Aston University

Some pages of this thesis may have been removed for copyright restrictions.

If you have discovered material in AURA which is unlawful e.g. breaches copyright, (either yours or that of a third party) or any other law, including but not limited to those relating to patent, trademark, confidentiality, data protection, obscenity, defamation, libel, then please read our Takedown Policy and contact the service immediately

CELLULAR UPTAKE AND BIOLOGICAL ACTIVITY OF SYNTHETIC HAMMERHEAD RIBOZYMES

PATRICIA LYNNE FELL

Doctor of Philosophy

ASTON UNIVERSITY

September, 1999

This copy of the thesis has been supplied on condition that anyone who consults it is understood to recognise that its copyright rests with the author and that no quotation from the thesis and no information derived from it may be published without proper acknowledgement.

ASTON UNIVERSITY

CELLULAR UPTAKE AND BIOLOGICAL ACTIVITY OF SYNTHETIC HAMMERHEAD RIBOZYMES

PATRICIA LYNNE FELL

Doctor of Philosophy

1999

SUMMARY

Glioblastoma Multiforme (GBM) is a highly malignant form of brain cancer for which there is no effective cure. The over-expression of a number of genes, including the epidermal growth factor receptor (EGFr), has been implicated as a causative factor of tumourigenesis. Ribozymes are a class of ribonucleic acid that possess enzymatic properties. They can inhibit gene-expression in a highly sequence specific manner by catalysing the *trans*-cleavage of target RNA. The potential use of synthetic hammerhead ribozymes as novel anti-brain tumour agents was investigated in this study. The successful use of synthetic, exogenously administered ribozymes for such applications will require chemical modifications that improve biological stability and a fundamental understanding of cellular uptake mechanisms. Chimeric 2'-O-methylated hammerhead ribozymes proved to be significantly more stable (>4000-fold) in serum than unmodified RNA ribozymes and exhibited high *in vitro* catalytic activity. The cellular association of an internally [^{32}P]-labelled 2'-O-methylated chimeric ribozyme in U87-MG human glioma cells was temperature-, energy- and pH-dependent and involved an active process that could be competed with a variety of polyanions. Indications are that the predominant mechanism of uptake is by adsorptive and / or receptor mediated endocytosis. Twenty 2'-O-methylated chimeric ribozymes were designed to cleave various sites along the EGFr mRNA. *In vitro*, 18 ribozymes exhibited high activity in cleaving a complementary short substrate. Using LipofectAMINE™ as a delivery agent, the efficacy of these ribozymes was evaluated in the A431 cell line, which expresses amplified levels of EGFr. Studies revealed that although the ribozymes were taken up by the cells and remained stable over a period of 4 days, no significant reduction in either EGFr expression or cell proliferation was evident. The presence of telomerase, a ribonucleoprotein responsible for telomere elongation, has been strongly associated with tumour progression. The biological activity of a 2'-O-methylated ribozyme targeted against the RNA component of telomerase was determined. The ribozyme exhibited specific dose-dependent inhibition of telomerase activity in U87-MG cell lysates with an IC_{50} of ~4μM. When 4μM ribozyme was delivered to intact U87-MG cells, complexed to LipofectAMINE™, telomerase activity was significantly reduced to 74.5± 4.17% of the untreated control. Free ribozyme showed no significant inhibitory effect demonstrating the importance of an appropriate delivery system for optimum delivery of exogenously administered ribozymes.

KEYWORDS: Ribozymes, Cellular uptake, EGFr, Telomerase, Glioblastoma Multiforme

ACKNOWLEDGEMENTS

The work in this thesis was jointly funded by a Total Technology case award from the Engineering and Physical Research Council (EPSRC) and Ribozyme Pharmaceuticals Inc.

I would like to thank my supervisor at Aston University, Saghir Akhtar, for his guidance during my studies. I would also like to acknowledge my external supervisor, Mark Reynolds at Ribozyme Pharmaceuticals Inc., for his technical advice and financial support.

The following people are kindly acknowledged: Chris Bache for his constant willingness to rapidly repair laboratory equipment; Sidwell Technologies Ltd. for repeatedly fixing my computer and to the lecturers at Aston Business School for their help in attaining the MBA modules required to complete the Total Technology coursework.

Finally I would like to thank my family, especially my husband Richard, whose support has kept me going during these past few years of research.

LIST OF CONTENTS

CHAPTER TWO: GENERAL MATERIALS AND METHODS

LIST OF FIGURES

LIST OF TABLES

LIST OF ABBREVIATIONS

2'-O-Me	2'-O-methyl
2'-NH_2	2'-amino
A,G,C,T,U	adenine, guanine, cytidine, thymidine, uridine
AAV	adeno-associated virus
AE	adsorptive endocytosis
ATP	adenosine triphosphate
BSA	bovine serum albumin
°C	degrees Celcius
cpm	counts per minute
CHAPS	3'-[(3-cholamidopropyl)dimethyl-ammonio]-1-propanesulphonate
CO_2	carbon dioxide
DMRIE	1,2-dimyristyloxypropyl-3-dimethyl-hydroxyethyl ammonium bromide
DOPE	dioleoyl phosphatidylethanolamine
DOSPA	N-[2-({2,5-bis[(3-aminopropyl)amino]-1-oxypentyl}amino)ethyl]-N,N-dimethyl-2,3-bis(9-octadecenyloxy)-1-propanaminium trifluoroacetate
DOTAP	N-[1-(2,3-dileoyloxy)propyl)-N,N,N-trimethylammonium methylsulphate
DOTMA	N-[1(-2,3-dioleyloxy)propyl]-N,N,N,-trimethylammonium chloride
DEPC	diethylpyrocarbonate
DMEM	Dulbecco's modified Eagle's medium
DMSO	dimethyl sulphoxide
DMT	dimethoxytrityl
DNA	deoxyribonucleic acid
DTT	dithiothreitol
ECACC	European collection of animal cell cultures
EDTA	ethylenediamine tetra-acetic acid
EGFr	epidermal growth factor receptor
FBS	foetal bovine serum
FITC	fluorescein isothiocyanate
Fpmp	1-(2-fluorophenyl)-4-methoxypiperidin-4-yl
FRET	fluorescence resonance energy transfer

ΔG	energy of formation of lowest energy structure
GBM	glioblastoma multiforme
GFAP	glial fibrillary acid protein
HBSS	Hank's balanced salt solution
HEPES	(N-2-hydroxymethylpiperazine)-N'-2-ethanesulfonic acid
HIV-1	human immunodeficiency virus, type 1
HPLC	high-performance liquid chromatography
HRP	horseradish peroxidase
hTR	RNA component of human telomerase
hTRT	catalytic protein subunit of telomerase
i.p	intra - peritoneal
i.v.	intra – venous
kDa	kilo Daltons
LSC	Liquid scintillation counting
ml,μl	millilitres, microlitres
μCi	micro Curies
MES	(2-[N-morpholine]-ethanesulphonic acid
MP-ODN	methylphosphonate oligonucleotide
mRNA	messenger ribonucleic acid
mw	molecular weight
OD	optical density
ODN	oligodeoxynucleotide
ON	oligonucleotide
ORN	oligoribonucleotide
PAGE	polyacrylamide gel electrophoresis
PBS	phosphate-buffered saline
PCR	polymerase chain reaction
PDGF	platelet-derived growth factor
PMSF	phenylmethylsulphonylamide
PNK	polynucleotide kinase
PO-ODN	phosphodiester oligodeoxynucleotide
Pre-mRNA	unspliced messenger ribonucleic acid
PS-ODN	phosphorothioate oligodeoxynucleotide
RME	receptor-mediated endocytosis
RNase-H	ribonuclease H
rpm	revolutions per minute
RZ	ribozyme
SD	standard deviation
SDS	sodium dodecyl sulphate

$t_{1/2}$	half-life
TBE	tris-borate EDTA buffer
TEMED	N,N,N',N'-trimethylethylenediamine
TETD	tetraethyl disulphide
TGF	transforming growth factor
TRAP	telomeric repeat amplification protocol
TRIS	Tris(hydroxymethyl)amino methane
UTR	untranslated region
VEGF	vascular endothelial growth factor
v/v	volume per volume
w/v	weight per volume
w/w	weight per weight

CHAPTER ONE

INTRODUCTION

1.1 ANTISENSE TECHNOLOGY

An important goal of drug design is the achievement of specificity. Conventional drugs are most typically directed against proteins such as enzymes, receptors or ion channels, the structure and mode of action of which are often incompletely understood. Such drugs are, in general, poorly selective and can cause toxic side-effects, imposing limits on drug dosage and duration of treatment. Recent advances in the understanding of the molecular basis of disease processes has, however, led to treatment strategies being pursued which offer important innovations in drug discovery.

One such strategy employs an antisense-based therapeutic approach. Antisense technology takes advantage of the natural tendency of complementary nucleic strands to form in solution. Through Watson-Crick base pairing, nucleic acids hybridise to complementary DNA, pre-mRNA or mRNA of a target gene, thus restricting or blocking the flow of information from the DNA of a specific gene to its protein product (see Figure 1.1). As a result gene expression is inhibited in a highly specific manner. Antisense technology, therefore, promises to provide the basis for a new generation of therapeutic drugs that specifically modulate the expression of aberrant genes without affecting normal cells.

Antisense modification of gene expression can be due to naturally produced nucleic acids, forming part of a cell's normal regulatory system, or those added exogenously as oligonucleotides (ONs).

1.1.1 Antisense Oligonucleotides

Antisense oligonucleotides are single-stranded nucleotide stretches whose sequences are synthesised complementary to specifically selected mRNA transcripts (sense strands) encoding particular proteins of interest. Such oligonucleotides can be composed of DNA (oligodeoxynucleotides, ODNs) or RNA (oligoribonucleotides, ORNs).

Zamecnik and Stephenson were the first to propose, in 1978, the use of synthetic antisense oligonucleotides for therapeutic purposes (Zamecnik & Stephenson, 1978). Using a 13-mer ODN that was complementary to the RNA of Rous sarcoma virus, they were able to demonstrate inhibition of the growth of this virus in cell culture. Since the pioneering work of Zamecnik and Stephenson, an enormous number of reports have been published demonstrating the inhibitory activity of ODNs on gene expression (for reviews see: Akhtar, 1995; Agrawal, 1996; Bennett, 1998; Gewirtz *et al.*, 1998). These studies have included ODNs targeted to a large variety of both cellular genes (e.g. oncogenes, growth factors, signal transduction) and foreign genes (e.g. viral).

In earlier studies, unmodified ODNs containing a phosphodiester backbone (PO-ODN) were administered, however, they proved unstable towards nucleases and their *in vivo* use is therefore limited. To overcome the nuclease instability of ODNs, various analogues have been synthesised including those containing phosphorothioate internucleotide bonds (PS-ODNs) and those containing methylphosphonate internucleotide linkages (MP-

ODNs) (for review articles see Uhlmann & Peyman, 1990; Crooke, 1992; Agrawal and Iyer, 1995; Reddy, 1996).

Various cellular processes can be inhibited by oligonucleotides depending on where the ON hybridises on single stranded regions of DNA or mRNA (Helene and Toulme, 1990). A schematic diagram describing the possible sites and mechanisms of action by which ONs can inhibit protein biosynthesis is shown in Figure 1.1.

Antisense oligonucleotides have the ability, once inside the cell, to bind to target mRNA either in the cytoplasm, in the nucleus or in both. Prevention of translation can occur, upon hybridisation, by two distinct mechanisms. Firstly, certain charged (but not uncharged) ODNs, including PO-ODNs and PS-ODNs, can inhibit mRNA translation by activating cellular RNase H, a ubiquitous enzyme which cleaves the RNA component of an RNA-DNA duplex (Dash *et al.*, 1987). Once cleaved, the mRNA is no longer competent for translation and may be rapidly degraded. Alternatively, translation can be blocked by simple steric hindrance. The antisense – mRNA duplex may simply block the RNA physically from interacting with cellular components required for translation of RNA into protein. ONs such as MP-ODNs, and ORNs are believed to act in this manner (reviewed in Milligan, 1993, Tidd, 1996). In the cytoplasm, steric blocking can inhibit protein synthesis processes such as translation, initiation or ribosomal movement. In the nucleus, such a blocking can inhibit pre-mRNA splicing, polyadenylation or transport of mRNA from the nucleus to the cytoplasm. Other possible target regions are the 5'- and 3'- untranslated regions, where bonding of an oligonucleotide may cause conformational changes or destabilisation of the mRNA (Helene and Toulme, 1990).

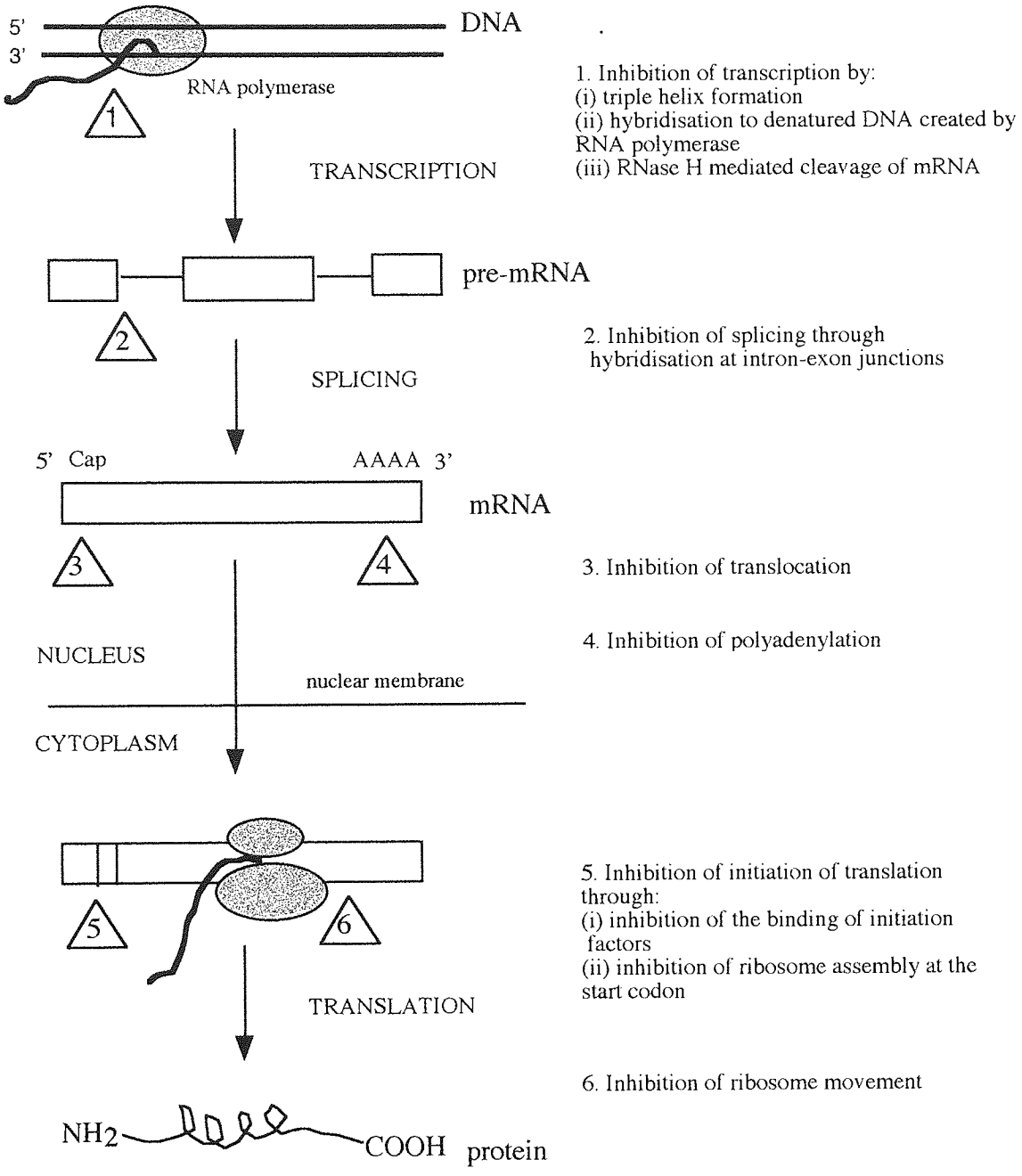

Figure 1.1 *Possible sites of action of antisense oligonucleotides* (Adapted from Helene and Toulme (1990)).

In addition to mRNA, chromosomal DNA is the other cellular target for sequence specific action of antisense ONs, preventing either initiation or elongation of transcription. This is achieved by either binding to segments of DNA that are partially unwound during transcription or alternatively by binding to the DNA double helix to form a triplex. The formation of a triple helix on DNA sequences by Hoogsteen hydrogen bonds requires regions of DNA containing a continuous series of purines on one strand and pyrimidines on the other strand. The ODN becomes the third strand by hydrogen bonding on a purine reference strand and lying in the major groove (reviewed by Helene and Toulme, 1990; Pierga and Magdelenat, 1994; Scanlon *et al.*, 1995). The advantage of this approach is that inhibition occurs at the first step of protein biosynthesis, and thus it is more efficient to target a small number of genes compared to a large number of mRNA molecules. However, the homopurine sequence requirements of triplex forming ODNs severely limits the choice of target regions and furthermore concerns exist that triple helixes with DNA might produce permanent biological effects such as mutagenicity and carcinogenicity.

1.1.2 Ribozymes

A development to the antisense strategy is the ribozyme - based therapeutic approach and is the subject of this report. Ribozymes are essentially a class of oligoribonucleotides that have an intrinsic capability of cleaving RNA in a sequence-specific manner. They similarly rely on the principle of complementary base formation and have evolved as a potential therapeutic agent as a result of the elucidation of the properties of ribonucleic acids.

In the early 1980s it was found that certain naturally occurring RNA molecules possess the property of self-catalysed cleavage activity, demonstrating that RNA can act as an enzyme in the absence of proteins and other molecules (Cech *et al.*, 1981; Guerrier-Takada *et al.*, 1983). The discovery that these catalytic RNAs, subsequently called ribozymes (derived from the terms: ribonucleic acid and enzyme), could in fact carry out functions that had been ascribed solely to proteins, fundamentally changed our understanding of the function of RNA. Previously, RNA had been considered to be purely passive carriers of genetic information.

At present, several naturally occurring ribozyme structures have been identified. Cech *et al.* (1981) were the first to demonstrate such RNA catalytic activity in the group I intron of the protozoan *Tetrahymena thermaphila.* The natural role of this ribozyme is to process ribosomal RNA by participating in autocatalytic cleavage during the RNA splicing process. Shortly afterwards, a second ribozyme structure was elaborated by Dr. Sydney Altman and colleagues during experiments which characterised the structure of RNase P enzyme, purified from *Escherichia coli* (Guerrier-Takada *et al.*, 1983). RNase P is an endoribonuclease which generates the mature 5'-end of tRNAs by endonucleocatalytic cleavage of precursor transcripts. Of the two subunits which comprise this molecule, the one subunit, M1-RNA, bears catalytic properties while augmentation of the endoribonuclease activity appears to be the function of a 14-kDa second subunit (Guerrier-Takada *et al.*, 1983).

Following the pioneering work of Cech and Altman, five more distinct classes of ribozymes have been defined which are capable of intramolecular cleavage (for general reviews see: James and Gibson, 1998; Carola and Eckstein, 1999; Tanner, 1999). These are often named after the appearance of their secondary structures and include the

following motifs: [1] The "hammerhead" ribozymes were discovered in plant viroids, virusoids and satellite viruses (Forster & Symons, 1987). They act in *cis* (intramolecular) during viral replication by the rolling circle method, cleaving the polycistronic message into individual RNA transcripts. [2] The "hairpin" ribozyme was identified in the minus strand of the satellite RNA of the tobacco ringspot virus (Hampel *et al.*, 1990). This ribozyme has a similar role in viral replication as the hammerhead. [3] The hepatitis delta virus is a helper virus whose RNA was found to have autocatalytic RNA processing similar to the function of the hairpin and hammerhead motifs (Wu *et al.*, 1989). This ribozyme is sometimes referred to as the "axehead" ribozyme. [4] and [5] Two additional catalytically active ribozyme motifs have been described in self-splicing group II introns, which are related to the *Tetrahymena* group I type ribozymes, (Cech and Bass, 1986) and in *Neurospora* self-cleaving RNA (Collins & Olive, 1992).

The predominant activity found in all of these naturally occurring ribozymes is the ability to cleave RNA molecules in a highly sequence-specific manner. Essentially ribozymes are small RNA molecules endowed with endoribonuclease activity at enzymatic rates. The ribozyme is composed of two domains: a binding domain and an RNA cleaving domain. The binding domain hybridises to target RNA by Watson-Crick base-pairing, causing the target RNA to be acted upon by the catalytic domain of the ribozyme. The ribozyme cleaves the target RNA, following which the cleavage products dissociate from the ribozyme, making it available to hybridise to another sequence.

Although evidently different in size, structure, specificity and mechanism of action, a common feature of all these different ribozyme motifs is that they act as metalloenzymes. Divalent metal ions, such as magnesium or manganese are required for both the

stabilisation of their tertiary structure and for maximum catalytic activity (Bratty *et al.*,1993).

The properties of these ribozymes make them extremely attractive for use as therapeutic agents, for they exhibit antisense behaviour to block translation by duplex formation, they have the ability to cleave and inactivate mRNA molecules and they have the potential to act on multiple target molecules. With the exception of RNase P RNA, however, naturally occurring ribozymes function in an intramolecular (*cis*) reaction to splice or cleave their own RNA sequences. Consequently, research was required to develop ribozymes for therapeutic use by modifying them to function as *trans*-acting enzymes, i.e. to perform intermolecular cleavage between two separate RNA molecules.

In 1987, Uhlenbeck demonstrated intermolecular cleavage by separating the catalytic and substrate domains of the hammerhead ribozyme through the removal of naturally occurring loops in the stem structure (Uhlenbeck, 1987). Subsequently, Haseloff & Gerlach (1988) achieved *trans*-cleavage of a target RNA unrelated to the natural substrate. Further investigations have led to the development of other *trans* reactive ribozymes including the group 1 intron ribozyme (Sullenger and Cech, 1994); the hairpin ribozyme (Hampel *et al.*, 1990); the hepatitis delta ribozyme (Been, 1994) and the *Neurospora* ribozyme (Guo and Collins, 1995). The development of such sequence specific *trans*-acting ribozymes offered exciting possibilities in the down-regulation of gene expression, for ribozymes could now be custom-designed to target and catalytically cleave any given cellular or viral RNA target species.

To date, almost all applications of ribozymes to the regulation of gene expression have used either hammerhead or hairpin ribozymes (for recent reviews see Hampel, 1998;

James and Gibson, 1998; Gaughan and Whitehead, 1999; Kruger *et al.*, 1999; Tanner *et al.*, 1999). The hammerhead ribozyme is the smallest of the ribozyme motifs and is by far the most widely studied in terms of therapeutic applications. Its small size makes it the most amenable ribozyme for exogenous delivery, since it can be readily synthesised via automated solid-phase chemical synthesis. It also has been the best characterised ribozyme with respect to optimised target sequence, conserved nucleotides sequences within the catalytic core and the kinetic parameters. In addition, the target RNA cleavage sites have the least restraints with respect to sequence compared to the other motifs. The hammerhead ribozyme will be discussed in further detail in section 1.2, since the experimental studies performed during this report are focused on the cellular uptake and activity of this type of ribozyme.

1.1.3 DNA Enzymes

In vitro selection has led to the recent development of DNA enzymes (also termed DNAzymes or deoxyribozymes) composed entirely of ODNs that can cleave RNA in a sequence-specific manner. One such type of DNAzyme has been reported to be able to cleave almost any targeted RNA substrate under simulated physiological conditions (Joyce, 1998). These DNA enzymes are similar to the hammerhead ribozyme, consisting of a catalytic domain of 15 deoxynucleotides and requiring Mg^{2+} for catalytic activity. Further characterisation has revealed that the DNAzymes can cleave with high substrate specificity, and very high catalytic activity, surpassing that of small ribozymes such as the hammerhead and hairpin by an order of magnitude (Santoro and Joyce, 1998). In addition, Sen and Geyer (1998) isolated an RNA-cleaving DNAzyme, termed 'G3', that reportedly functions with a 10^8-fold rate enhancement in the absence of either divalent cations or any other suitable co-factor. Their rapid catalytic turnover and stability to

nucleases make DNAzymes very appealing for future *in vitro* and *in vivo* applications. Not surprisingly, therefore, this is a rapidly expanding area of research in the antisense field (for reviews see: Sen and Geyer, 1998; Carola and Eckstein, 1999; Li and Breaker, 1999).

1.2 THE HAMMERHEAD RIBOZYME

1.2.1 Sequence Requirements of the Hammerhead Ribozyme

As stated previously, naturally occurring ribozymes were identified within a number of plant RNA viruses (Symons, 1992). Analysis of the different self-cleaving RNAs revealed a highly conserved nucleotide sequence relating to the catalytic region. From the profile of its secondary structure, this type of ribozyme became known as the hammerhead ribozyme. The sequence and secondary structure of the *trans* acting form of the hammerhead ribozyme, based on the design of Haseloff and Gerlach, is illustrated in Figure 1.2. In order to facilitate comparison of data from different research groups, a uniform numbering system has been adopted (Hertel *et al.*, 1992).

The hammerhead motif consists of 3 base-paired helical stems and a core of highly conserved non-complementary nucleotides which are essential for catalysis (for more recent structure / function reviews see: Birikh *et al.*, 1997; Amarzguioui and Prydz, 1998; Kore *et al.*, 1998). Detailed mutational analysis has revealed that changes at most unpaired positions results in lack of cleavage activity (Ruffner *et al.*, 1990). Nucleotide 7, however, may be changed to any other without major consequences, although highest cleavage rates have been observed with U, followed by G, A and C (Ruffner *et al.*, 1990).

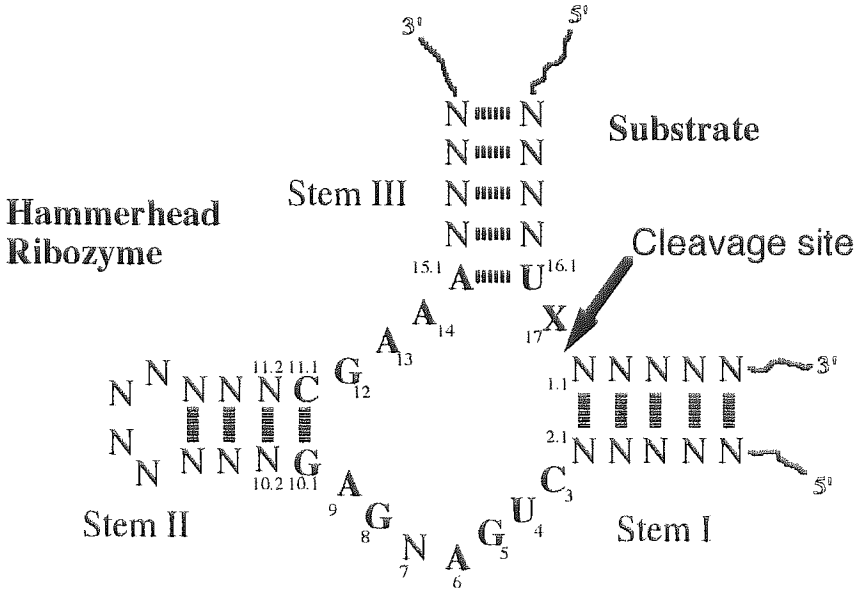

Figure 1.2 The *consensus sequence of the hammerhead ribozyme.* Numbering system according to Hertel *et al* (1992). Conserved nucleotides are in bold. N is any nucleotide, X is A, C or U.

Stem II is important in the stabilisation of the hammerhead structure and is thought to be responsible for associating with the divalent metal cation, required for catalytic cleavage of the substrate (Tuschl & Eckstein, 1993). Research indicates that this helical stem can vary both in sequence and in length. Tuschl and Eckstein (1993) found that the minimum base requirement for maximum cleavage activity was two base-pairs including the conserved base pair $G_{10.1}$:$C_{11.1}$. In order to maintain the conserved base-paired conformation, at least one additional base pair at positions 10.2:11.2 is required. This second base-pair is necessary in order to compensate for the helix destabilising effect of the terminal hairpin loop II (Jaeger *et al.*, 1989). Extension of this helix beyond four base pairs does not enhance *in vitro* activity (Homann *et al.*, 1994). In addition, the sequence of the loop nucleotides of helix II is not important and can be replaced by any nucleotide (Thompson *et al.*, 1993). Replacement of the whole stem and loop with a few nucleotides

that cannot form Watson-Crick base-pairing has resulted in the development in minimised ribozymes (minizymes) which retain cleavage activity (Hendry *et al.*, 1995).

Ribozyme and RNA substrate are held together by flanking regions of base-pairing (stems I and III) which must allow accurate positioning of the catalytic region relative to the potential cleavage site (Figure 1.2). The sequences of stems I and III must, therefore, be complementary to the substrate sequence adjacent to the cleavage site, so that binding of ribozyme and substrate can occur. Generally, 5 base-pairs or more are required on each side of the cleavage site to achieve stable binding, although cleavage has been observed when one substrate binding arm has contained only 2-3 base pairs, provided the other arm is tightly bound (Usman & Stinchcomb, 1996). The nature of substrate binding contributes to its specificity as single base-pair mismatches result in impaired cleavage activity. In contrast to oligonucleotides, increasing the recognition sequence can cause a reduction in specificity, since long recognition sequences result in strong binding which can lead to the toleration of mismatches in the ribozyme-substrate complex (Werner & Uhlenbeck, 1995). A study by Hertel *et al.*, (1996) reported that recognition sequences of up to 12 nucleotides could be used without significant loss of specificity.

In naturally occurring hammerhead ribozymes, cleavage after the GUC triplet sequence is the most predominant (Symons, 1992). Two exceptions are found in the GUA cleavage triplet of the satellite RNA of the lucerne transient streak virus (Forster & Symons, 1987) and the AUA cleavage triplet of the satellite RNA of barley yellow dwarf virus (Miller *et al.*, 1991). Systematic mutational studies have been undertaken to establish the sequence requirements of the cleavage triplet (for reviews see: Symons, 1992; Bratty *et al.*, 1993; Birikh *et al.*, 1997). The results indicate that any triplet sequence of NUX (where N= any nucleotide and X = A, C, or U) can be cleaved.

There are, however, inconsistencies in reports predicting the relative cleavage activity pertaining to each cleavage recognition site, although it is generally believed that the GUC triplet yields the highest rate of cleavage compared to other triplet sequences. For example, a substrate that contained AUC triplet was found to have an activity similar to the wild type substrate (Ruffner *et al.*, 1990) while in another study the same substrate was poorly cleaved (Perrimen *et al*, 1992). Such conflicting results could be due to the varying reaction conditions used by different research groups. Shimayama *et al.*, (1995) reported that the order of cleavage activity relative to cleavage site sequence varied according to ribozyme concentration, while Sullivan (1994) found that the sequence surrounding the triplet can strongly influence the cleavage efficiency.

Bratty *et al.*, (1993) has reported that the base trios; GUC, CUC, GUA and UUC can generally be cleaved providing incompatible structures are not formed by the nucleotides on either side. Further research mainly supports these findings. A detailed analysis of hammerhead ribozyme designs targeted against mutant substrates with all possible variations of the NUX triplet showed that GUC (wild type), AUC, CUC, GUA and AUA sequences were efficiently cleaved (Shimayama *et al.*, 1995). A more recent investigation has, however, revealed that contrary to previous opinion, triplets of NAX are also cleavable although cleavage efficiency was poor (2-10%) when compared with the conventional GUC triplet and the ribozyme had an altered core and stem-loop II sequence (Vaish *et al.*, 1998; Kore *et al.*, 1998). Furthermore, it has also been reported that substrates with an NCX triplet can be cleaved if position 15.1 in the ribozyme is replaced with an inosine (Ludwig *et al.*, 1998). Consequently, it appears from these recent findings that the NUX rule could be extended to NXX by the introduction of specific mutations in the conserved sequence of the native hammerhead.

It is apparent from these studies that there is no set rule predicting highly active cleavage sites; the optimal triplet appears to be dependent upon many factors including ribozyme concentration, the ribozyme binding arms and the composition and nucleotide composition of the target RNA.

The three-dimensional structure of the hammerhead ribozyme has more recently been elucidated by different means including x-ray crystallography (Pley *et al.*, 1994; Scott *et al.*, 1995), fluorescence resonance energy transfer (Tusch *et al.*, 1994), and electrophoretic mobility (Bassi *et al.*, 1995). A fairly consistent picture has emerged which suggests that this ribozyme should really be named the "wishbone" ribozyme for, in the presence of magnesium, the overall shape of the ribozyme adopts a Y-shaped or wishbone configuration, with stem I and II at the arms and stem III at the base (Figure 1.3).

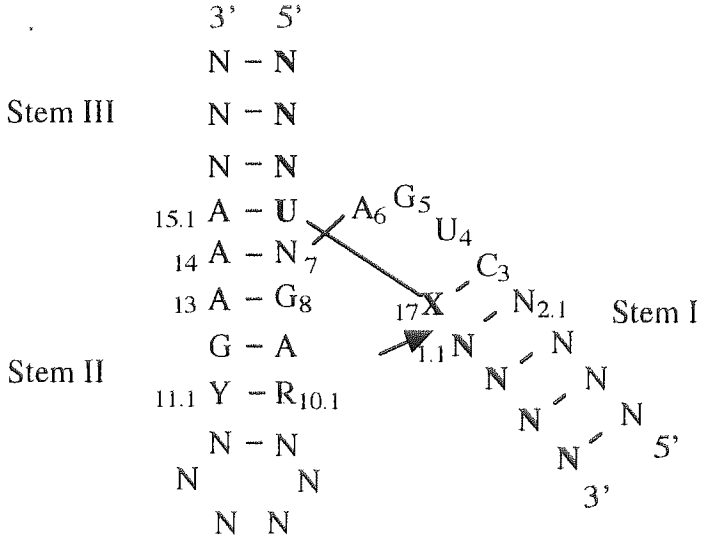

Figure 1.3 *Schematic representation of the hammerhead ribozyme based on the three-dimensional structure.* N represents any nucleotide; X represents the nucleotides A, U or C; R represents a purine nucleotide and Y a pyrimidine nucleotide; – represents Watson-Crick or reversed-Hoogsteen base pairs. Bold characters represent the substrate strand. The cleavage site is indicated by the arrow. Nucleotides in the core are labelled according to Hertel *et al.* (1992).

1.2.2 Hammerhead Ribozyme Catalytic Reaction Mechanism

The hammerhead ribozyme catalyses a transesterification, cutting the 3',5'-phosphodiester bond between nucleotides 17 and 1.1 and forming cyclic 2',3'-phosphodiester on nucleotide 17 and free 5'-hydroxyl on nucleotide 1.1 (Figure 1.4). The activity depends on the presence of divalent cations in millimolar concentrations (Bratty *et al.*, 1993).

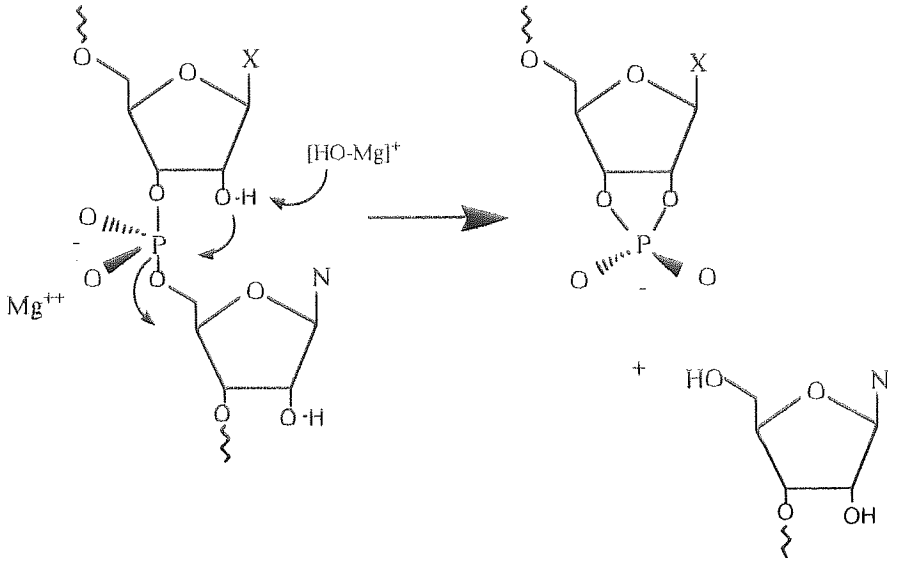

Figure 1.4 *Hammerhead ribozyme catalytic mechanism* (source: Dahm *et al*, 1993). N represents any base nucleotide, X represents the nucleotides A,U or C.

The proposed mechanism of action begins with deprotonation of the 2'-sugar at the 3'-side of the cleavage site. This results in nucleophilic attack of the adjacent phosphodiester bond and subsequently protonation of the 5'-oxyanion leaving group, generating 2',3'-cyclic phosphate and 5'-hydroxyl termini. The 2'-hydroxyl adjacent to the cleavage site is essential for cleavage (Sullivan, 1994). The Michaelis-Menten mechanism for the formation of the ribozyme-substrate complex and its subsequent conversion to products is outlined in Figure 1.5 and consists of at least three steps:

1. Firstly, the substrate (together with Mg^{2+} ions) binds to the ribozyme to form a complex via formation of base pairs with stems I and III (k_{ass}).
2. Then a specific phosphodiester bond in the bound substrate is cleaved as the ribozyme functions as a metalloenzyme (k_{cleave}).
3. Finally, the cleaved fragments dissociate from the ribozyme and the liberated ribozyme is now available for a new series of catalytic events (k_{diss}).

$$E + S \underset{}{\overset{k_{ass}}{\rightleftharpoons}} E{:}S \overset{k_{cleave}}{\rightleftharpoons} EP_1P_2 \overset{k_{diss}}{\rightleftharpoons} E + P_1 + P_2$$

Figure 1.5 *Minimal kinetic mechanism for intermolecular hammerhead catalysis.* E represents ribozyme; S represents substrate; P represents cleavage products.

The kinetic parameters K_m and k_{cat} can be derived for ribozymes in an analogous way to protein enzymes where K_m represents the ribozyme's affinity for the substrate and k_{cat}, the turnover number, is the chemical step to form products. The rates of ribozyme hybridisation to the substrate, dissociation of the ribozyme from the substrate and dissociation of the cleavage products from the ribozyme are controlled by the length and nucleotide sequence composition of the binding arms. If base-pairing between ribozyme and substrate is short i.e. less than 6 or 7 base pairs each arm then, under multiple turnover conditions (substrate saturating), k_{ass} and k_{diss} are fast relative to k_{cleave} and the cleavage event becomes the rate limiting step (Birikh *et al.*, 1997). When longer ribozymes are used, however, the elongation of the helical arms increases helix stability and drastically reduces the dissociation rates of substrate and products. In this case, the product dissociating step becomes the rate-determining step consequently reducing the turnover rate (k_{cat}).

The strong dependency of dissociation rates on helix stability is limiting to the design of ribozymes as multiple turnover catalysts. *In vitro*, only short ribozymes with flanking arms less than 6 or 7 nucleotides each will allow fast and efficient multiple cleavage reactions (Amarzguioui and Prydz, 1998). However, indications are that *in vitro* kinetic activities of ribozymes do not always translate into equivalent intracellular activities (Rossi, 1994), and reports have been published demonstrating effective use of ribozymes with long chain flanking sequences in *ex vivo* studies (for reviews see: Sczakiel, 1996; Birikh *et al.*, 1997; Amarzguioui and Prydz, 1998). This is probably due to the fact that *in vitro* experiments do not necessarily reflect the situation in the living cell, where proteins form complexes with RNA, influencing conformation and catalysis.

The influences of RNA-binding proteins on the catalytic activity of ribozymes have been investigated experimentally using the HIV encoded nucleocapsid protein NCp7 and the non-specific protein hnRNP A1 (Bertrand & Rossi, 1994; Herschlag *et al*, 1994 Tsuchihashi *et al*, 1993). Both types of protein enhanced ribozyme catalytic turnover (k_{cat}) over 10-20-fold by facilitating both the binding of ribozyme to target substrate and product release. In addition, the glycolytic enzyme glyceraldehyde-3-phosphate dehydrogenase (GAPDH) has been shown to enhance the *in vitro* cleavage rate of a ribozyme targeting tumour necrosis factor (TNFα) mRNA by up to 25-fold (Sioud and Jepersen, 1996).

Consequently, no general rules exist regarding the optimum arm length of ribozymes for effective biological activity and it is necessary, therefore, to experimentally optimise for a particular target and cell type.

1.3. CHEMICAL MODIFICATIONS OF RIBOZYMES

A major limitation in the development of ribozymes for use as therapeutic agents is the instability of ribozymes in the biological milieu. Unmodified RNA is rapidly degraded by nucleases which attack either the 5'-or 3'- ends of the molecule (exonucleases) or cleave the molecule internally (endonucleases). In addition, RNA is highly susceptible to attack by 2'-hydroxyl-dependent ribonucleases such as pancreatic RNase A. A significant challenge, therefore, in using ribozymes as drugs is to modify the RNA to increase ribozyme stability while retaining catalytic activity.

Methods for the chemical synthesis of RNA, using standard solid phase phosphoramidite techniques, have advanced rapidly in the past few years (Usman & Cedergren, 1992; Wincott *et al.*, 1995). The growing sophistication of chemical RNA synthesis has facilitated the study of ribozymes with various chemical modifications. The majority of this work has been undertaken with hammerhead ribozymes since their small size makes them the most suitable to chemically synthesise and modify. There are several potential target sites for modification in the basic nucleotide building block: the phosphodiester internucleotide linker, the ribose sugar moiety and the nucleotide base (Figure 1.6).

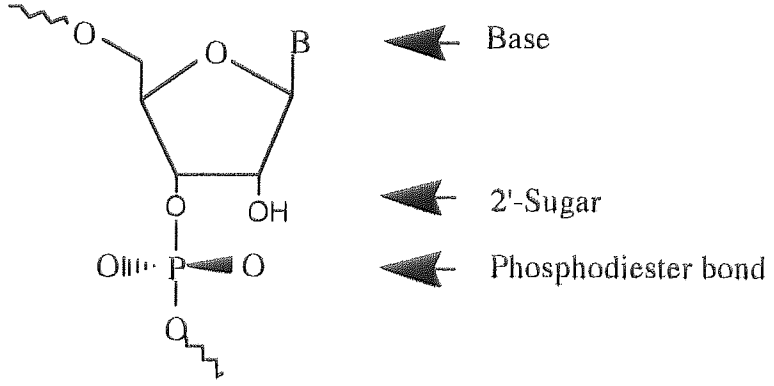

Figure 1.6 *Potential sites for chemical modification of ribonucleotides*

1.3.1. Phosphodiester Internucleotide Linkage Modifications

The internucleotide phosphate linkage is a structural feature common to all DNAs and RNAs. It is formed as a result of the action of DNA or RNA polymerases and is itself the target of a large number of enzymes such as nucleases, topoisomerases and activities associated with spliceosomes and RNA splicing (Heidenreich *et al.*, 1993). It is not surprising, therefore, that much research has been undertaken in modifying this site.

One of the most widely used modifications of the internucleotidic phosphate group in oligodeoxynucleotides is replacement by phosphorothioate groups (Eckstein, 1985; Gish & Ekstein, 1989). The increased nuclease resistant properties of such phosphorothioate oligodeoxynucleotides (PS-ODN) have been well documented (Marshall and Caruthers, 1993; Reddy, 1996; Agrawal, 1999), with reports indicating that PS-ODN can degrade up to 100 times more slowly than the unmodified phosphodiester oligonucleotide (PO-ODN) (Stein *et al.*, 1988). It was a logical step, therefore, to examine the effect of such modifications on the stability and catalytic activity of ribozymes.

The influence of phosphorothioate linkages on the activity and stability of ribozymes has been studied by several groups, who reported that while phosphorothioate linkage increased nuclease resistance significantly, activity was severely impaired (Ruffner & Uhlenbeck,1990; Shimayama *et al.*, 1993). Ruffner & Uhlenbeck (1990) identified critical phosphates at positions A_9, A_{13}, A_{14} and $N_{1.1}$ (cleavage site), where replacement by a phosphorothioate linkage severely impaired catalytic activity. Shimayama *et al.* (1993) showed that two phosphorothioate linkages 5'- to U_4 and G_5 in a DNA/RNA chimeric ribozyme stabilised the molecule but also significantly reduced catalytic activity. In

general, indications are that phosphorothioate substitution should be avoided in the catalytic domain of the ribozyme.

Successful use of phosphorothioates have been achieved, however, at the 5'- and 3'- ends of the binding arms of the hammerhead ribozyme, in conjunction with 2'-sugar modifications (Heidenreich *et al.*, 1994, 1996a). A modified ribozyme containing 2'-fluoro- and 2'-amino-pyrimidines in combination with terminal phosphorothioate linkages was shown to be significantly more stable and exhibited a three-fold higher cleavage efficacy than its unmodified counterpart. The increased resistance against nuclease degradation was mainly due to the terminal phosphorothioate linkages. Modified ribozymes with terminal phosphorothioates have since been used successfully *in vivo* (Lyngstadaas *et al.*, 1995; Flory *et al.*, 1996).

Potential problems associated with the use of phosphorothioate antisense molecules have, however, been highlighted in a recent report (Agrawal, 1999). Non-sequence specific and anti-protein effects of PS-ODNs have been observed (Krieg and Stein, 1995, Coulson *et al.*, 1996) arousing concerns as to the potential toxicity of these molecules. In addition, PS-ODNs have been shown to be immuno-stimulatory, reportedly inducing cytokine induction in mice (Zhao *et al.*, 1997, Kreig *et al.*, 1998; Hacker *et al.*, 1998). Nonetheless, PS-ODNs have been widely used in *in vivo* models, and have demonstrated sequence-specific antisense activity (Akhtar and Agrawal, 1997; Agrawal, 1999).

1.3.2 2'- Modifications at the Sugar Moiety

The prime target for modification in the ribose moiety of RNA is the 2' position. Modifications that have been introduced at this site mostly include 2'-deoxy, 2'-O-

methyl-, 2-O-allyl, 2'- amino, and 2'-fluoro replacements (for reviews see Aurup *et al.*, 1995; Bratty *et al.*, 1993; Sproat, 1996).

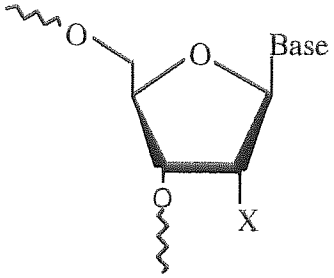

X = OH	unmodified ribonucleoside
X = H	2'-deoxynucleoside
X = OCH_3	2'-O-methyl ribonucleoside
X= NH_2	2'-deoxy-2'-amino ribonucleoside
X = F	2'-deoxy-2'-fluoro ribonucleoside
X = CH_2CHCH_2	2'-deoxy-2'-C-allyl ribonucleoside
X = OCH_2CHCH_2	2'-O-allyl ribonucleoside

Figure 1.7 *Commonly employed modifications at the 2'-site of ribose sugar.* 'Base' represents either A, C, G or U. 'X' represents the 2'-sugar residue.

Perreault *et al.*, (1990) were the first to embark on such studies by exchanging several ribonucleotides of a hammerhead ribozyme by their corresponding 2'-deoxy analogues and comparing the activities of the resulting RNA-DNA chimeras by kinetic analysis. Two 2'- hydroxyl groups were identified as being essential for full catalytic activity; those at G_5 and A_9 in the catalytic core of the ribozyme. Other research groups have confirmed these results, showing that the presence of a deoxyribonucleotide residue at position G_5 considerably lowers the activity of the hammerhead (Fu & McLaughlin, 1992; Williams *et al.*, 1992). By the reverse strategy, ribonucleotides have been inserted in an otherwise fully deoxyribonucleotide "nucleozyme" to reconstitute catalytic activity (Yang *et al.*, 1992). The results indicated that only four ribose residues are required to

sustain some catalytic activity (rG_5, rG_8, rA_9, & $rA_{15.1}$) although the activity reported was only about 0.3% of the parent, wild type ribozyme.

Hendry *et al.*, (1995) and Taylor *et al.*, (1992) have shown that hammerhead ribozymes with 2'-deoxyribonucleotides in place of ribonucleotides in stems I and III have an increased resistance against nuclease digestion and an enhanced catalytic activity. *In vivo* experiments have likewise shown that these chimeric DNA-RNA hybrid ribozymes are efficacious (Kiehntopf *et al.*, 1994; Snyder *et al.*, 1993).

The introduction of novel functional groups at the 2'-site of the ribose sugar has been examined. Substitution by 2'-O-methyl modified nucleotides at all positions in a hammerhead ribozyme except G_5, G_8, A_9, $A_{15.1}$ and $G_{15.2}$ resulted in a 1000-fold increase in stability but lowered catalytic activity significantly by a factor of 10^3 (Yang *et al.*, 1992). At the same time, Goodchild (1992) demonstrated that hammerhead ribozymes with nucleotides in stems I and III replaced with 2'-O-methylated RNA showed a two-fold higher cleavage efficiency when compared to an all RNA ribozyme and, in addition, enhanced stability four-fold.

Paolella *et al.* (1992) have used 2'-O methyl and 2'-O allyl groups for the replacement of the 2'-hydroxyl group in hammerhead ribozymes. Ribozymes containing these groups at positions G_5, G_8, G_{12}, and $A_{15.1}$ were catalytically inactive. In addition, cleavage was significantly reduced by changing U_4 and A_6 to their 2'-O-allyl derivatives. A ribozyme modified with 2'-O-allyl groups, except for at the critical positions mentioned, retained 20% of catalytic activity while considerably increasing biological stability (30% of the material remained intact after 2 hours compared to a <1 minute half life for an all RNA ribozyme).

Substitution of all the pyrimidine nucleotides in a hammerhead ribozyme by their 2'-amino or 2'- fluoro analogues resulted in a 1200-fold increase in stability in rabbit serum but also reduced activity 25-50-fold (Pieken *et al.*, 1991). Interestingly, specific substitution of 2'-amino or 2'-fluoro purines resulted in an even greater reduction in catalytic activity (Olsen *et al.*, 1991) indicating that, in general, modification of core nucleotides, particularly purine residues, severely impairs catalytic activity.

The problem of balancing nuclease resistance and catalytic activity was further addressed by Beigelman *et al.* (1995a) who were able to combine the results of Yang *et al.* (1992) and Paolella *et al.* (1992) to design a reportedly nuclease-stable hammerhead motif with native activity. This ribozyme motif consisted of only 5 ribose residues at positions G_5, A_6, G_8, G_{12} and $A_{15.1}$. Most of the remaining residues were 2'-O-methyl nucleotides with one or two other 2' modified sugars at positions U_4 and U_7 to block RNase A degradation. Ribozymes with either U_4 / U_7 2'-amino / 2'- amino or U_4 / U_7 2'- C-allyl / 2'-O-methyl modifications were reported to exhibit almost wild-type catalytic activity and substantially enhanced stability; their serum half lives were 5-8 hours compared to the all RNA parent ribozyme which demonstrated a stability half life of < 1 minute.

1.3.3 Nucleotide Base Modifications

Several base modifications have been incorporated into the hammerhead ribozyme to examine the effect on catalytic activity rather than to assess their ability to enhance stability. Most of the substitutions have been made at purines at the core of the hammerhead (for review see: Gait *et al.*, 1995; Usman & McSwiggen, 1995; Murray *et al.*, 1998) since they are thought to play an important role in catalysis. Many of these have involved replacement by inosine and purine ribonucleosides. In general, none of the

exocyclic amino groups of the conserved adenosine residues were found essential for catalytic efficiency. In contrast, however, removal of an amino group at the conserved guanosine residues G_5, G_8 or G_{12} proved to be detrimental to catalytic activity (Gait *et al.*, 1995). Recently, it has been discovered that substitution of nucleotide $A_{15.1}$ with inosine monophosphate resulted in a change of specificity, the preferred cleavage triplet altered from NUX to NCX (Lugwig *et al.*, 1998).

There have been few reports of pyrimidine analogue substitutions in hammerhead ribozymes. Since pyrimidine-specific nucleases have a particular requirement for base recognition, base modifications may provide nuclease stabilisation. Such an approach was directed at the nuclease sensitive positions U_4 and U_7 in the hammerhead ribozyme. These sites were replaced with either 6-methyluridine (Beigelman *et al.*, 1995b) or by an abasic ribose (Beigelman *et al*, 1995c). In both cases, the pyrimidine-base-modified ribozymes demonstrated both high catalytic activity and improved stability when compared to an all RNA molecule. Replacing the other core nucleotides with ribo-abasic residues, however, resulted in complete loss of cleavage activity.

Studies have revealed that nucleases present in serum are predominantly 3'-exonucleases (Tidd & Warenius, 1989). Protection from such 3'-terminal degradation has been demonstrated by introducing an unnatural, inverted internucleotidic linkage such as a 3'-3'-phosphate diester (Origao *et al.*,1992). The addition of an inverted (3'3'-linked) dT or abasic nucleotide to the 3'-terminus of a 2'-O-methyl modified hammerhead ribozyme has been shown to increase ribozyme half-life in human serum to greater than 260 hours (Beigelman *et al.*, 1995a). This represents a 10^5-fold increase in stability over the all RNA ribozyme with only a negligible reduction in catalytic activity.

These results indicate that, in addition to 2'-ribose sugar and phosphorothioate modifications, nucleotide base analogues may also be useful as nuclease stabilising elements in hammerhead ribozymes. Certainly, considerable advances have been made in stabilising synthetic ribozymes to produce nuclease stable, catalytically active ribozymes. Such enhanced stability coupled with the retention of activity make them eminently suitable for *ex vivo* and *in vivo* research and offer exciting possibilities for future *in vivo* therapeutic applications.

The chemical modifications described above relate to chemically synthesised, synthetic, ribozymes. There is, however, another method of obtaining ribozyme RNA. Ribozymes can be synthesised enzymatically by purified bacteriophage RNA polymerases, such as T7 or SP6. Such *in vitro* transcription is, however, limited to synthesis of unmodified RNA, as only natural ribonucleotides are recognised and incorporated by the phage enzymes (Elkins & Rossi, 1995). In this case ribozymes can be engineered to increase intracellular stability by creating secondary structures within the RNA that inhibit nuclease degradation. Increased stability has been demonstrated by embedding the hammerhead construct into either a tRNA (Perriman *et al.*, 1995) or by the addition of a stable hairpin structure at the 3'end of a ribozyme (Sioud *et al.*, 1992). Alternatively ribozymes have been expressed in such a way that the processing of the transcript yielded a circular ribozyme (Puttaraju *et al.*, 1993) to avoid the action of exonucleases. The circular *trans* acting hepatitis delta virus ribozyme was shown to retain catalytic activity while stability was greatly enhanced.

1.4 RIBOZYME DELIVERY

The method of ribozyme delivery to target cells must be effective for ribozymes to be used successfully in therapeutic applications. Efficient cellular uptake, specific mRNA targeting, sustained ribozyme expression, long half-life and safety are all desirable characteristics (Gaughan and Whitehead, 1999). Two options exist for ribozyme delivery: *Endogenous* delivery which involves the intracellular transcription of a ribozyme coding gene via an expression vector and *exogenous* delivery, which permits the uptake of preformed, synthesised ribozymes into the cell (Figure 1.8).

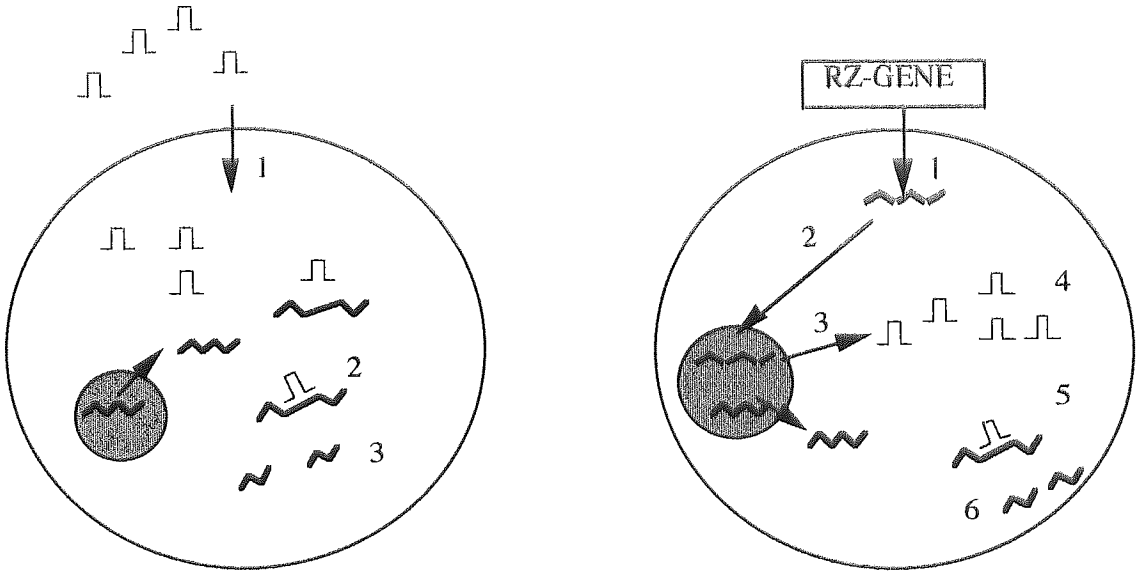

A: Exogenous

B. Endogenous

Figure 1.8 *Ribozyme delivery into cells.* **A**. The exogenous approach: Synthesised ribozyme enter cells (1); ribozymes bind to target RNA (2); cleavage takes place (3). **B**. The endogenous approach. A vector construct bearing RZ gene is introduced into cell (1); where it is integrated into host cell genome (2); transcription of RZ gene (3) leads to expression of active ribozymes (4) which bind to target mRNA (5). Cleavage then takes place (6). represents ribozyme; represents vector bearing ribozyme gene; represents target mRNA

1.4.1 Endogenous Delivery.

Endogenous delivery involves insertion of the ribozyme-encoding gene next to a promoter site in the host cell genome. Various different viral vectors can be exploited as potential ribozyme delivery vehicles including retroviruses, adenoviruses and adeno-associated viruses (for reviews see: Rossi, 1995; James and Gibson, 1998; Amarzguioui and Prydz, 1998; Gaughan and Whitehead, 1999). Retroviruses and adeno-associated viruses result in stable transfection whereas infection with adenoviruses results in transient transfectants (Rossi, 1995). Each viral delivery system has its advantages and disadvantages.

To date, RNA retroviruses have primarily been used for endogenous ribozyme expression. Stable transfection can be achieved in a variety of cell types with retroviral vectors, although integration into the host genome is rather non-specific, creating the danger of interruption of important gene sequences (Amarzguioui and Prydz, 1998). In addition, retroviruses have low vector titre and only transfect dividing cells, although the latter could be advantageous in the treatment of cancer where tumour cells would be selectively transduced. The stable transfectant adeno-associated virus vector offers a promising alternative. The adeno-associated virus (AAV) is a non-pathogenic virus which requires the presence of a helper virus (adenovirus) in order to replicate. It can infect a broad range of cell types, does not require cell division for integration and inserts non randomly into chromosome 19 (Ali *et al.*, 1994). A potential problem, however, in using the AAV as a vector for ribozyme-based therapeutics is that 40-80% of adults have pre-existing immunity to AAV (Gaughan and Whitehead, 1999). Infection with retroviruses and adeno-associated viruses yields permanent transfections that have the potential for continuous ribozyme expression.

Transient expression of ribozymes can be achieved with adenovirus vectors which do not integrate into the host genome. The advantages of using such vectors are a high transfection efficiency, they can transduce non-dividing cells and they produce high titres from packaging cell lines (Sullivan, 1994). Adenoviral vectors do not replicate, however and so expression is short-lived. The effectiveness of an adenovirus vector in mediating the expression of ribozymes was very recently demonstrated when an adenovirus, expressing ribozyme, targeted against c-myb mRNA, was shown to inhibit smooth muscle cell proliferation and neointima formation *in vivo* (Macejak *et al.*, 1999).

Once the ribozyme gene is delivered to the cell it must be expressed and the choice of promotor sequence for the intracellular expression of ribozyme transcripts is an important factor. A major consideration is the choice of expression system required; this may be involve inducible, tissue-specific or constitutive promoters (Rossi, 1995). Inducible promoters rely on external events to trigger expression. For example, heat shock protein promotors have been utilised for timed induction of ribozyme expression (Zhao and Pick, 1993). Tissue specific expression can potentially localise ribozyme expression and thus increase its effectiveness. Ohta *et al.*, (1996) used a tyrosinase, an enzyme which is synthesised solely in the melanocytic system, as a promotor to express an anti-H-*ras* ribozyme in human melanoma cells. The majority of reports demonstrating the efficacy of endogenously delivered ribozymes have, however, involved constitutive promotors (Amarzguioui and Prydz, 1999 for review). In particular, RNA polymerase II and III systems have proven efficacious for ribozyme expression (James and Gibson, 1998).

An interesting development in endogenous delivery is the co-localisation of ribozyme and substrate (for review see Arndt and Rank, 1997). In cells, RNAs appear to be highly compartmentalised and actively sorted to specific cellular locations. Consequently, such

RNA trafficking may result in ribozymes being located in a different part of the cell to their target substrate, thus limiting the effectiveness of the ribozyme to inhibit gene expression. In order for ribozymes to be effective, therefore, they must co-localise with the target to increase effective concentration (Sullenger and Cech, 1993).

Sullenger and Cech (1993) used a retroviral RNA packaging signal to facilitate intracellular co-localisation of ribozymes with its target by co-expressing murine retroviral genomic transcripts, one harbouring the lacZ target and the other a ribozyme to this target. Using this strategy, 99% inhibition of the lacZ mRNA was achieved, whereas lacZ mRNA expression levels were unaffected by the ribozyme when the packaging signal was not included. A similar strategy was utilised by Westaway *et al.*, (1995). A HIV-1 specific ribozyme was co-expressed as a fusion with tRNA-Lys^3 since a specific primer of this tRNA is bound by viral proteins and co-packaged with viral genomes. The ribozyme, which was targeted to HIV-1 reverse transcriptase was effective in inhibiting HIV replication. It has also been observed that the 3'-UTRs of some mRNAs carry the signal responsible for localisation. It is possible, therefore, that such localisation signals could be attached to ribozyme sequences to aid their co-localisation and efficiency (James and Gibson, 1998),

The major advantage of endogenous application of ribozymes lies in its continual expression, whereas multiple administrations of exogenously delivered ribozymes are necessary if long-term presence of the ribozyme is required. In addition, since the ribozymes are not chemically modified, they should be metabolised via natural routes, reducing the possibility of toxicity. It must be born in mind, however, that integration of foreign DNA into the host genome could represent a dangerous intervention into the

genetic structure of the recipient. For this reason much research is being undertaken to develop an efficient exogenous delivery system for nuclease stable synthetic ribozymes.

1.4.2 Exogenous Delivery.

In contrast to endogenous delivery, exogenous delivery of ribozymes offers the possibility of developing therapeutic agents that can be applied locally into, for example, solid tumours and inflammatory sites. In addition, exogenous delivery permits the use of chemically modified ribozymes that are relatively resistant to degradation to nucleases.

The vast majority of drugs that are useful therapeutics are small molecules. By contrast, even the smallest motif, the hammerhead ribozyme, is in the region of 30-40 nucleotides in length, highly charged and hydrophilic, properties which are not amenable to transversing the plasma membrane. While it has been demonstrated that chemically synthesised ribozymes can be directly delivered to cells and tissues (Marschall *et al.*, 1994), the uptake efficiency of free delivery is extremely low. Moreover, while the cellular uptake mechanism of oligodeoxynucleotides has been extensively reviewed (for reviews see Akhtar and Juliano, 1992; Crooke, 1992; Reddy, 1996), the extent and mechanisms by which ribozymes and ribonucleotides penetrate the cell membrane has received little attention. In fact, until this study (Fell *et al.*, 1997) a detailed report on the mechanism of cellular uptake of ribozymes had not been described (see Chapter Three). Such information will be useful, however, for their successful development as biological tools in cultured cells and as potential therapeutic agents *in vivo*. Furthermore, the optimisation of appropriate delivery strategies will require a fundamental understanding of the cellular uptake properties of synthetic ribozymes.

Since synthetic ribozymes share many characteristics with antisense ODNs, such as size and anionic charge, it had been postulated that ribozymes also enter cells by similar mechanisms to ODNs (Marschall *et al.*, 1994; Elkins and Rossi, 1995). Consequently the mechanism by which ODNs are reported to enter cells is detailed below.

1.4.2.1 *Cellular Uptake and Intracellular Distribution of Oligodeoxynucleotides*

The mechanisms of cellular uptake of ODNs are complex and not fully understood, however evidence suggests that they are taken up into cells predominantly by the active process of endocytosis (for reviews see Akhtar and Juliano, 1992; Reddy, 1996; Akhtar, 1998). Previous studies have indicated that ODN uptake is dependent upon time, temperature, energy, and concentration (Yakubov *et al.*, 1989; Loke *et al.*, 1989). These finding have led researchers to believe that, in certain cell types, endocytic uptake of PO- and PS- oligonucleotides may be mediated by specific receptors i.e via receptor mediated endocytosis (RME). To support this theory, various cell surface proteins have been suggested as putative receptor proteins to which ODNs specifically bind. Initially an 80-kDa cell surface protein, referred to as 'nucleic acid binding receptor-1' (NABR-1) was discovered. This protein was identified in a variety of cell types including HL60 (Loke *et al*, 1989), in mouse fibroblast L929 and ascites carcinoma Krebs 2 cells (Yakubov *et al*, 1989) and in CHO hamster cells (Vlassov *et al.*, 1994). Following these earlier reports, many more ODN binding proteins have been reported. Both Goodarzi *et al* (1991) and Kitajima *et al* (1992) identified a 34-kDa membrane protein to which ODN specifically bound; and another protein of 46-kDa, found on Caco-2 cells, T15 mouse fibroblast cells and a variety of human carcinoma cells was more recently identified as a PO-ODN binding protein (Akhtar *et al.*, 1996; Hawley and Gibson, 1996). Others have found that ODNs will bind to several proteins; Yao *et al.*, (1996) reported ODN binding to proteins

of 100 and 110-kDa in Hep G2 cells and in a study which examined the binding of biotinylated phosphorothioate ODNs to the cell membranes of K562 cells (Beltinger *et al.*, 1995) many binding proteins of various molecular weights ranging from 20-kDa to 147-kDa were identified. Interestingly, it has also been suggested that some of these binding proteins may act as cell membrane nucleic acid ion gated channels. (Hanss *et al.*, 1998).

The use of different cell lines or varying chemical modifications may explain the variety of identified ODN binding proteins. Another explanation, however, could be that oligonucleotides enter the cell through adsorptive endocytosis, where a ligand binds nonspecifically to proteins and lipids on the cell membrane before internalisation, as opposed to RME which requires a receptor protein specific to each particular ligand. In support of this theory, Stein *et al.*, (1993) found that ODNs which adsorb well to the cell surface (PO and PS) are internalised to a much greater degree than oligonucleotides, such as methylphosphonates and peptide nucleic acids, that do not. In addition, many researchers have reported that various polyanions competitively reduce the internalisation of charged ODNs (Loke *et al.*, 1989; Hawley and Gibson, 1996; Nakai *et al.*, 1996). In fact it has been suggested that 'ODN binding' proteins are actually a variety of membrane attached surface proteins such as heparin binding proteins (Benimetskaya *et al.*, 1997; Hawley and Gibson, 1996), fibrinogen receptors (Gerwitz, 1996) and serum albumin (Geselowitz and Neckers, 1995).

In contrast to the above, however, others have reported that uptake of oligonucleotides is non-specific, non-saturable and does not involve any detectable membrane binding, thus concluding that uptake occurs predominantly by fluid-phase endocytosis (FPE) / pinocytosis (Shoji *et al.*, 1991; Stein *et al.*, 1993; Wu-Pong *et al.*, 1994; Hughes *et al.*,

1995; Kreig and Stein, 1995). The concentration of ODN used in these experiments, however, could influence the mechanism of uptake. Yakubov *et al.*, (1989) and Beltinger *et al.*, (1995) have both provided evidence that at low concentrations of ODN (<1μM) receptor mediated or adsorptive endocytosis is the dominant mechanism but at high concentrations, when receptors become saturated, pinocytosis predominates.

Consequently, the exact uptake mechanism of ODNs still remains unclear and appears to be dependent upon many factors including oligodeoxynucleotide chemistry, concentration, length and cell type. Certainly the uptake of oligodeoxynucleotides is an inefficient process since only a small fraction of the input ODN becomes cell associated and a significant amount of that remains bound to the cell membrane (Milligan *et al.*, 1993).

1.4.2.2 *Enhanced Delivery Methods*

Since preformed / synthesised ribozymes are taken up so poorly following exogenous administration, various delivery vehicles are under investigation to enhance uptake efficiency. While most of these methods have been applied primarily to delivery of DNA (see Akhtar, 1998 for review), they are likely to function as well for RNA ribozymes.

One of the commonly used vehicles for delivering pre-synthesised ODNs and ribozymes to target cells is by liposome encapsulation. Liposomes are microscopically small spheres composed of phospholipids, arranged in a bilayer, which can either encapsulate nucleic acids within an aqueous centre, or can form lipid / nucleic acid complexes due to opposing electrostatic charges (for review see Juliano & Akhtar, 1992; Thierry and Tackle, 1995; Brown and Jarvis, 1997). The effectiveness of liposome mediated delivery

of ribozymes is dependent upon a number of factors including cell type and phospholipid composition. Sullivan (1993) reported that a liposome formulation composed of phosphatidylethanolamine, phosphatidylcholine and cholesterol was actively taken up by vero cells yielding 70% of the ribozyme in the cytoplasm. The same formulation was tested for uptake by HeLa cells. In this case, less than 5% of the offered dose was taken up into the cells and the ribozymes were sequestered inside intracellular vesicles. This clearly demonstrates that lipid composition needs to be designed for the cell type of interest and both uptake and intracellular release of the ribozyme must be taken into account.

While the effective use of liposome delivery of oligodeoxynucleotides was been well documented (Akhtar, 1998), fewer groups have reported the use of liposomes for the delivery of ribozymes. Thierry & Tackle (1995) reported the successful delivery of ribozymes via liposomes which had been prepared by a newly developed method termed the minimal volume entrapment (MVE) method. A ribozyme encapsulated within the MVE-prepared liposome formulation demonstrated increased resistance to serum ribonuclease, remaining stable for at least 24 hours in heat-inactivated foetal calf serum while the free ribozyme degraded within 5 minutes. In addition, cellular association of the ribozyme increased to 1.5% of the added dose after 24 hours. They did not, however, compare this level of association to free ribozyme and did not attempt to determine how must of the associated ribozyme was actually internalised.

Cationic liposomes appear to have been the most successful liposome-mediated delivery vehicle in facilitating delivery of synthetic ribozymes (see Table 1.1). Cationic lipids are one of the most well known microcarriers for oligonucleotide delivery; they bind to polynucleotides by virtue of their opposing charge and hydrophobic interactions (Hope *et*

al., 1998). The lipid moiety enhances cellular uptake through interaction with the plasma membrane.

Cationic liposomes have been employed to successfully deliver both *in vitro* transcribed (Sioud *et al.*, 1992; 1996; Sakamoto *et al.*, 1996; Gu *et al.*, 1997; MacKay *et al*, 1999) and chemically synthesised ribozymes into a variety of different cultured cells (Kariko *et al.*, 1994; Jarvis *et al.*, 1996; Scherr *et al.*, 1997). The effectiveness of using cationic lipids to enhance the delivery of ribozymes was clearly demonstrated in a report by Bramlage *et al.*,(1999), who studied the delivery and activity of two synthetic ribozymes targeted against luciferase mRNA in HeLa cells. Luciferase expression in cells was inhibited by 50% when the ribozymes were complexed to cationic lipids whereas the ribozymes applied without a carrier showed no inhibition. Furthermore, fluorescence microscopy using 5'-fluorescein labelled ribozymes identified ribozymes delivered with cationic liposomes localised both in the cytoplasm and the nucleus. The ribozymes that had not been delivered with the aid of a delivery vehicle were observed trapped in the cell membrane.

Cationic lipids have also been shown to facilitate ribozyme delivery *in vivo* as well as in cell culture (*ex vivo*). Cationic lipids were used to deliver synthesised ribozymes to peritoneal macrophages *in vivo* (Kisich *et al.*, 1995). Three different lipids were compared: DOTMA, DOSPA, DMRIE. The macrophages incorporated over ten times more ribozyme when delivered in conjunction with DOSPA than with the other two cationic lipids. Just recently, the same group reported specific inhibition of TNF-alpha expression *in vivo* following ribozyme treatment (Kisich *et al.*, 1999). Following inter-peritoneal injection of cationic lipid / ribozymes complexes, approximately 6% of the

administered ribozymes accumulated in target cells, macrophages. The catalytically active ribozymes suppressed TNF-alpha secretion by 50% relative to the inactive control.

An important issue when using exogenous delivery of ribozymes is the subcellular localisation of the internalised ribozyme. The exact mechanism by which nucleic acid – cationic lipid complexes enter the cell is not well understood. It was originally assumed that cationic lipid-ribozyme complexes fuse to the cell membrane leading to the ribozyme being directly transported to the cytoplasm (Bennett, 1995). However, more recent evidence suggests that they are in fact internalised by endocytosis (see reviews by Lappalainen *et al.*, 1997; Zabner, 1997; Hope *et al.*, 1998). Consequently, ribozymes may become trapped within endosomes, unable to reach target mRNA. DOTAP (Dioleoyl trimethyl-ammonium propane)-mediated transfection of a fluorescently labelled ribozyme resulted in a distinct punctate distribution in human MT-2 cells, a HTLV-I infected T lymphoblast line, representative of ribozyme entrapment in endosomal vesicles (Heidenreich *et al.*, 1996b). Similar findings were reported in which ribozymes once again complexed with DOTAP (Lange *et al.*, 1994) and also with ribozymes complexed to Lipofectin™ (Kariko *et al.*, 1994). Furthermore, lipid formulation can affect subcellular distribution. Konopka *et al.*, (1998) investigated the cationic liposome-mediated intracellular delivery of a fluorescein-labelled chimeric DNA-RNA ribozyme in different cell lines and observed different fluorescent patterns when the cells were exposed to LipofectAMINE™, Lipofectin™ or DMRIE:DOPE (1:1). With LipofectAMINE™ intense cell-associated fluorescence was found. Incubation with Lipofectin™ resulted in less intense diffuse fluorescence while with DMRIE:DOPE (1:1) an intense but sporadic fluorescence was observed. Such differences could be accounted for by differences in different charge ratios (see section 4.3.3.3). Consequently, the

efficiency of ribozyme delivery may differ with various cationic liposome formulations and careful optimisation is required for each cell line.

A variation of the use of cationic lipids to enhance ribozyme delivery was demonstrated when cationic liposomes were fused to the haemagglutinating virus of Japan (HVJ) (Kitajima *et al.*, 1997). Cellular uptake of ribozymes complexed with HVJ-cationic liposomes was 15-20 times higher than uptake of naked ribozyme. The complexes promoted accumulation of ribozymes in the cytoplasm and accelerated transport to the nucleus. Target protein (HTLV-1 Tax) levels were reduced by approximately 95% by the active ribozyme while an antisense effect of about 20% was observed with inactive ribozyme and antisense oligonucleotides.

It must be noted, however, that two restrictions must be born in mind when conducting efficacy studies using cationic lipids. Firstly cationic lipids are toxic to the cells at high concentrations and consequently a toxicity profile of the cationic lipid/ribozyme complex must be established prior to efficacy studies. Such toxicity problems may be compounded where repeated administration of ribozyme is required (Bennett, 1995). Secondly, cationic lipids are, in general, ineffective in the presence of serum proteins which may limit their application to *ex vivo* culture studies (Akhtar, 1998). A serum-resistant cationic lipid preparation, cytofectin, has been developed however, which reportedly enhances the delivery of nucleic acids in the presence of serum (Lewis *et al.*, 1996). In addition, enhanced nucleic acid delivery to cells using a cationic amphiphile containing cholic acid moieties linked via alkylamino side chains has recently been reported (DeLong *et al.*, 1999). The alkylamino side chains provide a handle for binding to nucleic acids while the cholic acid moieties interact with the lipid bilayer. This novel delivery vehicle produced a 250-fold enhancement of ODN association with cells, with fluorescent microscopy

fluorescent microscopy showing nuclear accumulation of the fluorescently tagged ODN. These amphiphiles showed substantial delivery activity even in the presence of high concentrations of serum.

Another strategy to enhance delivery of ribozymes is complex formation with receptor ligand glycoproteins in an attempt to hijack naturally efficient receptor mediated endocytic systems (Akhtar, 1998). Ribozyme delivery was increased 7-10 fold when ribozymes were delivered to leukaemia cells (which possess a large number of folate receptors) using folate-conjugated polylysine (Leopold *et al.*, 1995). A greater reduction in target mRNA levels was also evident (see section 1.5). A similar approach was used by Kilpatrick *et al.*,(1996) who complexed a fibrillin-1 (FBN-1)-specific ribozyme with transferrin and polylysine to deliver the ribozymes into cultured dermal fibroblasts. The complex was taken up into cells and efficiently reduced both cellular FBN-1 mRNA and deposition of fibrillin in the extracellular matrix. More recently, the cellular delivery of a 2'-O-methyl modified ribozyme to A431 tumour cells was enhanced three-fold by conjugating the ribozyme to a transferrin receptor antibody (Hudson *et al.*, 1999).

One approach of ribozyme delivery is to create a delivery vehicle which is capable of a controlled release at the site of administration. Such *in vivo* delivery of synthetic ribozymes was achieved for topical, ocular delivery using polyacrylic acid, a controlled release polymer (Ayers *et al.*, 1996). Polyacrylic acid has the unique property of being a liquid at pH 5 and a gel at pH 7. Permeation of cations into the gel polymer collapses the gel back into liquid. The ribozyme / polymer formulation is therefore administered as a gel. The ribozyme is then released since cations in the tear fluid and secretion from the corneal epithelial cells collapse the gel to a liquid thus releasing the ribozyme. A 2'-O-methyl chimeric ribozyme administered in this manner remained stable in the presence of

the polymer, retained its catalytic activity and enhanced retention of the ribozyme by 5-10 fold when compared to treatment with ribozyme alone. After a 30-minute period, the ribozyme had penetrated into the lower area of the epithelium layer and into the stromal layer. These findings show that synthetic ribozymes can be maintained at a level within tissues by local administration. The use of a controlled-release polymer has also been demonstrated by Hudson *et al.*, (1996). Synthetic hammerhead ribozymes were successfully incorporated into biodegradable poly L-lactic acid polymer films. Using this method, biological stability of ribozymes was significantly improved without affecting catalytic activity and a sustained release profile *in vitro* was documented.

Table 1.1 *Selected examples of delivery strategies for pre-synthesised ribozymes*

STRATEGY	REFERENCES
A. Receptor targeted delivery	
i) Transferrin	Hudson *et al.*, 1999; Kilpatrick *et al.*, 1996
ii) Folate	Leopald *et al.*, 1995
B. Liposomal mediated delivery	
i) MVE-prepared liposomes	Thierry and Tackle, 1995
ii) Cationic liposomes	
In vitro transcribed ribozymes	Sioud *et al.*, 1992, 1996; Sakamoto *et al.*, 1996; Gu *et al.*, 1997; MacKay *et al.*, 1999; Kisich *et al*,1999.
Chemically synthesised ribozymes	Kariko *et al.*, 1994; Lange *et al*, 1994; Heidenreich *et al.*, 1996b; Jarvis *et al.*, 1996; Scherr *et al.*, 1997; Konopka *et al.*, 1998; Masuda *et al.*, 1998; Bramlage *et al.*, 1999
iii) HVJ-cationic liposomes	Kitajima *et al.*, 1997
C. Biodegradable polymer devices	
i) Polyacrylic acid polymer	Ayers *et al.*, 1996
ii) Thin polymer films (Poly (L-lactic acid))	Hudson *et al.*, 1996

In general the exogenous delivery of ribozymes is still in its infancy, however, the strategies described above, and summarised in Table 1.1, have proved promising. Much

research still remains to be done, however, before an optimal exogenous delivery system for synthetic ribozymes is achieved

1.4.2.3 *Pharmacokinetics of Exogenous Ribozymes*

At present, very little has been reported with respect to pharmacokinetics and pharmacodynamics for synthetic ribozymes in animal model systems. In one study a synthetic 2'-O-allyl modified ribozyme, designed to cleave the mRNA of cytochrome P-450 3A2, was administered to rats via 0.25mg intravenous injections to investigate the pharmacokinetic properties of this ribozyme (Desjardins *et al.*, 1996). The chemically modified ribozyme was detected intact in the plasma up to 48 hours after injection. A biphasic plasma clearance with a distribution half-life of 12 minutes and an elimination half-life of 6.4 hours was observed. In addition, tissue distribution of the ribozyme was observed not only in the liver and kidney but also in the brain.

More recently, the pharmacokinetics of another chemically modified ribozyme was monitored in the mouse (Sandberg *et al.*, 1999). This 2'-O-methyl modified ribozyme, targeted against the vascular endothelial growth factor (VEGF) and termed ANGIOZYME, was administered as an intravenous (i.v.), intraperitoneal (i.p.) or subcutaneous (s.c.) injection. The ribozyme was well absorbed by either i.p. (90%) or s.c (77%) administration. The highest concentrations of angiozyme were detected in the kidney and femur with all three routes, although ribozyme was also detected in the lungs (s.c; i.p) and the liver (i.p). These findings indicate that extra-vascular injections (either i.p or s.c.) may be the most efficacious route of administration for chemically modified ribozymes, although further studies are required in this field to corroborate these findings.

1.5 THERAPEUTIC APPLICATIONS OF RIBOZYMES

Various successful applications of ribozymes for the inhibition of gene expression have been demonstrated (for reviews see: James and Gibson, 1998; Rossi, 1998; Armarzguioui and Prydz, 1999; Gaughan and Whitehead, 1999; Macpherson *et al.*, 1999). Ribozymes have been shown to effectively inhibit gene expression against a great many undesirable target genes although particular emphasis has been on the development of ribozyme based inhibition of HIV-1 and cancer oncogenes.

To date, most of the demonstrations of ribozyme efficacy have been carried out using expression vectors to deliver ribozymes into cells (endogenous delivery). In fact the first clinical trials using ribozymes as potential therapeutic agents have involved the endogenous expression of ribozymes targeted against the human immunodeficiency retrovirus type 1 (HIV-1). Retroviruses, such as HIV, induce cellular changes by reverse transcription followed by insertion into the host cell genome. Viral genes are then expressed along with host cellular genes, and viral proteins are produced. Consequently, ribozymes targeted against retroviral RNA would destroy RNA before reverse transcription. They also offer the potential for simultaneously targeting multiple sites along the viral genome to combat drug resistance. At present phase I / IIa clinical trials are in process, undertaken by several groups involving both the expression of hammerhead (Rossi 1998; Macpherson *et al.*, 1999) and hairpin ribozymes (Wong-Staal *et al.*, 1998). These trials involve retroviral-mediated transduction of anti-HIV ribozyme genes into either T-lymphocytes or stem blood cells expressing the $CD34^{+}$ antigen, isolated from the peripheral blood. Thus far these trials have utilised *ex vivo* transduction of cells with the viral vectors and subsequent reintroduction into patient. This rapid progress of ribozyme to clinic can be attributed in part to their great specificity which

minimises toxicity, this coupled with the fact that the ribozyme genes can be delivered by viral vectors directly to the target cells has hastened their pace to clinical trial (Rossi, 1998).

This report is, however, mainly focused upon the therapeutic applications of exogenously delivered chemically stabilised ribozymes. In the light of the recent advances in the development of nuclease stable synthetic ribozymes (section 1.3) and appropriate delivery systems (section 1.4.2.2), a number of investigators have reported ribozyme-mediated inhibition of gene expression using exogenous delivery of pre-synthesised ribozymes.

1.5.1 Cancer Related Applications

An exciting potential of ribozymes is the possibility of inactivating genes for treating neoplastic disorders. Ribozymes have the capability to distinguish RNA transcripts which differ from the wild type by only one nucleotide. Consequently, the opportunity exists to eliminate the transcript resulting from the mutated gene, while leaving the wild type transcript intact. In the area of cancer research, synthetic ribozymes have been reported to inhibit mutant gene expression in this way.

Chronic myelogenous leukaemia (CML) is an ideal candidate for ribozyme therapy. CML is a disorder of haematopoietic stem cells associated with the Philadelphia chromosome, the result of a chromosome translocation between chromosomes 22 and 9 that brings the *bcr* gene (on 22) into juxtaposition with the *abl* gene(on 9). This generates a *bcr / abl* chimeric gene which encodes a novel tyrosine kinase of 210-kDa (p210) with

transforming activity unique to the malignant phenotype. Specific targeting of the fusion gene by ribozymes should therefore spare wild type genes in normal cells while destroying the mutant genes in leukaemia cells. Specificity is essential, however, since both normal and CML cells have the same mRNA sequences, although in CML cells the order of the two sequences is altered (James *et al.*, 1996). Several groups have demonstrated the efficacy of exogenously delivered synthetic ribozymes targeting *bcr / abl* mRNA (see Table 1.2).

Lange *et al.* (1994) delivered ribozymes, synthesised enzymatically, with the lipofection agent DOTAP to the CML cell line K562, which carries this fusion gene. Treatment with the ribozyme produced up to five-fold reduction in *bcr / abl* mRNA. In addition, proliferation of the cells reduced by about 60% after 72 hours compared to cells treated with the transfection agent alone. Antisense and sense RNA controls also significantly inhibited cell proliferation however, reducing cell numbers by up to 35%. This casts some doubt on the specificity of the ribozyme. Furthermore, wild type *abl* and *bcr* controls were not used in order to confirm specificity.

Using a chemically modified chimeric DNA-RNA ribozyme, Snyder *et al.* (1993) demonstrated the *in vitro* potential of ribozymes directed against the *bcr / abl* transcript. Transfection of CML cells with these chimeric ribozymes also resulted in a significant reduction of *bcr / abl* mRNA and p210 protein expression. This effect on *bcr / abl* gene expression resulted in a significant decrease in the proliferative capacity of the cells. By comparison an unrelated ribozyme had very little effect.

By applying a slightly different strategy, Leopold *et al.* (1995) synthesised a transcript that contained three ribozymes directed against three contiguous sites near the *bcr / abl*

junction. This resulted in enhanced cleavage activity against the target mRNA relative to single ribozyme constructs. The specificity of this transcript, however, came into doubt when it was observed that the multiple ribozyme was also capable of cleaving the wild type *bcr* and *abl* mRNA substrates.

The effect on animal model systems was addressed by Mills *et al.* (1996) who have been examining the effect of *ex vivo* purging of a murine cell line containing the *bcr / abl* oncogene with anti-*bcr / abl* ribozymes before injection into SCID mice. Effectiveness of the ribozyme was demonstrated by increased survival of the mice when compared with mice injected with control ribozymes (James and Gibson, 1998).

The growth and differentiation of a cell depends upon a number of signal transduction pathways. Proteins encoded by *ras* genes (H-*ras*, N-*ras* and K-*ras*) are involved in these pathways. Mutant *ras* proteins stimulate growth or differentiation autonomously and such oncogenes have been detected in a wide variety of tumours such as pancreatic carcinomas and tumours of the stomach and breast (see Alberts *et al.*, 1989). A recent study investigated the effectiveness of a 2'-O-allyl modified ribozyme targeted against mutated Ki-ras mRNA in a pancreatic carcinoma cell line CFPAC-1 (Giannini *et al.*, 1999). The active anti-Ki-ras ribozyme was found to be at least 2-fold more potent in decreasing cellular Ki-ras mRNA levels and in inhibiting cell proliferation than a catalytically inactive ribozyme although some antisense effect was observed.

Successful cancer therapy may be impeded by formation of gene products in neoplastic cells which confer drug resistance. For example, the phosphoglycoprotein, P-GP, is associated with multiple drug resistance as it acts as a drug efflux pump (for review see

Endicott and Ling, 1989). The development of hammerhead ribozymes directed against the MDR-1 transcript, which encodes for P-GP, has been a goal of many investigators.

Kiehntopf *et al.* (1994) designed a synthetic MDR-1 directed and chemically modified DNA-RNA ribozyme which was capable of greater than 98% delivery by liposome mediated transfer into highly drug resistant mesothelioma cells. These nuclease resistant ribozymes were able to almost eliminate MDR-1 expression, resulting in 93% loss of P-GP surface expression. In addition, increased chemosensitivity towards the anti-neoplastic drugs, doxorubicin and vindesine was achieved. Control experiments using active and inactive all RNA ribozymes showed no effect. However, specificity of action can not be confirmed, since neither an inactivated modified ribozyme nor a modified ribozyme with scrambled arm sequence were used.

The importance of choosing the correct delivery vehicle for each cell line was also illustrated in a recent study (Masuda *et al.*, 1998). A synthetic ribozyme targeted against codon 196 of MDR-1 mRNA was delivered, complexed with the cationic lipid DOTAP, to MCF-7/R and MOLT-3/TMQ800 human cell lines. Treatment with the ribozyme caused significant decreases in both MDR-1 mRNA and P-glycoprotein expression levels in the breast cancer line MCF-7/R, resulting in reversal of vincristine resistance. No effect, however, was evident in MOLT-3/TMQ800 cells. Confocal microscopy imaging of fluorescently labelled ribozyme showed that while cytoplasmic fluorescence was clearly evident in MCF-7/R cells, no fluorescence was detected in the MOLT-3/TMQ800 cell line.

1.5.2 Applications in Treating Immunological Disorders

The overproduction of the cytokine, Tumour Necrosis Factor-α (TNF-α), is associated with inflammatory and auto-immune diseases such as rheumatoid arthritis (Kisich *et al.*, 1999). TNF-α, therefore, represents a suitable target for ribozyme-mediated treatment of such disorders.

One of the early reports of exogenously delivered ribozymes involved a hammerhead ribozyme targeted against the cytokine, tumour necrosis factor-α (TNF-α) (Sioud *et al.*, 1992). Treatment of human promyelocytic leukaemia cells (HL60 cell line) with this ribozyme, delivered complexed to Lipofectin™, reduced TNF-α mRNA levels by 80-90% and reduced secretion of TNF-α protein by 70-85%. A comparable antisense construct reduced TNF-α mRNA and protein but to a lesser degree. In subsequent studies, intraperitoneal injection in mice of *in vitro* transcribed anti-TNF-α ribozymes in complex with cationic liposomes was employed to reduce TNF-α levels following stimulation by lipopolysaccharide (Sioud, 1996). Up to 50% reduction in TNF-α protein secretion was achieved following a single injection of 10 nanomoles of ribozyme. The control animals, however, were dosed with an *E.Coli* tRNA rather than inactive and scrambled ribozyme constructs. Consequently, the mechanism and specificity of action of this ribozyme is not confirmed.

Ribozymes targeting murine TNF-α have also been shown to specifically inhibit TNF-α secretion by primary macrophages (Kisich *et al.*, 1995). Ribozymes were transcribed *in vitro* and applied with cationic lipids to isolated murine peritoneal macrophages. The active ribozyme inhibited TNF-α expression and secretion by 85%, while an inactive ribozyme inhibited secretion by only 45%. In addition, ribozymes with different binding

arms failed to significantly inhibit TNF-α secretion, thus confirming the specificity of ribozyme mediated inhibition. Successful ribozyme mediated inhibition has now been demonstrated *in vivo* (Kisich *et al.*, 1999). Following intraperitoneal injection of cationic lipid / ribozyme complexes, the catalytically active ribozyme suppressed TNF-α secretion by approximately 50% relative to an inactive ribozyme control without inhibiting secretion of another pro-inflammatory cytokine produced by macrophages, IL-1α.

1.5.3 Other Therapeutic Applications

Other *ex vivo* studies have demonstrated the efficacy of exogenously delivered, pre-synthesised ribozymes. Chemically synthesised and stabilised ribozymes were shown to reduce *c-myb* levels by approximately 80% in a variety of smooth muscle cells, resulting in a significant reduction in cell proliferation (Jarvis *et al.*, 1996). Inactive ribozymes or ribozymes with scrambled binding arm sequences had little effect on cell growth nor indeed did ribozymes which had not been modified. These findings demonstrate that inhibition of cell proliferation was sequence specific and required a nuclease stable catalytic core capable of cleaving the target mRNA.

To date, there are few reports of *in vivo* efficacy using synthetic chemically modified ribozymes. Surprisingly, ribozyme mediated inhibition has been demonstrated using exogenously administered ribozymes delivered without the aid of a delivery vehicle. Flory *et al.* (1996) utilised the rabbit model of interleukin 1-induced arthritis to assess the localisation, stability and efficacy of exogenous anti-stromelysin hammerhead ribozymes. 2'-O-methyl / 2'-C-allyl chemically modified synthetic ribozymes, directed against the mRNA encoding stromelysin, were injected in the absence of a delivery agent into the

synovial tissue of rabbit knees 24 hours prior to stimulation of stromelysin synthesis by human interleukin-1α (IL-1α). The ribozymes were taken up by cells in the synovial lining and remained stable in the synovium, with 80-90% of the administered ribozyme remaining intact 24 hours post-injection and trace quantities even detected 7 days after the injection. A dose of 100μg per knee joint caused a 60% reduction of stromelysin mRNA while no significant inhibition was observed by an inactive ribozyme control or with control ribozyme containing scrambled arms.

Sproat and colleagues developed a chemically modified ribozyme that eliminated amelogenin, the major translation product in developing mouse enamel (Lyngstadaas *et al.*, 1995). The ribozymes, designed to target amelogenin mRNA, were injected close to developing mandibular molar teeth in newborn mice, without the aid of any carriers to assist cellular uptake. A prolonged and specific arrest of amelogenin synthesis was observed with no apparent toxicity. Synthesis of amelogenin was inhibited by at least 90% up to 48 hours after injection of 50μg of ribozyme and did not recover completely until 96 hours post-injection. The effect of the injected ribozyme was considered specific as mutated ribozyme and antisense oligonucleotide controls had limited or no effect on amelogenin levels.

These two examples show that for disease in which local or *ex vivo* application is possible, direct delivery of chemically stabilised ribozymes may be sufficient (Usman and Stinchcomb, 1996).

Very recently, it has been announced that Phase 1a and 1b human clinical trails have successfully been completed on the first chemically synthesised ribozyme to be studied in human clinical trials (RPI. press release, July 1999). This ribozyme, termed

ANGIOZYME, is directed against the vascular endothelial growth factor (VEGF) receptors Flt-1 and KDR that regulate the growth of new blood vessels (angiogenesis) responsible for nourishing malignant tumours. Specific ribozyme mediated inhibition of this target has been shown in pre-clinical trials to prevent angiogenesis and the growth and spread of metastases (Parry *et al.*, 1999). During these trials single doses as high as 300 mg/m^2 were administered with no significant toxicity observed. Phase II clinical trials are planned for later on this year.

Overall, the demonstrations of ribozyme-mediated inhibition of gene expression highlighted in the above section and summarised in Table 1.2, clearly show that exogenously delivered synthetic ribozymes can be highly effective both *ex vivo* and *in vivo* and are as such most promising potential candidates for use as sequence-specific therapeutic agents. Care must be taken, however, in selecting suitable controls to demonstrate specific ribozyme cleavage. As a minimum, a catalytically inactive ribozyme control is required to show antisense effects and an active but unrelated ribozyme, possibly with scrambled arm sequences, is required to show specificity for the target mRNA together with a transfection agent only control if appropriate (James and Gibson, 1998).

Table 1.2. *Examples of specific gene inhibition using exogenously delivered ribozymes*

Appli-cation	Genetic Target	Ribozyme type/ delivery method	Cell line / animal model	Effects / comments (also see text)	Reference
Cancer	*bcr /abl* mRNA	DNA-RNA chimeric ribozyme / Cationic lipid (Transfectam™)	Human chronic myelogenous leukaemia (CML) cell line EM-2	50% decrease in *bcr /abl* mRNA. 84% decrease in cell proliferation after 72 hours.	Snyder *et al.*, 1993.
	bcr /abl mRNA	Unmodified all RNA ribozyme / Cationic lipid (DOTAP)	Human CML cell line K562	5-fold reduction in *bcr/abl* mRNA. 60% reduction in cell proliferation after 72 hours.	Lange *et al.*, 1994
	bcr/abl mRNA	Unmodified all RNA ribozyme / folic acid - polylysine carrier	Transformed 32D murine myeoblastoma cells	Decrease in *bcr /abl* mRNA after 24 hours by 1000-fold.	Leopald *et al.*, 1995
	bcr/abl mRNA	DNA-RNA chimeric ribozyme / LipofectAMINE™	32Db3a2 in SCID mice	Increased survival of SCID mice after injection with ribozyme treated 32Db3a2 cell.	Mills *et al.*, 1996
	Ki-ras mRNA	2'-O-allyl modified ribozyme	Human pancreatic adenocarcinoma cell line CFPAC-1	2-fold decrease in Ki-ras mRNA levels. Inhibition of cell proliferation.	Giannini *et al.*, 1999.
	MDR-1 mRNA	Chimeric DNA / RNA / 2'-fluoro modified ribozyme / Lipofectin™.	Drug resistant mesothelioma cell line PXF118	93% inhibition of P-GP protein expression. Increased chemosensitivity.	Kiehntopf *et al.*, 1994
	MDR-1 mRNA	DNA-RNA chimeric ribozyme / cationic lipid (DOTAP)	Drug resistant human breast cancer cells MCF-7/R	Reversal of Vincristine resistance and reduced levels of MDR-1mRNA and P-GP expression.	Masuda *et al.*, 1998
Immuno-logical disorders	Tumour Necrosis Factor alpha (TNF-∝)	All RNA ribozyme. i.p. injection of ribozyme / Lipofectin™ complex	BALB/c mice	50% reduction in TNF-∝ protein secretion.	Sioud, 1996
	Tumour Necrosis Factor alpha (TNF-∝)	All RNA ribozyme. i.p.injection of LipofectAMINE™ / ribozyme complex	Isolated murine peritoneal macrophages /Mice	TNF- ∝ protein secretion reduced by 85% in cell culture. *In vivo*, TNF-∝secretion inhibited by ~50%.	Kisich *et al.*, 1995 and 1999.
Other appli-cations	*c-myb*	2'-O-methyl / 2'-C-allyl modified ribozyme / LipofectAMINE™	Rat aortic smooth muscle cells	~80% reduction in *c-myb* mRNA. Significant (~70%) inhibition of cell proliferation	Jarvis *et al.*, 1996

Table 1.2 (continued)

Appli-cation	Genetic Target	Ribozyme type / delivery method	Cell line / animal model	Effects / comments (also see text)	Reference
Other appli-cations (cont)	Stromelysin mRNA	2'-O-methyl / 2'-amino modified ribozyme. Direct injection to the knee joint. No delivery agent.	New Zealand male white rabbits	60% reduction in stromelysin mRNA after 30 hours.	Flory *et al.*, 1996
	Amelogenin mRNA.	2'-O-allyl modified ribozyme. Direct sub-mandibular injection. No delivery agent	New-born BALB/c mice	At least 90% eradication of amelogenin synthesis for up to 48 hours.	Lyng-stadaas *et al.*, 1995.
	Vascular endothelial growth factor (VEGF) receptor	2'-O-methyl modified ribozyme. Human trials involved s.c, i.p and i.v administration	Human vascular endothelial cells/ Rat animal model / HUMAN CLINICAL TRIALS PHASE I	Significant reduction of proliferation in cell culture and animal models (anti-tumour effects). No significant drug related toxicity evident in clinical trials.	Parry *et al.*, 1999. Sandberg *et al*, 1999. RPI. Press release, July, 1999.

1.6 GLIOBLASTOMA MULTIFORME

Gliomas are the most common primary tumours arising from the brain, in fact each year malignant gliomas account for approximately 2.5% of the deaths from cancer (Bruner, 1994). These gliomas are morphologically and biologically heterogeneous and include neoplasms derived from several cell types. Astrocytomas form the largest single group among the primary tumours (75-90%) which also include oligodendrogliomas, ependymomas and mixed gliomas (Steinmetz and Schackert, 1996). Distinct histological features allow astrocytomas to be graded into levels of anaplasia, the most widely used today involves a three tiered grading system (Ringertz, 1950) dividing astrocytomas into

low-grade astrocytomas (Grade II), anaplastic astrocytomas (grade III) and glioblastomas (grade IV).

The most malignant and frequently occurring form, glioblastoma multiforme (GBM), accounts for approximately one third of all primary brain tumours (Wong *et al.*, 1994). This tumour is so undifferentiated that its cell of origin remains obscure; however, most examples are generally thought to arise from astrocytes because glial fibrillary acidic protein (GFAP), a histological marker for astrocytes, can be identified in the cell cytoplasm (Kurpad *et al.*, 1995). The histological morphology of glioblastoma can be highly variable, confirming the name "multiforme".

The characteristic feature of glioblastoma multiforme is tumour necrosis. The individual cells may be small with a high nuclear / cytoplasmic ratio or very large and bizarre with abundant eosinophilic cytoplasm. The small cells are the more proliferative ones and show a more aggressive course. These cells often appear to condense around areas of tumour necrosis forming characteristic 'pseudopalisades". They also have the propensity to infiltrate the brain extensively, giving the appearance of multifocal gliomas (Furnari *et al.*, 1995).

Despite advances in many areas of cancer research and treatment, glioblastoma multiforme almost always proves fatal, with a median survival rate of less than one year and a 5 year survival rate of 5.5% or less (Martuza *et al.*, 1991). At present, no therapeutic modality has substantially changed the outcome of patients with glioblastoma. Characteristics of this type of tumour, including its invasive nature, its ability to spread locally and distantly while avoiding recognition by the immune system, its relative resistance to radiation and a high local recurrence rate, limit the success of

conventional therapy. The effective treatment of glioblastoma multiforme, therefore, presents a tremendous challenge.

The current methods of treatment used in the management of malignant gliomas involve a combination of surgery, radiotherapy and chemotherapy. The cornerstone of therapy for glioblastoma multiforme tumours has been surgery. The use of microsurgical techniques makes the surgical procedure safe and accurate (Chamberlain and Kormanik, 1998). However, although surgery does improve the mean survival time of patients with glioblastoma multiforme to a limited degree (by a matter of months), it rarely provides a permanent cure (Alexander and Loeffler, 1998).

Malignant gliomas such as glioblastoma multiforme exhibit an extraordinary resistance to radiotherapy and as a consequence the effectiveness of this form of treatment is limited. The sensitivity of the surrounding, unaffected, brain limits the dose that can safely be delivered to 60 greys, which is well below the level required to completely eradicate the primary tumour in the majority of patients (Chamberlain and Kormanik, 1998).

Chemotherapy has been shown to be effective adjuncts to surgery and radiotherapy in the treatment of cancer. Unfortunately, however, adjuvant chemotherapy has only had a limited impact on the survival of patients with high-grade astrocytomas, improving the mean survival duration by a matter of months of only a quarter of patients with GBM (Chamberlain and Kormanik, 1998). Generally, the relatively lipid soluble and non-ionized nitrosourea drugs, such as carmustine, lomustine, and vincristine have proved to be the most active chemotherapy agents for treating malignant astrocytomas (Lesser & Grossman, 1994). New drugs continue to enter clinical trials for use on patients with glioblastoma; none so far, however, have substantially prolonged a patient's life span (for

reviews see Shapiro and Shapiro, 1998). A combination of physiological factors such as the blood brain barrier, heterogeneous and resistant tumour cell populations and unacceptable toxicity have limited the efficacy of these agents.

Advances in the understanding of the molecular basis of cancer has now made it possible to design molecules that specifically interact with cancer cells. The most promising modes of therapy for the treatment of GBM, therefore, may lie with molecular based technologies which employ genetic interventions to alter the properties or behaviour of specific cells. Many detailed cytogenetic studies have been performed on malignant gliomas and these reveal commonly occurring abnormalities (see Furnari *et al.*, 1995; Louis and Gusella, 1995; Feldkamp *et al.*, 1997; Rasheed *et al*, 1999 for reviews.). Such studies are now beginning to indicate the existence of several genetic pathways leading to the development of glioblastoma multiforme (see Figure 1.9).

Although glioblastomas are pathologically heterogenous, they arise from a single cell whose end point in transformation is usually marked by the loss of tumour suppressor genes on chromosome 10 (Rasheed *et al.*, 1999). Loss of chromosome 10 occurs in 86% of GBMs with most cases showing allelic loss of the entire chromosome (Luois and Gusella, 1995). The development of this final malignant state can occur in two ways.

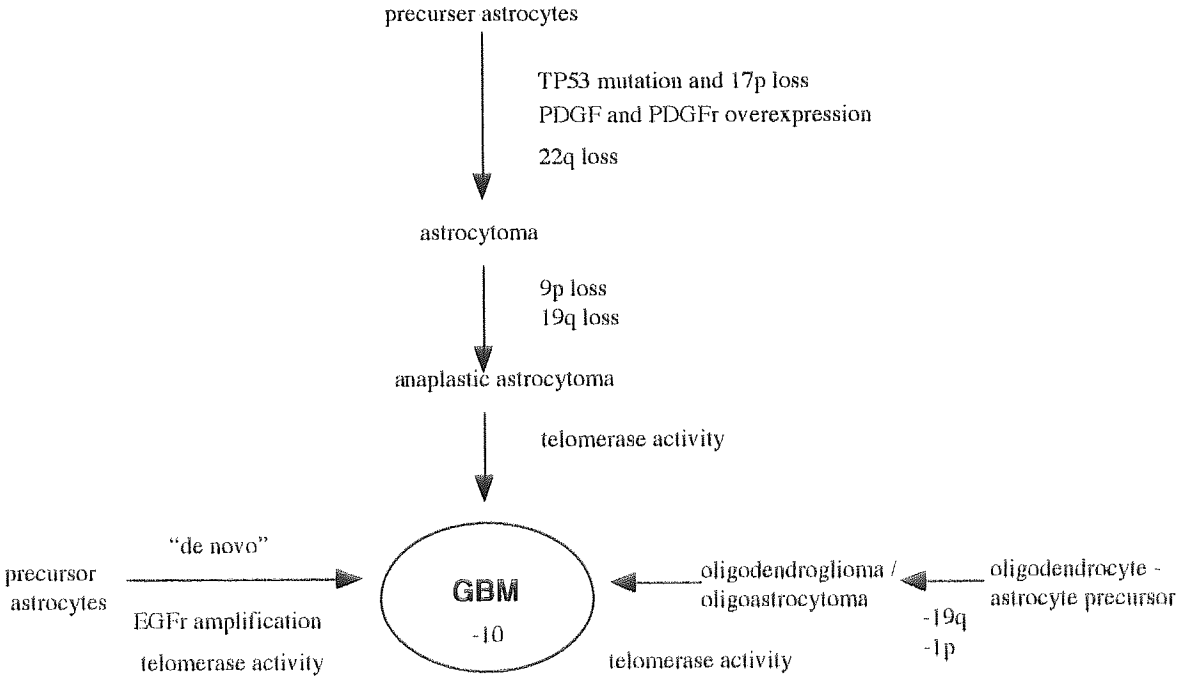

Figure 1.9 *Possible genetic pathways leading to glioblastoma multiforme (adapted from Furnari et al., 1995)*

Firstly, GBM tumours may arise by progression from lower grade gliomas such as astrocytomas. Inactivation of the *p*53 tumour suppressor gene, activation of the platelet-derived growth factor (PDGF) system and loss of a tumour suppressor gene on chromosome 22q are all alterations associated with this pathway. The *p*53 gene on chromosome 17p encodes a protein *p*53 which has an integral role in a number of cellular processes including cell cycle arrest and apoptosis. Inactivation of this gene, usually by mutation of one copy and chromosomal loss of the remaining allele, occurs in 50-80% of all GBM cases (Rasheed *et al.*, 1999).

Malignant progression "de novo' from normal glial cells is associated with the inactivation of putative tumour suppressor genes on chromosome 10 and amplification of the epidermal growth factor receptor (EGFr) gene (*c-erb*-B1). The EGFr gene is

amplified or overexpressed in at least 40% of glioblastomas (Shapiro and Shapiro, 1998). Overexpression of EGFr is often accompanied by the co-expression of growth factor ligands, suggesting an autocrine stimulatory loop by which tumour cells can escape normal physiological control (Modjtahedi and Dean, 1994). Those GBMs that exhibit EGFr gene amplification always show chromosome 10 losses, implying that inactivation of a chromosome 10 gene most probably precedes EGFr amplification. Interestingly, EGFr gene amplification almost never occurs in GBMs with *p*53 mutation or loss of chromosome 17p suggesting an independent pathway.

Recently telomerase, a ribonucleoprotein that directs the synthesis of new telomeric DNA repeats (see section 4.1), has been implicated in cell immortalisation and tumour progression. Over the past few years a number of studies have shown that telomerase is expressed and active in most brain tumours while being reportedly rare in benign tumours (Kim *et al.*, 1994; Langford *et al.*, 1996; Sano *et al.*, 1997; Le *et al.*, 1998; Falchetti *et al.*, 1999). One study revealed that the neoplastic progression of these malignant brain tumours is dependent upon telomerase activity (Blasco *et al.*, 1996). While expression of the RNA component of telomerase increased progressively in pre-neoplastic and early stage tumours, telomerase activity was observed only in late stage tumours. Such findings are supported in a study by Falchetti *et al.*, (1999) who when studying telomerase activity in 98 brain tumours reported a high degree of positivity for telomerase activity in glioblastomas while activity was poorly detected in anaplastic astrocytomas.

Consequently, therapeutic strategies that can be specifically directed to inhibit the expression of molecular targets such as EGFr and telomerase, in order to arrest tumour progression, offer considerable promise as potential anti-cancer agents in the treatment of GBM.

1.7 AIMS

The overall aim of this research was to investigate the biological properties of chemically synthesised hammerhead ribozymes in terms of their uptake, stability and biological activity, in order to assess their potential use as novel anti-brain tumour agents. Specific objectives addressed to achieve this aim were:

1. To characterise the stability, activity and cellular uptake properties of chemically modified hammerhead ribozymes.

For ribozymes to be of use as therapeutic agents they need to be both stable and active in the biological milieu. Factors that might limit the activity of ribozymes include the rate of degradation, their catalytic efficiency and the extent and mechanism by which they are taken into cells. Initial studies were therefore performed to characterise the stability, *in vitro* activity and cellular uptake properties of synthesised hammerhead ribozymes containing site-specific modifications introduced to enhance nuclease stability (Chapter Three).

2. To develop nuclease-resistant, synthetic ribozymes for down regulating the c-erbB1 gene (which encodes the epidermal growth factor receptor) and to investigate the biological activity of these ribozymes

The over-expression of EGFr is frequently associated with malignant gliomas (see section 1.6 and 4.1.1). Studies were undertaken to design and develop nuclease resistant, synthetic ribozymes to cleave target sites within the human EGFr mRNA molecule. The

biological efficacy of these ribozymes was then investigated both *in vitro* and in human cell culture models (Chapter Four).

3. To investigate the efficacy of chemically modified ribozymes directed to other molecular targets associated with the progression of glioblastoma multiforme.

Recent evidence suggests that telomerase activity is also implicated in tumour progression (section 1.6 and 5.1.1). Research was undertaken to design and develop a biologically stable ribozyme to cleave the RNA component of telomerase. The potential use of this ribozyme to inhibit telomerase activity was evaluated *in vitro* and *ex vivo* (Chapter Five).

CHAPTER TWO

GENERAL MATERIALS AND METHODS

ABSTRACT

General materials and methods used routinely throughout experimental work are described in this chapter. Specific directions for individual experiments are given in the relevant chapters.

2.1 RNA AND DNA SYNTHESIS

2.1.1 Synthesis of Oligodeoxynucleotides (ODN)

Oligodeoxynucleotides were synthesised in both phosphodiester and phosphorothioate forms on an ABI 392 automated DNA/RNA synthesiser (Applied Biosystems, Warrington, U.K.) using standard phosphoramidite reagents (Cruachem Ltd, Glasgow, U.K.). This automated method of solid phase synthesis has been developed from the technique devised by Merrifield (1963) and has become widely used in the synthesis of oligonucleotides (Brown and Brown, 1991). Various steps are involved in this procedure (Brown and Brown, 1991), the starting point of which is the 3'-end of the oligonucleotide, where a suitably protected nucleoside derivative is attached to a controlled pore glass support via a succinate linker. Cycles of addition of nucleotide units are then carried out by removal of 5'-terminal dimethoxytrityl (DMT) protecting groups, coupling to the next nucleotide unit, capping of unreacted chains (failure products) and oxidation. The process is continued until an oligonucleotide of desired length is synthesised. The completed oligonucleotide is then cleaved from the support and protecting groups are removed by treatment with ammonia solution.

2.1.1.1 *Phosphodiester Oligodeoxynucleotides*

Phosphodiester (PO) ODNs were synthesised on a 0.2μm scale using the pre-programmed 'CE Cycle' (Cruachem Ltd, Glasgow, U.K.). Synthesised PO ODNs with 5'-trityl groups removed were automatically cleaved from the solid support with 1.5ml of concentrated ammonium hydroxide and incubated at 55°C for 8 hours to remove the

protecting groups of the exocyclic amine of deoxyadenosine, deoxycytidine and deoxyguanosine.

2.1.1.2 *Phosphorothioate Oligodeoxynucleotides*

Phosphorothioate (PS) ODNs were synthesised on a 0.2μm scale using the preprogrammed "sulfur" cycle. Phosphorothioates were introduced by use of tetraethyl disulphide (TETD) as the sulphurising reagent. The addition of TETD replaced the oxidising step. Synthesised PS-ODNs with 5'-trityl groups removed were automatically cleaved from the solid support with 1.5ml of concentrated ammonium hydroxide and incubated at 55°C for 8 hours to remove the base-protecting groups.

2.1.1.3 *Determination of Coupling Efficiency*

When dimethoxytrityl (DMT) protecting group is cleaved from a nucleotide, it exists as a cation which produces a brilliant orange colour when in acid solution. The efficiency of coupling was determined by colorimetric quantification of these trityl fractions. The trityl fractions were collected after the addition of each phosphoramidite base and diluted to 25ml with 0.1M *p*-toluene sulphonic acid in acetonitrile (19.2g in 1000ml acetonitrile). The absorbance of the fractions was then measured in a UV visible spectrophotometer (Jenway Scientific Instruments,U.K.) at 498nm and the yield determined using the following formula (Brown and Brown, 1991):

Overall % yield = last or lowest / second or highest x 100

stepwise yield = overall yield $^{(1/\text{no of couplings})}$

percentage stepwise yield (coupling efficiency) = stepwise yield x 100

The O.D. of the first trityl fraction was ignored as this represents the first base that was attached to the column. A percentage stepwise yield of between 97-99% was expected for synthesis of PO- and PS- oligodeoxynucleotides.

2.1.1.4 *Purification of Oligodeoxynucleotides*

After deprotection, the resulting oligodeoxynucleotide was purified through Sephadex G-25 packed (NAP-10) columns (Pharmacia Biotech, St.Albans, U.K.) using gravity separation for maximum product recovery. Briefly, the sephadex column was equilibrated with 15ml of sterile RNase free water (elution buffer) after which 1ml of the sample was carefully added to the column, allowing the sample to enter the gel bed completely. The purified sample was eluted into a microcentrifuge tube by adding a further 1.5ml of elution buffer to the sephadex column. The purified sample was then dried by vacuum centrifugation using a Savant DNA Speed Vac (Savant,U.K.) and stored at –20°C.

2.1.2 Synthesis of Oligoribonucleotides / Ribozymes

Oligoribonucleotide synthesis requires a combination of compatible protecting groups for the ribonucleotide 5'- and 2'- hydroxyl groups. In solid phase synthesis 5'-terminal DMT protecting groups must be selectively removed at every cycle whereas the 2'- protecting groups must remain intact throughout and finally be removed at the end of synthesis.

2.1.2.1 *Chimeric 2'-O-Methyl / 2'-Amino Modified and 2'-O-Methyl /2'- C-Allyl Modified Ribozymes*

2'-O-methyl / 2'-amino modified and 2'-O-methyl / 2'- C-allyl modified chimeric ribozymes, used in Chapters Three and Four, were synthesised at Ribozyme Pharmaceuticals Inc. (Boulder, Colorado, U.S.A) on an automated ABI 394 DNA / RNA synthesiser using phosphoramidite chemistry according to the method of Wincott *et al.* (1995). The 2'- protecting group used was 2'-O-t-butyldimethylsilyl and deprotection was performed using methylamine and anhydrous triethylamine / hydrogen fluoride in *N*-methylpyrrolidinone (TEA.HF / NMP). Synthesised ribozymes were HPLC purified.

2.1.2.2 *Chimeric 2'-O-Methyl Modified Ribozymes*

The commercial availability of 2'-O-methylribonucleoside 3'-O-phosphoramidites allowed for synthesis of chimeric 2'-O-methyl modified ribozymes, used in Chapter Five, to be synthesised at Aston University on an ABI 392 automated DNA/RNA synthesiser using phosphoramidite reagents (Cruachem Ltd, Glasgow, U.K.). The 2'- protecting group used in this case was the modified acetal 1-(2-fluorophenyl)-4-methoxypiperidin-4-yl (Fpmp). The Fpmp group is reported to be stable during the non aqueous acidic treatment to remove 5'-DMT groups but is readily removed under aqueous conditions at pH 2 (Cruachem,U.K.).

A modified programme ('Fpmp cycle') based on the solid phase phosphoramidite method of ODN synthesis and custom designed by Andrew Hudson (Aston University) in conjunction with Cruachem Ltd was used to synthesise these chimeric ribozymes. The

ribozymes were synthesised without removal of 5'-O-DMT protecting groups and were manually cleaved from the solid support and deprotected as described in section 2.1.2.4.

2.1.2.3 *Oligoribonucleotides*

Oligoribonucleotides (ORNs) were synthesised on a 0.2μm scale using the custom designed 'Fpmp' cycle. ORNs were also synthesised without removal of the 5'-O-DMT protecting groups and were manually cleaved from the solid support and deprotected (section 2.1.2.4).

2.1.2.4 *Deprotection and Purification of Oligoribonucleotides / Ribozymes*

The 5'-O-DMT-2'-O-Fpmp-oligoribonucleotides were deprotected and purified according to the instructions given in Cruachem technical Bulletin No. 010. Firstly the support bound ORNs were transferred to a microcentrifuge tube and 0.5ml of concentrated aqueous ammonia was added. After sealing with parafilm and vortexing, the tube was then incubated at 55°C overnight or at 70°C for 5 hours. Following incubation the sample was cooled, centrifuged at 3000rpm for 2 minutes and the supernatant was removed and concentrated to a pellet by vacuum centrifugation using a Savant DNA Speed-Vac. These actions cleaved the ORN from the solid support and removed all protecting groups with the exception of the terminal 5'-O-DMT and all of the 2'-O-Fpmp groups.

For removal of these remaining protecting groups, 500μl of acidic buffer (0.5M sodium acetate, pH 3.25) was added to the pellet, the tube vortexed for 2 minutes and the solution incubated at 30°C for 36 hours. The acidic solution was neutralised by adding 100μl of

neutralising buffer (3.0M Tris-base), mixing for 1 minute and then centrifuging at 10,000rpm for 3 minutes. The supernatant, now containing fully deprotected ORNs in solution was carefully transferred to a sterile microcentrifuge tube and purified by ethanol precipitation. Three times the volume of analytical grade ethanol was added and the solution was placed in a –70°C freezer for 60 minutes then centrifuged at 10,000rpm for 5 minutes. The supernatant was carefully discarded and a further 900μl of analytical grade ethanol added. The tube was vortexed thoroughly and then centrifuged at 10,000 rpm for a further 5 minutes. Once again the supernatant was discarded and the purified, deprotected ORN / ribozyme pellet dried by vacuum centrifugation.

2.1.2.5 *Precautions taken while dealing with RNA*

Once deprotected, RNA is highly susceptible to degradation by the action of 2'-hydroxyl dependent ribonucleases. These ribonucleases (RNases) are present on the surface of the skin and are often present on laboratory glassware and plasticware. Stringent aseptic handling is, therefore, required to minimise the action of these RNases and, in view of this, the following precautions were taken:

All glassware and plasticware was treated with 0.1% (v/v) diethyl pyrocarbonate (DEPC) -water prior to use. DEPC is a strong, but not absolute inactivator of most ribonucleases. The plastics and glassware were soaked in DEPC treated water for at least 4 hours at 37°C, following which they were autoclaved for 15 minutes. RNase free water was prepared by adding 0.1% DEPC to double distilled water for a period of at least 12 hours and then autoclaved.

Where ever possible, solutions were also treated with 0.1% DEPC in the same manner as above. Solutions containing the buffer Tris, however, could not effectively be treated with this inhibitor as DEPC reacts readily with amines (Sambrook *et al.*, 1989). In this case, autoclaved double distilled water was used.

Electrophoresis tanks were also stringently cleaned prior to use with RNA. The rigs were washed with detergent, rinsed with water, dried with ethanol and then filled with a solution of 3% hydrogen peroxide for a period of 10 minutes. Following this treatment, they were then thoroughly rinsed with DEPC treated water (Sambrook *et al.*, 1989).

2.1.3 Quantification of Ribozymes / Oligodeoxynucleotides

The quantification of ribozyme / oligodeoxynucleotide was determined by UV spectroscopy at 260nm. The purine and pyrimidine bases of DNA and RNA strongly absorb light with maxima near 260nm. The following method converts O.D. units into milligrams based on the molecular weight of the sequence and is adapted from that of Brown & Brown, (1991).

2.1.3.1 *Estimation of the Molecular Weight.*

mol wt = (249 x nA) + (240 x nT) + (265 x nG) + (225 x nC) + (64 x n-1) +2

where:

(i) nA = number of adenine bases in the sequence and n= total number of bases.

(ii) (64 x n-1) accounts for the molecular weight of the phosphate groups

This method, however, does not allow for differences in molecular weight between phosphodiester and phosphorothioate oligodeoxynucleotides, oligoribonucleotides and modified ribozymes. The following adjustments are required to account for these differences:

For phosphorothioates, a sulphur (mw=32) replaces an oxygen (mw=16) on the phosphodiester side chain. Consequently an adjustment of +16 is made for n-1 bases.

i.e. mw = (249 x nA) + (240 x nT) + (265 x nG) + (225 x nC) + (80 x n-1) +2

For unmodified RNA adjustments are required to account for an additional oxygen (mw=16) on the 2' site of each nucleotide. The adjustment in this case is +16 for each base and an allowance for the difference in mw between thymine and uracil.

i.e. mw = (265 x nA) + (242 x nU) + (281 x nG) + (241 x nC) + (64 x n-1) +2

In the case of modified ribozymes adjustments are required to allow for each modification. For example, in the case of ribozyme RPI.4782 the following adjustments were made:

4 x phosphorothioates	= (4 x 16)	= + 64
5 x unmodified RNA	= (5 x 16)	= +80
29 x 2'-O-Me	= (29 x 30)	= + 870
2 x 2'-NH_2	= (2x15)	= + 30
Total Adjustment		= + 1044

2.1.3.2 *Calculation of Micromolar Extinction Coefficient, ε at* 264nm

$\varepsilon = \{(8.8 \times nT) + (7.3 \times nC) + (11.7 \times nG) + (15.4 \times nA)\} \times 0.9$*

* It is necessary to multiply the extinction coefficient of the sum of the individual bases by 0.9 because the base-stacking interactions in the single strand suppress the absorbance of DNA.

2.1.3.3. *To Convert O.D. Units to Milligrams*

1mg $= \varepsilon$ / (Mol wt /1000) $O.D._{260}$ units

Therefore 1 $O.D._{260}$ unit = (Mol. Wt / 1000) / ε milligrams

2.2 LABELLING OF NUCLEIC ACIDS

2.2.1 5' –end [^{32}P] -Radiolabelling

Synthetic oligonucleotides / ribozymes are synthesised without a phosphate group at their 5' termini and are therefore easily labelled by transfer of the $\gamma^{32}P$ from [γ-^{32}P] ATP using the enzyme bacteriophage T4 polynucleotide kinase (PNK) as described by Sambrook *et al* (1989).

$$DNA_{OH}^{5'} \text{ or } RNA_{OH}^{5'} \xrightarrow[[\gamma\text{-}^{32}P]ATP]{\text{T4 PNK}} 5'[^{32}P]DNA \text{ or } 5'[^{32}P]RNA + ADP$$

The ribozymes and oligonucleotides were labelled at the 5'-end with [γ-^{32}P] labelled ATP (ICN, U.K.) using bacteriophage T4 PNK (Bioline, U.K.) in 1x forward reaction buffer (100mM Tris pH 7.5, 20mM $MgCl_2$, 10mM DTT, 0.2mM spermidine and 0.2mM EDTA) at 37°C for 45 minutes. The reaction mixture is given below:

ribozyme / oligo solution (e.g.100 pmoles)		2µl*
T4 kinase (5units/μl)		2µl
10x reaction buffer		2µl
[γ^{32P}] dATP (4500Ci/ mmol)		5µl
sterile DEPC-treated ddH_2O	to	20µl

* volume of ribozyme/ oligo solution varied according to concentration of stock solution / number of moles required to be labelled.

2.2.2 Internal [^{32}P]-Radiolabelling

Chimeric ribozymes were internally labelled using T4 RNA ligase. RNA ligase catalyses the formation of a 3'-5'-phosphodiester bond between the 3' hydroxyl group of a single stranded 'acceptor' RNA and the 5' phosphoryl group of a single stranded donor RNA molecule (England *et al*, 1977; Middleton *et al*, 1985).

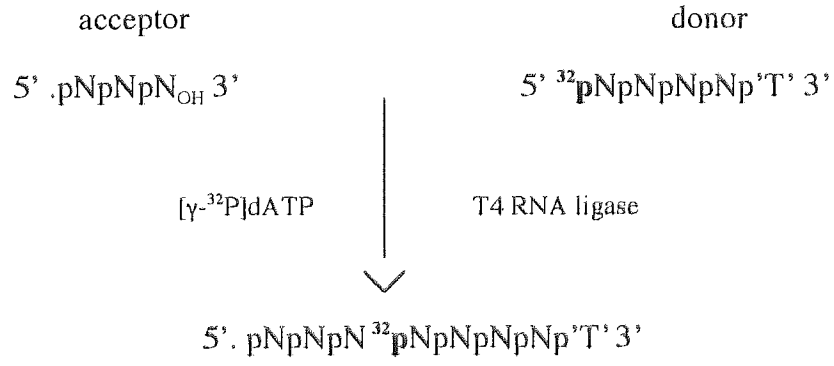

The internal labelling of ribozymes involved the following steps:

2.2.2.1 *Addition of 5'- Phosphate Group to Donor RNA*

One hundred picomoles of the dephosphorylated donor molecule was 5'-end labelled with [γ-^{32}P]ATP using T4 polynucleotide kinase as described in section 2.2.1. The reaction buffer used in this case, however, was a kinase/ ligase buffer (50mM Hepes pH 8.3; 3mM DTT; 5μg/ml BSA; 10mM $MgCl_2$). Following incubation at 37°C the sample was heated to 65°C for 5 minutes in order to inactivate the T4 kinase enzyme.

2.2.2.2 *Addition of Acceptor*

The acceptor RNA (e.g. 0.8μl of 121μM stock solution) was then added to the sample to give a donor : acceptor ratio of 1:1. The sample was dried by vacuum centrifugation in a Savant Speed Vac (Life Sciences, U.K.).

2.2.2.3 *Ligation of Donor and Acceptor*

The two halves of the ribozyme were ligated using T4 RNA ligase (Pharmacia Biotech, St.Albans, U.K.). The enzyme activity was determined by the supplier to be six units per microlitre. The dried sample containing both donor and acceptor was incubated at 37°C for 3 hours with 12 units of T4 RNA ligase, 1x kinase / ligase buffer and 9μM unlabelled ATP (Pharmacia Biotech, St. Albans, U.K.) in a final volume of 15μl. The inverted "T" on the 3' end of the donor RNA acted as a blocking agent to prevent either circular or multimeric products.

To ensure that ligation had occurred, internally labelled ribozymes were isolated from half ribozymes and unincorporated label by gel electrophoresis (see section 2.3.1). A representative example of the resulting autoradiograph is shown in Figure 2.1 below. This method gave reproducible 60-70% ligation of RNA fragments.

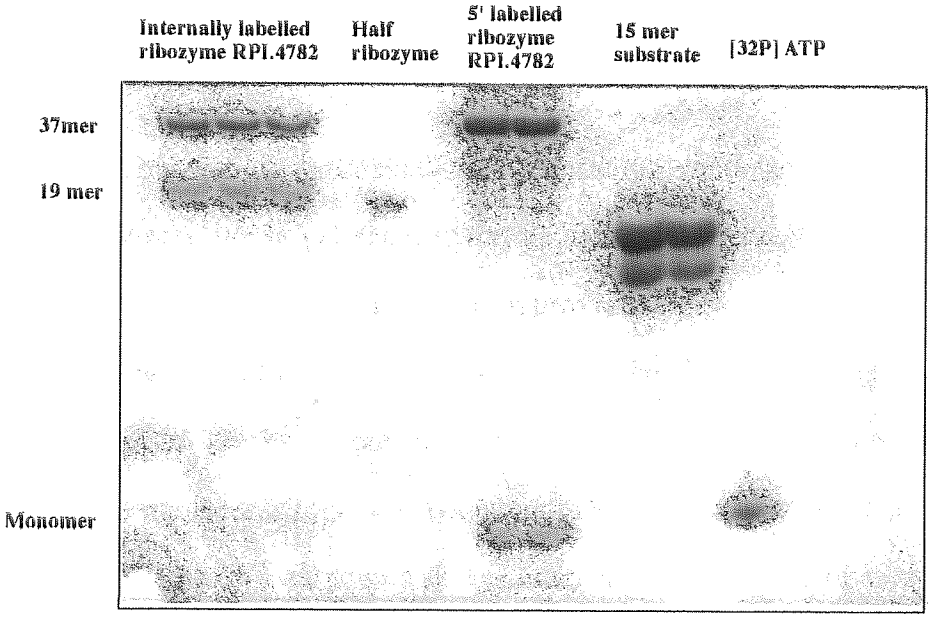

Figure 2.1 *Autoradiograph showing the successful ligation of 5'-labelled donor half ribozyme to acceptor half ribozyme* Samples of unligated half ribozymes, 5'-labelled 37mer ribozyme and a 5'-labelled 15mer all RNA substrate were used as size marker controls.

2.2.3 5'- end Fluorescein Labelling

FITC-labelled ribozymes were kindly synthesised and provided by RPI Pharmaceuticals (Colorado, USA) for use in fluorescent microscopy. The fluorescent label was attached to the 5'-end of a chimeric ribozyme as the terminal coupling step during automated synthesis by using fluorescein cyanoethyl phosphoramidite reagents (PerSeptive Bioresearch, USA).

2.2.4 Purification of Labelled Nucleic Acids

Once labelled, ribozymes and oligonucleotides were purified using one of the following methods:

2.2.4.1 *Purification by Polyacrylamide Gel Electrophoresis*

Following incubation, radiolabelled ribozymes / oligonucleotides were separated by 20% native polyacrylamide gel electrophoresis as detailed in section 2.3.1. Once the leading edge of the samples had migrated to approximately two thirds down the gel (estimated from marker dyes), the position of the required bands was visualised by autoradiography (section 2.3.2). The band containing the desired nucleic acid was excised and transferred to a sterile microcentrifuge tube containing DEPC-treated water. The excised bands were then incubated in the water on a shaker overnight at room temperature. Following elution, the supernatant was removed, transferred to a sterile microcentrifuge tube and lyophilised (Savant DNA Speed Vac). The resulting purified pellet was stored at –20°C until required for experimental purposes.

2.2.4.2 *Column Purification*

Alternatively, radiolabelled ribozymes and oligodeoxynucleotides were separated from unincorporated [^{32}P]ATP label and desalted by column purification. Separation was performed using Sephadex G-25 packed (NAP-10) columns (Pharmacia Biotech) using gravity separation for maximum product recovery as described in section 2.1.1.4.

2.3 GENERAL ANALYTICAL METHODS

2.3.1 Polyacrylamide Gel Electrophoresis (PAGE)

Short chain nucleic acids such as ribozymes and oligonucleotides can easily be separated according to size difference by polyacrylamide gel electrophoresis. Polyacrylamide gels are formed by the vinyl polymerisation of acrylamide monomers (CH_2=CH-CO-NH_2) into long random chains of polyacrylamide which are cross-linked by the inclusion into the mixture of small amounts of a co-monomer, *N-N'*-methylene-bis-acrylamide, commonly known as "*Bis*". The resulting cross-linked chains form a gel structure, the pore size of which is determined by the concentrations of both acrylamide and *Bis*-acrylamide.

Polyacrylamide gels were prepared as described by Sambrook *et al* (1989) using Biorad Protean II electrophoresis apparatus. Two glass plates (20cm x 20cm), cleaned with acetone and separated by 1mm spacers were sandwiched together and clamped vertically in the gel stand. The polymerisation reaction was activated by the addition of 0.6ml fresh ammonium persulphate (10%w/v) and 40μl of TEMED to 50ml of a stock gel mix, which had previously been prepared as shown in Table 2.1, and stored at 4°C. The polymerising mix was gently stirred and carefully poured into the gap between the two plates and a comb inserted. In general, and unless specified otherwise, ribozymes and oligodeoxynucleotides were separated using 20% polyacrylamide gel solutions and PCR products showing telomerase activity (Chapter 5) were separated using 8% polyacrylamide gel solutions.

Table 2.1: *Composition of stock polyacrylamide gel mixtures*

REAGENT	GEL CONCENTRATION	
	8%	20%
30% acrylamide / bis-acrylamide mix (19:1)	134ml	333ml
Urea *	420g (7M)	420g (7M)
5x TBE **	100ml	100ml
Double distilled water	to 500ml	to 500ml

* For a native gel the urea was omitted.

** 5x TBE (54g Tris base, 27.5g boric acid, 20ml 0.5M EDTA (pH8.0) to 1L with ddH_2O)

A minimum period of 30 minutes was allowed for the gel to set, the comb was then removed and the wells washed with sterile 1xTBE (diluted from 5x TBE stock solution). The gel was transferred into a BioRad electrophoresis tank and both upper and lower reservoirs filled with 1xTBE running buffer. Samples were diluted with an equal volume of loading buffer, (native: 5% glycerol in 1xTBE) or (denaturing: 9:1 (v/v) formamide:1xTBE) and carefully loaded into the wells using round tipped micropipettes (Costar,U.K.). Marker dyes (0.25% bromophenol blue; 0.25% xylene cyanole in 1xTBE) were used to track the progress of sample migration down the gel. Gels were run at 10-20W for 2-3 hours and cooled to 10°C using a thermostat controlled water circulator (Sarver Instruments, U.K.).

2.3.2 Autoradiography

2.3.2.1 *Sample Detection*

Radiolabelled samples, separated by PAGE, were detected by autoradiography. Following electrophoresis the gel was removed from the glass plates, wrapped in a single layer of Saran Wrap cling film and placed in a Hypercassette fitted with an intensifying screen (Amersham Life Sciences, Amersham,U.K.). Under dark room conditions, the gel was exposed to a sheet of Kodak HP autoradiograph film for the relevant exposure time (1 minute to 30 minutes). For weaker signals, the gels were exposed to autoradiograph film and stored, using the intensifying screen, at –70°C for the required period (4 hours to 14 days). The film was then developed using Kodak photographic reagents and once fixed allowed to dry naturally.

2.3.2.2 *Densitometric Analysis of Autoradiograph Images.*

Autoradiographs were scanned using an AGFA focus scanner connected to a Macintosh computer and images were saved as TIFF files. The images were then analysed using scanning densitometry. The programme NIH Image 1.58 (Division of Computing and Research Technology, NIH, Bethesda, USA) was used to plot and quantify the relevant image intensities of band patterns shown on the autoradiographs.

2.3.3 Liquid Scintillation Counting

Liquid scintillation counting (LSC) was used to quantify the activity of [^{32}P] and [^{14}C] radiolabelled nucleic acids. Samples were added to 5ml of Optisafe Hisafe III

(Pharmacia-Wallace, St Albans, U.K.) and counted for 5 minutes using a Packard 1900TR Scintillation Counter. Adjustments were automatically made for radioactive decay during the experimental period by entering the half life and reference date of the radioisotope used. For each experiment, counts were compared with background values.

2.4 CELL CULTURE

All cell culture procedures were undertaken under aseptic conditions in a Gelaire, biohazard level II, laminar flow cabinet from ICN (Thame, Oxfordshire, U.K.).

2.4.1 Cell Lines

U87-MG cell line was purchased from the European Collection of Animal Cell Cultures (ECACC), (Porton Down, U.K.). These human glioblastoma astrocytoma cells were originally derived from a grade 3 malignant glioma by explant technique (Ponten and Macintyre, 1968). A431 cells were a generous gift from Dr P.L. Nicklin, Ciba-Gigy Pharmaceuticals (Horsham, U.K.). This cell line is derived from a vulval carcinoma (Freshney, 1973) and expresses the EGFR at levels 10 to 50-fold higher than seen in other cell lines (Ullrich *et al.*, 1984). The cultured intestinal epithelial Caco-2 cells, derived from a human adenocarcinoma, were kindly donated by Dr. V. Moore (Aston University). Raw 264.7 is a murine macrophage cell line purchased from the ECACC (Porton Down, U.K.). These cells were established from the ascites of a tumour induced in a mouse by the intraperitoneal injection of Abelson Leukaemia virus (Raschke *et al*, 1978). IPFA cells are primary human astrocytes and were a gift from Dr. G. Pilkington, Institute of Psychiatry, (London, U.K).

2.4.2 Culture Media

The cell lines U87-MG; Raw 264.7 and IPFA were maintained in Dulbecco's modified Eagle's medium (DMEM) supplemented by 10% v/v mycoplasma screened foetal bovine serum (FBS), 1% penicillin/streptomycin and 1mM L-glutamine (all supplied from Gibco, Paisley, U.K.). A431 cells were maintained under the same conditions except glutamine was added to a final concentration of 2mM. The same medium, without the addition of the foetal bovine serum, was used in the stability and cell association studies.

Two media were prepared for culturing Caco-2 cells. A maintenance medium comprising DMEM supplemented with 10% v/v FBS, 1% v/v non essential amino acids, and 2mM L-glutamine was used to maintain stock cultures. A further plate medium was used to cultivate cells on 24 well plates and was comprised of maintenance medium supplemented to a final concentration of 1% v/v with penicillin and streptomycin.

2.4.3 Stock Cultures

Cells were cultured in $75cm^3$ plastic tissue culture vented cap T-flasks, with a non-wetting $0.2\mu m$ hydrophobic micro-porous membrane vent (Falcon, U.K.), using 25ml of the respective media. The cultures were incubated at 37°C in a humidified (95%) atmosphere of 5% CO_2 in air.

Stock cultures were maintained by changing the media every 48 hours and passaged when confluent (after approximately 3-4 days depending on cell line). Passaging was carried out using the following procedure:

The media was removed and the cells washed with 10ml of 0.25% v/v phosphate-buffered saline solution (PBS) (Sigma, Poole, U.K.). After aspiration of the PBS, 5ml of 1x Trypsin /EDTA solution (0.25% w/v trypsin, 0.2% w/v disodium ethylenediamine tetraacetate in PBS, pH 7.2) was added to the monolayers. After one minute, the trypsin /EDTA solution was removed by aspiration and the cells incubated at 37°C for 5 minutes. The flasks were tapped to dislodge the cell monolayer, examined by phase microscopy and re-incubated if necessary until detached from the flask. Fresh media was added to inactivate the trypsin and cells were pipetted to give a single- cell suspension. For stock cultures, the cells were split at a ratio of 1:5 and media was added to a final volume of 25ml. If the cells were to be used in a specific experiment, they were counted by haemocytometry and transferred at the required cell number to the appropriate culture vessel.

2.4.4 Determination of Cell Number / Viability

The viable cell density of stock cultures was measured by haemocytometry using a trypan blue exclusion test. 100μl of trypan blue (4mg ml^{-1}) was mixed with 400μl of cell suspension (1:1.25 dilution) and incubated at room temperature for 5 minutes. A small amount of the trypan blue cell suspension was then transferred to the counting chamber of a Neubauer haemocytometer (Weber Scientific International Ltd, U.K.). The cells were counted in five large (1mm) squares of the haemocytometer using a light microscope and a mean count per square obtained. Live cells exclude the trypan blue dye and appear with clear cytoplasm, whereas non-viable cells take up the stain and appear dark blue. Consequently the number of viable (unstained) cells can be determined. The cell density was calculated using the following equation:

Viable cells per ml = average number of viable cells per square x 10^4 x 1.25 (dilution factor of trypan blue)

% Cell Viability = total viable cells (unstained) / total cells (stained and unstained) x100.

Cells suspensions with a percentage cell viability of < 95% were disregarded.

2.4.5 Freezing / Thawing of Cell Lines

For long- term storage, frozen stock cultures were prepared in the following manner: Semi-confluent stock cultures were trypsinised as described previously (section 2.4.3) and neutralised with the addition of 10ml of DMEM medium. The cell suspension was then transferred to a 15ml universal tube (Falcon, U.K.) and centrifuged for 3 minutes at 350 revolutions per minute (Mistral 3000 I centrifuge, Sanyo MSE, Leicester, U.K.). The supernatant was decanted and the cell pellet was re-suspended in 1ml of 'freezing medium' (10% DMSO, 90% heat inactivated foetal calf serum) and transferred to a 2ml screw capped cryovial (Costar, U.K.). The ampoule was then placed in a –70°C freezer for 4-6 hours before being transferred into a liquid nitrogen (-196°C) cell bank. When required, the cells were recovered by rapid thawing at 37°C and gradual dilution with DMEM medium before seeding in 25cm^3 flasks (Falcon, U.K.).

2.5. CELL ASSOCIATION STUDIES

Most of the ribozyme cell association data presented in this thesis was obtained using U87-MG cells. The following general experimental procedure was used throughout cell association studies unless otherwise stated.

U87-MG cells were cultured on plastic 24-well plates (Falcon, U.K.). Confluent stock cultures were trypsinised and counted as described in section 2.5.3-2.5.4 and the cell density of the stock suspension diluted to 5 x 10^4 cells ml^{-1} with DMEM medium. Each well was seeded with 2ml of the diluted cell suspension to give a final concentration of $1x10^5$ $well^{-1}$. The plates were incubated at 37°C in a humidified (95%) atmosphere of 5% CO_2 in air. After approximately 20 - 24 hours, the cell monolayers had reached 80-90% confluency and were then ready for cell association experiments. The generalised method for cell association experiments is depicted in Figure 2. 2.

Initially the medium was removed and the monolayer carefully washed twice with PBS (2 x 1ml x 5min) to remove any traces of serum. The washing solution was aspirated and replaced with 200μl of serum free DMEM medium containing the radiolabelled ribozyme. Both PBS and serum free medium were equilibrated at 37°C for 1 hour prior to use. The plates were incubated at 37°C, unless otherwise stated, for the duration of the experiment. Once incubated for the desired period of time, the apical media was carefully collected and their radioactive content assessed by liquid scintillation counting (LSC). The cells were then washed 3 times (3 x 0.5ml x 5min) with ice cold PBS-azide to inhibit any further cellular metabolism and remove any ribozyme loosely associated with the cell surface. The washings were collected and their radioactive content determined by LSC.

Cell monolayers were solubilised by shaking with 0.5ml of 3% v/v Triton X100 (Aldrich Chemical Company, Gillingham, U.K.) in distilled water for 1 hour at room temperature. The wells were washed twice more (2 x 0.5ml) with Triton X-100 to ensure that all the cells had been harvested and the radioactivity content of the cellular fraction determined by LSC.

Unless otherwise indicated, all experiments were performed at a final concentration of 0.01μM [^{32}P]-internally labelled ribozyme and incubated for a period of 60 minutes. Furthermore, for all experiments three extra wells were seeded with cells and the viable cell density was determined by a trypan blue exclusion assay (section 2.4.4), so that cell association could be normalised to cell number when required.

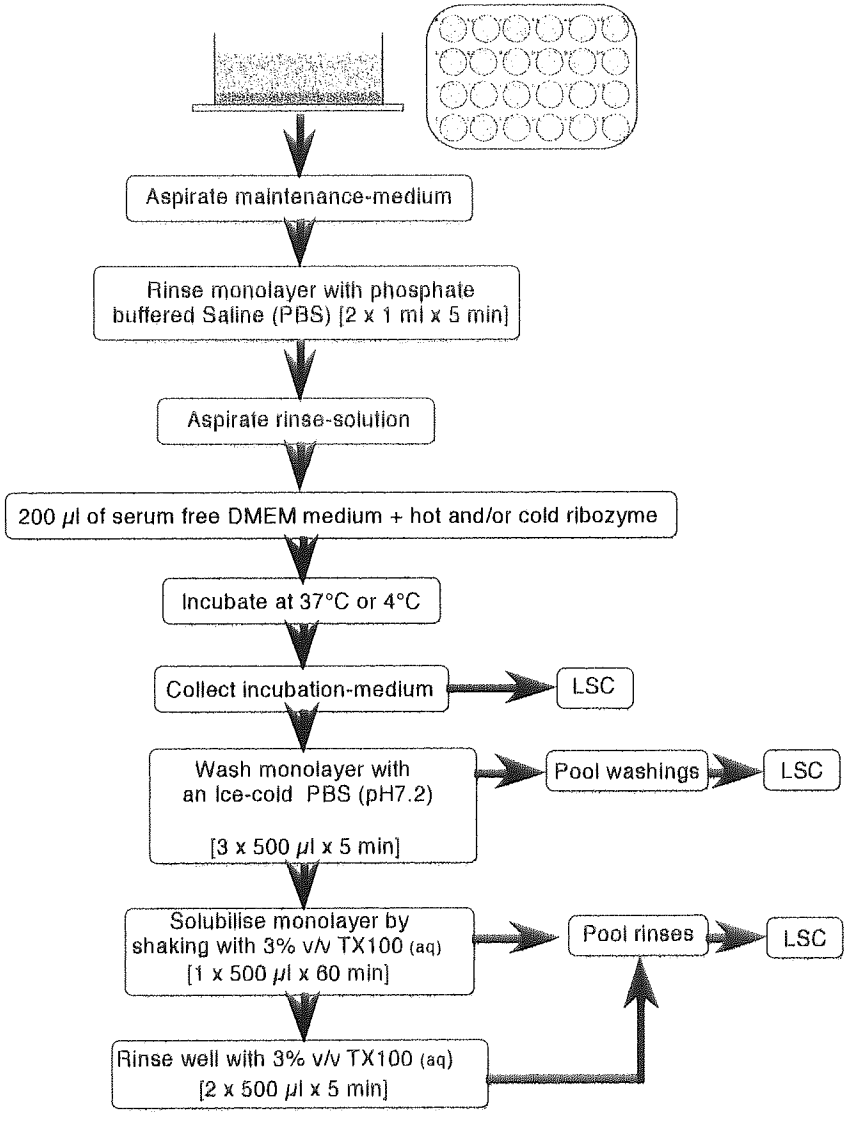

Figure 2.2 *Schematic diagram of generalised protocol for cell association experiments*

2.6 PROLIFERATION STUDIES

A431 and U87-MG cells were seeded in DMEM medium containing 10% FBS into 24 well plates ($2cm^2$) at 2.5-5.0 $x10^4$ cells/well and 3.0-6.5 $x10^4$ cells/well respectively. Following washes with serum free DMEM medium (2 x 0.5ml x 5min), ribozymes alone or ribozymes complexed with lipid enhancers were added in serum free culture medium 20- 24 hours after seeding. The total volume added per well was 200μl. After incubating over various time periods (from 4 hours to 4 days), cells were washed twice with PBS (2 x 0.5ml x 5min), trypsinised and the number of viable cells counted by trypan blue exclusion assay (sections 2.4.3 and 2.4.4). The morphology of cells after treatment was also examined by light microscopy and compared to untreated control cells.

Alternatively cells were plated out into 96 well plates ($0.3cm^2$) at 3.0–7.5 $x10^3$ cells/well (A431 cells) or at 3.5–8.0 x 10^3 cells/well (U87MG cells) in medium containing 10% FBS. After 20-24 hours, cell monolayers were washed twice with serum free DMEM medium (2 x 0.1ml x 5min) and ribozymes or ribozyme / lipid complexes added in a total volume of 100μl $well^{-1}$ of serum free medium. Following the required incubation time, cell number was determined by using a crystal violet assay as described below.

2.6.1 Crystal Violet Assay

An estimate of cell number can be obtained by staining the cells with crystal violet and measuring absorption on a densitometer. Crystal violet is a basic dye that attaches to negatively charged groups in the cell (e.g. DNA and proteins) and stains cells blue – violet. Since an increase in total DNA and protein correlates with cell number, this

colorimetric method can therefore be used in growth / proliferation experiments to measure the net increase in cell number over the experimental period.

Cells were washed by removing 50μl of medium and adding 50μl of wash solution (3% (w/v) sucrose in PBS). This process was repeated three times. The cells were then fixed by removing 50μl of wash solution, adding 50μl of fix solution (4% (w/v) paraformaldehylde in PBS) and incubating for 30 minutes. The wells were emptied completely and the cells incubated in 100μl of fresh fix solution for a further 60 minutes. Following removal of the fix solution, cells were washed three times with PBS solution and blotted dry. 50μl of stain solution (0.1% (w/v) crystal violet in PBS) was then added to each well and the cells incubated at room temperature on a shaker for a period of 30 minutes. Once the stain was removed, the plate was washed six times by total immersion in water and blotted dry. Finally, cells were solubilised by incubating in 50μl of 0.1% SDS in water for 10 minutes on a shaker at room temperature. The plate was read on an automatic plate reader at 550nm. A standard curve, correlating cell number to absorbance, was obtained by measuring the absorbance (OD_{550}) of plate replicates containing known number of cells (from $1x10^2$ to $1x\ 10^5$ cells /well). Cells were plated out at increasing concentrations in a volume of 100μl onto 96-well plates. The cells were left to attach to the plastic for four hours and then the crystal violet assay performed as described above. Cell number was plotted against OD_{550} and the equation for the best-fit line determined to convert OD_{550} to cell number for experimental samples.

2.7 PROTEIN ANALYSIS

2.7.1 Protein Sample Preparation

Cell samples were prepared under conditions that ensure the denaturing of proteins with minimal aggregation. This is achieved by using the strongly anionic detergent SDS in combination with a reducing agent and heat to dissociate the proteins. The denatured polypeptides bind SDS and become negatively charged enabling separation through gel electrophoresis according to size (Sambrook *et al.*, 1989).

2.7.1.1 *Lysis Method One*

Following ribozyme treatment (section 2.6), cells required for western blotting analysis were harvested from 24 well plates in Laemmli buffer (100mM Tris-HCl (pH 6.8), 4% SDS, 0.2% bromophenol blue, 20% glycerol, 5% mercaptoethanol). After washing the cells monolayers twice with PBS (2 x 0.5ml x 5 min), 30μl of hot (85°C) 1 x Laemmli buffer was added to each well. Triplicate sample wells were pooled. The lysate was scraped into a microcentrifuge tube and sonicated for 30 seconds to shear the chromosomal DNA and reduce the viscous lysate to manageable levels. The sample was then centrifuged at 10,000rpm for 10 minutes at room temperature, the supernatant transferred to a fresh tube and the pellet discarded. The samples were then loaded directly onto a gel or stored frozen at –70°C until required for analysis.

2.7.1.2 *Lysis Method Two*

Alternatively, after washing with PBS (2 x 0.5ml x 5min), cells were trypsinised (section 2.4.3) and pelleted by centrifuging at 1000rpm for 5 minutes at 4°C. The cells were re-suspended in 1ml of PBS, centrifuged at 1000rpm for 5 minutes at 4°C and washed in this manner twice more with PBS. The cells were then lysed by adding 100μl of lysis buffer (0.5M Tris-HCl, pH 6.8; 10% glycerol; 10% SDS; 0.1mM leupeptin and 0.1mM PMSF) for every 1 x 10^6 cells. The cells were vortexed and sonicated on ice until evenly mixed and then centrifuged at 14000rpm for 30 minutes at 4°C. The supernatant was stored at –70°C until required for analysis.

2.7.2 Protein Determination

Protein content of whole cell lysates was determined by means of a Bio-Rad protein assay. This assay is a dye-binding assay based on the differential colour change of a dye in response to various concentrations of protein (Bradford, 1976). The absorbance maximum for an acidic solution of Coomassie Brilliant Blue G-250 shifts from 465nm to 595nm when binding to protein occurs.

The following procedure was used; A protein standard solution (2mg /ml of bovine serum albumin) was diluted with distilled water to give a final volume of 795μl, and 5μl of lysis buffer was added to each tube of protein standard. This produced a range of concentrations (0μg/ml – 25μg/ml) for a calibration curve to be established. Whole cell lysate samples of unknown protein concentration were prepared in duplicate by diluting 5μl of the sample in 795μl of distilled water to give a total volume for both standards and samples of 800μl. The assay was initiated by adding 200μl of dye reagent concentrate to

each tube of standard and unknown and mixing well before incubating at room temperature for 15 minutes. Absorbance at 595nm was then read using a spectrophotometer (Jenway, U.K.). The absorbance of a blank control (0μg/ml of protein) was subtracted from the samples and a calibration curve constructed by plotting net absorbance vs. the concentration (μg/ml) of the protein standards at 595nm. The calibration curve was then used to determine the amount of protein in the unknown cell lysate samples.

2.7.3 SDS Polyacrylamide Gel Electrophoresis

All protein electrophoresis was carried out using Bio-Rad electrophoresis equipment (Bio-Rad, California, USA). Two glass plates (7cm x 8cm) were clamped together with spacers (1.5 mm thick) at the sides to form a gel sandwich which was placed in the gel stand and clamped to form a seal at the base of the plates. A 7.5% polyacrylamide separating gel was prepared as shown in Table 2.2 and poured into the gel sandwich. The gel was overlaid with 1ml of double distilled water and allowed to polymerise for 45 minutes. The water overlay was poured off and the area above the separating gel was then dried with filter paper. A 4% stacking gel was prepared (Table 2.3), poured on top of the separating gel and a comb inserted between the plates. After the stacking gel had set (after approximately 45 minutes), the comb was removed and the wells rinsed thoroughly with distilled water. The gels were assembled in the electrophoresis tank and both upper and lower reservoirs filled with running buffer (0.3% Tris.HCl; 1.44% glycine; 0.1% SDS).

Table 2.2 *7.5 % Separating gel mix*

STOCK /REAGENT	VOLUME	FINAL CONCENTRATION
30% Acrylamide / bis mix (29:1)	2.5ml	7.5%
1.5M Tris.HCl (pH 8.8)	2.5ml	0.375M
Distilled Water	4.8ml	N/A
10% (w/v) SDS	0.1ml	0.1%
10% (w/v) fresh Ammonium Persulphate	0.1ml	0.1%
TEMED	6μl	N/A

Table 2.3 *4% Stacking gel mix*

STOCK /REAGENT	VOLUME	FINAL CONCENTRATION
30% Acrylamide / bis mix (29:1)	650μl	4.0 %
0.5M Tris.HCl (pH 6.8)	1.25ml	0.125M
Distilled Water	3.0ml	N/A
10% (w/v) SDS	50μl	0.1%
10% (w/v) fresh Ammonium Persulphate	50μl	0.1%
TEMED	5μl	N/A

Protein samples, previously lysed as described in section 2.7.1.1, were heated at 90°C for 5 minutes prior to loading. Samples, were then loaded into the wells using round ended micropippette tips (Costar, U.K.). In addition to the working samples, a sample of high molecular weight markers of known molecular mass (205 kDa – 45 kDa) (Sigma, Poole, U.K.) was also loaded into one well of each gel. This product consisted of a range of

individually coloured and purified proteins resulting in identifiable bands when separated by SDS-PAGE. The coloured bands could be visualised on the gel and after transfer of proteins onto nitrocellulose filter, thus allowing comparisons with sample proteins of interest. Gels were run at 100V for about 90 minutes or until the bromophenol blue dye had run off the end of the gel.

2.7.4 Immunoblotting of Proteins

Electrophoretic transfer of the proteins on the gel onto the blotting membrane was performed using a Bio-Rad Trans-Blot electrophoretic transfer cell. Following electrophoresis the stacking gel was carefully removed and the separating gel was washed twice with distilled water before being equilibrated in transfer buffer (25mM Tris.HCl, 192mM glycine and 20% w/v methanol) for 10 – 15 minutes prior to blotting. In addition, the Hybond-ECL membrane (Amersham, U.K.) and six sheets of filter paper (Whatmann, 3MM) were cut to exactly the same size as the gel and soaked in the transfer buffer for 10-15 minutes. A blotting sandwich was assembled, consisting of three filter papers, nitrocellulose membrane, gel and three further filter papers, and placed in the apparatus of the transfer tank as show in Figure 2.3. At each stage of assembly, care was taken to remove any air bubbles by rolling over the surface with a glass pipette. The tank was filled with transfer buffer so that the sandwich was completely submerged and transfer was performed at either 30mV overnight or at 100mV for 2 hours.

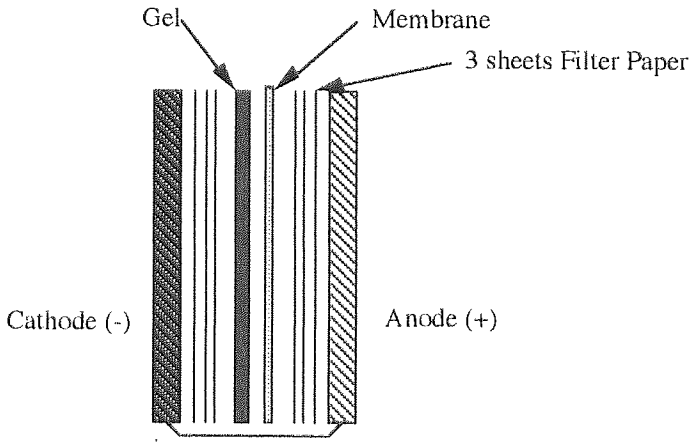

Figure 2.3 *Assembly of blotting sandwich*

After blotting was complete, the nitrocellulose membrane was either processed immediately by ECL immunodetection (section 2.7.5) or stored dessicated at 4°C.

2.7.5 Immunoblot Analysis

A commercial ECL immunodetection kit was used to analyse the immunoblots obtained. This is a light emitting method for detection of a specific antigen, conjugated directly or indirectly with horseradish peroxidase-labelled antibodies (Amersham, Buckinghamshire, U.K.). The principle of this procedure is highlighted in Figure 2.4.

Briefly, a primary antibody raised against the protein being studied is added to the membrane followed by a horseradish peroxidase (HRP) conjugated secondary antibody which is targeted to the primary antibody. ECL detection is initiated when detection reagents are added to the membrane and HRP catalyses the oxidation of luminol in the presence of a chemical enhancer (phenol). The light produced by this oxidation (maximum at 428nm) is detected by exposure to blue-light sensitive autoradiography film.

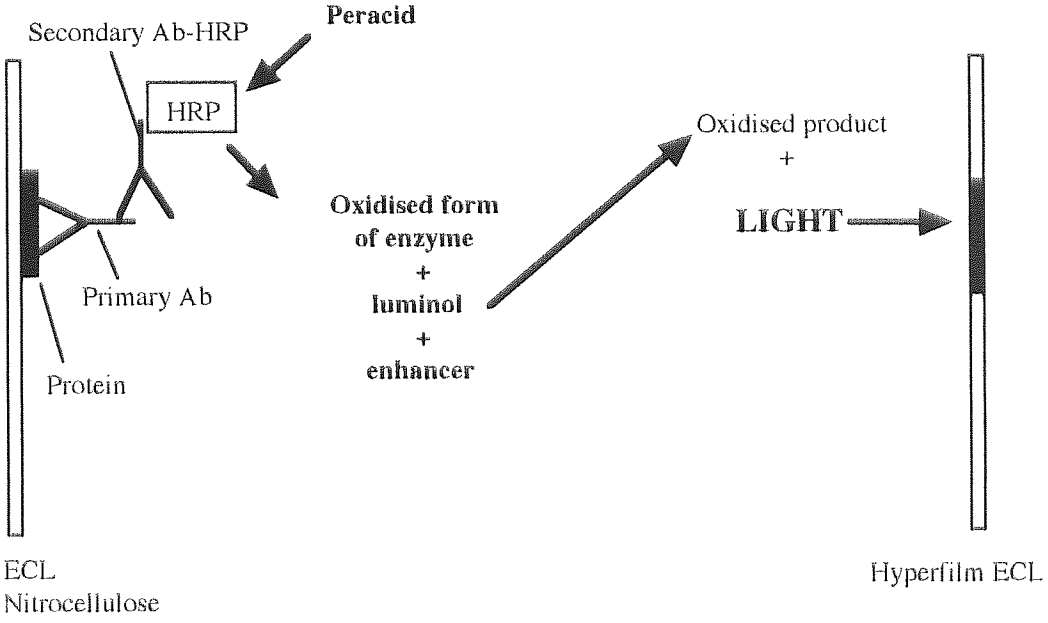

Figure 2.4 *Principles of ECL western blotting*

2.7.5.1 *Protein Detection*

Immunoblots were placed, with the protein bound side facing inwards, in screw topped containers. The various washings and incubations were performed at room temperature with the containers placed on an orbital shaker at low speed.

After blotting, the nitrocellulose filters were washed twice (2 x 50ml x 10min) in Phosphate Buffered Saline Tween (PBS-T) buffer (0.1% v/v Tween 20 in PBS pH 7.5) and incubated in blocking buffer (5% w/v low fat milk powder dissolved in PBS-T) for at least one hour. The blots were then washed three times for 10 minutes with PBS-T and then incubated for one hour with the appropriate concentration of primary antibody in 5ml of blocking buffer. Excess antibody was removed and the blots were then washed a

further three times with PBS-T buffer (3 x 50ml x10min). The HRP conjugated secondary antibody (anti-mouse or anti-rabbit) was diluted in blocking buffer and added at a concentration of 1:2500 (2μl in 5ml) and incubated for one hour. Excess secondary antibody was removed and the blot washed thoroughly (4 x 50ml x 10min). Following these washing, the blot was taken into a Dark Room where immunodetection was carried out using ECL reagents (Amersham, U.K.). Firstly, equal volumes of ECL detection solutions 1 and 2 were mixed together (final volume being 0.125 ml / cm^2), applied to the blot and incubated for one minute at room temperature without agitation. The excess reagent was drained off, the blot wrapped in Saran Wrap cling film and exposed to a sheet of autoradiography film (Hyperfilm-ECL) for between 10 seconds to 30 minutes. The film was placed in developer until bands appeared, rinsed in water and then fixed and allowed to dry naturally. Repeat exposures were undertaken to achieve an optimal image. The resulting autoradiographs were then analysed by scanning densitometry as described in section 2.3.2.2.

2.8 KINETIC CHARACTERISATION OF RIBOZYMES: *IN VITRO* ACTIVITY STUDIES

2.8.1 Standard Conditions.

Cleavage reactions were carried out in 50mM Tris.HCl, pH 7.5 and 10mM $MgCl_2$ at 37°C. In order to disrupt aggregates that can form during storage, unlabelled ribozyme and 5'-end labelled substrate were denatured and renatured separately in standard cleavage buffer (50mM Tris.HCl, pH 7.5) by heating to 90°C for 2 minutes and allowed to equilibrate to the reaction temperature of 37°C for 15 minutes. Each RNA solution was then adjusted to a final concentration of 10mM $MgCl_2$ and incubated at 37°C for a further

15 minutes. Cleavage reactions were initiated by combining the ribozyme and the substrate samples to the required concentrations in a final volume of 100μl. Aliquots of 10μl were removed at appropriate time intervals between 0 and 120 minutes and quenched by adding an equal volume of formamide loading buffer (9:1 (v:v) formamide : 1x TBE) and frozen on dry ice. Product and substrate were separated by denaturing 20% polyacrylamide (7M urea) gel electrophoresis as detailed in section 2.3.1. To determine the fraction of cleavage, substrate and product bands were located by autoradiography of wet gels and quantified by densitometry of these autoradiograms (see section 2.3.2). Alternatively, the relevant bands were excised from the gel and quantified by scintillation counting (Packard Tricarb 2000 CA liquid scintillation analyser) as described in section 2.3.3.

2.8.2 Single -Turnover Reactions

Experiments were performed with ribozyme in excess over substrate (40nM ribozyme: 1nM substrate) to determine the activity half-time ($t_{1/2}$) under single turnover conditions. Reaction rate constants (k) were obtained from the slope of semi-logarithmic plots of the amount of substrate remaining versus time. Plots tended to fit a double exponential curve where the fast portion of the curve was generally 60-90% of the total reaction. Consequently, the observed cleavage rates (k) and activity half-times ($t_{1/2}$) were taken from fits of the first exponential. The activity half-time $t_{1/2}$ was calculated as 0.693 / k.

2.8.3 Multiple -Turnover Reactions

Cleavage rates were also determined under multiple turnover conditions where substrate concentration was at least ten-fold greater than ribozyme concentration. Reactions were performed with a final concentration of 10nM ribozyme and concentrations of substrate between 100nM and 1μM. Initial rates of reaction were measured at seven substrate concentrations and the Michaelis-Menten equation was used for kinetic analysis. Values of K_m and V_{max} were derived from Eadie-Hofstee plots. The k_{cat} values were calculated as V_{max} divided by the concentration of ribozyme.

2.9 STATISTICAL ANALYSIS

Significant testing was performed using an unpaired students t-test assuming equal variance (Gaussian population) using the Microsoft Excel statistical software package. Data sets were assumed to be significantly different when the two-sided P values were calculated below 0.05. Unpaired t-tests assumed that data were randomly sampled, that each value was obtained independently of the others and that the populations were scattered according to a Gaussian distribution. The software package was used to perform F-tests which indicated whether or not the standard deviations of the two populations tested were significantly different. Where the variance of the two experimental populations were significantly different, a Welsh's test was used. The Welsh test is a modification of the unpaired t-test and does not assume that data follow a Gaussian distribution.

CHAPTER THREE

CHARACTERISATION OF 2'-O-METHYL-MODIFIED CHIMERIC HAMMERHEAD RIBOZYMES: BIOLOGICAL STABILITY, *IN VITRO* ACTIVITY AND CELLULAR UPTAKE PROPERTIES

ABSTRACT

Catalytic RNA or ribozymes have important potential applications as molecular biological tools in the study of gene expression and as therapeutic inhibitors of disease-causing genes. The successful use of synthetic, exogenously administered ribozymes for such applications will require chemical modifications that improve the biological stability without significant loss in catalytic activity compared to unmodified RNA. In addition, the optimisation of appropriate delivery strategies will require a fundamental understanding of the cellular uptake properties of synthetic ribozymes.

In this study, we have characterised two synthetic, 2'-O-methyl modified hammerhead ribozymes containing either 2'-amino groups at position U_4/U_7 (designated RPI.4782) or a 2'-C-allyl modification at U_4 only (designated RPI.5993). The serum stability of these ribozymes, targeting the 3'-UTR of the human epidermal growth factor receptor mRNA, was more than 4000-fold greater than an unmodified RNA molecule with stability half-lives ($t_{1/2}$) of 18 hours for ribozyme RPI.4782 and 20 hours for ribozyme RPI.5993. The chimeric ribozymes also proved to be significantly more stable than phosphodiester (PO) ($t_{1/2}$~10 minutes) and phosphorothioate (PS) ($t_{1/2}$~ 5 hours) oligonucleotides (ODNs) and remained largely intact over 4 days in U87-MG glioma cells. Furthermore, both ribozymes exhibited significant *in vitro* activity in cleaving a 15-mer RNA sequence representing the 3'-UTR target site within the EGFr mRNA.

The cellular association of the internally [^{32}P]- radiolabelled ribozyme RPI.4782 in U87-MG glioma cells was temperature-, energy- and pH- dependent and involved an active process that could be competed with cold ribozyme of the same chemistry and sequence, antisense PS- and PO-ODNs and the 2'-O-methyl / 2'-C-allyl ribozyme RPI.5993, as well as a variety of other polyanions. The extent of cellular association varied according to cell type, showing that ribozyme uptake is cell specific. Subcellular distribution studies of fluorescently labelled ribozymes confirmed an extranuclear, punctate localisation similar to that observed for an endosomal marker, dextran. This research highlights that hammerhead ribozymes, despite exhibiting a defined secondary structure, enter cells by an endocytic mechanism that appears to be similar to that reported for a variety of antisense ODNs. These observations should facilitate the development of more efficient delivery systems.

3.1 INTRODUCTION

A primary challenge for the application of ribozyme technology to an investigative or clinical situation is the delivery of chemically stable, biologically active ribozymes to the appropriate cells. The efficacy and general applicability of RNA-based therapeutic approaches may be limited, however, by poor biological stability (Beigelman *et al.*, 1995a), inefficient uptake into living cells (Elkins & Rossi, 1995; Ayers *et al.*, 1996) and limited cellular targeting (Sullinger & Cech, 1993; Rossi, 1998). Unmodified RNA is extremely unstable in biological systems and is rapidly degraded by intra- and extra-cellular nucleases. Most of the demonstrations of ribozyme efficacy have, until recently, involved endogenous delivery of ribozymes using expression vectors, since poor biological stability has limited the exogenous delivery of pre-synthesised ribozymes. Over recent years, however, significant progress has been made in the generation of RNA molecules by chemical methods (Usman & Cedergren, 1992: Wincott *et al.*, 1995) and a number of modifications have been applied to enhance stability (for reviews see: Bratty *et al.*, 1993; Aurup *et al.*, 1995; Sproat, 1996: see also section 1.3). This has led to the synthesis of chemically stabilised ribozymes that contain site specific modifications to improve nuclease resistance without significant loss of catalytic activity (Usman and Cedergren, 1992; Heidenreich *et al.*, 1994; Beigelman *et al.*, 1995). Consequently we are now seeing an increasing number of reports demonstrating efficacy in cell culture and in animal models using exogenously delivered synthetic ribozymes (Lyngstadaas *et al.*, 1995; Florey *et al.*, 1996; Jarvis *et al.*, 1996; Kisich *et al.*, 1999; Parry *et al.*, 1999).

Despite rapid progress in the development of such RNA-based therapeutics, little is known about the cellular uptake mechanisms of exogenously administered ribozymes.

Although it has been demonstrated that chemically synthesised ribozymes can be directly delivered to cells and tissues (Marschall *et al.*, 1994), the uptake efficiency of free delivery is extremely low. The success of ribozyme based therapeutics using such nuclease stable synthetic ribozymes is largely dependent, therefore, upon the development of delivery strategies which will improve cellular targeting and uptake. The optimisation of such strategies requires a fundamental understanding of the cellular uptake properties of synthetic ribozymes.

While a cellular mechanism has been widely described for the uptake of oligodeoxynucleotides (discussed in detail in section 1.4.2.1; for reviews see also; Akhtar and Juliano, 1992; Akhtar, 1995; Rojanasakul, 1996), there is a distinct lack of published information regarding the mechanisms of uptake of ribozymes and ribonucleotides. In fact, until this study (Fell *et al*, 1997), a detailed mechanism for cellular uptake of ribozymes had not been reported.

Exogenously administered ODNs reportedly enter cells by a combination of different endocytic mechanisms including fluid phase (pinocytosis), adsorptive and receptor-mediated endocytosis (for reviews, see section 1.4.2.1 and also Akhtar & Juliano, 1992; Reddy, 1996). Various specific oligonucleotide receptors have also been proposed including an 80-kDa cell surface protein (Loke *et al.*, 1989; Yakubov *et al.*, 1989), a 34-kDa membrane protein (Goodarzi *et al*, 1991; Kitajima *et al.*, 1992) and a 46-kDa protein (Akhtar *et al.*, 1996; Hawley and Gibson, 1996), although at the present time, there is no definitive evidence for a specific oligonucleotide uptake receptor of the Brown and Goldstein LDL-receptor type (Stein, 1997). The precise mechanisms of ODN uptake however appears to be dependant upon a whole host of factors including ODN length, chemistry, conformation, concentration and cell type as well as cell culture conditions

used (Akhtar, 1998). As synthetic ribozymes share many similar characteristics with antisense ODNs, such as large molecular weight, anionic charge and polar nature, it seems probable that ribozymes may enter cells by the same endocytic mechanisms, although the effect of partial modifications and secondary structure must be born in mind. Despite being termed "hammerhead," studies have shown that in solution, this motif actually adopts a defined "wishbone" configuration (Tuschl *et al.*, 1994; Scott *et al.*, 1995) and the extent to which this defined secondary structure affects cell association characteristics requires investigation. The physicochemical properties of modified ribozymes are likely to affect membrane transport since both chemistry and sequence have been shown to affect ODN uptake.

PS-ODNs have an increased affinity for the cell membrane and competitively inhibit the uptake of PO-ODNs (Stein, 1997). Consequently they are thought to at least partially share the same mechanism of entry, possibly through the same binding proteins and enter through either receptor-mediated endocytosis or adsorptive endocytosis. (Zhao *et al.*, 1993). Methyl-phosphonates, however, which are uncharged and lipophilic, do not compete with either PO- or PS-ODNs for uptake and are thought to enter cells by a distinct uptake pathway, namely by fluid phase endocytosis or by adsorptive endocytosis (Shoji *et al.*, 1991). In addition, other modifications have been shown to influence cellular uptake. Hughes *et al.* (1995) studied the membrane association of 2'-O-alkyl phosphorothioate oligonucleotides and reported that cell association increased with increasing length of the lipophilic 2'- moiety. Much of this increased association, however, was found to be due to accumulation of ODNs at the cell membrane rather than internalisation.

The evidence determining the effect of sequence on cellular uptake is equivocal. It has been reported that purine rich ODNs demonstrate greater cellular uptake than pyrimidine-rich sequences (Zhao *et al.*, 1993) and more recent research by Agrawal *et al.* (1996) suggests that sequence and the resulting secondary structure influences the magnitude of cellular association, since G rich ODNs that form tetraplexes were shown to become cell associated in greater quantities that other ODNs as a result of their defined secondary structure. Other studies, however, have failed to show any correlation between ODN sequence and cellular uptake (Yakubov *et al.*, 1989).

The objectives of this chapter were to characterise the properties of chemically modified ribozymes, which were intended to be used throughout this thesis, in terms of stability, catalytic activity and in particular cellular uptake characteristics. The specific chemical modifications applied to the ribozymes are shown in Figure 3.1 and consist of a hammerhead motif containing 5 ribose residues, with all remaining residues being 2'-O-methyl (2'-O-Me) nucleotides except at positions U_4 and / or U_7 which contained either 2-amino (2'-NH_2) modifications at positions U_4 and U_7 (designated RPI.4782) or 2'-C-allyl modification at U_4 only (designated RPI.5993). The chemical motif of these ribozymes has been reported to substantially enhance nuclease stability while preserving catalytic activity (Beigelman *et al.*, 1995a). Although such modifications can protect ribozymes against nuclease degradation, they can also have the inherent drawback of reducing the catalytic efficiency. Stability and activity were investigated to ensure that the chemical modifications applied to these ribozymes afforded suitable resistance to nuclease degradation for future *ex vivo* and *in vivo* work while still remaining biologically active.

Since at the time of this study, no mechanism for cellular uptake had been reported for chemically stable synthetic ribozymes, we addressed this issue by studying uptake of the chimeric ribozyme RPI.4782 using the human glioma cell line U87-MG as a model. These cells are derived from a grade III glioblastoma (Ponten & Macintyre, 1968) and have many of the distinguishing phenotypic features of malignant gliomas. Subsequent work was planned (see Chapter Four) to investigate the potential use of chemically stabilised synthetic ribozymes in down regulating the *c-erb*B1 oncogene, which encodes for the EGFr and has been shown to be both amplified and overexpressed in a number of cancer cells (Khazaie *et al.*,1993). In glioblastoma multiforme, a highly malignant form of brain cancer for which there is no effective cure, the amplification of the EGFr gene is one of the most consistent genetic alterations known, with the EGFr being overexpressed in approximately 40% of malignant gliomas (Black, 1991). The ribozymes used in this study was targeted against the 3'- untranslated region of EGFr mRNA.

3.2 MATERIALS AND METHODS

General materials and methods are detailed in Chapter Two. Any alterations, additions and specific methods relevant only to this chapter are given below.

3.2.1 Synthesis and Labelling of Nucleic Acid Sequences

A 37-mer hammerhead ribozyme designed against the 3'-untranslated region of the human EGFr mRNA was synthesised by Ribozyme Pharmaceuticals Inc. (Boulder, Colorado, USA) as described in section 2.1.2. The ribozyme contained site specific chemical modifications to increase stability (Figure 3.1). Most substitutions were with 2'-

O-methyl residues (nucleotide 2 in Figure 3.1) with five essential ribose residues situated within the 'catalytic core' of the molecule left unmodified to retain catalytic activity (nucleotide 1 in Figure 3.1). The remaining modifications were introduced at positions U_4 and / or U_7. Either 2'-amino residues (nucleotide 3 in Figure 3.1) were introduced at positions U_4 and U_7 (ribozyme designated RPI.4782) or alternatively a 2'-C-allyl group (nucleotide 4 in Figure 3.1) was introduced at position U_4 and a 2'-O-methyl group at U_7 (ribozyme designated RPI.5993). To resist exonucleases, a 3'-3'-linked thymidine (nucleotide 5 in Figure 3.1) or an abasic nucleoside was added at the 3'-end and the ribozyme contained four phosphorothioate linkages at the 5'-end.

To facilitate internal labelling, ribozyme RPI.4782 was synthesised in two halves with the junction 5'- to the GAA sequence in loop II. The following two fragment sequences (modified as described above and in Figure 3.1) were consequently produced.

Donor: 5'- gaa agg ccG aaA cug aac 'iT'-3'

Acceptor: 5'-$u_s g_s u_s g_s$ug ucU GAU Gag gcc-3'

In order to assess the *in vitro* catalytic activity of both the 2'-O-methyl / 2'-amino and the 2'-O-methyl / 2'-C-allyl modified forms of this ribozyme, a 15-mer, unmodified region of the target substrate molecule (5'-GUUCAGUCACACACA-3') was also synthesised by Ribozyme Pharmaceuticals Inc. All syntheses were performed on a 2.5μmol scale and were HPLC purified.

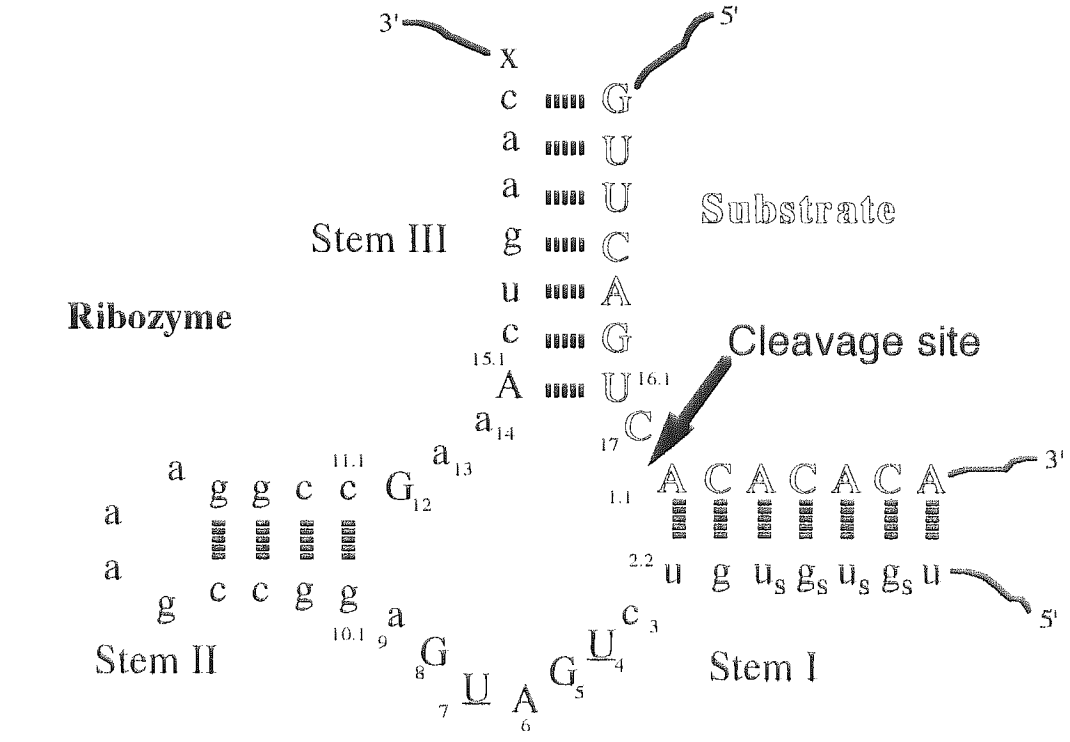

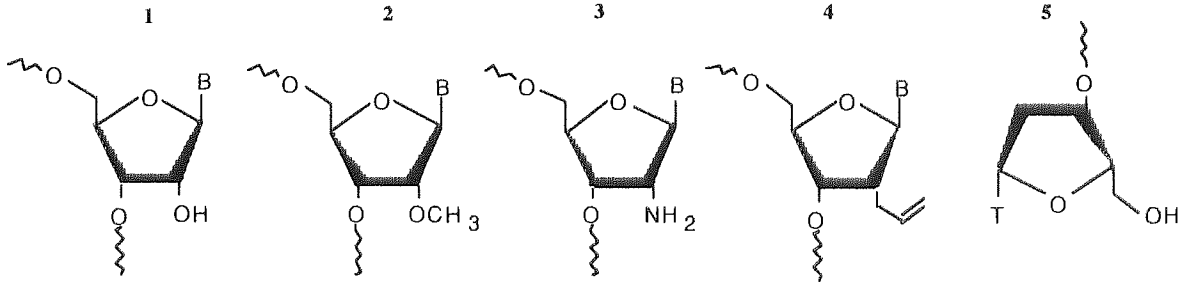

Figure 3.1 *The sequence and structure of a chimeric hammerhead ribozyme targeting epidermal growth factor receptor (EGFr) mRNA.* Conserved nucleotides within the central core are numbered according to Hertel *et al* (1993). Uppercase indicates 2'-hydroxyl (ribo) nucleotides (1). Lowercase indicates 2'-O-methyl nucleotides (2). U indicates modifications which are either 2'-amino (3) at positions U4 and U7 (ribozyme designated RPI.4782) or alternatively 2'-C-allyl (4) at position U4 and 2'-O-methyl at U7 (ribozyme designated RPI.5993). X indicates the addition of a 3'-3' inverted thymidine (5). The ribozyme contained four phosphorothioate linkages at the 5'-end; all other backbone linkages are phosphodiesters.

In addition, 37-mer ODNs, with a base sequence identical to that of the ribozyme were synthesised (0.2μmol scale) in both phosphodiester (PO-ODN) and phosphorothioate (PS-ODN) forms at Aston University, Birmingham, U.K. as described in section 2.1.1. An unmodified, all RNA version of the ribozyme was also synthesised (section 2.1.2.3). Following synthesis the ODNs and unmodified ribozyme were deprotected (sections 2.1.1.1; 2.1.1.2 and 2.1.2.4), desalted using Sephadex G-25 packed (NAP-10) columns (section 2.1.1.4) and lyophilised using a Savant DNA Speed Vac.

Ribozymes, substrates and ODNs were radiolabelled at the 5'-end with ^{32}P using using [γ-^{32}P]ATP (ICN, U.K.) and bacteriophage T4 polynucleotide kinase (Bioline, UK) as described in section 2.2.1. For internal labelling, ribozymes were synthesised in two halves with the junction 5' to the GAAA sequence in loop II. The 3'-half ribozyme portion was 5'-end labelled using T4 polynucleotide kinase and [^{32}P]ATP and then ligated to the 5'-half ribozyme portion using T4 RNA ligase (see section 2.2.2). Following radiolabelling, ribozymes, substrates and oligonucleotides were purified by native 20% polyacrylamide gel electrophoresis as described in section 2.3.1. Excised bands were eluted in 0.1% diethyl pyrocarbonate treated water, lyophilised and stored at –20°C.

3.2.2 Stability Studies

3.2.2.1 *Stability in Foetal Bovine Serum (FBS)*

Radiolabelled ribozymes / oligonucleotides were incubated in 100μl of FBS at 37°C to give a final concentration of 200nM. Samples (10μl aliquots) were removed at timed intervals, mixed with a loading buffer containing 9:1 v/v formamide:1 x TBE, 0.25%

xylene cyanol, 0.25% bromophenol blue, and frozen at –20°C prior to gel loading. Degradation profiles were analysed by 20% polyacrylamide (7M urea) gel electrophoresis and autoradiography of wet gels as detailed in sections 2.3.1 - 2.3.2.

3.2.2.2 *Stability in U87-MG Cell Supernatants*

U87-MG cells were seeded onto 24-well plates at a density of 1 x 10^5 cells / $well^{-1}$ as previously described (section 2.5) and used approximately 24 hours post seeding. Internally [^{32}P]-labelled ribozymes were added to 200μl of serum-free DMEM medium to give a final concentration of 0.01μM. Cells were then washed twice with PBS (2 x 0.5ml x 5 min) and then incubated with ribozyme containing medium at 37°C. 10μl aliquots of the apical solution were collected at variable time points over a period of 4 hours, mixed with an equal volume of formamide loading buffer (9:1 v/v formamide: 1 x TBE) and stored at –20°C. Prior to gel loading the samples were heated at 100°C for 5 minutes and separated on 7M urea / 20% PAGE (section 2.3.1) Bands were detected by autoradiography of wet gels (section 2.3.2).

3.2.2.3 *Intracellular Stability in U87-MG Cells*

U87-MG cells were seeded onto 24-well plates at a density of 3 x 10^4 cells/well as described in section 2.6 and used approximately 24 hours post-seeding. Cells were incubated with 0.1μM internally [^{32}P]-labelled ribozyme for varying time points over a 96 hour period. At each time point, cells were washed twice with PBS (2 x 0.5ml x 5min), lysed and harvested from the wells as described in section 2.7.1.2. Aliquots of 2μl were mixed with formamide loading buffer and stored at –20°C prior to gel loading.

Degradation profiles were analysed by 20% PAGE containing 7M urea (section 2.3.1) and detected by autoradiography of wet gels (section 2.3.2).

3.2.3 Cell Association Studies

Cell culture conditions and the experimental procedure undertaken for all cell association studies are detailed in sections 2.4 and 2.5..

3.2.3.1 Assay to Determine the Number of PBS-Azide Washes

Cells were seeded onto 24-well plates at a density of 1 x 10^5 cells / well and used approximately 24 hour post-seeding. Cells were incubated for 1 hour at 37°C with 0.01μM internally [^{32}P]-labelled ribozyme RPI.4782 as described in section 2.5. Following incubation, cells were washed with ice-cold PBS-azide (0.05% w/v sodium azide in sterile PBS) (0.5ml x 5min) an increasing number of times i.e. from 1 wash (protocol A) to 4 washes (protocol D), The radioactivity associated with the apical samples, respective wash samples and cell fractions from each assay were counted by LSC (section 2.3.3).

3.2.3.2 *Cell Association of Radiolabelled Mannitol.*

To assess the cell association of the fluid phase D-[1-^{14}C] Mannitol marker, cell association studies were performed as described in section 2.5 except radio-labelled ribozyme was replaced with D-[1-^{14}C] Mannitol (Amersham Life sciences, Amersham, U.K.). Quantities of radiolabelled mannitol in each of the three fractions collected were assessed by LSC. In this case, however, fractions were added to 10ml of Optiphase Hi-

safe 3 (Pharmacia-Wallace, St.Albans, U.K.) and counted for 10 minutes using an appropriate programme for the detection of ^{14}Carbon.

3.2.3.3 *The Effect of Time and Temperature on Cellular Association*

The cells were seeded onto 24-well plates as previously described and used approximately 24 hour post-seeding (section 2.5). U87-MG monolayers were incubated with 0.01μM internally [^{32}P]-labelled ribozyme at 37°C for varying time periods (30 minutes, 1h, 2h, and 4h). For low temperature experiments (at 4°C), the following amendments were adopted. After the required growth period (24 hour post seeding), cells were washed twice with ice-cold sterile PBS (2 x 0.5 x 5min at 4°C). The washing solution was aspirated and replaced with 200μl of serum-free DMEM medium containing the radiolabelled ribozyme. The serum free medium containing the ribozyme had been equilibrated at 4°C for 15 minutes prior to addition to the cells. Cells were then incubated at 4°C for the required times in parallel with the experiment conducted at 37°C.

3.2.3.4 *Efflux of Intracellular Ribozyme*

The cells were seeded onto 24-well plates as previously described and used 20-24 hour post-seeding (section 2.5). For efflux studies, cells were incubated for 2 hours at 37°C with 0.01μM ribozyme in serum-free medium. After incubation, the apical medium was removed, the cells washed with PBS (3 x 0.5ml), and 0.5ml of fresh serum-free medium (without the addition of ribozyme) was added. The efflux of internalised ribozyme was monitored at fixed intervals over 4 hours. At each timed interval, 0.5ml of serum-free medium was removed and equivalent of fresh serum-free medium was added. The

radioactivity pertaining to all fractions collected was determined by LSC as described in section 2.3.3.

3.2.3.5 *The Effect of Metabolic Inhibitors on Cellular Association*

The cells were seeded onto 24-well plates as previously described and used approximately 24 hour post-seeding (section 2.5). U87-MG monolayers were pre-incubated with 10mM sodium azide / 20mM 2-deoxyglucose (Sigma, Poole, U.K.) for 60 minutes at 37°C in serum-free medium. After pre-treatment, the cells were incubated with 0.01μM internally [^{32}P]-labelled ribozyme RPI.4782 for a further 60 minutes in the continuing presence of the inhibitors.

3.2.3.6 *The Effect of pH on Cellular Association*

The cells were seeded onto 24-well plates as previously described and used 20 - 24 hour post-seeding (section 2.5). For these experiments an incubation solution of hank's balanced salt solution (HBSS) containing 0.01% phenol red, 5mM D-glucose and buffered with 25mM HEPES (pH 7.0 & 8.0) or MES (pH 5.0 & 6.0) was used instead of serum-free DMEM medium. The pH adjusted incubation solution was filter sterilised using 0.2μM cellulose acetate bottle filters (Costar, U.K.) and stored at 4°C. U87-MG cells were incubated with 0.01μM ribozyme for 60 minutes at 37°C at pH 5.0, 6.0, 7.0 and 8.0.

3.2.3.7 *Octanol:Aqueous Buffer Distribution Coefficients*

The distribution between n-octanol and aqueous incubation solution (section 3.2.4.6) was determined over a range of pH 5 to 8. Prior to distribution studies, the two immiscible phases were pre-saturated at room temperature by shaking for 24 hours. Trace amounts of internally [^{32}P]-labelled ribozyme were then added to the phases and shaken for three hours. Samples from each phase were taken and counted using LSC (section 2.3.3). Data are expressed as log distribution coefficient (log D) between the two phases, where log D = log $[\text{ribozyme}]_{\text{octanol}}$ / $[\text{ribozyme}]_{\text{aqueous incubation solution}}$.

3.2.3.8 *The Effect of Post-uptake Trypsin Washing*

U87-MG cells were seeded onto 24-well plates as previously described and used 20 - 24 hour post-seeding (section 2.5). After the required growth period, cell monolayers were incubated with 0.01μM internally [^{32}P]-labelled ribozyme RPI.4782 for a period of 60 minutes. To remove surface-bound ribozyme, after washing with ice-cold PBS-azide, cells were treated with 200μl of trypsin-EDTA until all cells came off the wells. PBS (1ml) was then added, and the cells were recovered by centrifugation at 1000rpm for 5 minutes. The supernatant was collected, and cells were then resuspended in a further 1ml of PBS. The cell-associated radioactivity pertaining to both fractions (washing solution and cell) was determined by LSC.

3.2.3.9 *The Effect of Competitors on Cellular Association*

Competition studies were performed as described in section 2.5 with the following additions. Following initial washings with PBS, cells were pre-incubated with potential

competitors for a period of 15 minutes at 37°C. Cells were then incubated at 37°C with 0.01μM internally [^{32}P]-labelled ribozyme RPI.4782 in the continued presence of the competitors. Salmon testes DNA (molecular biology grade), the nucleotide monomer dATP (molecular biology grade), dextran sulphate and heparin (sodium salt, Grade I-A, cell culture tested) were all purchased from Sigma (Poole, U.K.).

3.2.3.10 *The Effect of Cell Line on Cellular Association*

Cellular association was investigated in a range of human cell lines and the procedure described in section 2.5 followed. The cells were seeded onto 24 well plates in the following manner in order to achieve 70-90% confluency: U87-MG cells were seeded at 1 x 10^5 cells/well as previously described (section 2.5); A431 cells were seeded at a density of 7.5 x 10^4 cells/well, 24 hours prior to the experiment; Raw 264.7 cells were plated out at a density of 5 x 10^5 cells/well, 24 hours prior to the experiment; Caco-2 cells were cultured onto 24 well plates at a density of 2 x 10^5 cells/well and used for uptake studies 7 days post seeding.

3.2.3.11 *Subcellular Distribution of Fluorescently Labelled Ribozymes.*

5'-FITC labelled ribozymes were synthesised and purified as described in section 2.2.3. Fluorescein isothiocyanate (free FITC) was obtained from Sigma (Poole, U.K.). For experiments concerning the subcellular distribution of ribozymes, cells were seeded at a density of 2 x 10^4 cells per well onto plastic chamber slides (Nunc, Gibco, U.K.) and incubated at 37°C in DMEM medium containing 10% FBS for 24 hours. Following the required growth period, cells were washed carefully with serum-free medium at 37°C (2 x 100μl per well).

The FITC-labelled ribozyme (or free FITC) was diluted to the required concentration (10μM) in serum-free DMEM medium and equilibrated to 37°C prior to the experiment. The ribozyme or free fluorophore containing medium was added to the wells in a total volume of 300μl per well and the cells incubated at 37°C for the required time period. Following incubation cells were carefully washed six times with serum-free medium (6 x 100μl x 1min) to remove all traces of non-associated fluorophores. Cells were then fixed with 2% v/v paraformaldehyde in PBS (1 x 100μl per well) for 30 minutes at room temperature. The fixative was then removed, the cells washed twice with PBS (2 x 100μl per well) and the plastic chamber gasket separated from the slide. Cells were mounted in a drop (10μl) of Vector Shield®, an anti-fading agent which enhances fluorescein detection, and a cover slip added.

Cells were then observed under an inverted Jenamed fluorescence microscope (Jena Instruments, Oberkochen, Germany). A 510nm wavelength blocking filter was used for detection of fluorescein as supplied by the microscope manufacturers. Cells were photographed using an Olympus camera with Jenamed adapter and Kodak colour film (iso 200).

3.3 RESULTS AND DISCUSSION

3.3.1 Stability of Chemically Modified Ribozymes

A molecule designed to be used as a drug must be sufficiently stable to resist the harsh environment of the biological milieu and remain intact long enough to reach its target site. As stated previously (section 1.3), RNA is notoriously unstable and extremely susceptible to the action of biological nucleases. Consequently, chemical modifications were applied to the ribozymes used in this study (see Figure 3.1) which have been reported to enhance ribozyme stability significantly (Beigelman *et al.*, 1995a). It was necessary, before proceeding with cellular association and efficacy studies, to validate this claim and investigate the extent of enhanced nuclease resistance afforded by these modifications ensuring the suitability of these ribozymes for future *in vitro* and *ex vivo* work.

3.3.1.1 *Stability of 2'- Modified Chimeric Ribozymes in Foetal Bovine Serum (FBS)*

A comparative stability study was undertaken in 100% FBS to compare the degradation profiles of the two chemically modified ribozymes, RPI.4782 (2'-O-methyl / 2'-amino modified) and RPI.5993 (2'-O-methyl / 2'-C-allyl modified), to those of unmodified RNA, phosphodiester (PO) and phosphorothioate (PS) oligodeoxynucleotides of the same sequence (Figure 3.2). Serum displays substantial nuclease activity and serum stability is frequently used in the antisense field as a general indication of the extra-cellular stability of molecules *in vivo*. Although the nuclease activity of sera derived from different species varies, foetal bovine serum is reportedly more active than either mouse serum or indeed human serum (Crooke, 1992).

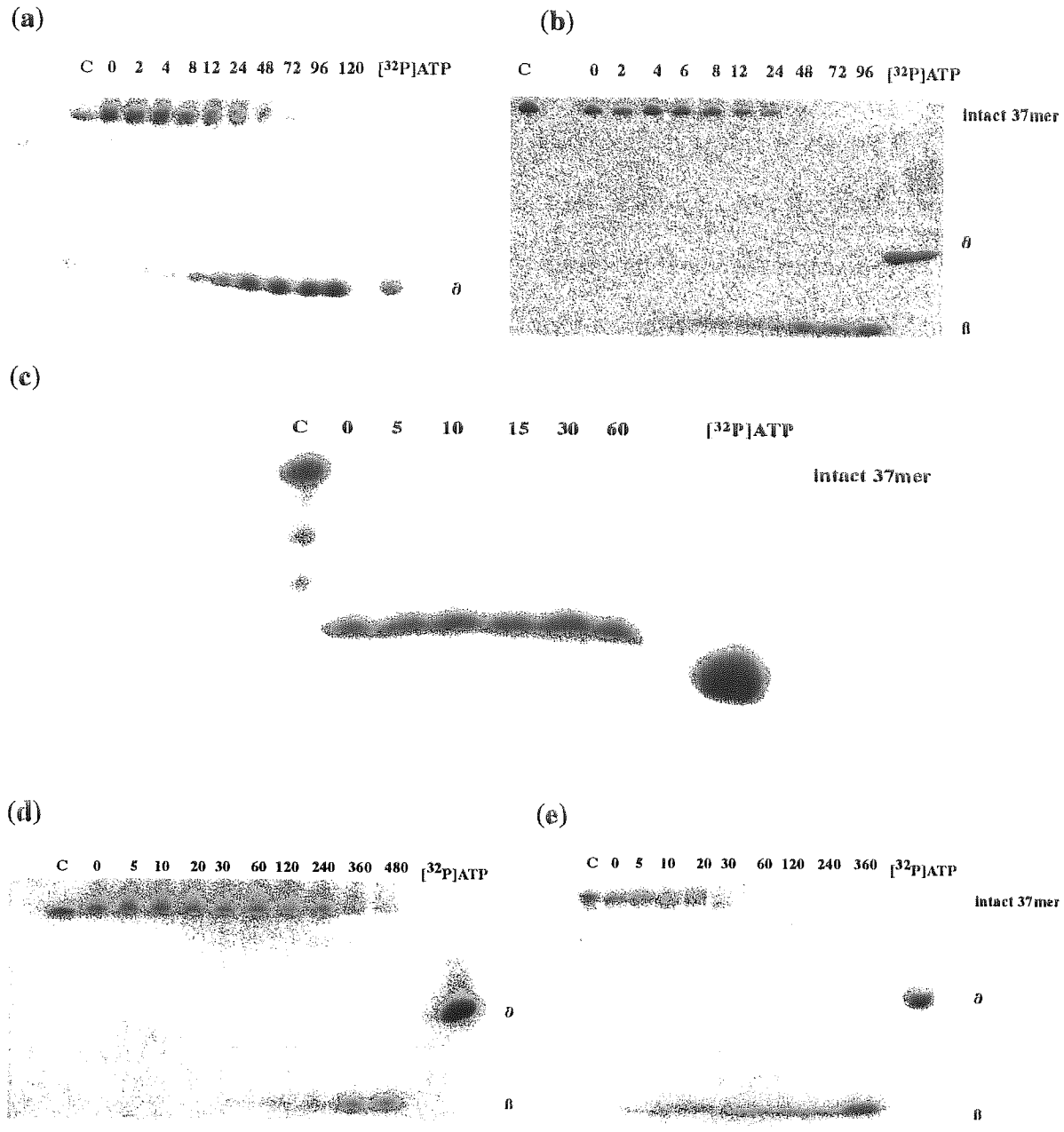

Figure 3.2 *Degradation of 5'-end [^{32}P]-labelled nucleic acids in foetal bovine serum* (FBS). Degradation profiles of (a) 2'-O-Me / NH_2 modified ribozyme RPI.4782. (b) 2'-O-Me / C-allyl modified ribozyme RPI.5993. (c) Unmodified (all RNA) ribozyme. (d) PS-ODN. (e) PO-ODN. Ribozymes and ODNs were added to neat FBS at a concentration of 200nM and incubated at 37°C for the time intervals indicated. Degradation times are given in hours for (a)and (b) and in minutes for (c) – (e). The control C represents unexposed ribozyme / ODN. Zero time represents minimal exposure to FBS before sample removal. Band ∂ is a degradation product which comigrates with the monomer [^{32}P]ATP and band ß is free phosphate. Degradation profiles were analysed by 20% PAGE (7M urea).

The chemical modifications applied to both these ribozymes resulted in a substantial increase in stability over that of unmodified RNA, with the chimeric ribozymes showing over a 4000-fold improvement in nuclease resistance over that of the all RNA ribozyme which was completely degraded within the time it took to add the RNA to serum, mix and quench the reaction (Figure 3.2c). Analysis of the band intensities of the results shown in the autoradiographs of Figure 3.2 are summarised graphically in Figure 3.3

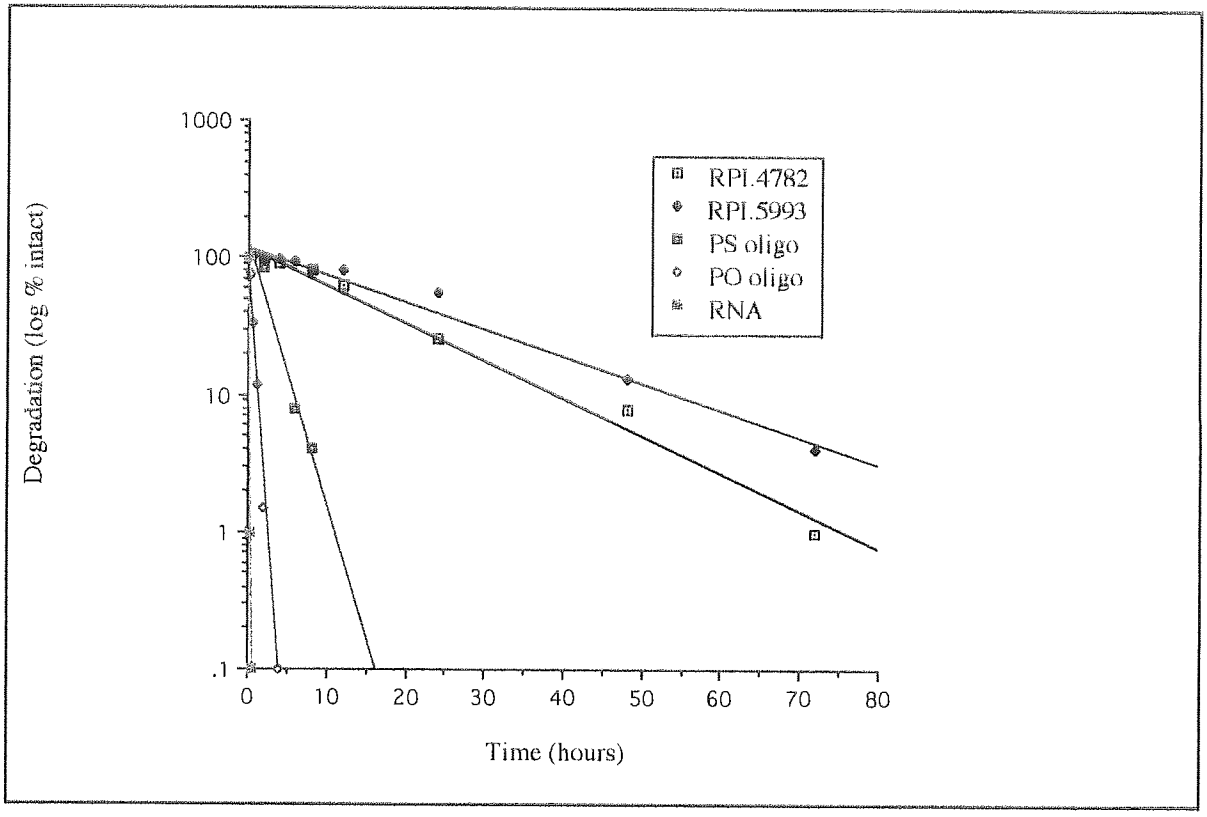

Figure 3.3 *Graphical representation of the comparative stabilities of chimeric ribozymes with unmodified RNA and modified ODNs in FBS.* Ribozymes and oligonucleotides were added to 100% FBS at a concentration of 200nM and incubated at 37°C for the time periods indicated. Degradation profiles were analysed by 20% PAGE (7M urea), quantified by densitometry of gel analysis and expressed as log of the percentage intact DNA /RNA remaining with time. Approximate stability half-lives are: ribozyme RPI.5993- 21hrs; ribozyme RPI.4782- 18hrs; PS-ODN- 5hrs; PO-ODN – 10min; all RNA ribozyme - < 30sec.

The half-lives of ribozymes RPI.5993 and RPI.4782 were approximately 21 hours and 18 hours respectively indicating that the 2'-O-methyl / 2'-C-allyl modified ribozyme conferred slightly more resistance to degradation than the 2'-O-methyl / 2'-amino modified ribozyme. Both chimeric ribozymes were substantially more stable in FBS than either PO- or the PS-ODNs: their approximate half-lives being 10 minutes and five hours respectively. Thus, under the conditions of this experiment, the chemically modified ribozymes proved to be the most stable to nuclease degradation, the order of stability being as follows: 2'-O-methyl / 2'-C-allyl modified ribozyme RPI.5993 > 2'-O-methyl / 2'-amino modified ribozyme RPI.4782 > PS ODN > PO ODN > unmodified RNA.

It must be noted, however, that all the nucleic acids were 5'-end labelled and as a result, degradation products may denote dephosphorylation at the 5'-end by phosphatases rather than by the action of exo- and endo- nucleases. Consequently, an internal radiolabel was incorporated into ribozyme RPI.4782 (which had been synthesised in two halves to facilitate this procedure; see section 2.2.2) and the stability of the internally labelled ribozyme in FBS (Figure 3.4) was compared to that of the 5'-end label. The incorporation of the internal radiolabel was intended to reduce the effects of phosphatases which act at the 5-end of the molecule to remove the [^{32}P] radiolabel.

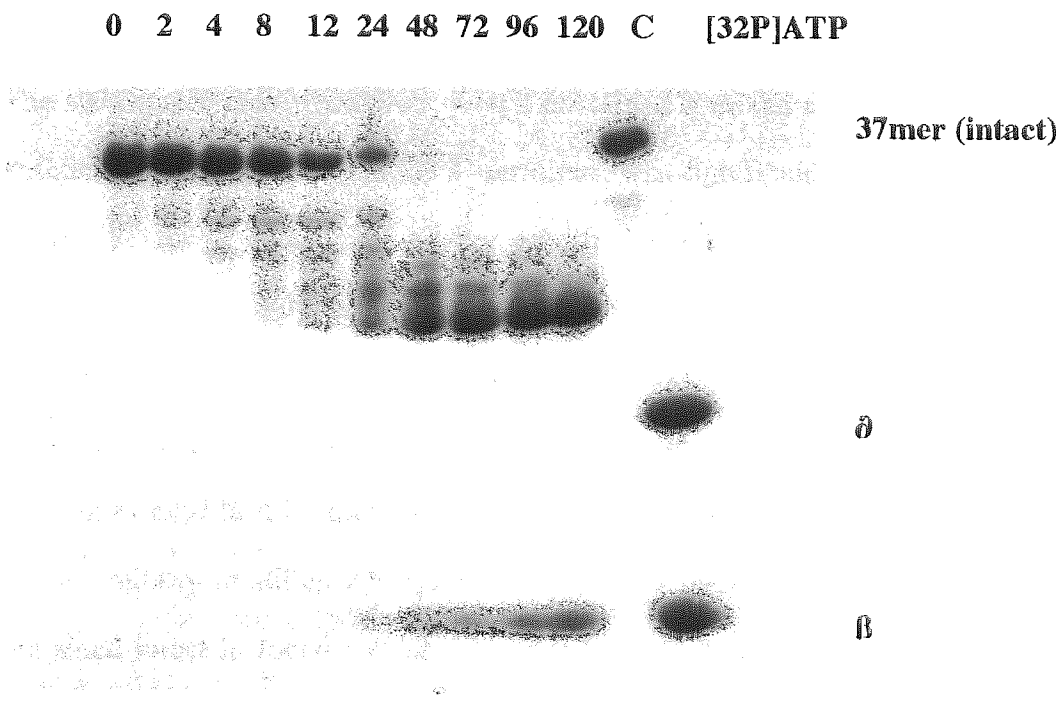

Figure 3.4 *Stability of internally [^{32}P]-labelled 2'-O-methyl / 2'-amino modified ribozyme RPI.4782 in 100% foetal bovine serum* (FBS). Ribozyme was added to 100% FBS at a concentration of 200nM and incubated at 37°C for the time intervals indicated. Degradation profiles were analysed by 20% PAGE (7M urea). Degradation times are given in hours (zero time represents minimal exposure of ribozyme to FBS before sample removal). The control (C) represents unexposed 37-mer ribozyme. Band ∂ is a degradation product which co-migrates with the monomer [^{32}P]ATP and band ß is free phosphate.

It was interesting to note that although the patterns of degradation were clearly different for the internally labelled ribozyme (Figure 3.4) and the 5'-end labelled ribozyme (Figure 3.2a), the kinetics of degradation were strikingly similar ($t_{1/2}$ of approximately 18 hours for both). This suggests that there was little phosphatase activity in the assays undertaken for this study. The 'laddering' effect of banding of degradation for the internally labelled ribozyme indicates either the progressive shortening of the ribozyme by the action of exo-nucleases, probably working at the 5'-end in view of the protection offered by the inverted T residue at the 3'-end, and/or possibly the action of endonucleases which cleave RNA at the unmodified sites of the ribozyme.

The stability of both ribozymes, which contained a mixed chemistry backbone together with an inverted T residue at the 3'-terminus, was significantly greater than that reported by many groups investigating other modified ribozymes. For example, Paolella *et al* (1992) found that only 30% of a 2'-O-allyl modified ribozyme remained intact in neat FBS after 2 hours, while Goodchild *et al* (1992), who used a 2'-O-methyl modified ribozyme, reported a half-life of approximately 15 minutes. Indeed, the stability of the ribozymes used in this study approaches that observed by Beigelman *et al* (1995a), who using similarly modified ribozymes, showed that these chemically stabilised ribozymes remained intact in foetal calf serum for at least 48 hours. It is acknowledged, however, that the nuclease activity in FBS varies considerably between batches and it is therefore difficult to make direct comparisons with other studies.

3.3.1.2 Stability of 2'-Modified Chimeric Ribozymes in U87-MG Cell Supernatants

To ensure that any findings obtained from proposed cellular association studies represented the uptake of intact 37-mer ribozyme and not that of shorter degraded fragments or free [^{32}P] label, the degradation of 5'-end and internally [^{32}P]-labelled 2'-O-methyl / 2'-amino modified ribozyme RPI.4782 was examined while incubated with U87-MG cell monolayers in serum free medium i.e. under the same conditions used for cellular association experiments. As Figure 3.5 demonstrates, the internally labelled ribozyme remained intact throughout the four hour incubation period (Figure 3.5a), while the 5'-end labelled ribozyme did exhibit increasing degradation after only 30 minutes (Figure 3.5b).

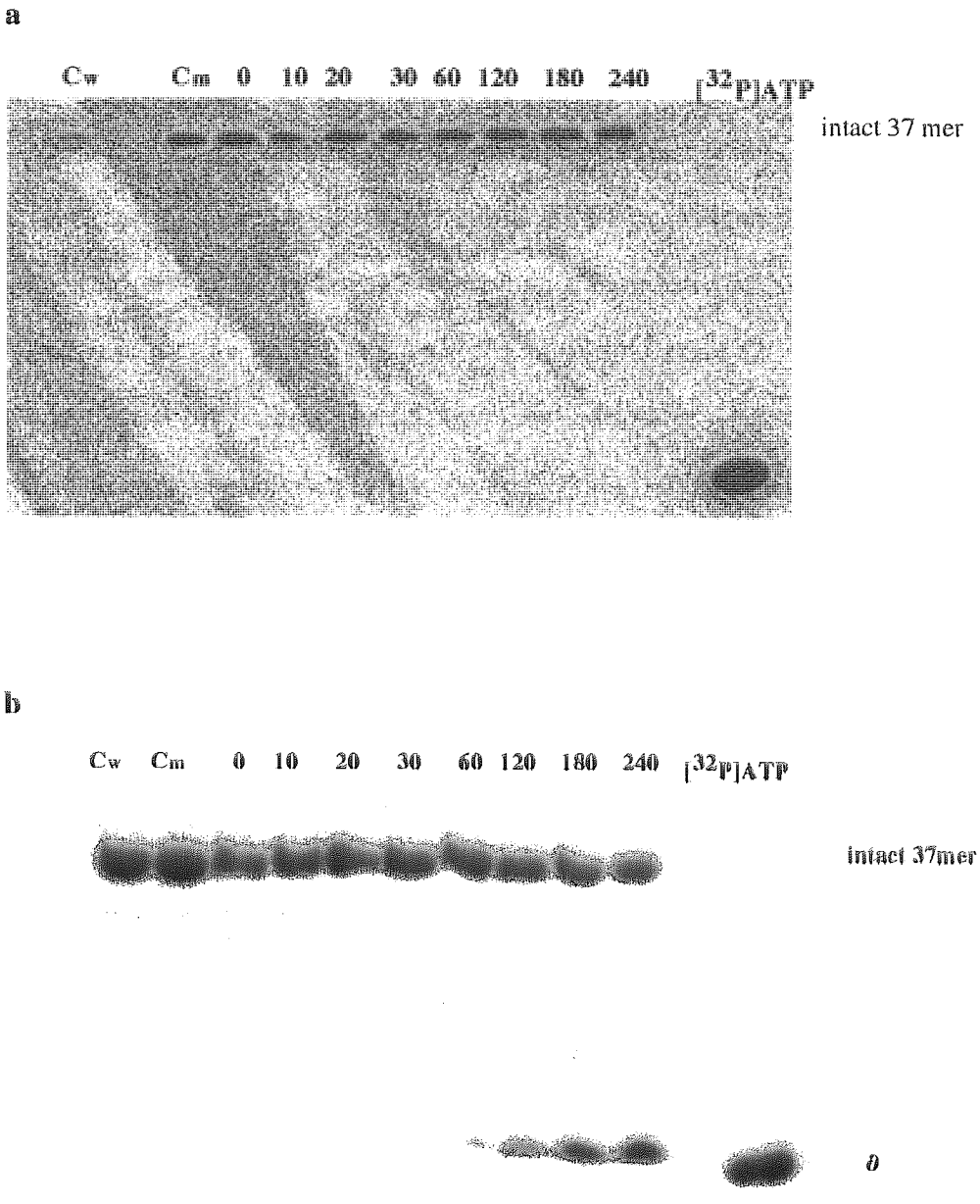

Figure 3.5 *Stability of 2'-O-methyl / 2'-amino modified ribozyme RPI.4782 in U87-MG monolayer apicals.* (**a**) degradation of internally [^{32}P]-labelled ribozyme RPI.4782. (**b**) degradation of 5'-end [^{32}P]-labelled ribozyme RPI.4782. The ribozyme was added to U87-MG cell culture in serum-free medium at a final concentration of 10nM. The ribozyme / substrate were recovered from the cell medium at variable time points and analysed on 20% PAGE (7M urea). Degradation times are given in minutes. Cw represents intact ribozyme in sterile water. Cm represents ribozyme in serum-free medium at time 240 min.

This demonstrates the importance of using an internal radiolabel for cell association studies. Phosphatase activity, which results in the removal of the 5'-end [^{32}P] radiolabel, may cause erroneous results due to the fact that the uptake of free phosphate is measured rather than that of the intact ribozyme. The free phosphate may have different uptake characteristics to the full-length molecule. This result also highlights the need for caution when interpreting data from previous published research into ODN uptake. In earlier studies some researchers used 5'-end labelled ODNs without fully assessing the stability of these nucleic acids under the experimental conditions used. For instance, Loke *et al.* (1989) measured the uptake of 5'-end acridine labelled ODNs over a period of up to 50 hours without any attempt to monitor the stability of the ODN during this time. Similarly, in an article on the importance of calcium concentration on cellular uptake Wu- Pong *et al.*(1994b) used 5'-end [^{32}P] radiolabelled PO-ODNs without providing any evidence of its stability.

3.3.1.3 Stability of 2'-Modified Chimeric Ribozymes Extracted from U87-MG Cells

Future efficacy studies will involve the addition of ribozymes to cells for periods of up to 4 days (96 hours). To establish the stability of the ribozyme for this period, internally labelled ribozyme RPI.4782 was extracted from U87-MG cells as described in section 3.2.2.3. The results, as shown in Figure 3.6, were extremely encouraging since over 60% of the ribozyme remained intact even after 96 hours.

All of the above stability assays demonstrate that both the 2'-O-methyl / 2'-C-allyl modified ribozyme and the 2'-O-methyl / 2'-amino modified ribozyme offer significant resistance to the many nucleases present in the biological environment and that either of

the chimeric ribozymes are sufficiently stable to use with confidence in future *ex vivo* and possible *in vivo* experiments.

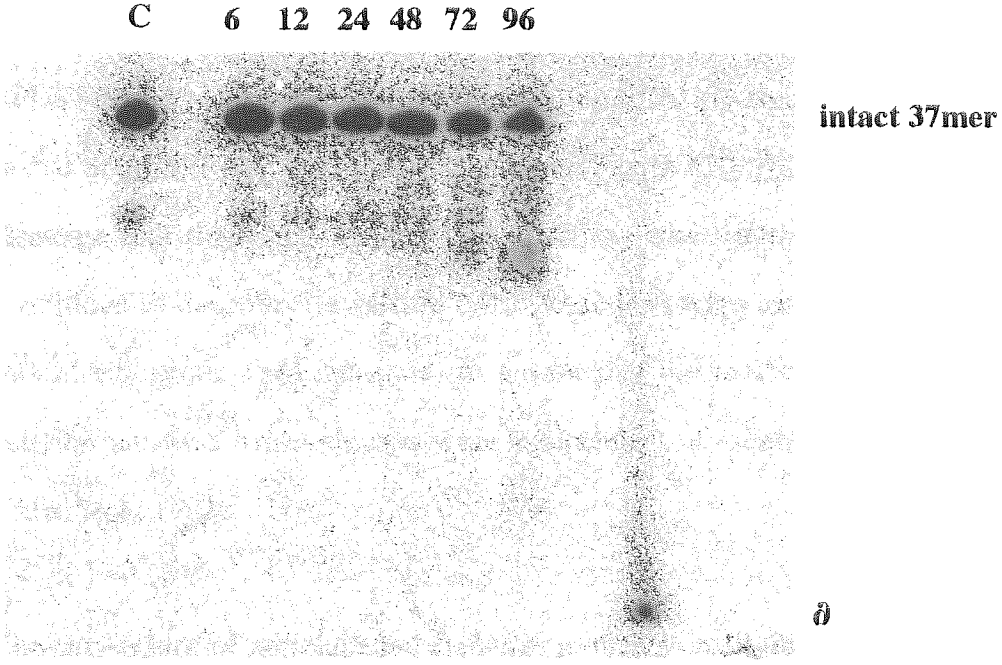

Figure 3.6 *Intracellular stability of internally [^{32}P]-labelled 2'-O-methyl / 2'-amino modified ribozyme RPI.4782 in U87-MG cells.* The ribozyme was added to U87-MG cell culture in serum-free medium at a final concentration of 0.1μM. The ribozyme was recovered from lysed cells at variable time points and analysed on 20% PAGE (7M urea). Incubation times are given in hours. C represents intact ribozyme in sterile water.

3.3.2 Kinetic Characterisation of Chemically Modified Ribozymes

Chemical modifications which enhance nuclease resistance can often have the inherent drawback of reducing catalytic efficiency (as detailed in section 1.3). Consequently the two chimeric ribozymes RPI.4782 and RPI.5993 were tested for their ability to cleave the target substrate *in vitro*.

3.3.2.1 In vitro Cleavage Activity under Single Turnover Conditions

To examine whether or not the chemical modifications applied had any effect upon the catalytic activity, the activity of both the 2'-O-methyl / 2'-C-allyl modified ribozyme RPI.5993 and the 2'-O-methyl / 2'-amino modified ribozyme RPI.4782 were compared to that of an all RNA, unmodified ribozyme (Figure 3.7). Ribozyme activity, expressed as cleavage half-time ($t_{1/2}$) against the substrate, was determined under single turnover conditions as described in section 2.8.2. Reactions were carried out with enzyme excess (40nM ribozyme: 1nM substrate) to ensure that the reactions were first order and that activity half-time measurements were independent of substrate concentration (Fedor and Uhlenbeck, 1992).

The appearance of radiolabelled cleavage products on all three autoradiographs in Figure 3.7 indicates that all the ribozymes retained the ability to cleave the target substrate. It can be seen that in each case after 20 minutes that majority of the substrate had been cleaved. In order to compare the rate and extent of cleavage, the intensity of the autoradiograph bands were quantified as described in section 2.3.2.2 and the activity half-time ($t_{1/2}$) calculated from semi-logarithmic plots of the amount of substrate remaining versus time (Figure 3.8) as described in section 2.8.2.

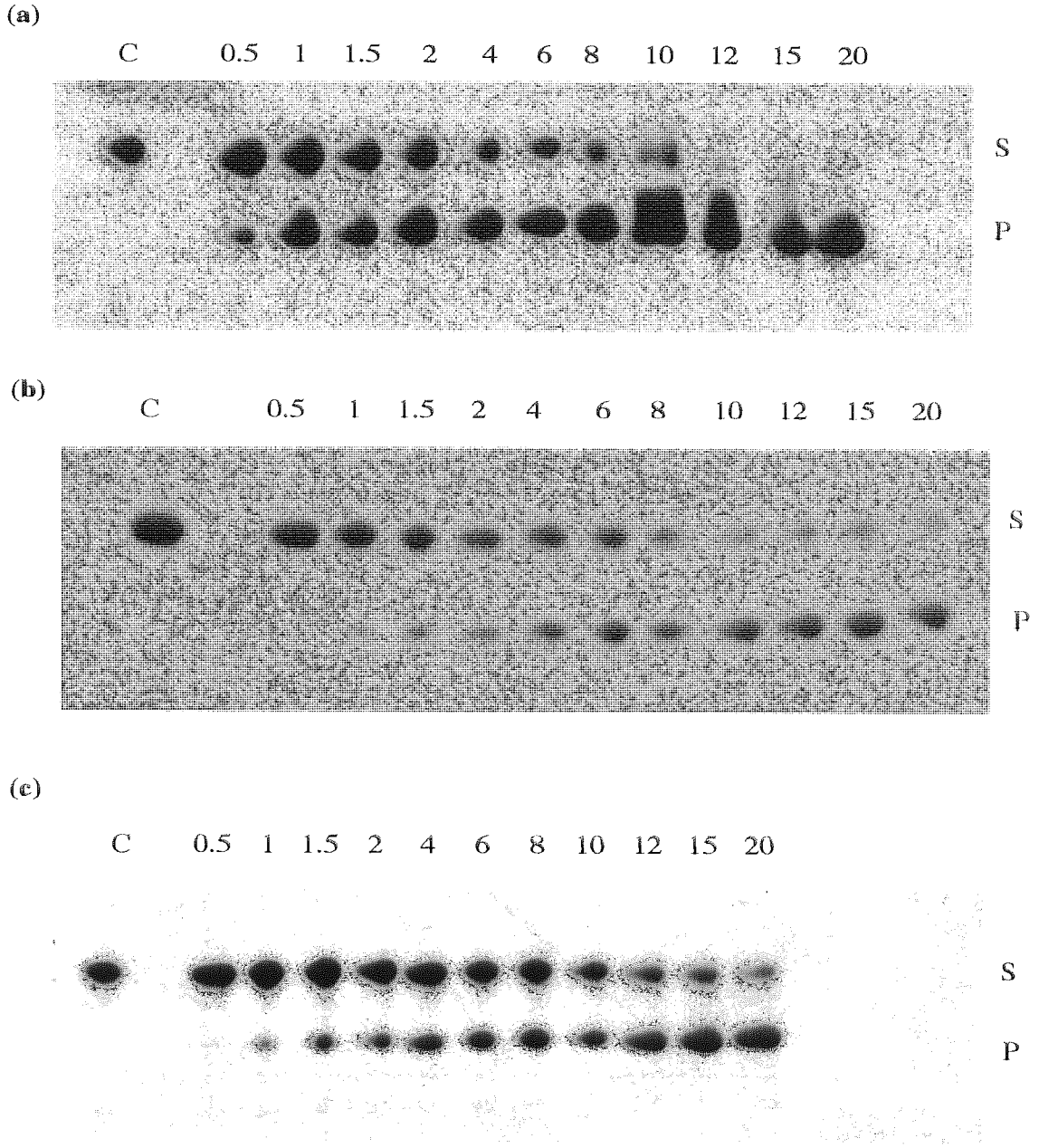

Figure 3.7 *Autoradiographs demonstrating the in vitro cleavage activity of 2'-O-methyl modified chimeric ribozymes under single turnover conditions.* (**a**) activity of all RNA unmodified ribozyme; (**b**) activity of 2'-O-Me / NH_2 modified ribozyme RPI.4782; (**c**) activity of 2'-O-Me / C-allyl ribozyme RPI.5993. Reactions were performed in the presence of 50mM Tris.HCl (pH 7.5), 10mM $MgCl_2$ at 37°C as described in sections 2.8.1-2.8.2. Reaction times, in minutes, are given above the lanes. C represents intact substrate in Tris.HCl buffer without the addition of ribozyme. Band S refers to intact substrate and band P refers to cleaved product.

The unmodified ribozyme cleaved the target substrate at the fastest rate, the half-life of the substrate being only 1.43 minutes. Although applied chemical modifications did impede the cleavage rate slightly, both modified ribozymes exhibited high activity with the activity half time of the 2'-O methyl / 2'-amino modified ribozyme being only 2.41 minutes and the activity half time of the 2'-O-methyl / 2'-C-allyl modified ribozyme being slightly slower at 4.24 minutes.

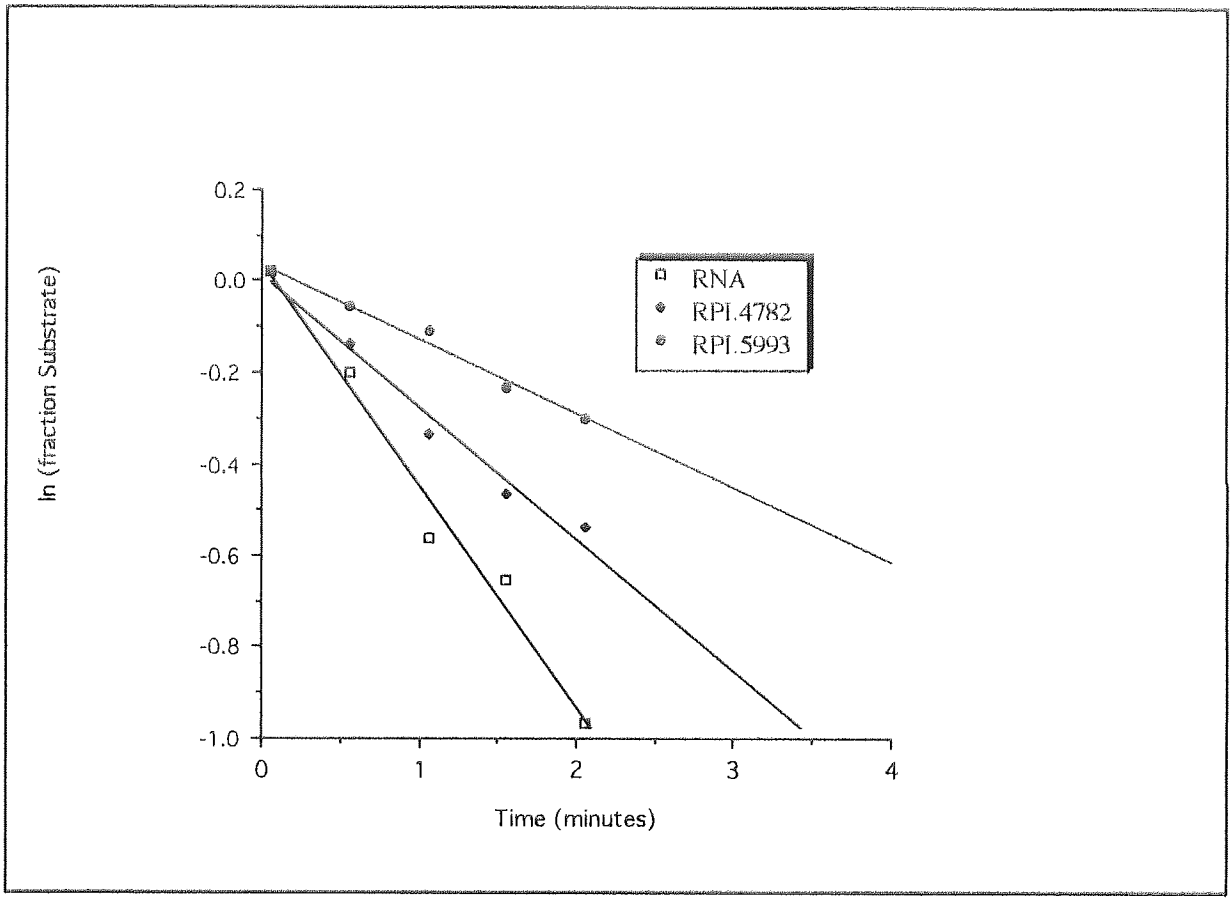

Figure 3.8 *Time course of in vitro activity profiles comparing 2'-O-methyl / 2'-C-allyl and 2'-O-methyl / 2'-amino chimeric ribozymes with an unmodified RNA ribozyme of the same sequence under single turnover conditions.* Activity half-times are: all RNA ribozyme - 1.4min; ribozyme RPI.4782- 2.4min; ribozyme RPI.5993- 4.2min.

The high activity of both these chimeric ribozymes is in agreement with the findings of Beigelman *et al.* (1995a) who reported that ribozymes of a different sequence but modified in the same manner as those in this study exhibited almost wild type activity, with activity half-times *in vitro* being under 3 minutes.

A ratio of relative stability / activity half-times can be used to compare the performance of the ribozymes considered in this study. The results are summarised in Table 3.1 below. It is clear that the benefits of enhanced nuclease resistance far outweigh the slight impairment in catalytic activity that results from applying such chemical modifications. There is absolutely no point in administering highly active unmodified ribozymes that will degrade before reaching the target site! In overall performance terms, there is little to distinguish the two chimeric ribozymes used in this study; both appeared to be stable and active. While the *in vitro* activity of the 2'-O-methyl / 2'-amino modified ribozyme was superior to that of the 2'-O-methyl / 2'-C-allyl modified ribozyme, the latter proved to be the more stable.

Table 3.1. *Summary stability and cleavage activity of chimeric ribozymes.*

Chemical Modifications	**Stability half-life* (minutes)**	**Activity half-time** (minutes)**	**Relative stability/activity**
None – all RNA	0.25	1.4	0.18
2'-O-methyl / 2'-amino (RPI.4782)	1080	2.4	450
2'-O-methyl / 2'-C-allyl (RPI.5993)	1260	4.2	300

*estimated ribozyme stability expressed as half-life of ribozyme in 100% FBS at 37°C
**estimated ribozyme activity expressed as cleavage half-time against substrate

3.3.2.2 In Vitro Catalytic Activity under Multiple Turnover Conditions

While multiple turnover may not be essential for utility, it seems desirable that the ribozyme act in a truly catalytic fashion under physiological conditions. Such conditions, where the concentration of substrate is in excess of ribozyme would, in theory, result in multiple turnover as the cleavage of several substrate molecules occurs. Consequently lower concentrations of ribozyme would be required than other potential drugs, such as antisense oligonucleotides, which do not have the advantage of enzymatic properties.

The kinetic characteristics of the most active modified ribozyme, RPI.4782, were examined further to verify the true catalytic nature of such ribozymes and to determine the kinetic parameters K_m and k_{cat} in order that the activity of this construct may be compared with other ribozymes / enzymes. The reactions were performed under multiple turnover conditions (i.e. excess substrate – see section 2.8.3) and initial cleavage reaction velocities were measured at several substrate concentrations that were at least ten fold greater than the ribozyme concentration of 10nM (see Figure 3.9 for representative autoradiographs of these reactions). Initial reaction velocities were determined via analysis of autoradiograph bands as described in section 2.8.3 and reaction velocities plotted against time (see Figure 3.10).

Reaction rates appeared to follow saturation kinetics with respect to concentration of substrate. As Figure 3.10 demonstrates, cleavage rates appeared to be first-order at low substrate concentrations, however, as the concentration of substrate increased, the reaction rates levelled off suggesting that ribozymes were effectively saturated with substrate. These results suggest that the ribozyme did indeed exhibit multiple turnover catalysis indicating that the cleavage reaction was truly catalytic. The data, therefore,

were amenable to analysis using Michaelis -Menten rate equation of enzyme kinetics (Ferscht, 1977).

(a) 10nM ribozyme : 300nM substrate

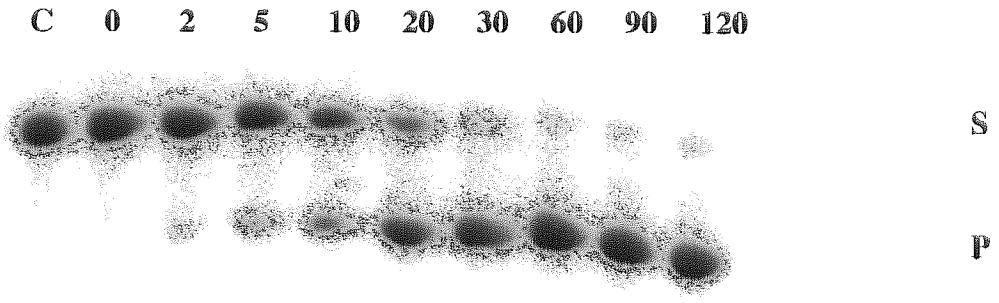

(b) 10nM ribozyme : 1μM substrate

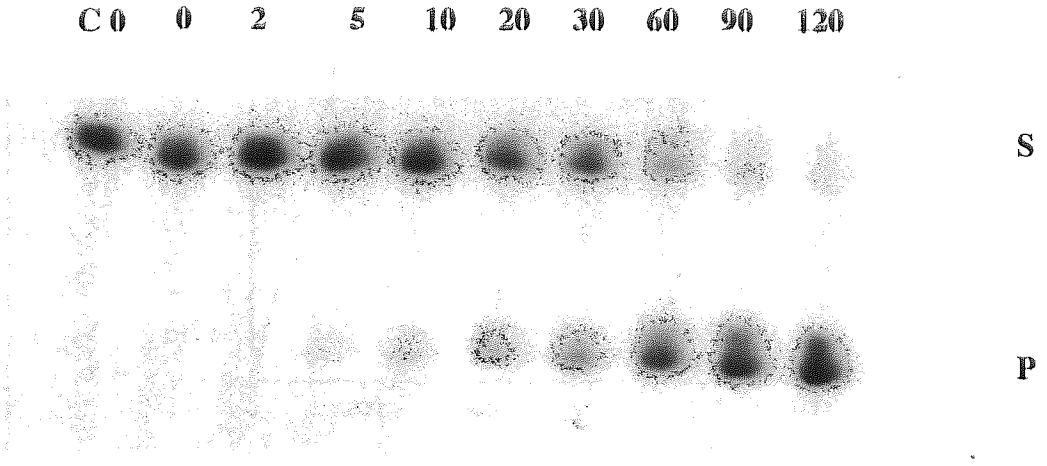

Figure 3.9 *Representative examples of autoradiographs depicting the time course of cleavage reactions exhibited by ribozyme RPI.4782 against its target substrate under multiple turnover reactions.* **(a)** *In vitro* activity of 10nM ribozyme with 300nM of 5'-[^{32}P] labelled substrate RNA **(b)** *In vitro* activity of 10nM ribozyme with 1μM of 5'-[^{32}P] labelled substrate RNA. Reactions were performed in the presence of 50mM Tris.HCl (pH 7.5), 10mM $MgCl_2$ at 37°C as described in section 2.8.3. Reaction times, in minutes, are given above the lanes. C represents intact substrate in Tris.HCl buffer without the addition of ribozyme. Band S refers to intact substrate and band P refers to cleaved product.

From an Eadie-Hofstee plot (Figure 3.11), the kinetic parameters K_m and V_{max} were determined. K_m represents the concentration of substrate at which the reaction rate is half its maximal value ($v=1/2V_{max}$) and can often be an indication of strength of binding; the higher the K_m value the weaker the binding of the ribozyme to substrate. V_{max} represents the maximum reaction rate (Fersh, 1977). The turnover number, k_{cat}, was calculated from the equation $k_{cat} = V_{max} / [ribozyme]$. From Figure 3.11, V_{max} was measured to be 11.98nM min^{-1} and the ribozyme exhibited a K_m value of 87nM. The k_{cat} value was calculated as being 1.2 min^{-1}

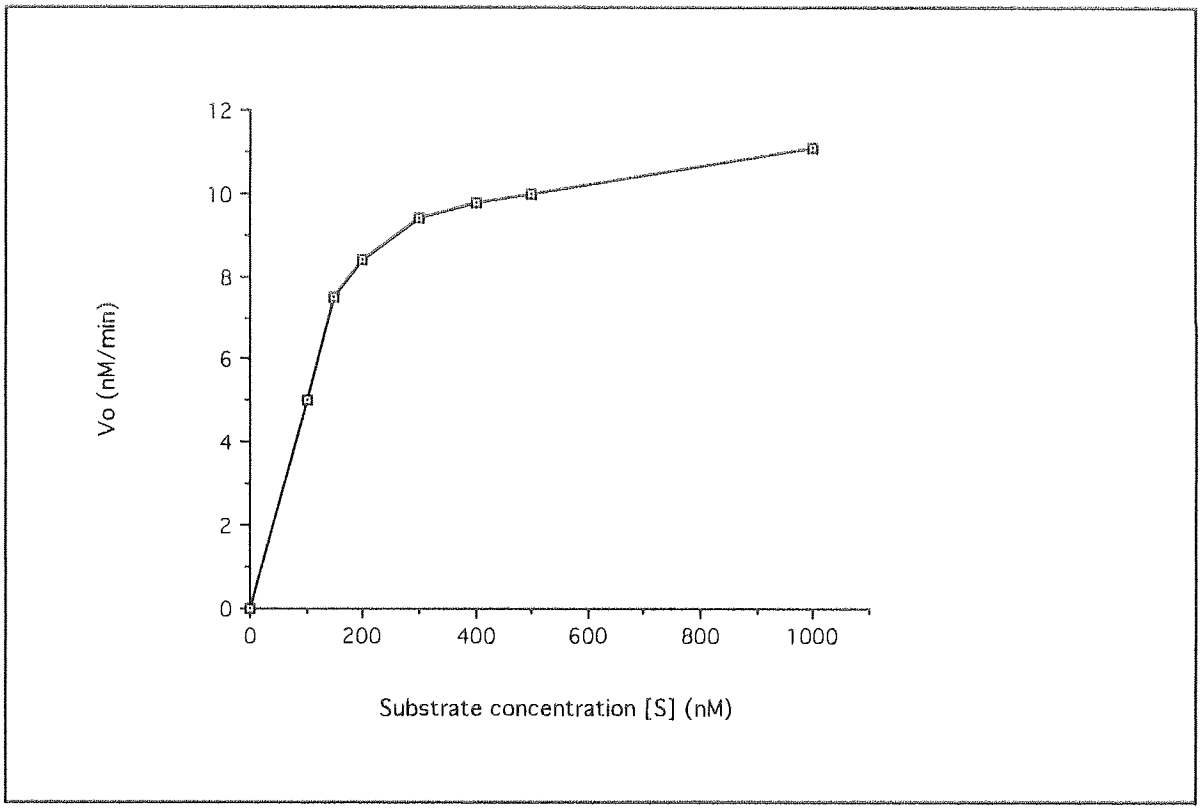

Figure 3.10 *Kinetics of hammerhead cleavage reactions exhibited by 2'-O-methyl / 2'-amino modified ribozyme RPI.4782 under multiple turnover conditions.* The initial rate of the reaction (Vo) is plotted versus substrate concentration [S]. Ribozyme concentration was 10nM while substrate concentration varied as indicated.

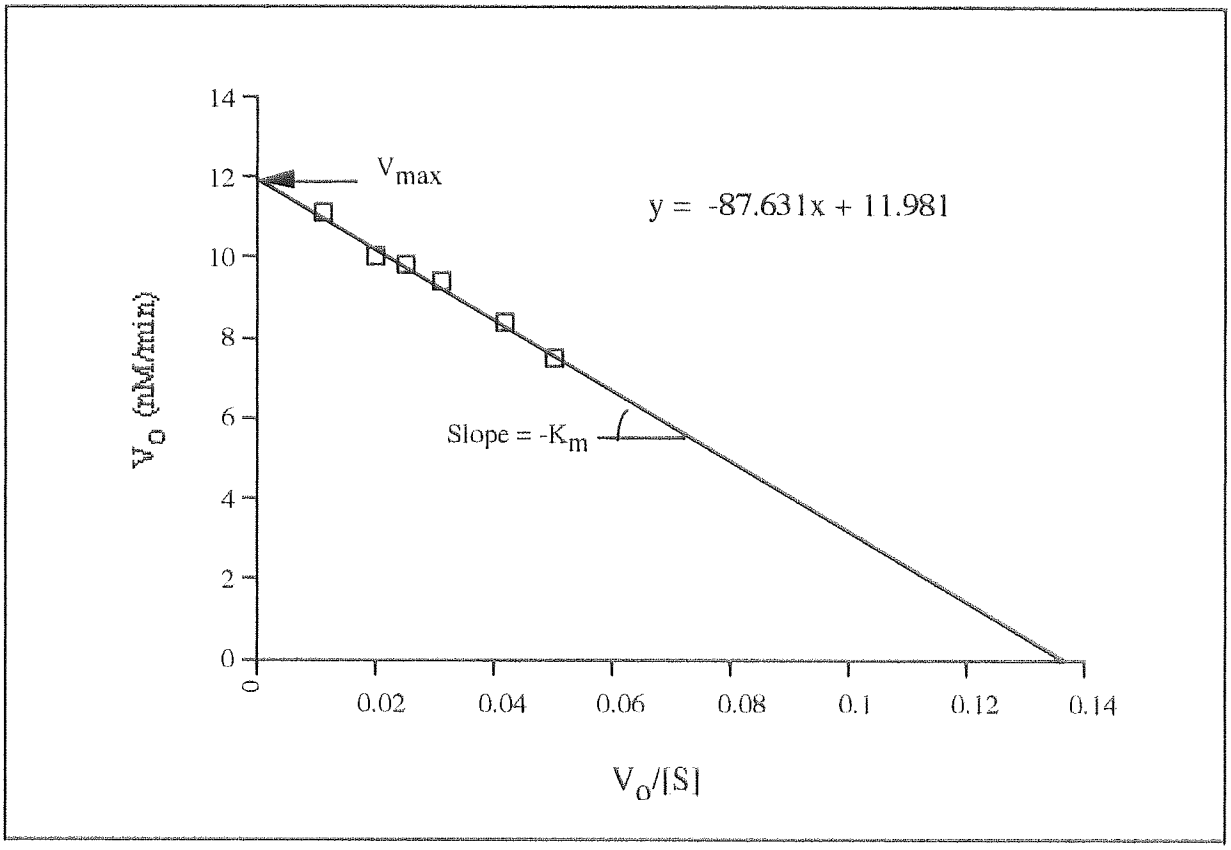

Figure 3.11 *Eadie-Hofstee plot of the hammerhead cleavage reactions exhibited by 2'-O-methyl / 2'-amino modified ribozyme RPI.4782.* Vo represents the initial reaction velocity. [S] represents nanomolar substrate concentration.

These results fall in line with typical values reported for short unmodified synthetic hammerhead ribozymes which range from 1-2 min^{-1} and 20-200nM for k_{cat} and K_m respectively (Thompson *et al*, 1996; Birikh *et al.*, 1997). These figures apply to ribozymes that contain seven nucleotides or less in each of the substrate binding arms ensuring that product release is fast and is not the rate limiting step (Fedor and Uhlenbeck, 1992).

It must be noted, however, that in general the kinetic parameters of ribozymes fall short of those exhibited by conventional protein enzymes. For instance, carbonic anhydrase

exhibits a K_m value of 87mM and a k_{cat} value of 600,000s^{-1} and even the relatively slow protein enzyme, lysozyme, has a turnover rate of 0.5s^{-1} and a K_m value of 6μM (Stryer, 1988). The significant discrepancy between ribozyme and the protein enzyme kinetic parameters is probably associated with the slower formation and disruption of RNA duplexes that takes place in reactions involving ribozymes and ensures their high specificity as compared to protein enzyme-substrate interactions (Zhenodarova,1993).

3.3.3 Cell Association of Chemically Modified Ribozymes

As a result of the promising biological stability and *in vitro* cleavage activity exhibited by the modified chimeric ribozymes, the issue of ribozyme uptake into living cells was next examined, an important consideration for the potential application of synthetic catalytic RNAs as both biological laboratory tools and as novel therapeutic agents. The results described in section 3.3.1.2 highlights the importance of using internally radiolabelled ribozymes for monitoring cell uptake. For this reason the 2'-O-methyl / 2'-amino modified ribozyme RPI.4782 was chosen for these studies since this construct had been synthesised in two halves to facilitate internal [^{32}P]-labelling.

3.3.3.1 Optimisation of Cell Association Study Protocol

The uptake of the chimeric ribozyme RPI.4782 was examined using the human glioma cell line U87-MG as a model. These cells are derived from a grade III glioblastoma and have many of the distinguishing phenotypic features of malignant gliomas (Ponten and Macintyre, 1968). The rate of cell growth was initially examined to determine the optimum cell concentration at which to conduct the experiments. U87-MG cells were plated out in serum-containing medium at a concentration of 1x10^4/ml and incubated for

various time periods at 37°C. Cells were trypsinised (section 2.4.3) and viable cell counts were calculated by trypan blue exclusion assay as described in section 2.4.4

The growth curve (Figure 3.12) showed exponential growth (log phase) until day five at which time the plateau/stationary phase was reached when cells became confluent and nutrients limited. At this stage the growth rate was reduced until proliferation almost ceased. Surprisingly, there was little evidence of an initial lag phase, however, this could have occurred in the first few hours post seeding, when sample counts were not measured. Using the method of Griffiths (1992), the cell doubling time during the exponential growth period was calculated to be 18.5 hours. Consequently, a seeding density of 1 x 10^5 cells/well would ensure that cells were still in the active exponential growth phase 20 – 24 hours post-seeding when cell association experiments were to be performed.

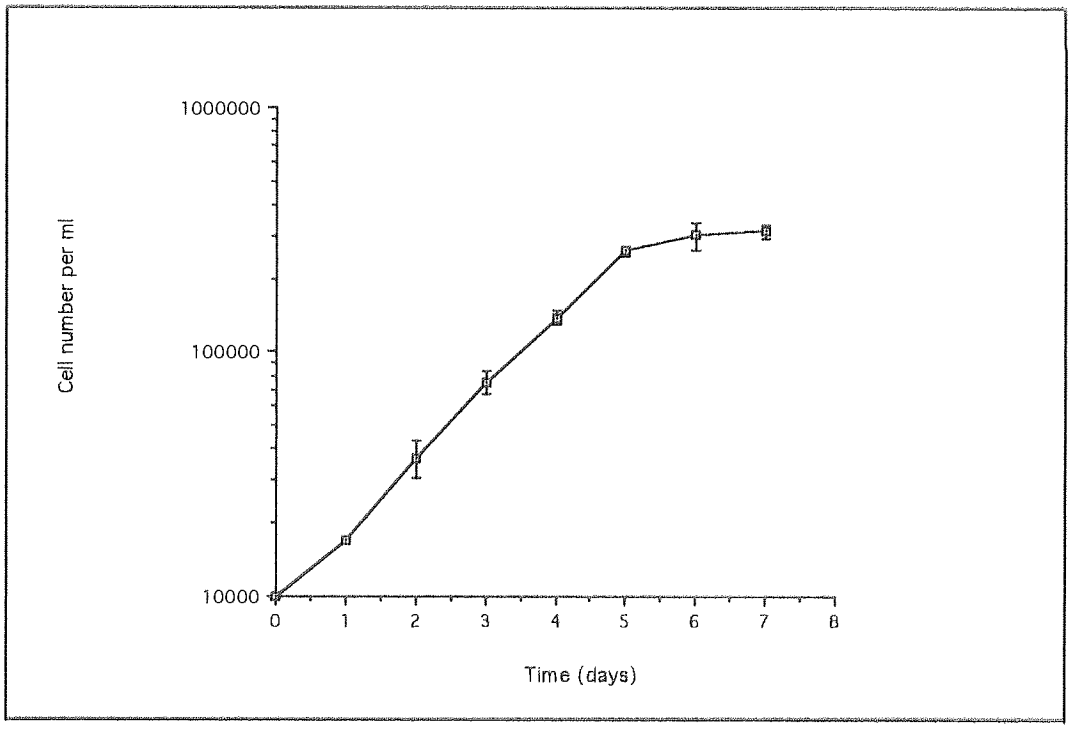

Figure 3.12 *Growth curve for U87-MG cells.* Cells were seeded at 1x 10^4 cells/ml into 24-well plates and incubated at 37°C for the time periods indicated. At each time point viable cells were trypsinised and counted using trypan blue exclusion assay.

An assay was conducted to determine how many PBS-azide washes were required, post-incubation to remove unbound and loosely bound ribozyme (see section 3.2.3.1). The percentage of non-cell associated radiolabelled ribozyme present in each of a successive number of post-incubation washes was measured and the results shown in Figure 3.13.

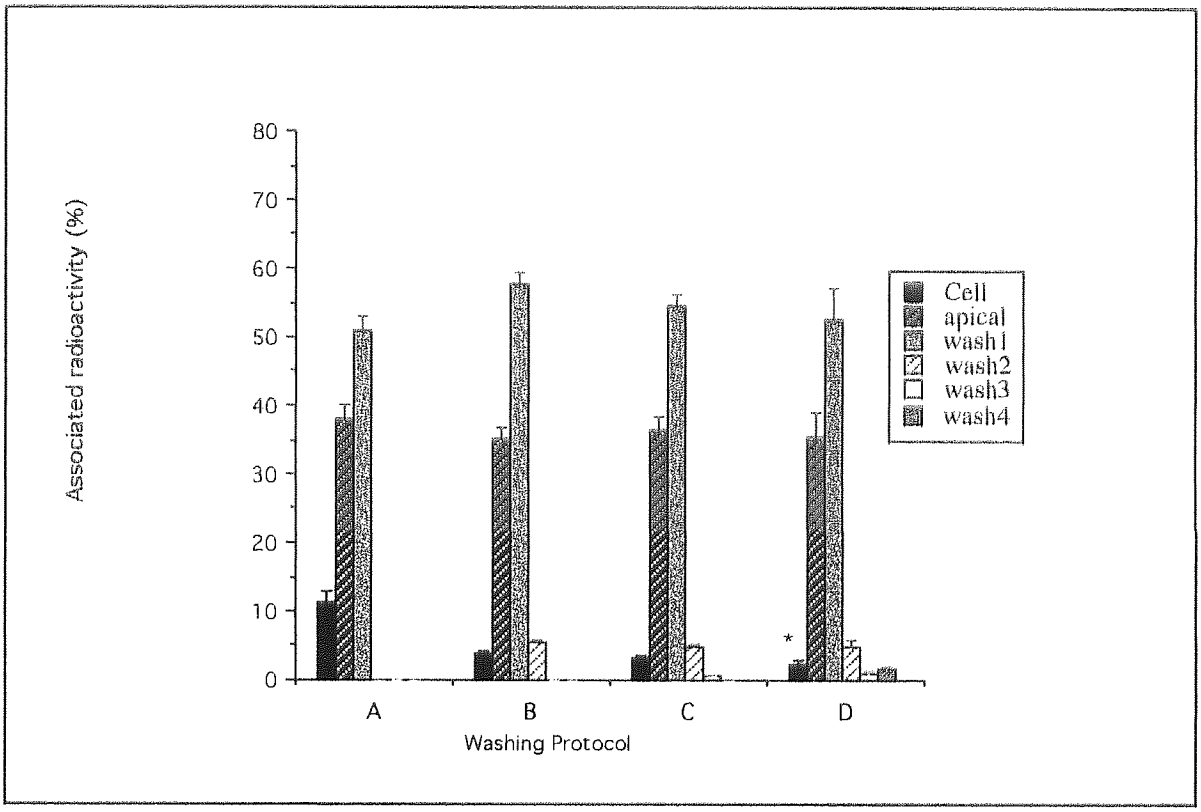

Figure 3.13 *Assay to determine the number of PBS-azide washes.* Following incubation with 0.01μM internally labelled ribozyme at 37°C, cells were washed with PBS-azide (0.5ml x 5min) at 4°C using the following protocols: A) 1 x 500μl x 5min ; B) 2 x 500μl x 5min ; C) 3 x 500μl x 5min ; D) 4 x 500μl x 5min. The amount of unbound / loosely bound ribozyme associated with each fraction (i.e. apical, respective washes, cell) is expressed as mean (n=6 ±SD) % of total ribozyme associated radioactivity applied to the monolayer. *Denotes a significant ($p<0.05$) reduction in total uptake from protocols B and C.

It was evident from the findings of this assay that one or two washes were insufficient to remove all traces of unbound radiolabelled ribozyme. By the third wash, however, only a small degree (0.6%) of ribozyme – associated radioactivity was observed. Further washings resulted in increased radioactivity levels being recorded for each subsequent wash (e.g. as in the case of wash 4), whilst a reduction in cell-associated radioactivity was observed. This suggests that the cells had begun to lift off the bottom of the wells. On microscopic examination, it was apparent that sloughing of the monolayer had indeed occurred and that further washing was potentially damaging to the cells. On the basis of these findings, a washing protocol of 3 PBS-azide washes (3 x 0.5ml x 5min) was implemented which ensured that over 99.4% of non-associated ribozyme was removed while no damage to monolayers occurred.

Cellular uptake becomes more pronounced in dead, unviable cells as the membrane loses its selective properties (Freshney, 1992). Consequently, before proceeding with these studies, a cell viability experiment was undertaken to ensure that the levels of ribozyme intended to be used throughout these experiments were not toxic to the cells. Cells were plated onto 24-well plates at a density of 1 x 10^5 cell / well as described in section 2.5 and used 20-24 hours post-seeding. Increasing concentrations of ribozyme (0μM – 25μM) were added to U87-MG cells in serum-free medium and after an incubation period of one hour, cells were trypsinised and viable cells counted using a trypan blue exclusion assay (see section 2.4.4). The results shown in Figure 3.14 show no significant difference ($p>0.05$) in viable cell number at all ribozyme concentrations examined when compared to the control sample (no ribozyme added). This demonstrates that under these conditions ribozyme concentrations of up to 25μM proved to be non toxic to U87-MG cells.

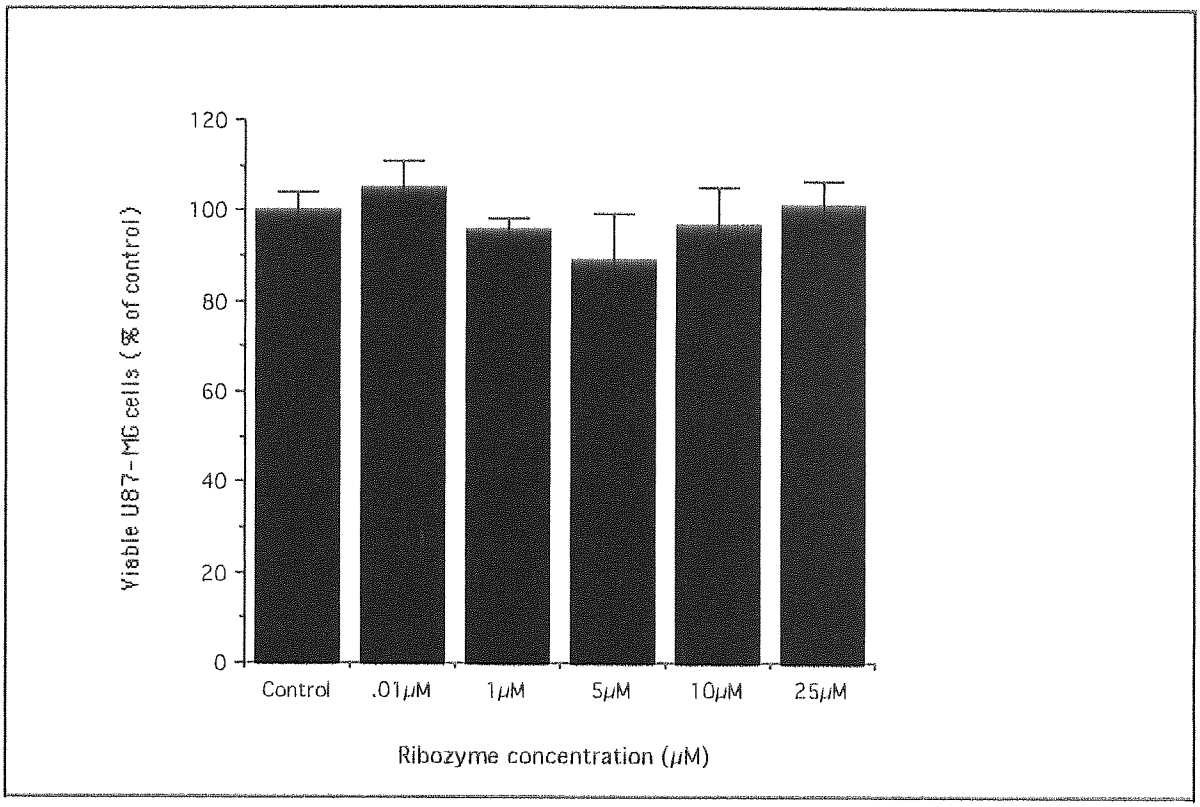

Figure 3.14 *The effect of ribozyme concentration on U87-MG viable cell numbers.* Cell monolayers were incubated with increasing concentrations of chimeric ribozyme RPI.4782 in serum-free DMEM at 37°C for a period of 1 hour. Following incubation cells were trypsinised and viable cells counted using a trypan blue exclusion assay. Data represents means (of at least four monolayers) ± SD.

3.3.3.2 *Temperature and Time Dependence of Cellular Association.*

The cell association of ribozyme RPI.4782 in U87-MG cells was determined at selected time intervals between 30 minutes and 240 minutes. As Figure 3.15 demonstrates, at 37°C cell association of ribozyme RPI.4782 occurred rapidly for the first two hours, after which time the rate of uptake began to level off. Statistical analysis showed that while significant increases in cell association occurred at all time points up to 120 minutes, there was no significant difference ($P>0.05$) in cell association between time points 120 minutes and 240 minutes.

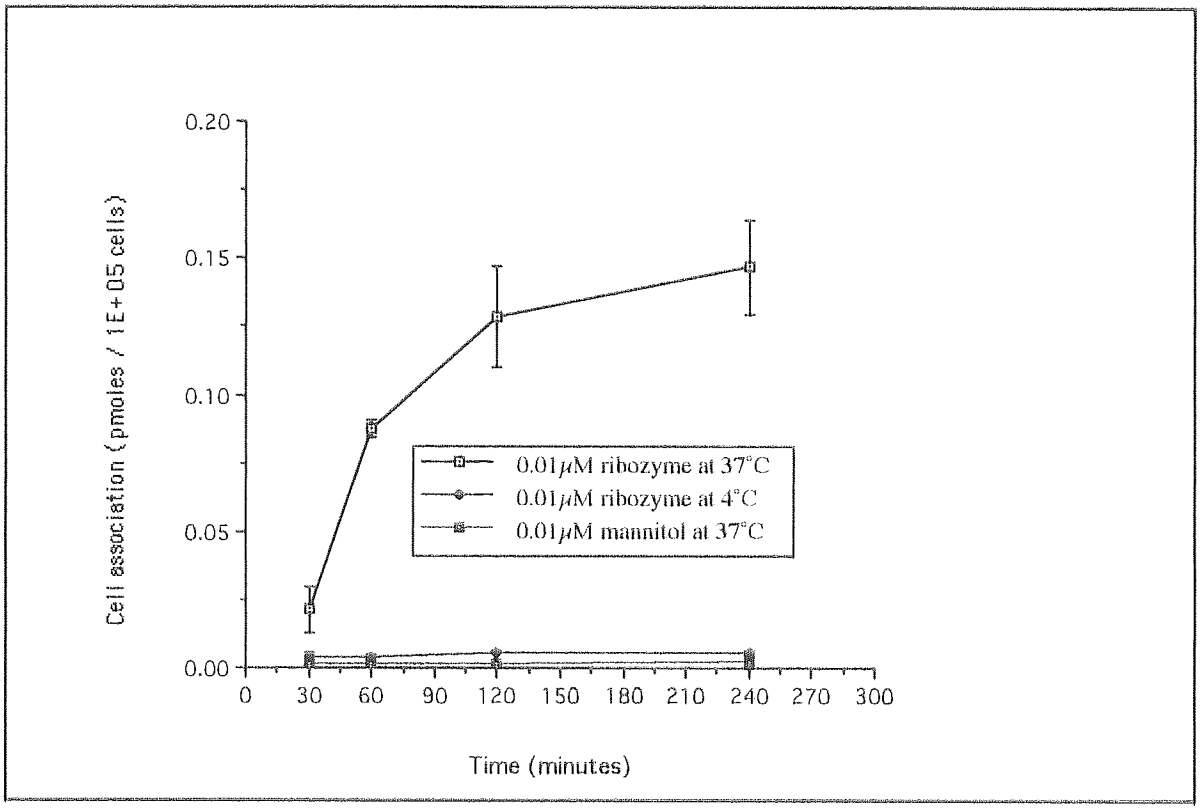

Figure 3.15 *Effect of temperature and time on cellular association of ribozyme RPI.4782 to U87-MG cells.* Cell monolayers were incubated with 0.01μM [^{32}P]-labelled ribozyme in serum-free DMEM medium at 4°C or 37°C for various times over a 4-hour period. To determine the extent of pinocytosis in the cells, uptake of [^{14}C] mannitol was also measured at 37°C over the same period. Cell associated ribozyme / mannitol is expressed in picomoles per 10^5 cells.

This is consistent with the pattern of cellular uptake of DNA oligonucleotides where cellular uptake has been shown to plateau after a few hours (Yakubov *et al.*, 1989; Iverson *et al.*, 1992; Levis *et al.*, 1995). In contrast, however, at 4°C cellular association was significantly reduced at all time points ($p<0.01$) when compared to the association seen at 37°C and remained at a relatively constant low level (at approximately 0.001 picomoles/10^5 cells) over the 240-minute period; thereby demonstrating that ribozyme uptake is strongly dependent upon temperature in this cell line.

The plateauing of cell association evident in Figure 3.15 suggests that after two hours of incubation, ribozyme uptake is in equilibrium with ribozyme exocytosis. In fact, cell association of the chimeric ribozyme was indeed found to be dynamic, representing both uptake and efflux processes. The export of ribozyme out of the cell was measured following an initial two hour incubation to achieve steady state association (as described in section 3.2.3.4). The profile of such efflux is shown in Figure 3.16a and represents the rate of loss of radiolabelled ribozyme from U87-MG cells as a function of time. Efflux of the internally labelled ribozyme was rapid in the first 60 minutes, when approximately 40% of internalised ribozyme was released, followed by a slower efflux over the remaining 3 hour period during which time a further 20% of ribozyme was released. After 4 hours 37% of the internalised ribozyme stayed sequestered within the cells. Similar results have been observed for oligonucleotides (Gao *et al.*, 1993; Tonkinson & Stein *et al.*, 1993; Temsamani *et al.*, 1994) and it has been suggested that this biphasic pattern of efflux is representative of release from two intracellular compartments (Tonkinson & Stein, 1994). Thus, the initial fast efflux of ribozyme may represent release of ribozyme from "shallow" compartments situated near the surface of the cell (e.g. strongly bound to the cell surface or within primary endosomal vesicles), whereas the slower efflux comes from ribozymes sequestered in "deeper (e.g. late endosomes or lysosomes or from other, as yet unidentified sites within the cell). The exact identity of these mathematically derived compartments remains unknown, but such patterns of efflux are thought to indicative of intracellular trafficking subsequent to endocytosis (Stein *et al.*, 1993).

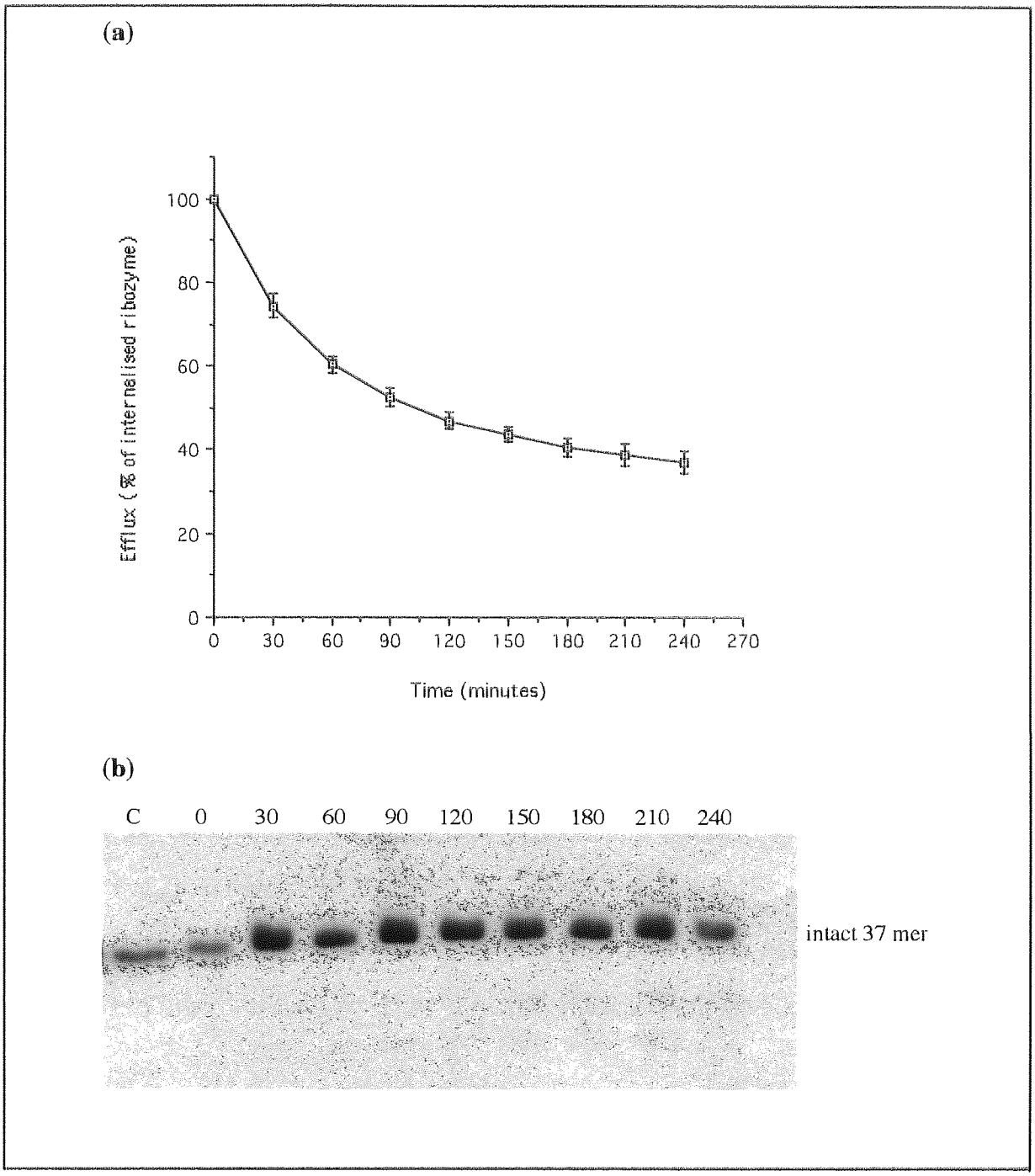

Figure 3.16 *Efflux of chimeric ribozyme RPI.4782 from U87-MG cells* (a) Efflux profile over time. Internally [^{32}P]-labelled ribozyme was incubated with U87-MG cells at 0.01μM concentration. After a 2-hour incubation at 37°C, the cells were washed with PBS and incubated with fresh serum-free medium (without ribozyme) for different periods. The efflux is represented by the percentage of [^{32}P]-labelled ribozyme remaining in the cell (n=5±SD). (b) Autoradiograph demonstrating the stability of ribozyme exported by U87-MG cells over time.

To ensure that any findings obtained from this efflux study represented uptake of intact ribozyme and not that of shorter degraded fragments or free [^{32}P] label, the degradation of internally labelled ribozyme RPI.4782 from efflux samples was examined. Apical samples collected at each efflux time point were analysed by denaturing gel electrophoresis. As Figure 3.16b demonstrates, the chemically modified ribozyme which had effluxed the cell was found to be stable and remained intact throughout the four hour incubation period.

3.3.3.3 *Energy Dependence of Cellular Association*

The temperature dependence of ribozyme uptake suggests that an active process is involved and largely discounts the possibility that ribozymes are taken up by passive diffusion. To further investigate, effects of energy depletion on cellular association was studied. U87-MG cells were pre-incubated with 10mM NaN_3 (a cytochrome oxidase inhibitor) and 20mM 2-deoxyglucose (a glycolytic inhibitor) for 1 hour prior to the addition of the ribozyme. Binding was significantly reduced by 65.8±7.0% in the presence of these inhibitors (Figure 3.17), clearly indicating that an energy-dependant process is involved in ribozyme uptake. Similar effects have been noted for PO-ODN and PS ODN by other workers (Wu-Pong *et al.*, 1994; Shoji *et al.*, 1996,).

The temperature and energy dependence of cellular association of this ribozyme in U87-MG cells suggested that endocytosis may account for the uptake of ribozymes, as is presumed for antisense ODNs (Akhtar and Juliano, 1992). They do not, however, distinguish whether fluid phase, receptor mediated or adsorptive endocytosis is involved, since all of these mechanisms will be affected by these parameters. In an attempt to evaluate the pathway of internalisation and determine the extent of pinocytosis in U87-

MG cells, the uptake of [^{14}C]-labelled mannitol, a classic, non metabolizable marker for fluid phase pinocytosis (Cohn & Ehrenreich, 1969) was measured over a four hour time period at 37°C (Figure 3.15). Compared to the uptake of radiolabelled ribozyme, the basal rate of pinocytosis in these cells remained extremely low throughout this time period ($p<0.01$) and is unlikely, therefore, to account for a significant fraction of ribozyme uptake at the concentrations used in this cell line.

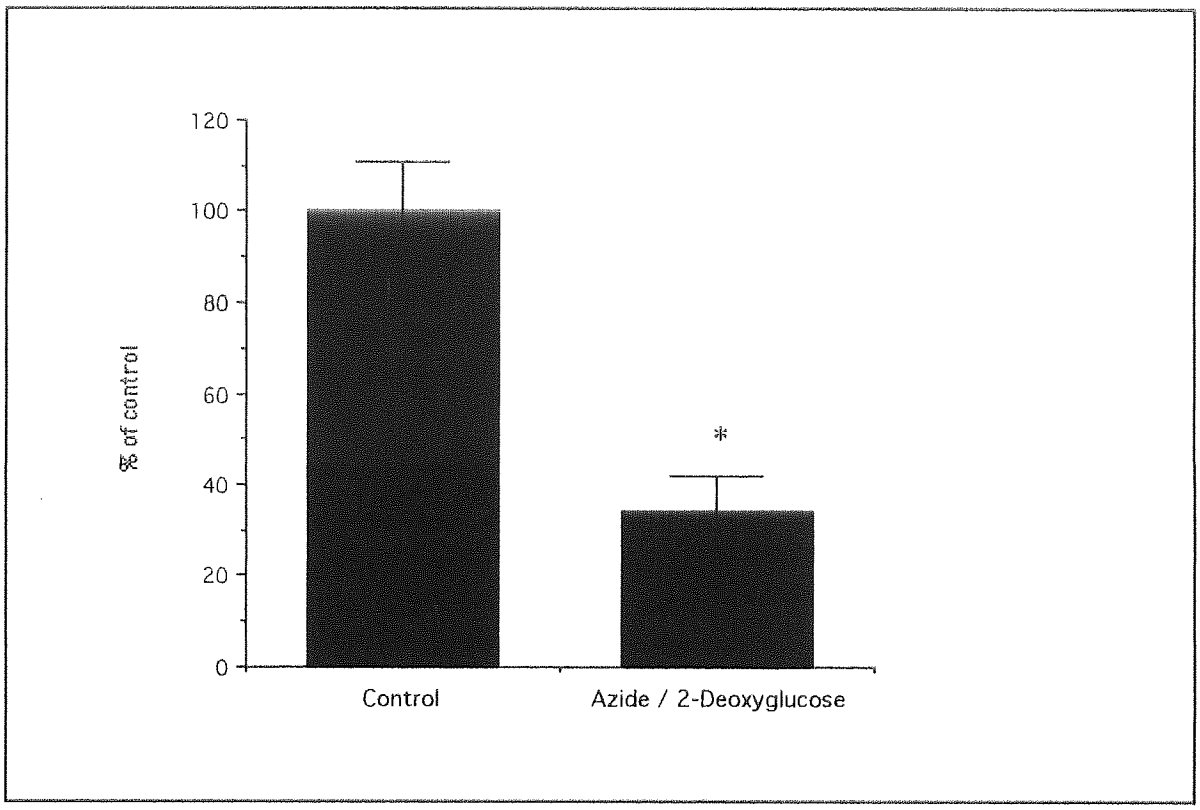

Figure 3.17 *The influence of metabolic inhibitors on cellular association of chimeric ribozyme RPI.4782 to U87-MG cells.* Cell monolayers were pre-incubated with 10mm NaN_3 and 20mM 2-deoxyglucose at 37°C in serum free DMEM medium for 1 hour. Cellular association of the ribozyme was measured after 60 minutes incubation in the continued presence of the aforementioned inhibitors. Data are expressed as mean (n=6) ± SD. * denotes a significant reduction ($p< 0.05$) from the appropriate control value.

3.3.3.4 Binding Characteristics of Cellular Association

The concentration dependence of cellular association of the chimeric ribozyme in U87-MG cells was determined by adding increasing amounts of unlabelled ribozyme to the incubation solutions containing fixed amounts of radiolabelled ribozyme. Ribozyme uptake was found to be inhibited by competition with unlabelled ribozyme in a dose-dependent manner, with a 500-fold excess of competitor significantly reducing cellular uptake by 92.2 ± 6.5 % (Figure 3.18).

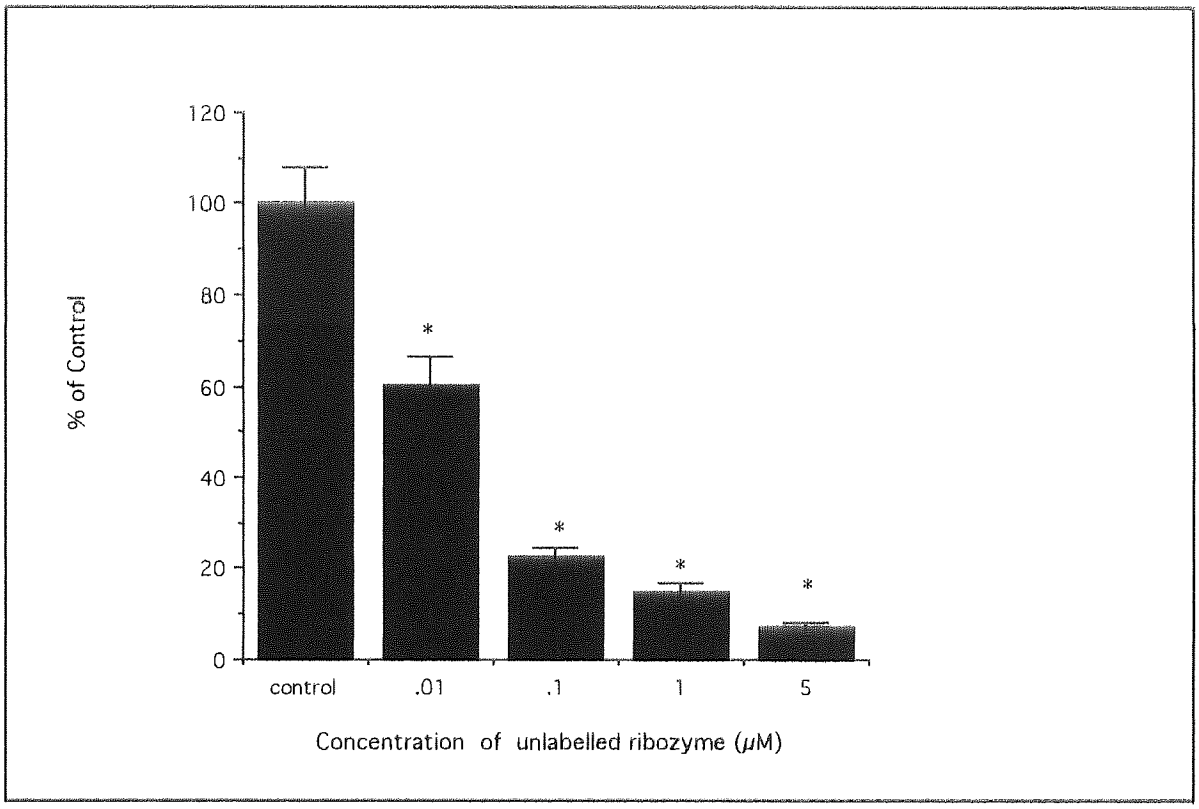

Figure 3.18 *Self competition of [^{32}P]-labelled ribozyme by unlabelled ribozyme.* U87-MG cells were incubated with 0.01μM [^{32}P]-labelled ribozyme RPI.4782 in serum-free medium for 1 hour along with varying concentrations of unlabelled ribozyme as shown. Data represents means (of at least four monolayers)±SD. * denotes a significant reduction ($P< 0.05$) from the appropriate control value (no addition of unlabelled ribozyme).

The self competable nature of ribozyme uptake is indicative of a specific cell surface binding mechanism which could be mediated by binding proteins. Receptor mediated and adsorptive endocytosis both involve the internalisation of molecules via membrane protein cell surface receptors. Consequently, a proteolytic enzyme such as trypsin or Pronase® can be used to determine the extent to which membrane proteins mediate uptake (Shoji *et al.*, 1991; Wu-pong *et al.*, 1994; Beck *et al.*, 1996). In a study investigating the cellular association of oligonucleotides in intestinal CaCo-2 cells, Beck *et al.* (1996) reported a 50% reduction of uptake upon cell surface washing with pronase, while 60% of oligonucleotide uptake was reported to be trypsin sensitive in Rauscher Red 5-1.5 erythroleukaemia cells (Wu-Pong *et al.*, 1994). Thus, to assess the extent of protein bound component of ribozyme cell association, trypsin-EDTA was used to strip off surface bound ribozymes by digesting cell surface protein binding sites (see section 3.2.3.8). Trypsinisation, following incubation of the ribozyme for 1 hour at 37°C, removed 75.24± 3.35% of cell associated radioactivity (Figure 3.19) showing that a large proportion of binding occurred via cell surface proteins. The remaining components may have become internalised or even represent tight binding to either non-trypsin sensitive (glyco)proteins or even cell surface lipids (Beck *et al.*, 1996).

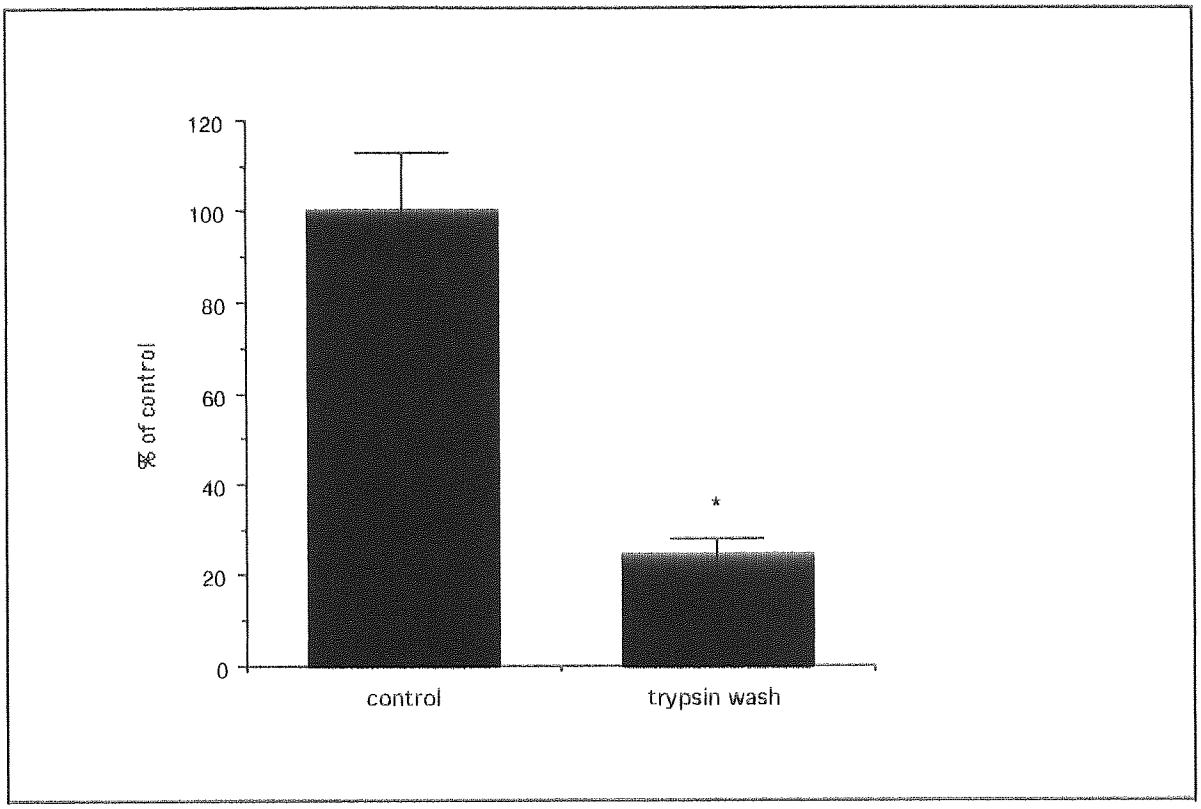

Figure 3.19 *Effect of trypsin washing on cellular association of ribozyme RPI.4782 to U87-MG cells.* Cells were incubated with 0.01μM ribozyme at 37°C for 60 minutes in serum-free DMEM medium. After incubation, cells were washed with trypsin to strip off surface bound ribozyme as described in section 3.2.3.8. Data are expressed as a percentage of the control (no trypsin treatment). Bars represent SD where n=5.

To examine the influence of pH on cellular association, U87-MG cells were incubated with ribozyme under various pH conditions. As Figure 3.20 illustrates, the binding of the ribozyme to U87-MG cells was found to be pH-dependent with increases evident as pH decreased. In fact, a decrease in pH from pH 8.0 to 5.0 resulted in a dramatic increase in cellular association from 0.647 ± 0.06 ng/10^5 cells at pH 8 to 1.75 ± 0.11 ng/10^5 cells at pH 5: an increase of nearly three fold.

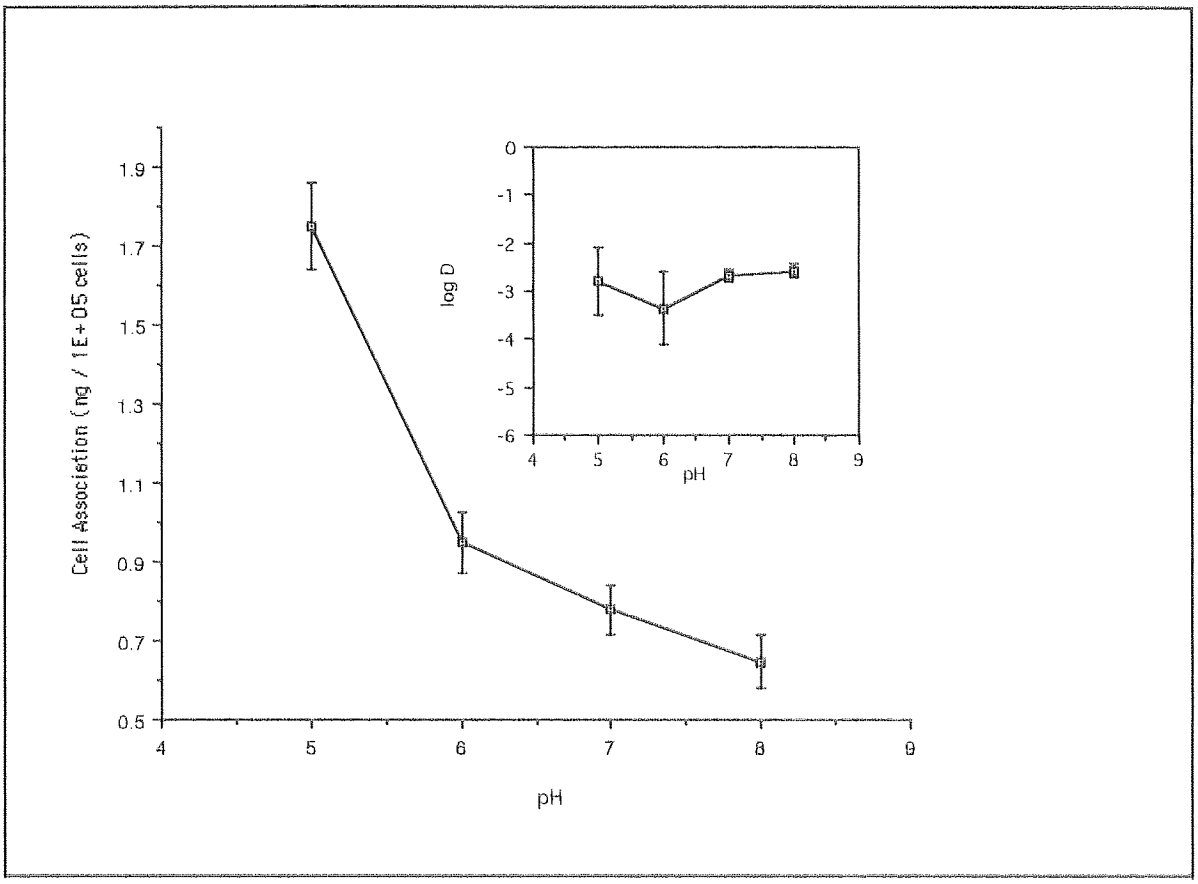

Figure 3.20 *Influence of pH on cellular association of ribozyme RPI.4782 to U87-MG cells.* Cell monolayers were incubated with 0.01μM ribozyme for 60 minutes at 37°C in an incubation solution of Hanks' balanced salt solution (HBSS) containing 0.01% phenol red, 5mM D-glucose, and buffered with 25mM HEPES (pH 7.0 and 8.0) or MES (pH 5.0 and 6.0). Cell associated ribozyme is expressed as ng / 10^5 cells. Data represents the means (n=5) ± SD. *Inset* Graph showing the effect of pH on n-octanol:aqueous buffer distribution coefficients for ribozyme RPI.4782. Distribution coefficients are expressed as log D, n= 6±SD.

To assess whether this increase in cellular association at low pH resulted from an increase in partition coefficient, octanol: aqueous buffer distributions were measured over this range. There was no significant change in distribution coefficient between pH 8.0 and 5.0 (Figure 3.20 *inset*) demonstrating that the oil-water partition coefficient of the ribozyme was not affected by pH. The fact that ribozyme association at low pH (5-6) was higher than at physiological pH suggests that the cellular binding / uptake sites are pH sensitive,

as has been reported for antisense PO-ODN and PS-ODN (Akhtar *et al.*, 1996; Beck *et al.*, 1996). It has been postulated that enhanced binding at low pH could be due to the presence of a 34-kDa membrane protein receptor that functions around pH 4.5 (Goodarzi *et al.*, 1991). In addition, the α amino group of lysine, the guanidium group of arginine and protonated imidazole of histidine have also been suggested to be possible oligonucleotide binding sites (Blackburn and Gait, 1990). Histidine, having a pKa of 6.5 is susceptible to protonation over a pH range of 7.2 to 5.0. Therefore, the enhanced affinity of ribozyme RPI.4782 to U87-MG cells at pH 5.0 could be due to protonation of susceptible amino or carboxylic acid groups present on the amino acids of possible binding proteins.

3.3.3.5 *Inhibition of Uptake by Competitors*

To further characterise the specificity of ribozyme uptake, the effect of nucleic acid and anionic competitors was examined. Potential competitors, including unlabelled oligonucleotides, salmon sperm DNA, ATP, and polyanions such as dextran sulphate and heparin were pre-incubated with cells for 15 minutes at 37°C. After pre-treatment, internally [^{32}P]-labelled ribozyme RPI.4782 was added and the cells incubated for 60 minutes in the continued presence of competitors. The results are summarised in Table 3.2.

The results from these experiments demonstrate that ribozyme uptake also involves a non-specific component, as other nucleic (salmon sperm DNA, ATP, ODNs, 2'-O-methyl / C-allyl ribozymes) and non nucleic acid molecules (dextran sulphate, heparin) significantly decreased ribozyme uptake by up to 96%. As PO-ODN and PS-ODN are generally considered to enter cells via receptor-mediated, adsorptive (binding protein-

mediated) or fluid phase endocytosis, the fact that uptake of ribozyme RPI.4782 was subject to competition with ODNs indicates that there could be an overlap in their mechanisms of entry and that ribozymes may compete for cell uptake via one or more of these processes. As Table 3.2 demonstrates, PS-ODN inhibited ribozyme uptake to a greater degree (82.0 ± 5.9% inhibition) than that seen with PO-ODNs (53.0 ± 7.5% inhibition). It has been well documented that phosphorothioates adsorb more avidly to cell membrane lipid components than phosphodiesters (Akhtar and Juliano, 1992) resulting in the PS-ODNs being more potent competitors of uptake than PO-ODNs. It has been postulated that this is due to their increased anionic charge allowing greater ionic interaction with cell surface proteins (Beck *et al.*, 1996). In addition, the 2'-O-methyl / 2'-C-allyl modified ribozyme RPI.5993 also significantly inhibited ribozyme association causing 94.1 ± 0.7 % inhibition at a concentration of 5μM (Table 3.2). This suggests that both chimeric ribozymes largely share the same mechanism of entry into the cells; the slight differences in modifications between the two ribozymes having little or no effect upon the uptake process.

The high potency of salmon sperm DNA in inhibiting ribozyme association could be accounted for by their large size (587-831 base pairs, Sigma D-9156) and high number of anionic charges; resulting in a high affinity for the cell membrane proteins. Beck *et al.*, (1996) demonstrated that increasing the length of antisense ODNs resulted in greater cell association. This could also explain why the small nucleotide monomer, ATP, inhibited ribozyme uptake to a much lesser degree (55.3±7.1% inhibition).

Such non-specific competition by unrelated polyanions has also been demonstrated for antisense ODNs and highlights the importance of ionic interaction with cell surface structures in the cellular uptake of these entities. Bennett *et al.*,(1985) reported a 30-kDa

DNA binding protein that could be inhibited by heparin, while Loke *et al.*, (1989) described an 80-kDa surface protein to which binding could be inhibited by single nucleotides as well as tRNA and plasmid DNA. More recently, a 46-kDa binding protein has been identified that can be competed a variety of polyanions including ssDNA, ds DNA, RNA and heparin (Akhtar *et al.*, 1996; Hawley and Gibson, 1996). Further studies are required to establish whether any of these putative binding proteins are also involved involved in mediating the transport of chemically modified RNA.

Table 3.2 *Influence of competitors on cellular association of ribozyme RPI.4782*

Competitor / inhibitor	Final concentration	% inhibition	n	p
PO-DNA oligo	5μM	53.0 ± 7.5	5	<0.05
PS-DNA oligo	5μM	82.0 ± 5.9	5	<0.05
2'-O-Me/C-allyl - ribozyme(RPI.5993)	5μM	94.1 ± 0.7	3	<0.05
Salmon sperm DNA	5μM	94.5 ± 1.1	5	<0.05
ATP	5μM	55.3 ± 7.1	5	<0.05
Dextran sulphate	10μM	96.9±0.7	5	<0.05
Heparin	10μM	94.0±0.6	4	<0.05

U87-MG cells were pre-incubated with potential competitors for 15 minutes at 37°C. Cells were then incubated with 0.01μM internally [^{32}P]-labelled ribozyme RPI.4782 in the continued presence of competitors. Values listed represent the mean of n experiments. Values of $p<0.05$ are considered to be significant.

3.3.3.6 *Cell-Type Specific Cellular Association*

Antisense ODN uptake has been reported to be cell type dependent (Noonberg *et al.*, 1993; Wu-Pong *et al.*, 1994; Beck *et al.*, 1996; Hawley and Gibson, 1996; Nakai *et al.*, 1996) which may reflect differences in, among others, the relative expression levels of the putative binding proteins. In an attempt to compare the magnitude of ribozyme association observed in U87-MG cells with other cell lines, ribozyme association with A431 (vulval), Raw 264.7 (macrophages) and Caco-2 (colonic) cells was also examined.

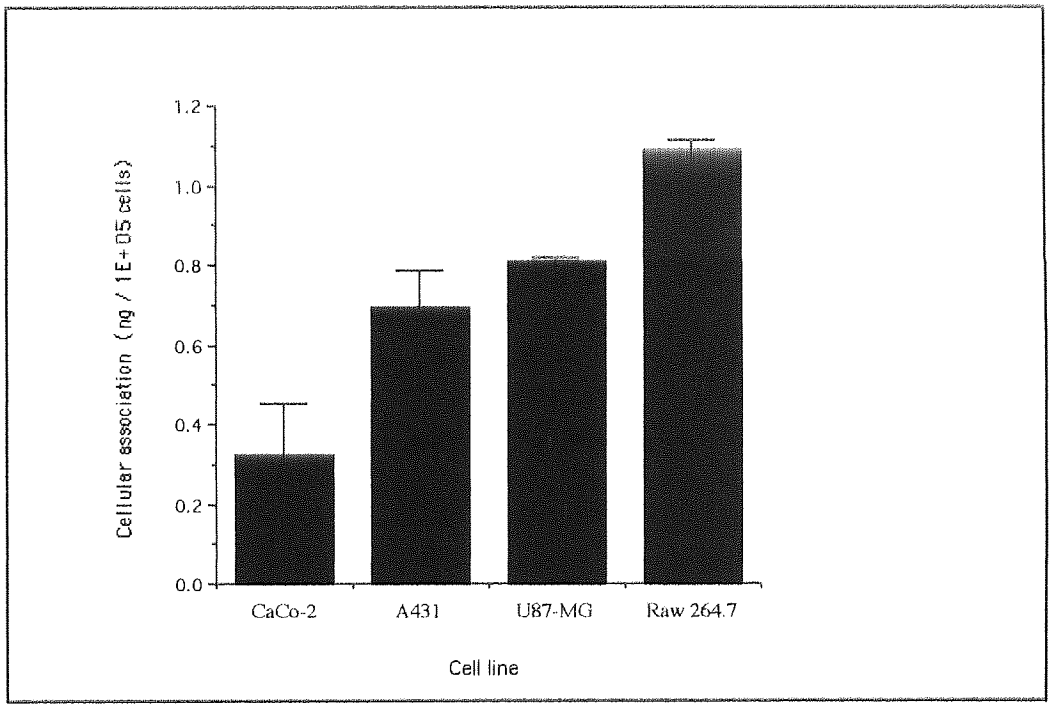

Figure 3.21 *Cellular association of ribozyme RPI.4782 to a range of cell lines.* Cell monolayers were incubated with 0.01μM ribozyme in serum-free DMEM medium for 60 minutes at 37°C. Cellular associated ribozyme is expressed as ng / 10^5 cells. Data represents the mean (n=5) ± SD.

When normalised to cell number, cell association was indeed found to be cell type dependent (Figure 3.21), with at least a 3-fold difference in cell association of ribozyme between those cells showing the greatest association (Raw 264.7) and those showing the least (Caco-2). Although these results are useful in demonstrating that, like antisense ODN, cell association of ribozymes is cell line specific, the limitations of this type of comparison are acknowledged. Various factors such as differences in cell size, gross morphology and varying stages in cell cycle could influence cell binding. Thus, quantitatively accurate comparisons between different cell types is difficult.

3.3.3.7 Subcellular Distribution of Fluorescently Labelled Ribozyme in U87-MG Cells

To study the uptake and intracellular distribution of ribozymes, cells were incubated with FITC-labelled ribozyme for a period of four hours, washed to release loosely bound ribozyme, fixed with paraformaldehyde and visualised using an inverted fluorescence microscope as described in section 3.2.3.11. In preliminary experiments, cells were incubated with a range of concentrations of ribozyme (from 0.1μM to 50μM) for a period of four hours, washed and then immediately viewed under the microscope. A concentration of 10μM FITC-labelled ribozyme was found to be the lowest dose that gave sufficiently intense fluorescent images to record.

The punctate distribution of ribozyme that was evident, as shown in Figure 3.22, is indicative of entry through endocytosis and subsequent compartmentalisation within vesicles (Shoji *et al.*, 1991). Studies monitoring the subcellular distribution of fluorescently labelled dextrans, which are known to accumulate in endocytic vesicles following cell uptake (Berlin and Oliver, 1980), have observed similar distribution patterns in a number of cell lines (Shoji *et al.*,1991). In addition, it was interesting to

observe that there was some cell to cell variability in fluorescence intensity although no consistent differences in intracellular localisation. This indicates that cellular uptake of chimeric ribozymes is heterogenous. Such heterogeneity may be due to differences in cell cycle and their influence on cell uptake. It has been reported that uptake occurs at the greatest rate during the S-phase of the cell cycle (Wu-Pong *et al.*, 1994). Consequently, cells demonstrating the greatest intracellular fluorescent intensity could represent those cells in S-phase of the cell cycle. On further examination (Figure 3.23) it can be seen that while internalised fluorescently-labelled ribozymes are clearly located in the periphery of the cytoplasm, close to the cell membrane, there is little indication of inter-nuclear localisation. This suggests that the chimeric ribozymes have a tendency to remain trapped in endocytic vesicles and may be liable to degradation in lysosomes. Researchers studying the sub-cellular distribution of ODNs have also observed such punctate distribution in the perinuclear region (Shoji *et al.*, 1991; Beltinger *et al.*, 1995a) and it been suggested that the rate limiting step in determining antisense efficacy may be escape of the ODN from the endosomes (Kreig and Stein, 1995). To be effective as a therapeutic agent, ribozymes and ODNs must be able to exit endosomes to reach their target site. These results, therefore, suggest that delivery methods may be required to overcome the problem of endosomal entrapment associated with entry into the cells through endocytosis.

To discount the possibility that uptake and localisation were driven by the properties of the fluorophore rather than the ribozyme (i.e. to ensure that these results represented distribution of ribozyme and not the FITC label) cells were also incubated with free FITC alone (Figure 3.24). In this case, a more random and diffuse distribution pattern was observed which was clearly distinct from that seen for the FITC labelled ribozyme. Fluorescence was observed throughout the cytoplasm and the nucleus. Furthermore, the

free FITC label produced a more intense fluorescence within U87-MG cells although this could not be measured with the method used. Flow cytometry would be required to directly quantify the differences in fluorescent intensity. As fluoresence microscopy in fixed cells can introduce artefacts, treated cells were also observed unfixed and the same intracellular distribution patterns were seen.

The potential toxicity of using the fluorescently -labelled ribozyme was evaluated. Cells were incubated with experimental amounts of ribozyme (10μM) or free FITC (10μM) for 4 hours at 37°C as described previously (section 3.2.3.11). The results showed that neither the ribozyme nor the FITC caused apparent toxic effects to the cells. Firstly, phase contrast microscopy indicated that the morphology of treated cells did not alter when compared to control (untreated) cells (Figure 3.25). In addition, trypan blue exclusion assays confirmed that treatment with either free FITC or FITC-labelled ribozymes did not significantly ($p>0.05$) affect viability when compared to control samples that had not been exposed to the fluorescent molecules.

When untreated cells were observed under the fluorescent microscope, no auto-fluorescence was detectable, ensuring that the results obtained from these experiments solely reflected the subcellular distribution of exogenously delivered fluorophores.

(a)

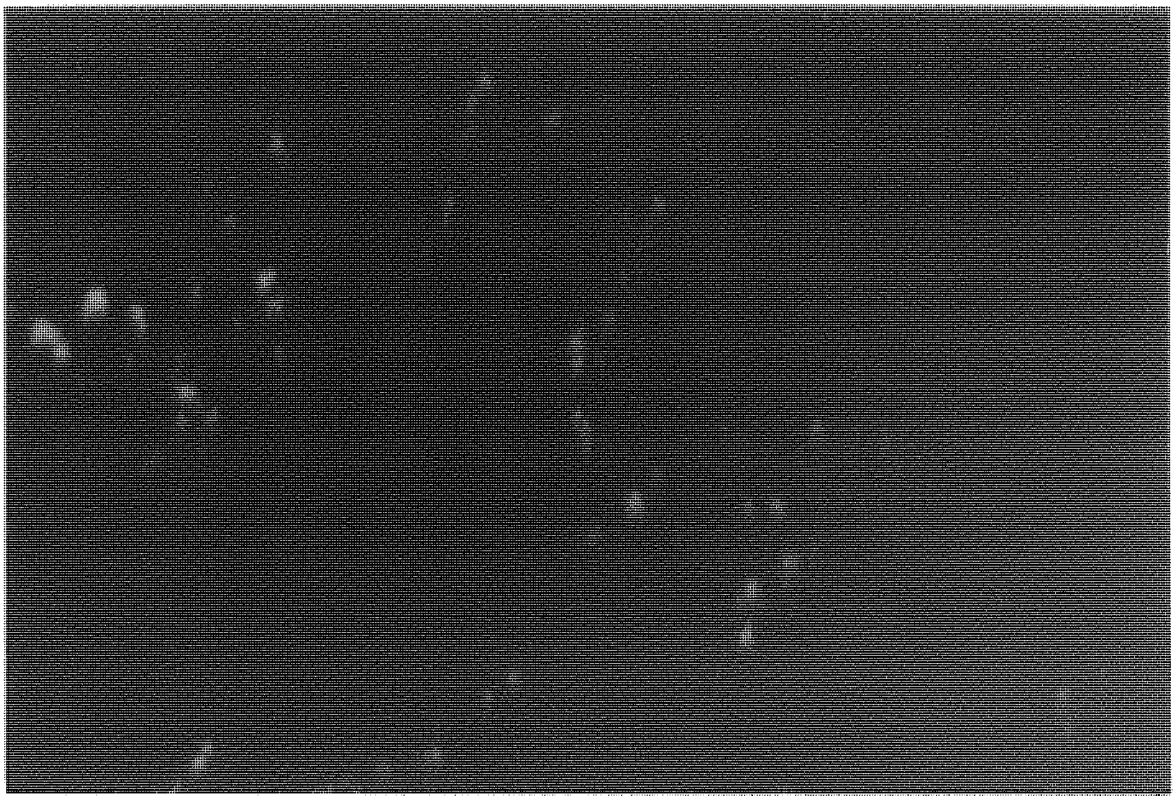

(b)

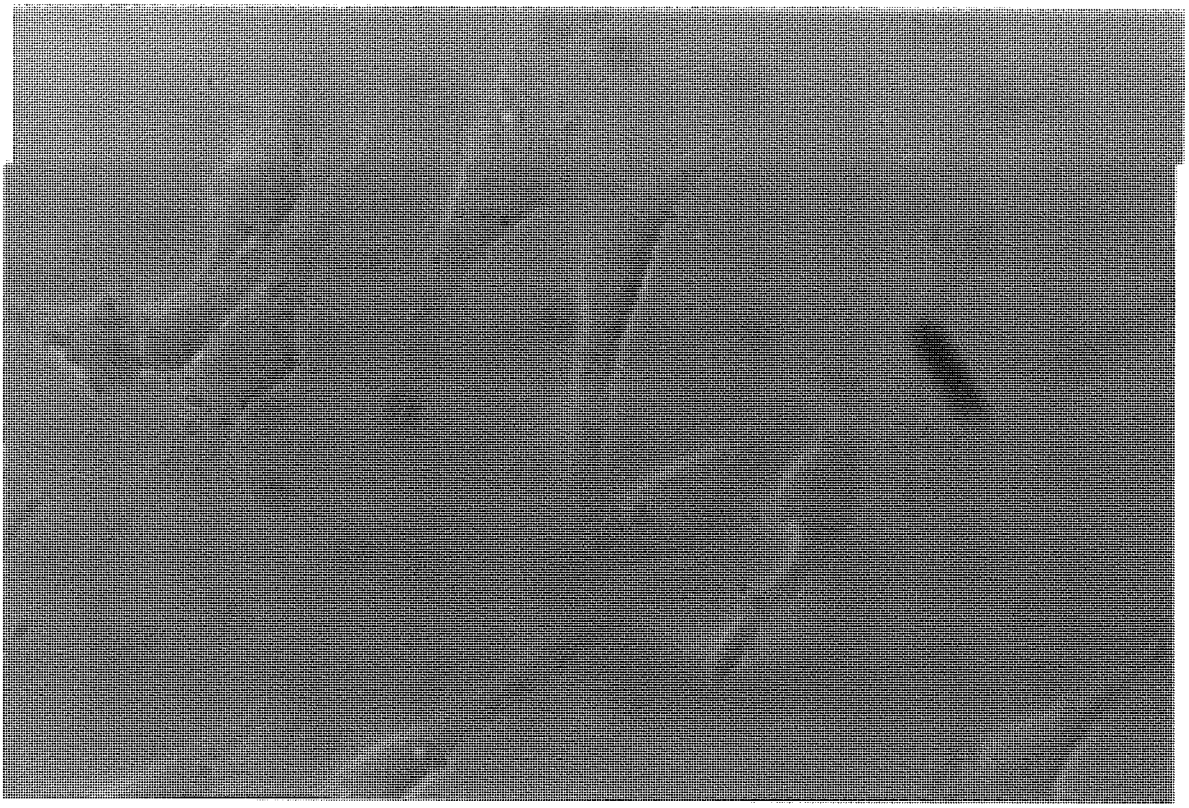

Figure 3.22 *Subcellular distribution of FITC-labelled chimeric ribozyme in U87-MG cells (magnification x 40).* Cell monolayers were incubated with 10μM FITC-labelled ribozyme in serum-free DMEM medium for 4 hours at 37°C. (a) Fluorescent illumination (b) Phase contrast image.

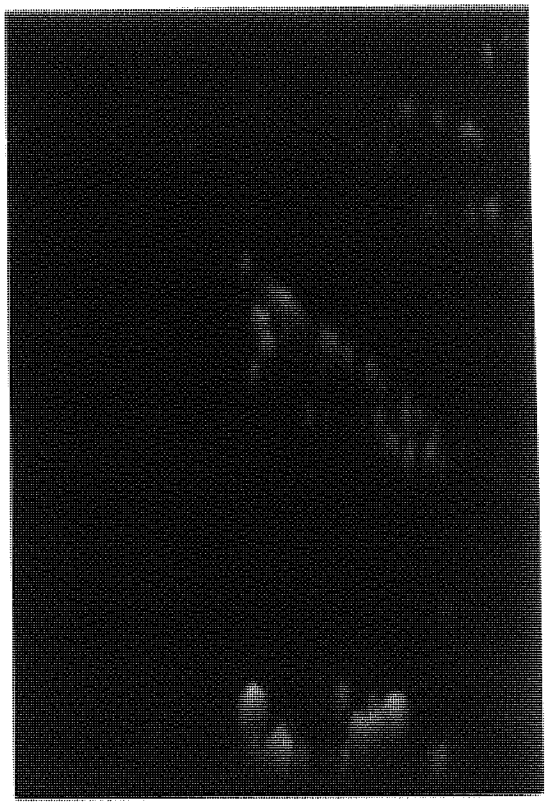

Figure 3.23 *Subcellular distribution of FITC-labelled chimeric ribozyme in U87-MG cells (magnification x 100).* Cell monolayers were incubated with 10μM FITC-labelled ribozyme in serum-free DMEM medium for 4 hours at 37°C.

(a)

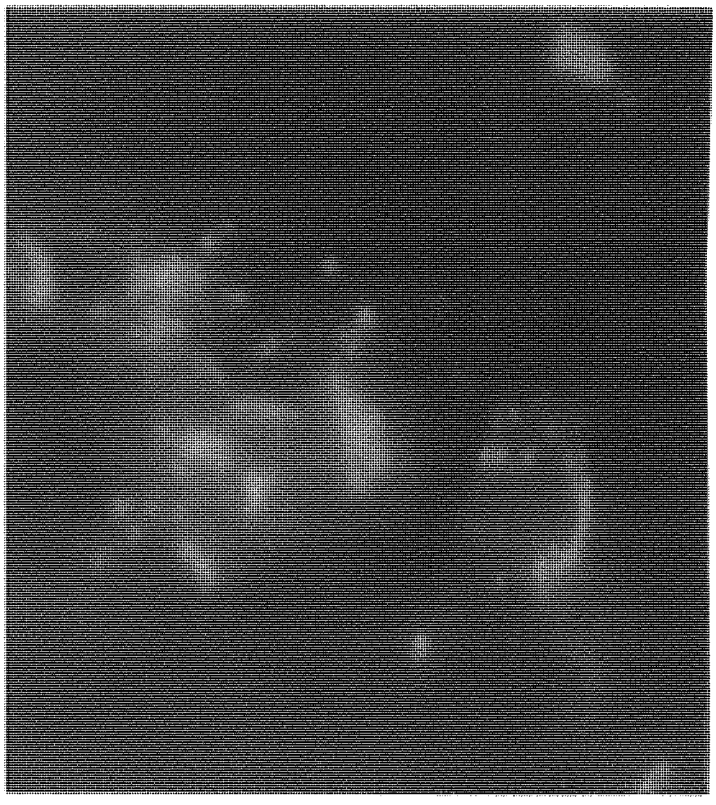

(b)

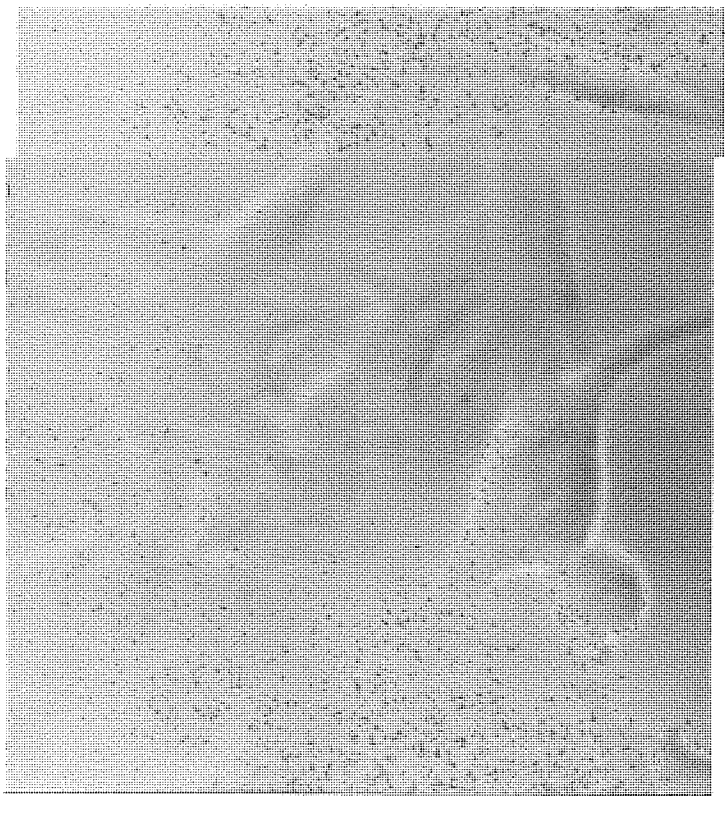

Figure 3.24 *Subcellular distribution of free FITC* in U87-MG cells. Cell monolayers were incubated with 10μM free FITC in serum-free DMEM medium for 4 hours at 37°C as described in section 3.2.3.11. (a) Fluorescent illumination (magnification x 40) (b) Phase contrast image (magnification x 40)

(a)

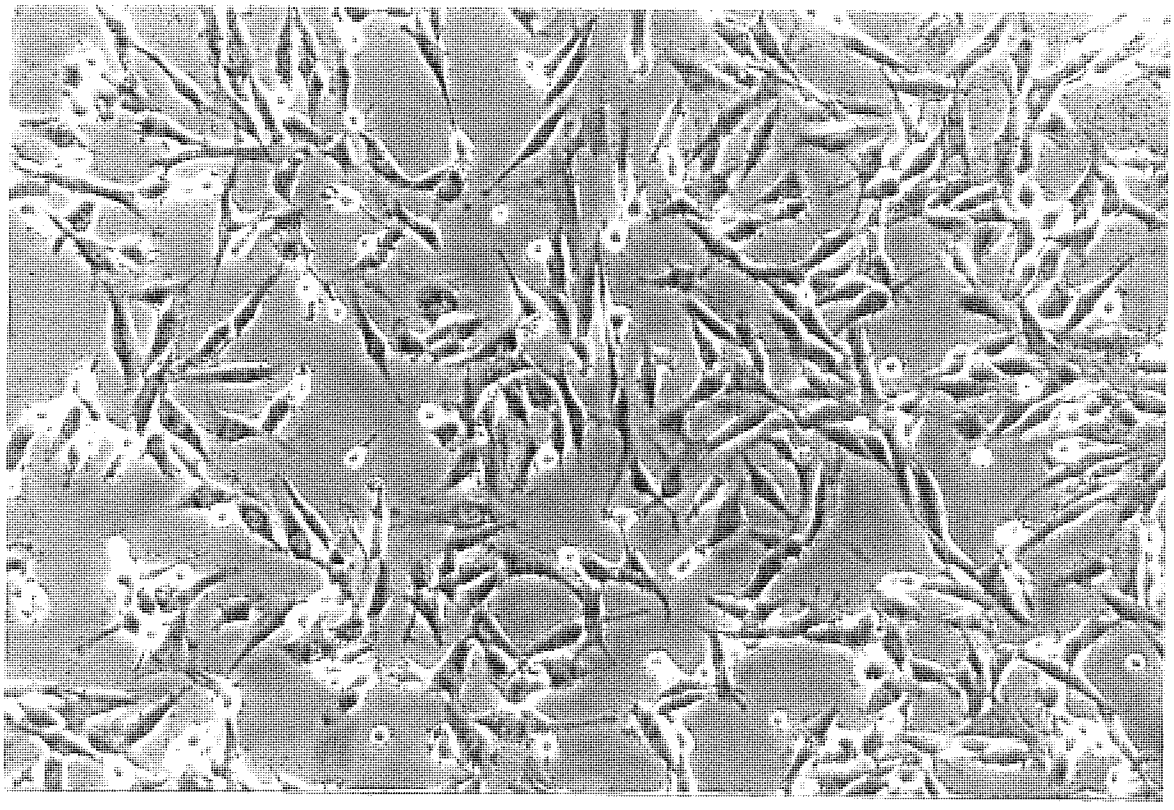

(b)

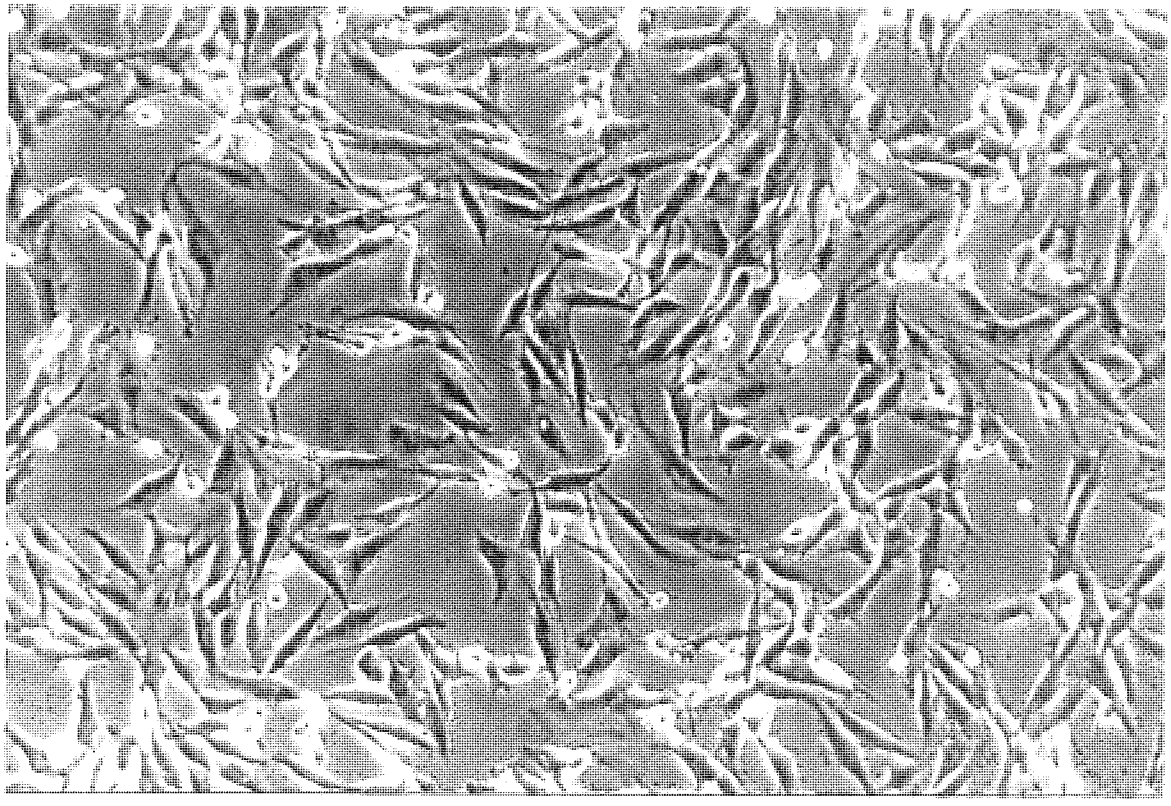

Figure 3.25 *Phase Contrast images of U87-MG cells.* Cells were incubated for four hours in serum-free DMEM medium as described in section 3.2.3.11. (a). In the absence of any fluorophores (serum-free medium only). (b). In the presence of 10μM FITC-labelled ribozyme (magnification x 10).

3.4 CONCLUDING REMARKS

One of the major limitations of using unmodified ribozymes as drugs is their instability in both the extracellular and intracellular environment. The chemical modifications applied to both the ribozymes used in this study appear to have overcome this limitation. We have shown that the two chimeric 2'-O-methyl-modified ribozymes containing either U_4/U_7 amino groups (RPI.4782) or U_4 C-allyl group (RPI.5993) within the catalytic core nucleotides of the hammerhead motif and an inverted thymidine at the 3'-terminus (Figure 3.1) exhibit good *in vitro* cleavage activity with substantially improved nuclease stability in serum compared to all RNA and commonly used DNA oligonucleotides. In fact, both chimeric ribozymes proved sufficiently stable and active to use with confidence in future *ex vivo* and possible *in vivo* experiments.

The mechanism by which these ribozymes enter cells is also an important consideration in the development of these agents as therapeutics. The findings of this study suggest that the pathway of cellular uptake of these synthetic ribozymes in the human glioma-derived cell line, U87-MG, involves an active cellular process. Indications are that the predominant mechanism of uptake is by adsorptive and / or receptor mediated endocytosis, mediated by a variety of cell surface proteins and possibly other membrane components. It is also evident from these studies that the cellular uptake properties of the chemically modified ribozyme in cultured glioma cells show many similarities to those observed by many research groups for antisense ODNs. These data, which are consistent with an endocytic mechanism of entry into cultured glioma cells, suggest that the known wishbone secondary structure of hammerhead ribozymes (Cech and Uhlenbeck, 1994; Pley *et al.*, 1994; Tuschl *et al.*, 1994; Scott *et al.*, 1995) is not responsible for altering the mechanism of uptake from the many DNA oligonucleotide sequences reported in the

literature (For review see Akhtar and Juliano, 1992; Rojansakul, 1996) that presumably exhibit a variety of different secondary structures. It is likely therefore that the large molecular weight and polyanionic characteristics of the ribozyme molecule are more important factors in governing the uptake mechanism. However, recent data on the secondary structure of G-quartet-containing ODNs that form tetraplexes in solution suggest that the magnitude of ODN uptake is strongly dependent upon secondary structure (Agrawal *et al.*, 1996) even if the gross cellular mechanism may be the same.

The entry of these chimeric ribozymes by endocytosis suggests that delivery strategies, such as cationic lipids that facilitate endosomal exit of ODNs by a putative lipid exchange mechanism (Zelphati and Szoka, 1996), will be required for *in vitro* (cell culture) applications. Indeed, effective use of liposomes / cationic lipids has been reported in facilitating delivery of pre-synthesised ribozymes (Jarvis *et al.*, 1996; Bramlage *et al.*, 1999; Kisich *et al.*, 1999; see also section 1.4.2.2). However, lipid complexes with ribozymes will require optimisation for a given cell / nucleic acid system, as data obtained with other analogues / chemistries are not directly transferable to ribozymes (M. A. Reynolds, unpublished data). In addition, the optimal intracellular localisation of ribozymes is thought to be important for activity *in vitro* (Sullenger and Cech, 1993; see also Arndt and Rank, 1997). Recent *in vivo* studies with ODNs (for review see Akhtar and Agrawal, 1997) and chemically modified ribozymes (Lyndgstadaas *et al.*, 1995; Flory *et al.*, 1996) suggest, however, that cellular uptake in animal models is sufficient to achieve biological effects in the absence of such delivery methods.

CHAPTER FOUR

DESIGN, *IN VITRO* ACTIVITY AND BIOLOGICAL EFFICACY OF 2'-O-METHYL-MODIFIED CHIMERIC HAMMERHEAD RIBOZYMES TARGETED AGAINST EGFR

ABSTRACT

In this chapter the potential use of chemically stabilised, synthetic ribozymes was investigated in down regulating the *c-erb*B1 gene which encodes for the epidermal growth factor receptor that is both amplified and over-expressed in a number of cancers (Khazaie *et al.*, 1993) including the malignant brain cancer, glioblastoma multiforme (Shapiro and Shapiro, 1998).

With the aid of RNAFOLD folding program (Denman, 1993), twenty hammerhead ribozymes were designed to cleave various target sites along the EGFr mRNA containing either GUC or GUA triplets. These ribozymes were synthesised containing 2'-O-methyl / 2'-C-allyl modifications to enhance nuclease stability. *In vitro*, 18 out of 20 ribozymes exhibited high activity in cleaving a complementary short substrate, with the activity half-life of the substrate being under 8 minutes for all the active ribozymes.

Two different commercially available cationic liposomes, LipofectAMINE™ and PerFect™ Pfx-6, were investigated as a means of improving the efficiency of ribozyme delivery to A431 cells, a vulval carcinoma cell line which over-expresses EGFr protein levels. Optimisation studies revealed that optimal association of ribozymes to A431 cells was achieved when the overall charge ratio was net positive, although maximum association of the lipid/ribozyme complex to A431 cells was found to be dependent upon a number of factors including ribozyme concentration, lipid concentration and formulation.

Using LipofectAMINE™ as a delivery vehicle, the efficacy of the twenty ribozymes was evaluated in the A431 cell line. Studies revealed that although the ribozymes were taken up by the cells and remained remarkably stable over a period of 4 days, no significant reduction in either EGFr expression or cell proliferation was evident. Further research is required to determine whether ribozyme design or delivery method is responsible for limiting the activity of these ribozymes in cell culture.

4.1 INTRODUCTION

4.1.1 Epidermal Growth Factor Receptor (EGFr)

The epidermal growth factor receptor (EGFr) is a 170-kDa transmembrane glycoprotein consisting of an extracellular 'ligand' binding domain, a transmembrane region and an intracellular domain with tyrosine kinase activity (Moghal and Sternberg, 1999). The binding of growth factors to the EGFr results in signal transduction, activating a tyrosine kinase in the intracellular region of the receptor. This results in autophosphorylation of the receptor and phosphorylation of other intracellular substrates, leading ultimately to DNA synthesis and cell division (Volborg *et al.*, 1997). The external ligand binding domain is stimulated by a variety of growth factors including EGF, TGFα, amphiregulin and some viral growth factors (see Ciardiello and Tortota, 1998; Hackel *et al.*, 1999; Wells, 1999 for reviews).

One of the striking characteristics of the EGFr gene (*c-erbB1*), located on chromosome 7, is it's homology to the avian erythroblastosis virus oncogene (*v-erbB*), which induces malignancies in chickens. The *v-erbB* gene codes for a truncated product that lacks the extracellular ligand binding domain. The tyrosine kinase domain of the EGFr has been found to have 97% homology to the *v-erbB* transforming protein (Downward *et al.*, 1984).

Studies have shown that the EGFr is over-expressed in a number of malignant human tissues when compared to their normal tissue counterparts (for reviews see Modjtahedi and Dean, 1994; Davies and Chamberlin, 1996; O'Rouke *et al.*, 1997; Wells, 1999). Over-expression of the EGFr is often accompanied by the co-expression of the growth

factors EGF and TGFα, suggesting that an autocrine pathway for control of growth may play a major part in the progression of tumours (Sporn & Roberts, 1985). Both pre-clinical and clinical data have established a high correlation in cancer patients between EGF receptor / ligand expression and poor prognosis (reviewed in Fry, 1999).

Growth factors and their receptors appear to have an important role in the development of human brain tumours. A high incidence of over-expression, amplification, deletion and structural rearrangement of the gene coding for the EGFr has been found in biopsies of brain tumours (Ostrowski *et al.*, 1994). In fact the amplification of the EGFr gene in glioblastoma multiforme tumours is one of the most consistent genetic alterations known, with the EGFr being over-expressed in approximately 40% of malignant gliomas (Black, 1991).

The amplified genes may also be rearranged and associated with polymorphism leading to abnormal protein products. The rearrangements that have been characterised usually show deletions of part of the extracellular domain, resulting in the production of an EGFr protein that is smaller in size. Three classes of deletion mutant EGF receptor genes have been identified in glioblastoma tumours. Type I mutants lack the majority of the external domain, including the ligand binding site; type II mutants have a deletion in the domain adjacent to the membrane but can still bind ligands; and type III, which is the most common and found in 17% of malignant gliomas, have a deletion of 267 amino acids spanning extracellular domains of the EGFr (Wong *et al.*, 1994). The significance of these receptor mutations in GBM has not as yet been elucidated.

The discovery that up-regulated EGFr signalling correlates with the formation and progression of human cancers has prompted interest in experimental therapies to target

the receptor. Current strategies being employed involve two approaches. The first exploits the presence of EGFr to direct cytotoxic agents to tumour cells (see review by Davies and Chamberlin, 1997). The second approach attempts to modulate EGFr response by a variety of means including the use of specific tyrosine kinase inhibitors (for reviews see Fry, 1999; Traxler and Furet, 1999), monoclonal antibodies directed against the ligand binding site (see Mendelsohn, 1997 for review) and antisense strategies (Coulson *et al.*, 1997; Yamazaki *et al.*, 1998; Witters *et al.*, 1999).

The aim of this chapter was to design nuclease stable synthetic ribozymes which will down regulate the *c-erb*B1 gene that encodes for the EGFr. The extent, specificity and mechanisms of biological efficacy of these ribozymes in cells would then be investigated in cell culture models which over-express the EGFr, in particular model systems of the malignant brain cancer GBM.

4.2 MATERIALS AND METHODS

General materials and methods are detailed in Chapter Two. Any alterations, additions and specific methods relevant only to this chapter are given below.

4.2.1 Using RNAFOLD Computer Program to Predict RNA Secondary Structures

A computer-assisted method for predicting the relative activity of small catalytic RNAs was performed using the RNAFOLD program in accordance with the method of Denman (1993). This program uses computer-based folding algorithms (Zuker *et al.*, 1991) in the suite of programs available from the University of Wisconsin Genetics Computer Group (GCG) (Madison W.I. USA), available on the seqnet database, located at Daresbury Laboratories, U.K. and accessed through Telnet. The program authors request that the following acknowledgement is cited for copyright purposes: 'Program manual for the Wisconsin Package, Version 8, Genetics Computer Group, Madison, USA and the program manual for the EGCG package, Hinxton Hall, Cambridge, UK'.

4.2.1.1 *Folding of Ribozyme Sequence*

The sequence of each ribozyme was inputted into the RNAFOLD package starting at the 5'-end. The sequence was then folded into its lowest energy structure using a standard RNA folding algorithm (Zuker *et al.*, 1991). If the correct hammerhead conformation was achieved, the structure folded as shown in Figure 4.1 and the predicted free energy of formation (ΔG) was -3.3 kcal/mol. Negative values of ΔG indicate stable base-pair formation and a value of –3.3 kcal/mol reflects the energy of base-pairing solely at stem

II of the ribozyme. Only ribozymes which demonstrated this favourable folding conformation were considered as candidates for synthesis

```
5'-GUCUGCGCUGAUGA     G
                  GGCC A        Energy: ΔG =-3.3 kcal/mol
                  CCGG A
     3'-ACCUUCAAAG     A
```

Figure 4.1 *RNAFOLD analysis of a candidate ribozyme folded into a favourable hammerhead secondary structure.* The energy value given represents the energy required for Watson-Crick base-pair formation within a particular construct.

4.2.1.2 *Folding of Substrate Sequence*

A short section of the substrate mRNA sequence (usually a 15-mer sequence) was also folded using this program. In this case a positive free energy value was desirable, as this indicates weak bonding. Misfolding of the substrate could prevent hybridisation with the ribozyme and result in poor cleavage activity of the relevant ribozyme when tested *in vitro*. This information may be useful in predicting the *in vitro* activity of ribozymes against short synthetic substrates; a preliminary step in screening candidate ribozymes.

4.2.1.3 *Folding of Ribozyme / Substrate Complex*

Since only single RNA species can be folded by this computer program, the *cis*-acting counterparts of each *trans*-acting ribozyme were created. The process is outlined in schematic form in Figure 4.2.

Briefly, substrate and ribozyme were joined at the end of either stem I or stem III with a 5-base loop of A or U residues, thus forming 4 different *cis*-acting ribozymes for each variant. Each of the 4 ribozyme / substrate complexes was then folded into its lowest energy structure by RNAFOLD. The number of structures (out of the 4 possibilities) correctly folding into a hammerhead secondary structure and the free energy value of formation of each lowest energy structure were scored. The greater the number which adopted the correct secondary structure, the more favourable the prediction.

Consequently, only ribozymes which folded into the correct conformation in all of the above cases (i.e. ribozyme only, substrate only and all 4 structures of ribozyme / substrate complexes) were considered as suitable candidates for synthesis.

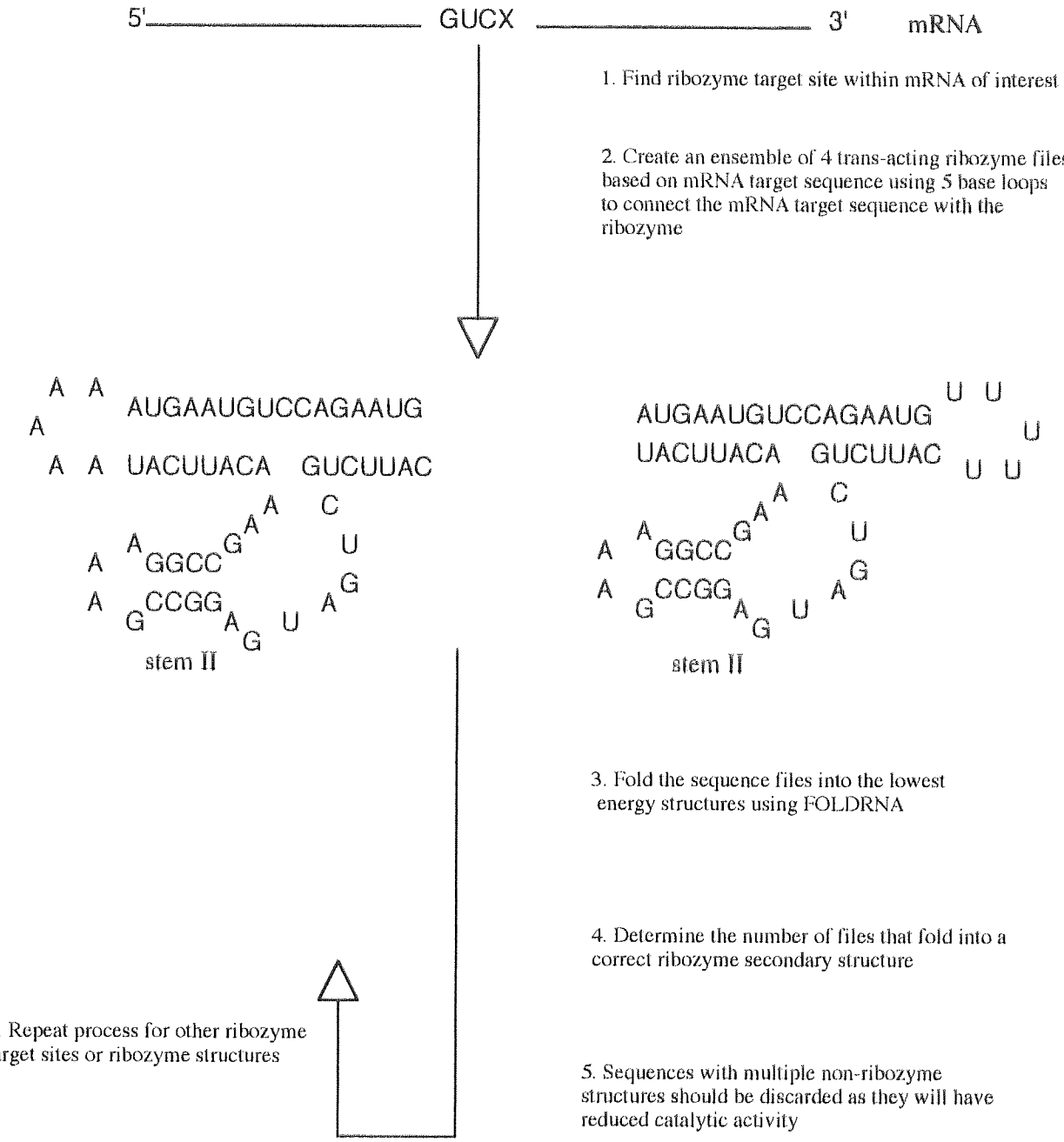

Figure 4.2 *Schematic diagram depicting the procedure used to predict the secondary structure of ribozyme / substrate complexes* (Denman, 1993).

4.2.2 Western Blot Analysis

4.2.2.1 *EGFr Expression in Different Cell Lines*

Whole cell-lysates were prepared as described in section 2.7.1.2. The protein concentration of each cell sample was quantified using a standard BSA assay (section 2.7.2) and 20μg (U87-MG & IPFA) or 10μg (A431) of protein per well was analysed by 7.5% SDS-PAGE electrophoresis and transferred to nitrocellulose membrane as described in sections 2.7.3-2.7.4. Immunodetection was performed as detailed in section 2.7.5. using a primary mouse monoclonal antibody, E-3138, (Sigma, Poole, U.K.) targeted to the intracellular domain of the epidermal growth factor receptor. The antibody was used at a 1:1000 dilution in PBS-Tween buffer. A HRP-conjugated secondary anti-mouse antibody was used at a 1:2500 dilution. Following immunoblot analysis, the blot was washed thoroughly in PBS-Tween and then re-probed with an anti-actin primary antibody, A-2066 (1:200 dilution) (Sigma, Poole, U.K.) followed by HRP-conjugated anti-rabbit secondary antibody (1:2500 dilution).

4.2.2.2 *Effect of Ribozyme Treatment on EGFr Expression*

A431 cells were seeded at 5 x 10^4 cells/well in 24 well plates for efficacy studies to be conducted over 24 hours and at 3 x 10^4 cells/well for efficacy studies to be performed over a period of four days. Following ribozyme treatment (as described in sections 4.2.3.2-4.2.3.5) cells were lysed, analysed by 7.5% SDS-PAGE (20μg/ml cell lysate protein / well) and immunoblotting performed with anti-EGFr antibody E-3138 at a dilution of 1:1000 as detailed in sections 4.2.2.1 and 2.7.3-2.7.5. After immunoblot analysis, the blot was washed thoroughly in PBS-Tween and then re-probed with an anti-

actin primary antibody, A-2066 (1:200 dilution) (Sigma, Poole, U.K.) followed by HRP-conjugated anti-rabbit secondary antibody (1:2500 dilution).

4.2.3 Proliferation Studies

4.2.3.1 *Effect of Tyrphostin A25 on Cell Growth*

The effects of tyrphostin A25 (a gift from Dave Poyner, Aston University) on cell growth was investigated in U87-MG and in A431 cells. Both cell lines were seeded in 24-well plates at a concentration of 5 x 10^4 cell / well. 24 hours post-seeding cells were washed twice with sterile PBS (2 x 0.5ml x 5min) and culture medium containing the desired concentration (10μM – 1000μM) of tyrphostin added. Tyrphostin stock solutions were made in 100% DMSO at 200mM and kept at –70°C until use in growth assays. For growth assays tyrphostins were diluted in DMEM culture medium containing 10% FBS. Control media were obtained using serial dilutions of DMSO in culture media. Cell were allowed to proliferate in the presence of tyrphostin A25 for a period of 24 hours, at which time cells were trypsinised (100μl trypsin-EDTA per well) and viable cells counted by trypan blue exclusion assay (section 2.4.4).

4.2.3.2 *Treatment of A431 Cells with Ribozyme over 24 hours.*

A431 cells were seeded in 96-well plates at 6.5 x 10^3 cells per well. Approximately 24 hours later, cells were washed twice with sterile PBS (2 x100μl x 5min) and ribozyme, complexed to LipofectAMINE™ (as described in section 4.2.4.2) were added at the appropriate concentration in a total volume of 100μl of serum-free medium per well. Following a four-hour uptake period, the medium was removed and replaced by fresh

serum-free medium. Controls contained LipofectAMINE™ reagent alone. Cells were then incubated at 37°C for a further 20 hours at which time cell number was determined by means of crystal violet assay (section 2.6.1).

4.2.3.3 *Treatment of A431 Cells with Ribozyme over 4 days.*

A431 cells were seeded in 96-well plates at 4 x 10^3 cells per well. Approximately 24 hours later, cells were washed twice with sterile PBS (2 x100μl x 5min) and ribozyme, complexed to LipofectAMINE™ (as described in section 4.2.4.2) was added at the appropriate concentration in a total volume of 100μl of serum-free medium per well. Following a four-hour uptake period, the medium was aspirated and replaced by fresh medium containing 10% FBS and cells were incubated at 37°C. Every 24 hours, the medium was removed and the equivalent dose of ribozyme (either 0.1μM or 1μM), complexed to LipofectAMINE™, was reapplied in exactly the same manner as above. After 4 days growth cell number was determined by means of crystal violet assay (section 2.6.1).

4.2.3.4 *Effect of EGF on Growth of A431 Cells.*

A431 cells were plated in 24-well plates at 3 x 10^4 cells per well in DMEM medium containing 10% FBS. Approximately, 24 hours post-seeding, cells were washed twice with sterile PBS and incubated for 96 hours with a range of concentrations (0.01ng/ml – 100ng/ml) of EGF diluted in DMEM medium containing 10% FBS. Following incubation, viable cell number was determined by means of a trypan blue exclusion assay (section 2.4.4).

4.2.3.5 *Effect of Ribozyme Treatment on A431 Cells Stimulated with EGF*

A431 cells were plated in 96-well plates at 4 x 10^3 cells per well in 10% DMEM. 24 hours post-seeding, cells were washed twice (2 x 0.5ml x 5min) with PBS and chimeric ribozyme, complexed with LipofectAMINE™ (as described in section 4.2.4.2), was added at the appropriate concentration in a total volume of 100μl of serum-free medium per well. Following a four hour uptake period, the medium was aspirated and replaced by fresh medium containing 10% FBS and 1.7pM EGF (10pg/ml) and the cells incubated at 37°C. Every 24 hours, the medium was removed and the equivalent dose of ribozyme (0.1μM) complexed to LipofectAMINE™, was reapplied in exactly the same manner as above. Cells were incubated in the continued presence of ribozyme and EGF for a total of 96 hours (4 days) at which time cell number was determined by means of a crystal violet assay (section 2.6.1).

4.2.4 Cellular Delivery of Chimeric Ribozymes using Cationic Liposomes

4.2.4.1 *Assay to Determine the Toxicity of Cationic Lipids to A431 Cells.*

A431 cells were seeded onto 24-well plates at a concentration of 5 x 10^4 cells/well as described in section 2.6. 24 hours post-seeding, cells were washed twice with sterile PBS (2 x 0.5ml x 5 min) and a range of cationic lipid concentrations were added to the wells in a final volume of 200μl / well. Cells were then incubated at 37°C for a period of 4 hours. Following incubation, cells were washed twice with sterile PBS (2 x 0.5ml x 5min) and viable cell number determined by trypan blue exclusion assay (section 2.4.4)

4.2.4.2 *Complexation of Ribozymes with Cationic Liposomes*

LipofectAMINE™ reagent containing the polycationic (+5) lipid 2,3-dioleyloxy-*N*-[2(sperminecarboxamido)ethyl]-*N*,*N*-dimethyl-1-propanaminium trifluoroacetate (DOSPA) and the neutral lipid, dioleoyl-phosphatidylethanolamine (DOPE) (a 3:1 w/w formulation of DOSPA and DOPE, equivalent to 1.5mg of DOSPA per ml of LipofectAMINE™) was obtained from Gibco BRL Life Technologies, Inc., (Paisley, U.K.). PerFect™ lipid, Pfx-6, containing the lipid S-(2-((2,5,-*p* amino-1-oxopentyl)amino)ethyl) carbamic acid, 1-hepta decyl octa decyl ester, dihydrotrifluoroacetate) and DOPE (a 1:1 w/w mix of cationic lipid and DOPE; moles of positive charge / μg lipid mix is given by the manufactures to be 1.07×10^{-9}) was purchased from Invitrogen Corporation (Leek, The Netherlands).

For cellular association studies, cationic lipid / ribozyme complexes were prepared according to the manufacturers instructions as follows: The lipid formulation, at 10-fold the required concentration, was diluted in 100μl serum-free DMEM medium. In a separate microfuge tube, the ribozyme was also diluted, at 10-fold the required concentration, to 100μl with serum-free DMEM medium. The two solutions were then combined, vortexed gently for 2 minutes and incubated for 30 minutes at room temperature to allow the complexes to form. Following incubation, the solution was diluted with serum free DMEM medium to a final volume of 1ml, achieving a 1X concentration of both lipid and ribozyme.

4.2.4.3 *Cellular Association Studies with Ribozyme / Cationic Liposome Complexes*

In all experiments, cationic: anionic (+ / -) charge ratios were calculated on the basis that each molecule of DOSPA carried a net charge of +5 (Gibco BRL LifeTechnologies, U.K.) and each molecule of Pfx-6 carried a net charge of +1 (Invitrogen Corporation, Netherlands). The 37-mer ribozyme was calculated as having an anionic charge of –36, representing the number of inter-nucleotide phosphate linkages contained within the molecule (Jaaskelainen *et al.*, 1994).

A431 cells were seeded onto 24 well plates at a concentration of 5 x 10^4 cells/well as described in section 2.6. 24 hours post-seeding, internally [^{32}P]-radiolabelled ribozyme were complexed to lipids, as described in section 4.2.4.2, using differing (+/-) charge ratio combinations. Cells were then washed twice with sterile PBS (2 x 0.5ml x 5 min) and the liposome / ribozyme complexes were added to cells in a total volume of 200μl of serum-free DMEM medium. The percentage of complexed, radiolabelled ribozyme that became cell associated after 4 hours was determined as described in section 2.8 and normalised to viable cell number (% cell association per 1 x 10^5 cells).

4.2.5 Intracellular Stability of 2'-Modified Chimeric Ribozyme in A431 Cells

A431 cells were seeded onto 24-well plates at a concentration of 3 x 10^4 cells/well and used approximately 24 hours post-seeding. At this time, 0.1μM internally [^{32}P]-labelled ribozyme, complexed with LipofectAMINE™ (at the optimal +/-charge ratio of 5) was added to the A431 cells in serum-free medium. Following a four hour incubation period, the medium was replaced with complete DMEM medium (10% FBS) and cells incubated for varying time points over a 96 hour period. At each time point, cells were washed

twice with PBS (2 x 0.5ml x 5min), lysed and harvested from the wells as described in section 2.7.1.2. Aliquots of 2μl were mixed with formamide loading buffer and stored at –20°C prior to gel loading. Degradation profiles were analysed by 20% PAGE containing 7M urea (section 2.3.1) and detected by autoradiography of wet gels (section 2.3.2).

4.2.6 Efflux of Ribozyme from A431 Cells over 96 hours

A431 cells were seeded onto 24-well plates at a concentration of 3 x 10^4 cells/well and used 20-24 hour post-seeding. For efflux studies, cells were incubated for 4 hours at 37°C with 0.1μM internally [^{32}P]-labelled ribozyme, either free or complexed with LipofectAMINE™ (+/- charge ratio of 5) as described in section 4.2.4.2, in serum-free medium. After incubation, the apical medium was removed, the cells washed with PBS (3 x 0.5ml x 5 min), and 0.5ml of fresh DMEM medium (without the addition of ribozyme) was added. The efflux of internalised ribozyme was monitored at fixed intervals over 96 hours. At each timed interval, 0.5ml of DMEM medium was removed and equivalent of fresh medium was added. The radioactivity pertaining to all fractions collected was determined by LSC as described in section 2.3.3.

4.3 RESULTS AND DISCUSSION

4.3.1 Ribozyme Design

In preparation for future *in vitro / ex vivo* efficacy studies, a number of ribozymes were designed against various sites along the EGFr mRNA. Two major considerations were addressed in the design of ribozymes for this study: the choice of motif (involving the sequence of catalytic core, length of flanking arms and chemistry) and the selection of target site.

4.3.1.1 *Sequence and Structure of Ribozyme Core Motif*

All ribozyme designs were based on the hammerhead motif, since its small size and minimal substrate requirements make it a most suitable candidate for exogenous ribozyme delivery. The sequence of this ribozyme motif was designed to promote optimal intracellular activity based on the findings of Jarvis *et al.*, (1996b). The basic structure is shown in Figure 4.3. The base sequence of stem II and the catalytic core have been shown to be highly active *in vitro* (reviewed in Symons 1992; Bratty *et al.*, 1993) and are based on the design of Haseloff and Gerlach (1988). The terminal loop on stem II of the catalytic core did not contain any uridine bases since pyrimidine bases are reportedly more susceptible to endonucleases than purine bases (Beigelman *et al.*, 1995a). The lengths of the guide sequences, stems I and III, were kept relatively short to either 6 or 7 bases each and designed to be antisense to a particular region of the target mRNA. Short binding arms (in the region of 13-15 total nucleotides) have been reported to achieve optimal cell efficacy (Jarvis *et al.*, 1996b; Birikh *et al.*, 1997).

Chemical modifications were required to ensure enhanced resistance to nuclease activity. The findings of Chapter Three revealed that 2'-O-methyl modified chimeric ribozymes containing either U_4/U_7 2'-amino groups or U_4 2'-C-allyl modifications within the catalytic core of the hammerhead motif and an inverted thymidine or abasic residue at the 3'-terminus (Figure 3.1) conferred considerable stability without significant loss of catalytic activity. The 2'-O-methyl modified ribozymes synthesised for this study contained the 2'-C-allyl modification at position U_4; four phosphorothioate linkages at the 5'-end and an abasic nucleoside at the 3'-end as detailed in Figure 4.3 below.

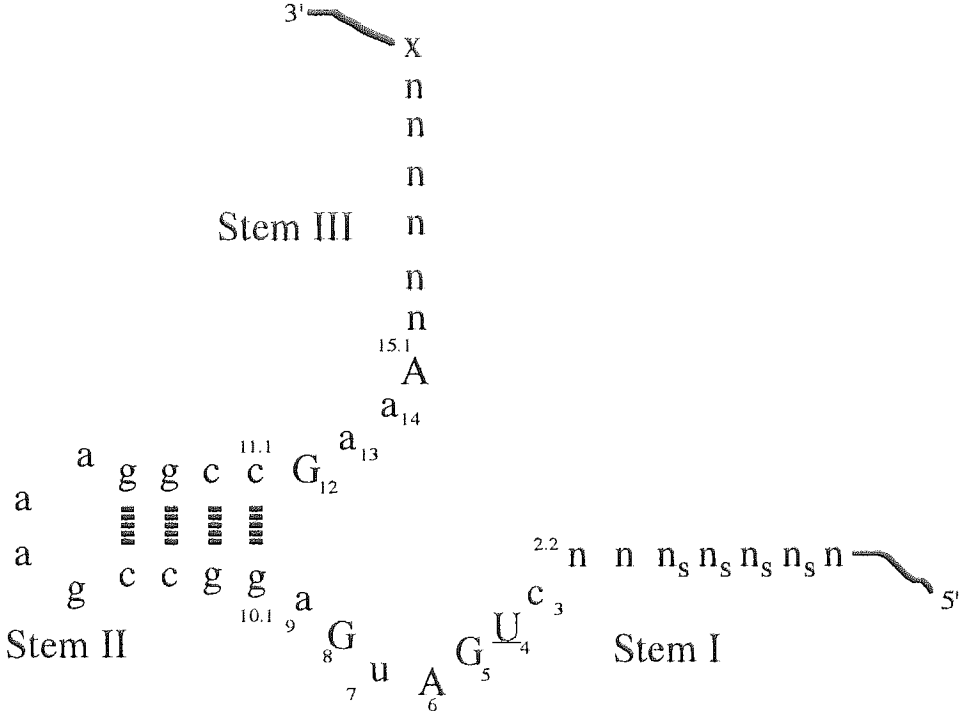

Figure 4.3 *Generic sequence and structure of synthetic ribozymes targeting EGFr mRNA*. Conserved nucleotides within the central core are numbered according to Hertel *et al.* (1993). n is any nucleotide. Uppercase indicates 2'-hydroxyl (ribo) nucleotides. Lowercase indicates 2'-O-methyl nucleotides. U indicates 2'-C-allyl modification at position U_4. X represents a 3'-3'-linked (inverted) abasic nucleotide. The ribozyme motif also contains four phosphorothioate linkages at the 5'-end; all other backbone linkages are phosphodiesters.

4.3.1.2 *Selection of Target Sites along Human EGFr mRNA*

Determining which region to target along the mRNA can be problematic. The ability of an antisense molecule to exert its biological effect is governed by its ability to interact with the targeted mRNA sequence. Yet most RNAs have very complex secondary and tertiary structures and are often associated with proteins. It is difficult, therefore, to identify where accessible sites may lie.

Although sequences designed against the AUG initiation codon have been thought to yield accessible sites, this is more often not the case (Rossi, 1998). A direct method to select accessible sites is simply to synthesise a large number of ribozymes and directly screen them for their ability to affect target gene expression in cell culture or in animals. The ribozyme that proves to be the most efficacious in reducing the level of target mRNA is thereby the best site (Usman & Stinchcomb, 1996). With the collaboration of Ribozyme Pharmaceuticals Inc. (Boulder, Colorado, USA), the strategy used to select accessible mRNA sites for this study was to design and synthesise a number of ribozymes (approximately 20) targeted to different sites along the human EGFr mRNA, and to directly screen the biological efficacy of each of these ribozymes in both *in vitro* and *ex vivo* experiments. The intention was to ultimately test the most efficacious ribozymes for inhibition of primary tumour growth in a murine xenograft model of Glioblastoma Multiforme.

The sequence of the human EGFr mRNA was retrieved from Genbank database (Accession no X00588) using programs from University of Wisconsin Genetics Computer Group (UWGCG), available on seqnet database, located at Daresbury Laboratory U.K. and accessed via Telnet as described in section 4.2.1.

Potential cleavage sites require only the triplet 5' - XUN - 3' in the sequence (where X = any base and N = A, C or U) (section 1.2.1). However, for a large target sequence such as the human EGFr mRNA, which is 5532 bases long (Ullrich *et al.*, 1984), this would yield a vast number of possible target sites - certainly far too many to feasibly synthesise and screen. Consequently, potential cleavage sites including only GUC, GUA, CUC and UUC triplets were investigated. This option still revealed a total of almost 300 possible cleavage sites (68 GUC sites, 39 GUA sites, 96 CUC sites and 78 UUC sites). In order to narrow the possibilities down to a reasonable number to synthesise, a computer prediction program, RNAFOLD, was used to predict secondary structures and eliminate unfavourable ribozyme designs (as described in section 4.2.1).

As mentioned above, folding of the mRNA can render target sites inaccessible to attack by ribozymes or antisense oligonucleotides. The folding of the ribozyme itself and in relation to its target substrate sequence, however, is also important in the design of catalytically active ribozymes. Sequences in the substrate binding arms of the ribozyme can affect its propensity to fold correctly and cleave its target. Misfolding of the ribozyme will prevent the ribozyme hybridising to the substrate and, in addition, if the ribozyme / substrate complex adopts an incorrect conformation then catalytic activity can be severely impaired (Clouet-D'Orval and Uhlenbeck, 1996).

RNAFOLD is a program which uses computer based algorithms (Zuker *et al.*, 1991) to predict the secondary structure of RNA and is accessed using the Genetics Computer Group (UWGCG) package as previously described (section 4.2.1). Consequently, the program was used to assess the folding characteristics of each of the candidate ribozymes and allowed potentially inactive ribozymes to be eliminated from consideration in the *in vitro* screening.

From nearly three hundred potential cleavage sites, only 36 ribozyme designs folded into the required secondary structure conformations as described in section 4.2.1.3 Consequently, from these folding algorithms, it is predicted that these ribozyme constructs will be less likely to adopt inactive conformations when reacted with substrate RNA molecules *in vitro*. In collaboration with Ribozyme Pharmaceuticals Inc., it was decided to limit synthesis to 20 of the most favourable designs, targeting GUC and GUA sites only. The target sites selected and ribozyme sequences chosen are detailed in Tables 4.1 and 4.2

TABLE 4.1 *Chosen target sites identified along human EGFr mRNA*

REGION	TARGET SITE (BASE NO)	RIBOZYME NAME	SEQUENCE OF TARGET SUBSTRATE
5' untranslated region			
	146	egfr-146	5'-GUCCAGU A UUGAUCG-3'
coding region			
	549	egfr-549	5'-UAGCAGU C UUAUCUA-3'
	690	egfr-690	5'-ACAUAGU C AGCAGUG-3'
	1165	egfr-1165	5'-CAAGUGU A AGAAGUG-3'
	1210	egfr-1210	5'-AAUAGGU A UUGGUGA-3'
	2015	egfr-2015	5'-UGGAAGU A CGCAGAC-3'
	3126	egfr-3126	5'-ACCUUGU C AUUCAGG-3'
3' untranslated region			
	4094	egfr-4094	5'-AAAGAGU A UAUUUGA-3'
	4165	egfr-4165	5'-UCAUUGU A GCUAUUG-3'
	4280	egfr-4280	5'-CACAAGU C UUCCAGA-3'
	4394	egfr-4394	5'-AUCAAGU C AUGGCAG-3'
	4404	egfr-4404	5'-GGCAGGU A CAGUAGG-3'
	4409	egfr-4409	5'-GUACAGU A GGAUAAG-3'
	4484	egfr-4484	5'-CUUUUGU A AAAAUGU-3'
	4501	egfr-4501	5'-CCACGGU A CUUACUC-3'
	4793	egfr-4793	5'-AUCAGGU C CUUUCGG-3'
	4944	egfr-4944	5'-AAAGAGU A UAUGUUC-3'
	5008	egfr-5008	5'-AAAGUGU C UCUGCCU-3'
	5110	egfr-5110	5'-UUCAGGU A GUAAAUA-3'
	5401	egfr-5401	5'-GUUCAGU C ACACACA-3'

TABLE 4.2 *Sequence of synthesised hammerhead ribozymes designed against target sites along human EGFr mRNA.*

RIBOZYME NAME	STEM I	CATALYTIC CORE	STEM III
egfr-146	5'-CGAUCAA	CUGAUGAGGCCGAAAGGCCGAA	ACUGGAC -3'
egfr-549	5'-UAGAUAA	CUGAUGAGGCCGAAAGGCCGAA	ACUGCUA -3'
egfr-690	5'-CACUGCU	CUGAUGAGGCCGAAAGGCCGAA	ACUAUGU -3'
egfr-1165	5'-ACUUCU	CUGAUGAGGCCGAAAGGCCGAA	ACACUU -3'
egfr-1210	5'-CACCAA	CUGAUGAGGCCGAAAGGCCGAA	ACCUAU -3'
egfr-2015	5'-UCUGCG	CUGAUGAGGCCGAAAGGCCGAA	ACUUCC -3'
egfr-3126	5'-CUGAAU	CUGAUGAGGCCGAAAGGCCGAA	ACAAGG -3'
egfr-4094	5'-UCAAAUA	CUGAUGAGGCCGAAAGGCCGAA	ACCUCUU -3'
egfr-4165	5'-CAAUAGC	CUGAUGAGGCCGAAAGGCCGAA	ACAAUGA -3'
egfr-4280	5'-CUGGAA	CUGAUGAGGCCGAAAGGCCGAA	ACUUGU -3'
egfr-4394	5'-UGCCAU	CUGAUGAGGCCGAAAGGCCGAA	ACUUGA -3'
egfr-4404	5'-CCUACUG	CUGAUGAGGCCGAAAGGCCGAA	ACCUGCC -3'
egfr-4409	5'-CUUAUCC	CUGAUGAGGCCGAAAGGCCGAA	ACUGUAC -3'
egfr-4484	5'-ACAUUUU	CUGAUGAGGCCGAAAGGCCGAA	ACAAAAG -3'
egfr-4501	5'- AGUAAG	CUGAUGAGGCCGAAAGGCCGAA	ACCGUG –3'
egfr-4793	5'-CCAAAG	CUGAUGAGGCCGAAAGGCCGAA	ACCUGA –3'
egfr-4944	5'-GAACAUA	CUGAUGAGGCCGAAAGGCCGAA	ACUCUUU –3'
egfr-5008	5'-GGCAGA	CUGAUGAGGCCGAAAGGCCGAA	ACACUU –3'
egfr-5110	5'-UAUUUAC	CUGAUGAGGCCGAAAGGCCGAA	ACCUGAA- 3'
egfr-5401	5'-UGUGUGU	CUGAUGAGGCCGAAAGGCCGAA	ACUGAAC –3'

4.3.2 *In vitro* Catalytic Activity of Chimeric Ribozymes Targeted against the EGFr mRNA

The twenty ribozymes selected as described above and detailed in Table 4.2 were kindly synthesised by Ribozyme Pharmaceuticals Inc. (Colorado,USA) according to the method of Wincott *et al.*,(1995) (section 2.1.2.1). The 2'-O-methyl / 2'-C-allyl chimeric ribozymes were synthesised with site-specific modifications as shown in Figure 4.3. In addition, short complementary sequences of the target mRNA substrates (15-mer

sequences) were also synthesised (section 2.1.2.4) and 5'-end [^{32}P]-radiolabelled as described in section 2.2.1.

The *in vitro* catalytic cleavage activity of each of the ribozymes synthesised was determined on a complementary short substrate under single turnover conditions. In each case, activity measurements were performed using an excess of ribozyme at concentrations of 40nM ribozyme to 1nM substrate (see section 2.8.2). Ribozyme mediated cleavage should result in the production of two products, a radiolabelled 8-mer 2',3'-cyclic phosphodiester product which is detectable on an autoradiograph and an unlabelled 7-mer 5'-hydroxyl sequence which is not detectable. Figure 4.4 depicts representative autoradiographs demonstrating the activities of three of these ribozymes. Where cleavage products were clearly evident (as in the case of ribozymes egfr-690 and egfr-3126 shown in Figure 4.4 a and b), the extent of substrate cleavage was quantified using scanning densitometry on the autoradiograph bands (section 2.3.2.2). A profile of the cleavage reaction was obtained by plotting the percentage of intact substrate as a function of time (sample graphs are illustrated in Figure 4.5). In most cases, the plots exhibited a double exponential curve, with rapid cleavage of 60-90% of the substrate occurring in the first 2-10 minutes, after which a steady state was reached. A semi-log plot of the reaction during the initial fast portion of the curve was linear suggesting that the reaction was first order or pseudo-first order during this period. Consequently, the observed reaction rates (k) and activity half-times ($t_{1/2}$= ln(2)/k) were taken from the first exponential. It has been postulated that the slower steady state part of the curve represents inefficient cleavage due to a small proportion of the ribozyme or substrate adopting alternative conformations (M.A.Reynolds, personal communication).

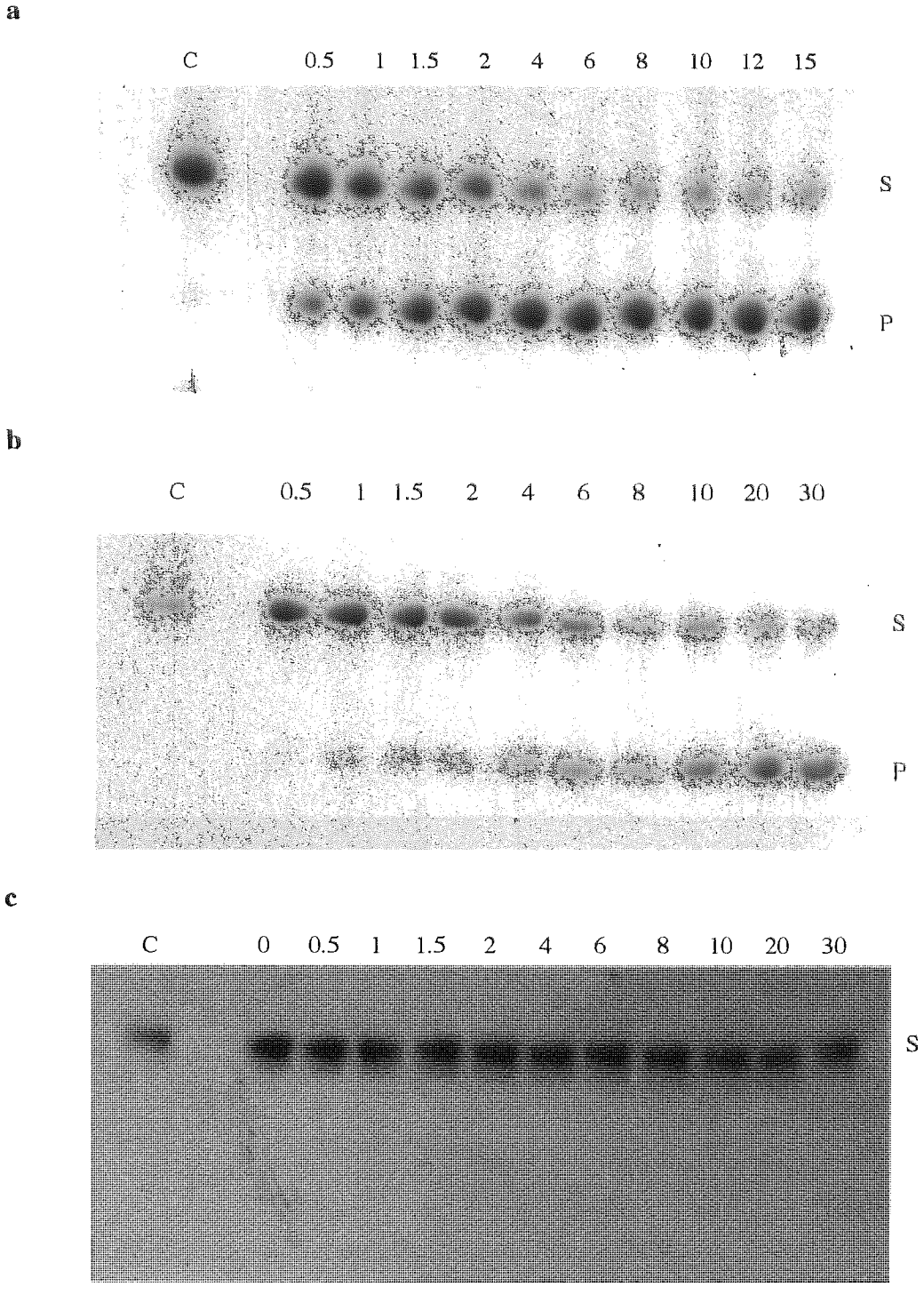

Figure 4.4 *Representative autoradiographs demonstrating the in vitro activity of selective ribozymes against complementary short substrates relating to sites along the human EGFr mRNA.* (a) Activity of ribozyme egfr-690; (b) Activity of ribozyme egfr-3126; (c) Activity of ribozyme egfr-4094. 40nM ribozyme was added to 1nM substrate in presence of 50mM Tris.HCl (pH 7.5), 10mM $MgCl_2$ at 37°C (section 2.8). Times of the reaction in minutes are given above the lanes. Band S refers to intact substrate and band P refers to cleaved product.

a

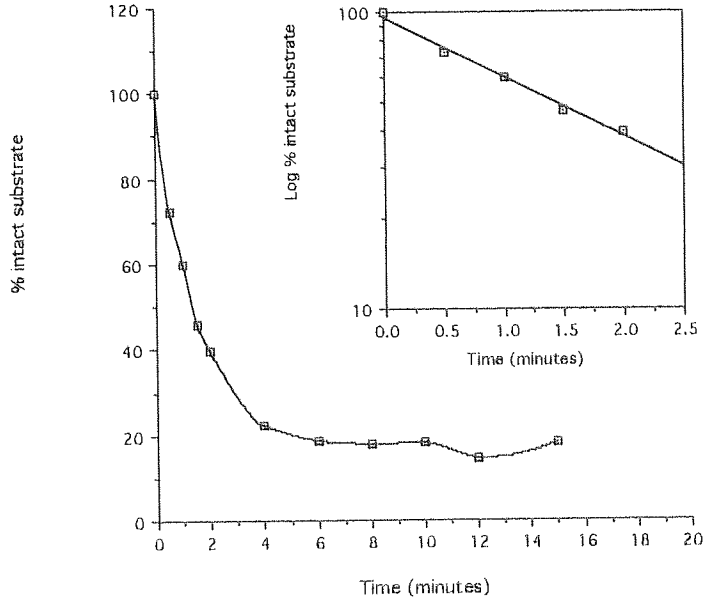

b

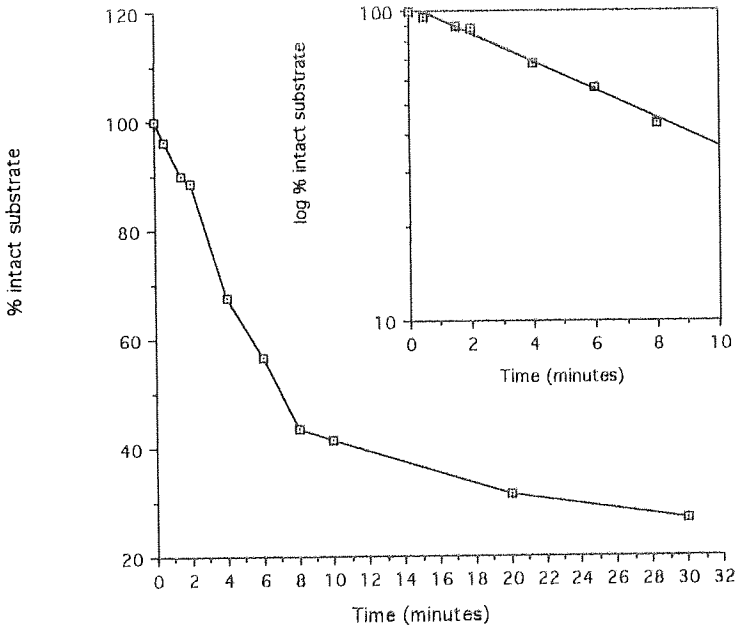

Figure 4.5 *Representative activity profiles of anti-EGFr ribozymes.* (**a**) Activity of ribozyme egfr-690 *inset* semi-log plot of this data to determine activity half-time($t_{1/2}$). (**b**) Activity of ribozyme egfr-3126 *inset* semi-log plot of this data to determine activity half-time($t_{1/2}$). Reactions were performed under single turnover conditions (section 2.8).

The cleavage reactions described above were performed in triplicate for each anti-EGFr ribozyme and an average activity half-time ($t_{1/2}$) calculated. A summary of the results is given in Table 4.3 below.

Table 4.3. *Cleavage activity of anti-EGFr ribozymes targeted against short complementary substrates under single turnover conditions.*

RIBOZYME	ACTIVITY HALF-TIME ($t_{1/2}$) *IN VITRO* (minutes)
egfr-146	1.78 ± 0.16
egfr-549	5.00 ± 0.64
egfr-690	1.57 ± 0.07
egfr-1165	1.40 ± 0.07
egfr-1210	1.99 ± 0.22
egfr-2015	1.51 ± 0.17
egfr-3126	7.43 ± 1.05
egfr-4094	no cleavage
egfr-4165	1.48 ± 0.19
egfr-4280	2.09 ± 0.31
egfr-4394	2.92 ± 0.57
egfr-4404	4.92 ± 1.09
egfr-4409	3.48 ± 0.34
egfr-4484	3.73 ± 0.43
egfr-4501	2.09 ± 0.43
egfr-4793	2.55 ± 0.18
egfr-4944	no cleavage
egfr-5008	1.87 ± 0.12
egfr-5110	5.11 ± 0.42
egfr-5401	2.44 ± 0.36

Ribozyme activity is expressed as cleavage half-time against short (15mer) complementary substrate. Reactions were performed in the presence of 50mM Tris.HCl (pH 7.5), 10mM $MgCl_2$ with 40nM ribozyme and 1nM substrate as described in sections 2.8.1-2.8.2. Values listed represent the mean (n=3) ±SD.

It can be seen from these results that 18 out of the 20 ribozymes successfully cleaved their target substrate. In fact, these experiments show that the chimeric ribozymes have the capacity to cleave their target very efficiently, with the activity half-life of the

substrate being under 8 minutes for all the active ribozymes. Despite the computer predictions of RNAFOLD using folding algorithms, it is probable that the inactivity of ribozymes 4094 and 4944 is due to either the ribozyme and / or the substrate adopting alternative, catalytically inactive conformations.

The ability of ribozymes to cleave their target enzymatically provides evidence of at least three important advantages of these RNA enzymes as potential therapeutics. Firstly it demonstrates their mechanism of action which destroys the substrate; secondly, it illustrates their capacity for multiple turnover to increase potency and finally it suggests increased specificity when compared to small molecules or other antisense therapeutic agents. In order to establish a correlation between cleavage rate and target substrate sequence, the results were analysed further (Table 4.4). Any pattern detected may assist in identifying future efficient cleavage sites along a target mRNA.

When the ribozymes were placed in order of activity (Table 4.4) it appeared that the ribozymes could be roughly classified into two groups; 'fast cleavers' which exhibited activity half-times of under three minutes and 'slower cleavers' which demonstrated activity half-times of over three minutes (usually in the region of 4-5 minutes or over).

To investigate why there are such differences in observed cleavage rates, the kinetics of ribozyme cleavage must first be considered. Ribozyme catalysis may be described by the Michaelis-Menton mechanism as detailed in section 1.2.2. In its simplest form, this involves ribozyme:substrate binding, cleavage of the phosphodiester bond of the bound substrate and release of cleaved products from the ribozyme which is now liberated and available for a new series of catalytic events (Fedor and Uhlenbeck, 1992).

Table 4.4 *Analysis of ribozyme activity in vitro against short complementary substrates*

RIBOZYME	*SEQUENCE OF TARGET SUBSTRATE*	*ACTIVITY HALF LIFE (minutes)*	*ΔG (kcal / mol)*	*%C-G*
egfr-1165	CAAGUGU A AGAAGUG	1.40 ± 0.07	-15	33
egfr-4165	UCAUUGU A GCUAUUG	1.48 ± 0.19	-13.7	36
egfr-2015	UGGAAGU A CGCAGAC	1.51 ± 0.17	-19	58
egfr-690	ACAUAGU C AGCAGUG	1.57 ± 0.07	-18.9	43
egfr-146	GUCCAGU A UUGAUCG	1.78 ± 0.16	-17.2	50
egfr-5008	AAAGUGU C UCUGCCU	1.87 ± 0.12	-17.4	50
egfr-1210	AAUAGGU A UUGGUGA	1.99 ± 0.22	-15.5	42
egfr-4280	CACAAGU C UUCCAGA	2.09 ± 0.31	-13.7	42
egfr-4501	CCACGGU A CUUACUC	2.09 ± 0.11	-17.7	50
egfr-401	GUUCAGU C ACACACA	2.44 ± 0.36	-16.7	42
egfr-793	AUCAGGU C CUUUGGG	2.55 ± 0.18	-16.9	50
egfr-4394	AUCAAGU C AUGGCAG	2.92 ± 0.57	-16.3	42
			83%	83%
			≤ -15	> 40
egfr-4409	GUACAGU A GGAUAAG	3.48 ± 0.34	-14.8	43
egfr-4484	CUUUUGU A AAAAUGU	3.73 ± 0.43	-9.9	21
egfr-404	GGCAGGU A CAGUAGG	4.92 ± 1.09	-20.2	64
egfr-549	UAGCAGU C UUAUCUA	5.00 ± 0.64	-13.9	29
egfr-5110	UUCAGGU A GUAAAUA	5.11 ± 0.42	-12.8	29
egfr-3126	ACCUUGU C AUUCAGG	7.43 ± 1.05	-10.3	36
egfr-4094	AAAGAGU A UAUUUGA	no cleavage	-11.6	21
egfr-4944	AAAGAGU A UAUGUUC	no cleavage	-12.8	29
			88%	75%
			> -15	< 40

The Michaelis-Menten parameters K_m and k_{cat} can be derived for ribozymes in an analogous way to protein enzymes, where K_m (k_1/k_{-1}) is the ribozyme's affinity for a particular substrate and the catalytic rate constant (or turnover number) k_{cat} is a measure of the rate limiting step; which can be cleavage, conformational transitions of the ribozyme-substrate complex or product release (Fersht, 1977). The length and sequence

of substrate can influence many of the elemental rate constants involved (Hertel *et al.*, 1994). For ribozymes with relatively short arms, in the region of 5-6 base-pairs in each of the substrate binding stems I and III, product release is fast and hence k_{cat} represents the rate of phosphodiester cleavage (Fedor and Uhlenbeck, 1992). Elongation of the arms increases helix stability and thereby shifts the rate-limiting step to that of product dissociation. To demonstrate this point, Thompson *et al.* (1996) observed that a hammerhead ribozyme containing 5 base-pairs in each arm had a k_{cat} value of $1.4min^{-1}$ whereas a ribozyme containing 8 base-pairs in each arm was reported to have a k_{cat} of only $0.008min^{-1}$. Under the conditions of these experiments, however, the variance in observed cleavage rates cannot be accounted for by difference in ribozyme arm length. Although ribozymes contained a variety of either six or seven base-pairs per helical arm (Table 4.2), which may result in a shift in the rate limiting step from chemical cleavage to product dissociation, experiments were performed under single turnover conditions. Single turnover does not involve a product release step and the cleavage rate is solely dependent upon ribozyme:substrate affinity and the speed of the chemical cleavage step (Birikh *et al.*, 1997). Since stem II, containing the catalytic core which performs the chemical cleavage step, is identical in all 20 ribozymes, this suggests that differences in observed activity rates may result from variances in ribozyme:substrate affinity.

Ribozymes and substrates may fold into alternative conformations so that the establishment of the equilibrium between the reactants and the ribozyme-substrate complex (k_1/k_{-1}) is no longer rapid. This could account for the distinction between fast and slower cleavers. The computer program RNAFOLD had previously been used, however, to predict possible secondary structures using folding algorithms (Zuker *et al.*, 1991) and discount ribozymes which were most likely to adopt such unfavourable folding conformations (Denman, 1993). The free energy values of formation, ΔG_{hh}, quoted by

this program for folding of the 20 ribozyme-substrate complexes into a hammerhead configuration were compared to *in vitro* performance (column 4; Table 4.4). Certainly a pattern emerges to validate these predictions. Over 83% of the 'fast cleavers' were predicted to have ΔG_{hh} of values more negative or equal to –15 kcal/mol, whereas ΔG_{hh} for the 'slower cleavers' were given to be less negative than –15 kcal/mol. Very low (negative values) of ΔG_{hh} are an indication of stable base-pair formation and consequently for the 'fast cleavers' the formation of a ribozyme-substrate complex is, in general, thermodynamically favoured *in vitro*. Since this study, Hertel *et al* (1998) have conducted a thermodynamic dissection of substrate-ribozyme interaction and have reported that observed free energies of substrate binding to hammerhead ribozymes correlated well with binding energies calculated from computer folding algorithms.

The number of G.C base pairs in the substrate-binding arms has been reported to influence substrate dissociation (Birikh *et al.*, 1997), consequently the number of potential G.C base-pairs were calculated for each target site (column five, Table 4.4). It can be seen that, in general, the 'fast cleavers' contained a high proportion of G.C bases in their substrate recognition sites (83% containing over 40% of C.G bases) whereas the majority of the 'slower cleavers' contained a low proportion of C.G bases (75% contained less than 40% of C.G bases). This suggests that reducing the number of G.C base-pairs in the substrate:ribozyme binding arms does indeed favour substrate dissociation. It must be noted, however that a high level of G.C base pairs can result in reduced specificity (Hertel *et al.*, 1996).

In vitro experiments such as those described above allow testing of a number of ribozymes and selection of the most efficient cleavers for cell culture and *in vivo* investigations. Although a number of hammerhead ribozymes selected on the basis of

efficient cleavage of target substrate *in vitro* have been shown to exhibit high activity *in vivo* (see review by Birikh *et al.*, 1997), the usefulness of such *in vitro* results is, however, limited in predicting performance *in vivo*. This is because many factors within the cell can influence cleavage activity. One of the most rate-limiting factors when dealing with long mRNA substrates is usually association of the ribozyme with the target RNA. This complication arises because RNA folds readily into complex secondary and tertiary structures, which interfere with binding of the ribozyme. In addition the presence of certain RNA binding proteins within the cell have also been shown to influence ribozyme cleavage rates (Bertrand and Rossi, 1994). Consequently, efficient cleavage sites on long substrate RNA cannot easily be predicted. Commonly, in the past, either a trial and error approach has been used for choosing cleavage susceptible sequences or site selection has been based upon secondary structure predictions of the target mRNA (Zuker and Steigler, 1981; Christoffersen, 1994). However, an experimental approach to identify cleavage sites has clear advantages.

Following identification of active ribozymes through *in vitro* cleavage assays on short unstructured substrates, as described above, one can probe for accessible sites along the full length target mRNA by use of *in vitro* screening assays such as RNase H mapping of target mRNA with random ODN libraries or by using ribozyme-library. A more direct approach, however, would be to directly screen the ribozymes in tissue culture. This latter option provides a more realistic assessment of the ability of a ribozyme to attack its target mRNA in a cell. The next step, therefore, in characterising ribozyme activity of the anti-EGFr chimeric ribozymes selected for this study was to screen them directly in cell culture models.

4.3.3 Biological Efficacy of anti-EGFr Ribozymes in Cell Culture (*ex vivo*)

As discussed previously (section 4.1) amplification and rearrangement of the EGFr gene occurs frequently in human glioblastomas. Transcription of numerous gene copies per cell leads to increased EGFr mRNA and high levels of receptor expression. The evaluation of ribozymes as a potential therapy in the treatment of brain tumours requires a versatile implantable brain tumour model utilising glioma cells with high level target expression (Fenstermaker *et al.*, 1995). The human glioma cell line U87-MG are grade III astrocytoma cells and have been shown to exhibit many of the phenotypic features of primary glioblastoma including an autocrine form of proliferation, high levels of protein kinase Cα and infiltration via white matter tracts (Yazaki *et al.*, 1996). This cell line has also been successfully implanted intracranially into the frontal lobe of nude mice to produce subcutaneous U87-MG xenograft tumours for *in vivo* experiments (Yazaki *et al.*, 1996). The phenomena of EGFr over-amplification and rearrangement, however, are less commonly observed in cultured glioma cell lines than in solid tumours (Filmus *et al.*, 1985). In addition, cell lines derived from primary tumours often lose any mutated alleles when maintained in cell culture (Han *et al.*, 1996). Consequently, the suitability of using the U87-MG cell line as a model for testing the efficacy of the anti-EGFr ribozymes was initially investigated.

4.3.3.1 *The Expression of EGFr in Cell Culture Lines*

The levels of EGFr protein expressed in U87-MG cells was assessed by western blotting of whole-cell lysates (as described in section 4.2.2) and compared to EGFr expression in A431 epithelial cells and IPFA human astrocyte cells (Figure 4.6). The A431 cell line is derived from a human epidermoid carcinoma of the vulva and is known to over-express

an unusually large number of EGF receptors (1-3 x 10^6 per cell) (Ullrich *et al.*, 1984). An antibody to the intracellular domain (E-3138; Sigma) was used to detect the EGFr and loading of the gels was standardised by quantification of the levels of actin detected (section 2.4.2).

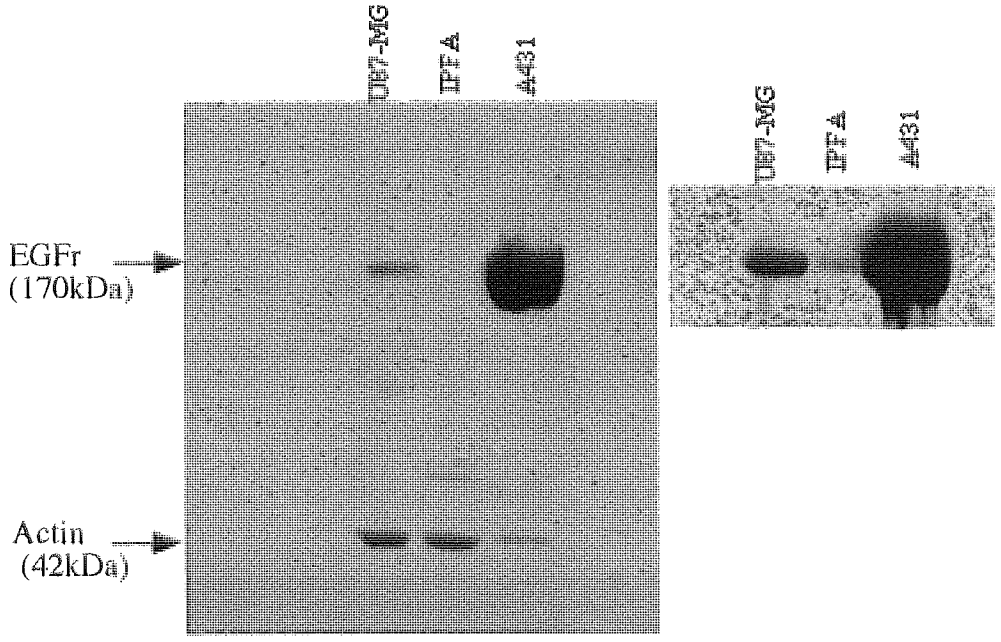

Figure 4.6 *Western blot of EGFr expression in different cell lines.* Total cell lysates from U87-MG, IPFA astrocytes (20μg/well each) and A431 epidermoid cells (10μg/well) were subjected to 7.5%SDS-PAGE at 100V for 1.5h. The proteins were then transferred onto nitrocellulose membrane at 30V overnight and the membrane probed with an anti-EGFr antibody (E-3138) and an anti-actin antibody (A-2066) as described in sections 2.7 and 4.2.2.1. *inset.* Overexposed image of the same blot.

It is clearly evident from Figure 4.6 that the A431 cell line does indeed greatly over-express the EGFr protein. Analysis by densitometry (section 2.3.2.2) revealed that, after normalising for protein loading, the level of EGFr expression in the U87-MG cell line was approximately 6% of that detected in A431 cells. The level of EGFr expression in

this glioma cell line, when compared to that seen in A431 cells, is slightly higher to that observed by Hoi Sang *et al.*, (1995a) who reported EGFr expression to be 100 times greater in A431 cells (1.36 x 10^6 receptors / A431 cell) than in U87-MG cells (1.36 x 10^4 receptors / cell). In addition, U87-MG cells were shown to express approximately three times more receptor than the IPFA astrocytes, demonstrating upregulation at the protein level in the glioma cell line relative to the normal human astrocytes.

In order that the EGFr protein band may be unequivocally identified and to confirm that the protein detected in the above experiment did in fact represent full length EGFr, a control sample of pure EGFr (Sigma, Poole, U.K.) was blotted and compared to bands obtained from whole-cell lysates. Figure 4.7 represents the resulting blot.

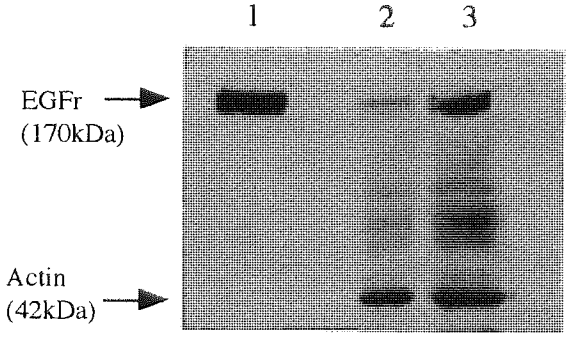

Figure 4.7 *Western blot determining the specificity of anti-EGFr antibody E-3138.* Lanes **1.** 1ng of EGFr; **2.** 10μg A431 cell lysates; **3.** 20μg A431 cell lysates. Cell samples were subjected to 7.5%SDS-PAGE at 100V for 1.5h. The proteins were then transferred onto nitrocellulose membrane at 30V overnight and the membrane probed with anti-EGFr antibody (E-3138) and an anti-actin antibody (A-2066) as described in sections 2.7 and 4.2.2.2.

A clearly discernible sharp protein band representing pure full length EGFr protein of molecular weight 170-kDa, was detected in the control lane 1. The positioning of the

most prominent protein bands detected from the lysates of A431 cells (lanes 2 + 3) corresponds to that of the EGFr control demonstrating the specificity of antibody E-3138.

It can be seen, therefore, that despite being propagated under cell culture conditions the glioma cell line U87-MG does appear to have retained the ability to overexpress the EGFr to a certain degree, although upregulation is not as pronounced as that seen in A431 cells.

4.3.3.2 *Growth Modulation by Tyrosine Kinase Inhibitor, Tyrphostin A25.*

Tyrphostins are small molecular weight compounds that have been shown to preferentially inhibit the EGFr tyrosine kinase and thus may inhibit EGFr-dependent growth (Sion-Vardy *et al.*, 1994). Preliminary proliferation assays using a known tyrosine kinase inhibitor, tyrphostin A25, were conducted on both A431 and U87-MG cells to confirm that the targeting of the EGFr receptor in these model systems will cause a reduction in proliferation. A dose response was investigated over a period of 24 hours as described in section 4.2.3.1. The results, shown in Figure 4.8, produced some interesting findings. While, tyrphostin A25 significantly inhibited growth in A431 cells in a dose dependent manner (IC_{50} of approximately 350μM) there was no significant inhibition evident in U87-MG cells for the range of concentrations of tyrphostin A25 applied. At the highest concentration of tyrphostin (1000μM) tested, however, a change in morphology of U87-MG cells was clearly visible. Cells appeared to have become more rounded with decreased extension of processes. It has been reported that the EGFr mediates the stimulative effects of EGF on glial process extension and glial fibrillary acid protein (GFAP) expression (Hoi-Sang *et al.*, 1995b). Consequently, it is possible that while tyrphostin A25 did not have significant effect on growth, possibly due to relatively

modest levels of EGFr over-expression, inhibition of EGFr specific tyrosine kinase activity was sufficient to affect glial process extension in this cell line.

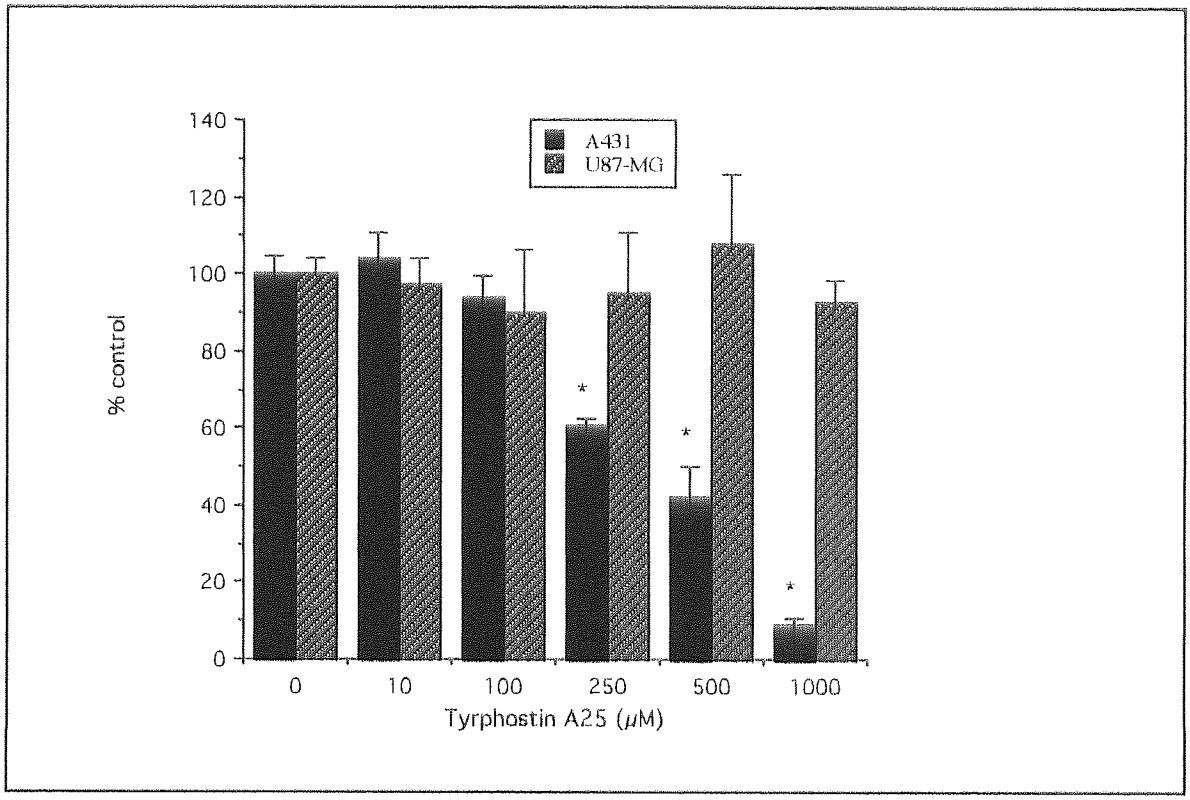

Figure 4.8 *Effects of Tyrphostin A25 on cell growth in U87-MG and A431 cell lines.* Cells were incubated with increasing concentrations (10-1000μM) of Tyrphostin A25 for 24 hours as described in section 4.2.3.1. Cell numbers were determined by trypan blue exclusion assay. Data are expressed as percentage of control (untreated) cell number. Bars represent SD where n=3. * denotes a significant reduction ($P<0.05$) from the untreated control.

Furthermore, the growth of glioma cells has also been reported to be independent of EGFr expression on flat culture dishes suggesting that the primary function of the EGFr in this glioma cell line does not appear to be mediation of the growth-promoting effect of EGF (Hoi-Sang *et al.*, 1995a). This group reported that instead, the level of EGFr expression correlated with the cell's ability to survive and divide when deprived of a solid substratum, especially in response to EGF. The findings of this study may be

supported by the fact that research undertaken by Coulson *et al.*, (1996) found that an ODN directed to EGFr, which specifically inhibited EGFr tyrosine kinase activity, significantly reduced cell growth in A431 cells but not in U87-MG cell line.

Consequently, the results from the above two assays imply that U87-MG glioma cells may not, after all, be the most appropriate model system for targeting of the EGFr. It was decided therefore, to initially screen the 20 anti-EGFr ribozymes in A431 cells with the view to screening any lead ribozymes identified from these studies in a glioma model. A glioma cell line that expresses higher levels of EFGr than U87-MG may be more suited for this purpose. The T-98G cell line, derived from explants of a human glioblastoma multiforme tumour, has been reported to express 10-times the levels of EGFr protein than U87-MG cells and is therefore a likely candidate for future efficacy studies (Hoi-Sang *et al.*, 1995a). It must be noted, however, that it may be easier to detect a reduction in protein levels in a cell line that expresses lower levels of EGFr and testing the most efficacious ribozymes in both U87-MG and T-98G glioma cell lines is most probably the best option.

4.3.3.3.Optimisation of Cellular Delivery of Chimeric Ribozymes using Cationic Liposomes

The research detailed in Chapter Three revealed that, similar to ODNs, exogenously delivered 2'-O-methyl modified ribozymes enter cells by endocytic mechanisms, predominantly by adsorptive and / or receptor mediated endocytosis. These processes are extremely inefficient, however, with only a small fraction (~1-3%) of exogenously applied ribozyme being taken up into the cells. Furthermore, internalised ribozyme is

often trapped within endosomes and unavailable for action against the target mRNA. Clearly, therefore, before proceeding with the proposed efficacy studies, a delivery strategy that enhances ribozyme uptake and bioavailability is required.

Cationic liposomes have proved to be a successful delivery vehicle for achieving biological effects with both antisense ODNs and ribozymes in cultured cells (See Akhtar, 1998; and also section 1.4.2.2). These lipids not only improve cellular association, mainly by adsorptive endocytosis (Akhtar, 1998) but also facilitate endosomal exit via a proposed lipid-exchange mechanism (Zelphati and Szoka, 1996). Studies have revealed that cationic lipids can alter intracellular localisation of nucleic acids, with ODN being observed not only in the cytoplasm but also within the nucleus following delivery with such lipid formulations (Bennet *et al.*, 1992; Lappalainen *et al.*, 1997).

The enhancement properties of two different cationic lipids were investigated and compared in A431 cells: Lipofectamine reagent containing the polycationic (+5) lipid 2,3-dioleyloxy-N[2(sperminecarboxamido)ethyl]-N,N-dimethyl-1-propanaminium trifluoroacetate (DOSPA) and the neutral lipid, dioleoyl-phosphatidylethanolamine (DOPE) (3:1w/w), and 'PerFect™ lipid, Pfx-6' reagent containing the monocation (+1) lipid S-(2-((2,5,-p amino-1-oxopentyl)amino)ethyl) carbamic acid,1-hepta decyl octa decyl ester, dihydrotrifluoroacetate) and DOPE (1:1w/w). The fusogenic DOPE acts as a helper lipid to destabilise endosomal membrane, thus permitting release of nucleic acids from endosomes (Jaaskelainen *et al.*, 1998).

A preliminary study was initially conducted to assess the toxicity of these two cationic liposomes on A431 cells. The effects of lipofectAMINE™ and PerFect™ Pfx-6 on this cells line is represented in Figure 4.9.

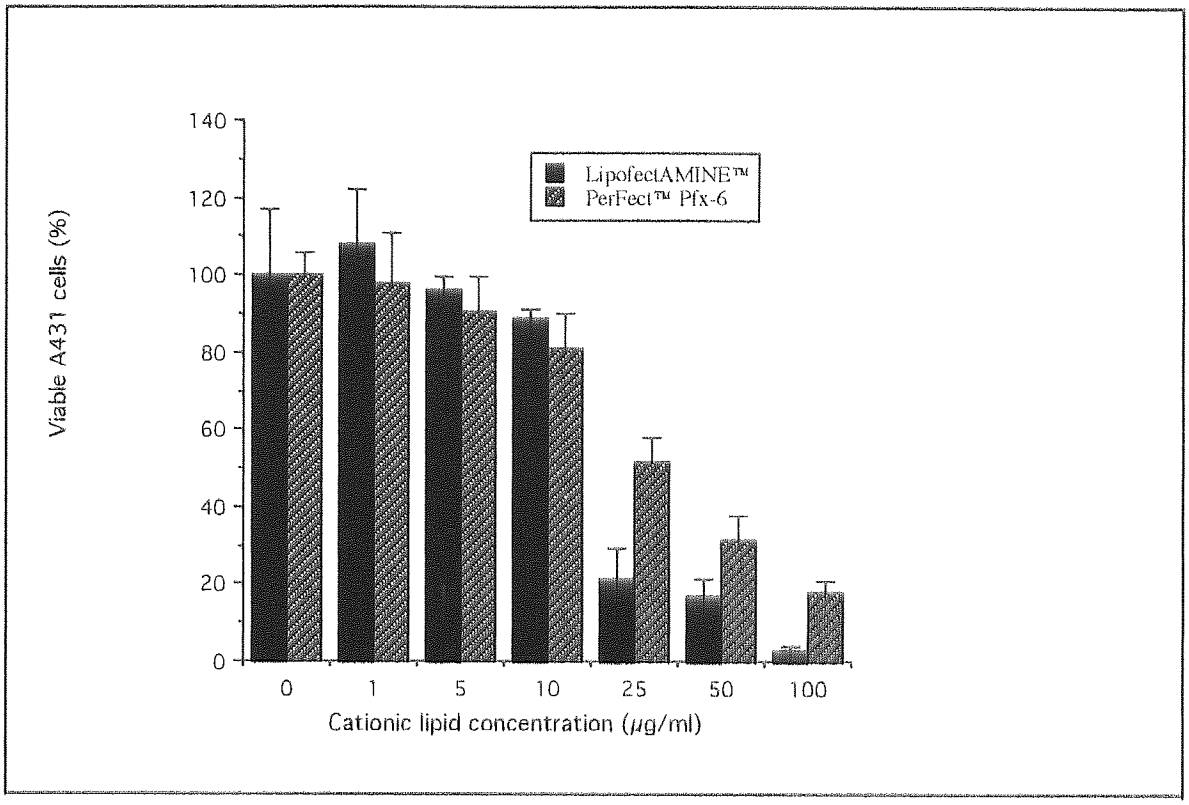

Figure 4.9 *Toxicity of cationic lipid formulations, LipofectAMINE™ and PerFect™ Pfx-6 on A431 cells.* Cationic lipids LipofectAMINE™ and PerFect™ Pfx-6, diluted in serum-free DMEM medium, were added to A431 cells at concentrations ranging from 1μg/ml to 100μg/ml as described in section 4.2.4.1. The cell numbers, 4 hours after addition of the lipids are shown as a percentage of the untreated cell number. Data are expressed as mean (n=3) ±SD.

The results illustrate that both cationic lipid formulations were clearly non-toxic in these cells up to concentrations of 10μg/ml since the mean percentage of viable cells did not reduce significantly ($p>0.05$) over this concentration range. Above this concentration, however, a progressive loss in cell number was apparent after treatment with both LipofectAMINE™ and PerFect™ Pfx-6. The reduction in cell viability appeared more pronounced after treatment with LipofectAMINE™, with cell viability falling steeply from 88.8 ± 2.22% to 21.5 ± 8.01% in the concentration range from 10μg/ml to 25μg/ml. The increased toxicity observed at the higher concentrations of LipofectAMINE™ when

compared to that of PerFect™ Pfx-6 could possibly be due to the greater cationic charge carried by DOSPA. Positively charged molecules have been implicated in cellular toxicity in other models (Filion and Phillips, 1997). These results demonstrate that cationic liposomes should be used with caution for the intracellular delivery of ribozymes, since lipid formulations such as these can be toxic *in vitro* if used at high concentrations.

The importance of charge to charge interactions in the formation and properties of lipid complexes has been recognised. In fact, in most cases it has been reported that transfection of nucleic acids becomes efficient only when the nucleic acid – lipid complex has a net neutral or positive charge (Eastman *et al.*, 1997; Lappalainen *et al.*, 1997; Hope *et al.*, 1998; Jaakelainen *et al.*, 1998). Since the ratio of positive to negative charge is known to be an important factor in transfection, studies were undertaken to determine the optimal charge ratio for both types of lipid formulation (LipofectAMINE™ and PerFect™ Pfx-6) in increasing cellular association in A431 cells.

Internally [^{32}P]-labelled ribozyme, at a concentration of 0.1μM, was complexed with these two liposome formulations at a variety of different cation:anion charge ratios. The effect on cellular association was examined after a period of 4 hours incubation at 37°C (as detailed in section 4.2.4.3) and the results shown in Figure 4.10a (lipofectAMINE™) and Figure 4.11a (PerFect™ Pfx-6). Parallel studies were also performed to assess the cytotoxicity of these lipid-ribozyme complexes (Figure 4.10b and Figure 4.11b).

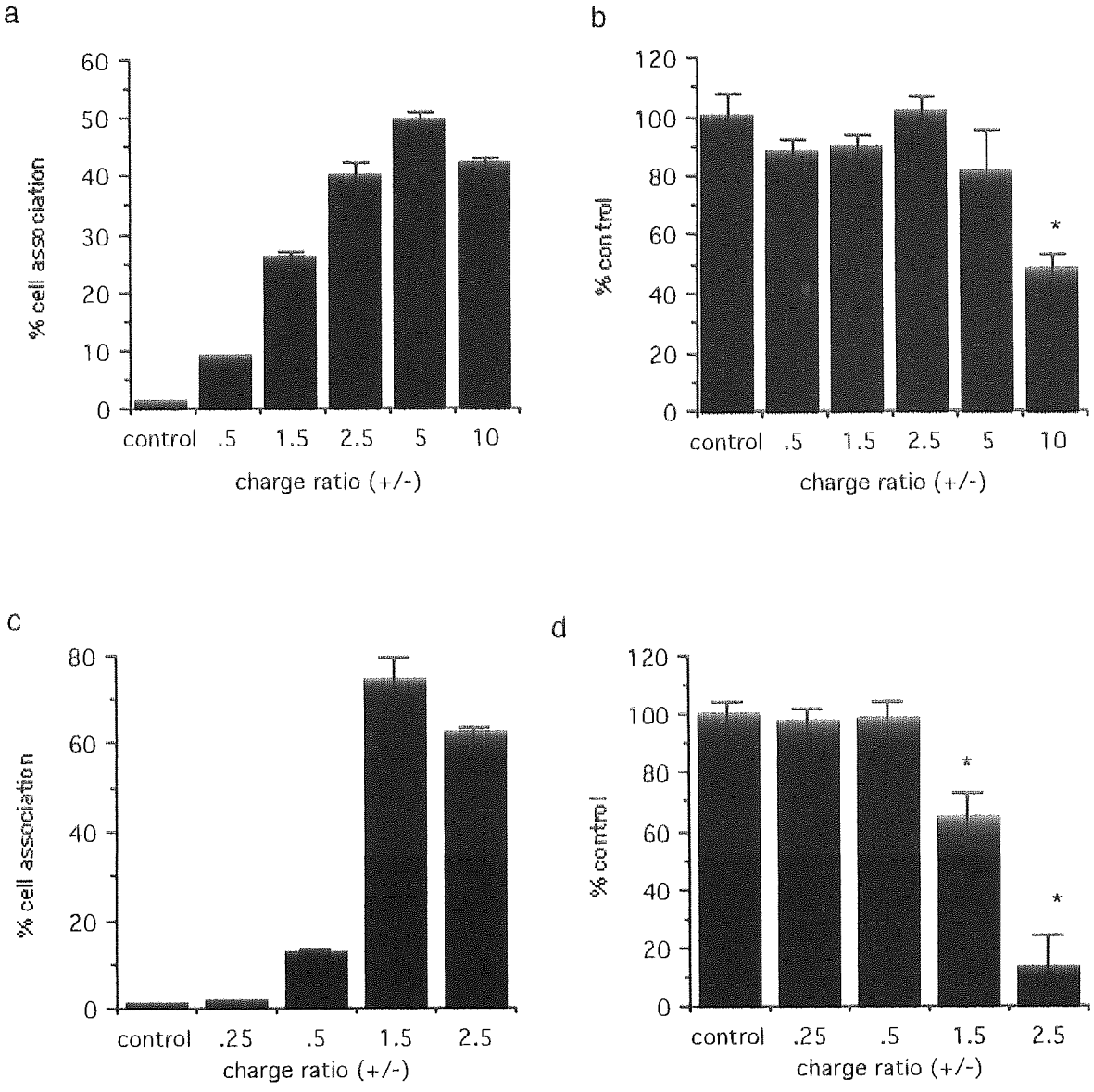

Figure 4.10 *Optimisation of ribozyme association to A431 cells using LipofectAMINE™.* (a) Cell association of 0.1μM ribozyme when complexed with LipofectAMINE™ at various charge ratios after 4 hours incubation at 37°C (section 4.2.4.3). (b) Parallel assay representing the toxicity of the lipid:ribozyme complexes when complexed to 0.1μM ribozyme. (c) Cell association of 1μM ribozyme when complexed with LipofectAMINE™ at various charge ratios after 4 hours incubation at 37°C . (d) Parallel assay representing the toxicity of the lipid:ribozyme complexes when complexed to 1μM ribozyme. Data are expressed as mean (n=3)±SD. * denotes a significant reduction ($p<0.05$) from the untreated control.

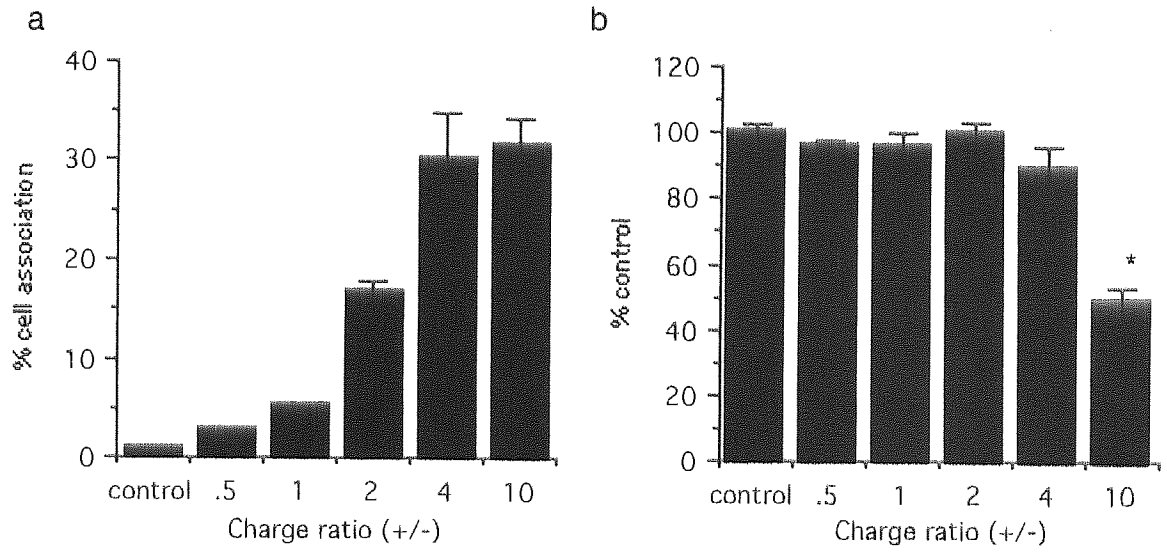

Figure 4.11 *Optimisation of ribozyme association to A431 cells using PerFect™ Pfx-6.* (a) Cell association of 0.1μM ribozyme when complexed with PerFect™ Pfx-6, at various charge ratios after 4 hours incubation at 37°C (section 4.2.4.3). (b) Parallel assay representing the toxicity of the lipid:ribozyme complexes when complexed to 0.1μM ribozyme.

It is apparent from these results that at all the charge ratios tested both cationic lipid formulations significantly ($P<0.001$) increased the percentage of chimeric ribozyme which became cell associated when compared with the free ribozyme control (Figure 4.10a and 4.11a). LipofectAMINE™ however, appeared to be the most effective agent since the level of association increased up to 75–fold (from 0.65 ± 0.03% association of 'free' ribozyme to 49.29 ± 1.44 % association at (+/-) charge ratio of 5) (Figure 4.10a). Increased cellular association observed with PerFect™ Pfx-6 was not as pronounced, with the greatest increases in percentage association, seen at a (+/-) charge ratio of 10, being 40-fold that observed by free, uncomplexed, ribozyme (Figure 4.11a).

The results also confirm that variations in cationic:anionic charge ratio does, indeed, have a considerable effect upon the cellular association of the chimeric ribozyme to A431 cells. The optimum lipid:ribozyme charge ratios for improving cellular association of the chimeric ribozyme to A431 cells were formed in the presence of excess liposome

(positively charged complexes). The greatest increases in cellular association were seen at a (+/-) charge ratio of 5 when the ribozyme was complexed to LipofectAMINE™ and at 10 when the ribozyme was complexed to PerFect™ Pfx-6. It must be noted, however, that in the latter case there was no significant difference ($p>0.05$) in % cellular association at (+/-) charge ratios of 4 and 10. These findings concur with many other studies which have shown that the net charge of the liposome- nucleic acid complex has to be positive for effective transport of nucleic acids into cells (Zhou and Huang, 1994; Farhood *et al.*, 1995; Hope *et al.*, 1998). Cationic liposomes are thought to enter cells through adsorptive endocytosis and it has been postulated that Lipid-DNA particles that exhibit a net positive surface charge are more readily endocytosed by cells in culture. In addition, Lappalainen *et al.*, (1997), while studying the liposomal delivery of ODNs at the ultrastructural level, demonstrated that release from vesicles and transport into the nuclear area was faster when complexes had a positive net charge. Furthermore, it has been reported that complexes prepared with excess DNA (on a charge basis) do not result in release of vesicle contents (Jaaskelainen *et al.*, 1994).

Maximal activity, however, has been reported to occur near the point of charge neutralisation (see Hope *et al.*, 1998 for review). Consequently optimal charge ratios in the region of 4, 5 and 10 do appear to involve excessive quantities of cationic lipid. This increased requirement for liposome could be due to the ionic strength of the cell culture medium (DMEM). A study by Eastman *et al.*, (1997) reported that increased amount of cationic lipid was required to change the negative zeta potential on the complex. Their research revealed that a cationic lipid:DNA charge ratio of >1.5:1 was necessary to produce a complex with an overall net positive charge and in Opti-MEM cell culture medium DOSPA complexes remained negatively charged up to a ratio of > 2.5:1.

The initial surface charge of the complex may serve an indirect purpose other than direct interaction with the cell surface, for instance adsorption of proteins. These roles may include compaction of DNA or to promote escape from endosomal compartments (Hope *et al.*, 1998). The differences in apparent optimal charge ratios between LipofectAMINE™: ribozyme complexes and PerFect™: ribozyme complexes could be due to a variety of factors including differences in cationic lipid:DOPE ratio or differences in the composition of the polar head group of the cationic lipid (Bennet, 1995). It must also be noted that few studies clearly describe how they calculated the net charge of lipid formulations used. There appears to be some confusion on this matter and consequently it is difficult to verify optimum charge ratios quoted.

The importance of undertaking parallel toxicity studies when optimising lipid delivery was clearly demonstrated by Figures 4.10b and 4.11b. When first considering ribozyme delivery using LipofectAMINE™, it can be seen from Figure 4.10b that concentrations of LipofectAMINE™ required for obtaining a (+/-) charge ratio of 10 or greater (≥14μg/ml) resulted in significant toxicity of the cells, as analysed by a trypan blue exclusion assay (section 2.4.4). Similar observations were made when considering ribozyme delivery using PerFect™ Pfx-6. At a (+/-) charge ratio of 10 (30μg/ml), viable cell number significantly ($p<0.001$) reduced to 48±4.3% of the control untreated value. It is evident from these results that the optimal concentration of cationic lipid to deliver ribozymes ex-vivo may, therefore, require a compromise between efficacy and toxicity. Consequently, an optimal +/- charge ratio of 5 (7μg/ml) is required when delivering 0.1μM ribozyme to A431 cells using LipofectAMINE™ whereas, in view of the toxicity seen at charge ratio of 10, the optimal +/- charge ratio to be used with PerFect™ Pfx-6 is 4 (12μg/ml).

The optimal charge ratio of lipid:ribozyme complex was also found to be dependent upon the concentration of ribozyme to be delivered. The optimal +/- charge ratio of LipofectAMINE™ to deliver 1μM chimeric ribozyme was determined to be 1.5 (Figure 4.10c). The concentration of LipofectAMINE™ (21μg/ml) used to achieve this ratio however proved to be significantly toxic to the cells, as viable cell number was reduced to 64.7 ± 8.4% of the control value at this ratio (Figure 4.10d). In order to avoid such cytotoxicity, it was decided that a maximum of 10μg/ml of LipofectAMINE™ could be used for transfection of ribozymes in A431 cells.

It is apparent, therefore, that many factors are involved when optimising ODN and ribozyme delivery using cationic lipids. The importance of both the cationic lipid charge, cationic to neutral lipid ratio, lipid to nucleic acid ratio, dose and concentration are all factors which appear to affect efficacy of delivery and this makes the screening process more and more complex. In general, it appears that it is too simplistic to claim that a certain charge ratio is optimal in all *ex vivo* cases. These experiments show that careful optimisation is required accounting for cell line, choice of lipid formulation, lipid and ribozyme concentrations and time of exposure. Since LipofectAMINE™ appeared to be the most efficient formulation in delivering chimeric ribozyme to A431 cells, it was decided to mainly use this reagent to facilitate delivery when screening the anti-EGFr ribozymes for efficiency in this cell culture model.

4.3.3.4 *Optimisation of Cell Proliferation Assay Protocol*

One of the main issues to be addressed when considering whether exogenously delivered chimeric ribozymes, targeted to EGFr, provide a realistic therapeutic approach to the treatment of Glioblastoma Multiforme is whether ribozymes will be effective in

inhibiting the activity or expression of the chosen target protein and whether this will be sufficient to inhibit proliferation of a glioblastoma. The ability of each of the twenty anti-EGFr ribozymes to achieve these goals was assessed by initially screening for reduction in both cell number and receptor protein levels. Once lead ribozyme/s were identified, further demonstration of efficacy would be undertaken by quantifying mRNA levels by Northern blot analysis.

The efficacy of the ribozymes in inhibiting tumour growth was assessed by determining cell number by means of a crystal violet assay as described in section 2.6.1. To ensure accurate assessments of cell numbers, a standard curve correlating cell number to optical density was obtained for each experiment. To this end, A431 cells were seeded in 96-well plates at densities ranging between and 1 x 10^3 – 4 x 10^4 cells per well and the colorimetric assay was performed 4 hours post-seeding, at which time no significant proliferation had occurred. A representative standard curve is shown in Figure 4.12 below and demonstrates the linear relationship between cell number and absorbance readings within this range of cell densities.

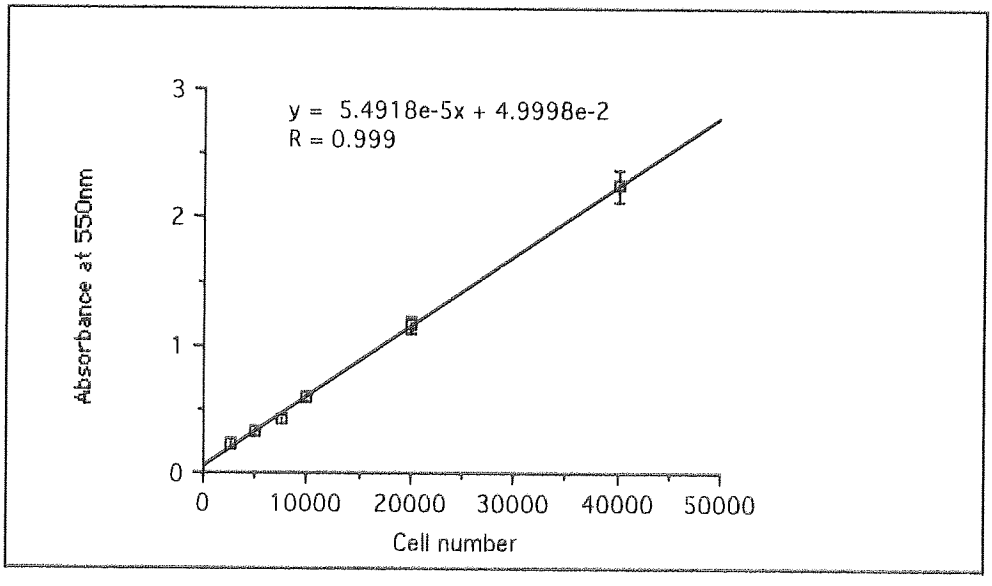

Figure 4.12 *Standard curve showing the correlation between cell numbers of A431 cells and absorbance at 550nm using the crystal violet assay.*

To assess optimal growth conditions for inhibition experiments, the rate of proliferation of A431 cells in the presence or absence of serum was determined. Cells were seeded onto 96-well plates at a density of 7.5 x 10^3 cells/well (time 0) in either serum-free medium or medium containing 10% FBS. Cells were then incubated at 37°C for the time periods indicated, at which point cell number was determined by crystal violet assay (section 2.6.1). The results are given in Figure 4.13.

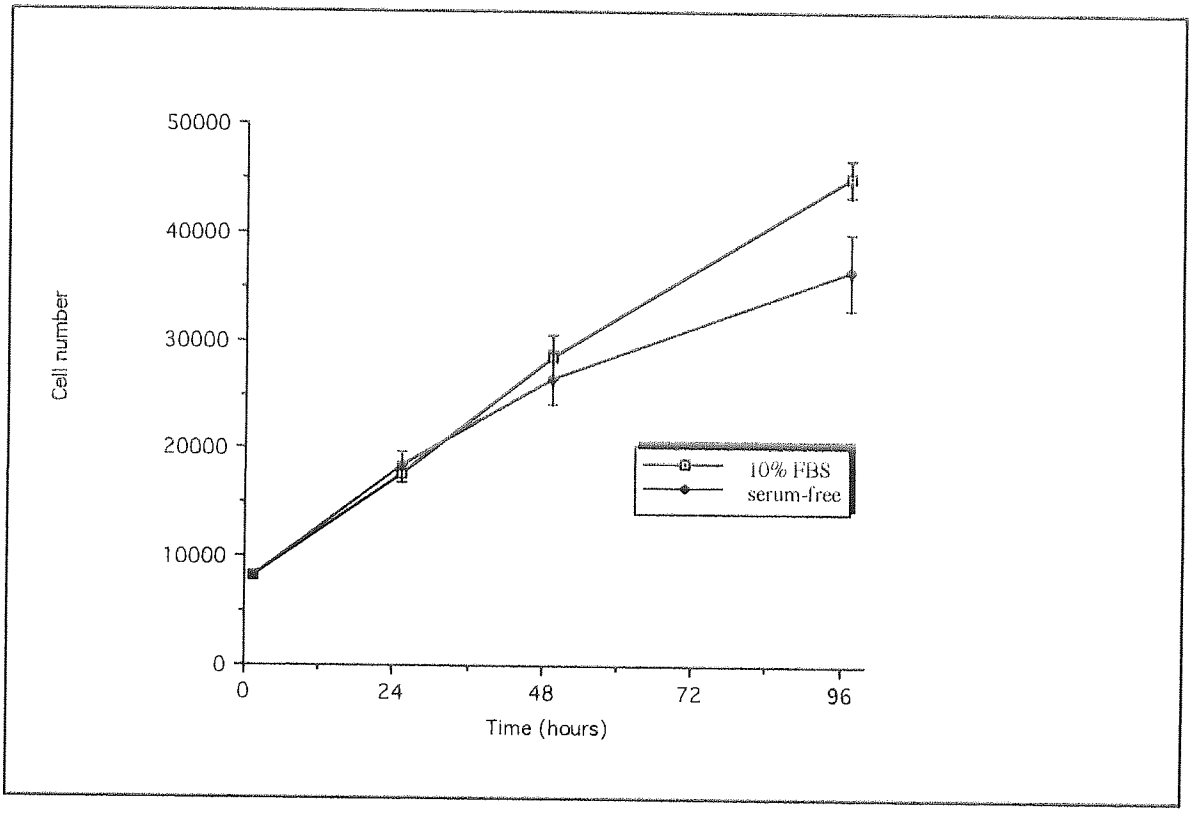

Figure 4.13 *Effect of growth conditions on proliferation of A431 cells.* Cells were incubated in either serum-free medium or medium containing 10% FBS at 37°C for the time periods indicated. Results (mean of 5 ± SD) are shown as cell number at each time point as determined by crystal violet assay.

Proliferation of A431 cells appeared to be independent of the presence of exogenous growth factors for 48 hours post-seeding since there was no significant difference in growth rates during this period between cells incubated in serum-free medium and those incubated in medium containing 10% FBS. An autocrine pathway for control of growth

in this cell line is likely to be responsible for the non-reliance on exogenous growth factors evident in this study, due to the over-expression of both EGFr and co-expression of the growth factor, EGF. By 96 hours post-seeding, however, cell growth in serum-free medium had slowed significantly ($P<0.001$) when compared to those cells incubated in the presence of FBS. These results indicated, therefore, that proliferation inhibition studies to be conducted over periods of up to 48 hours could be performed in serum-free conditions but those experiments requiring longer incubation periods of over 48 hours would require the cells to be incubated in serum containing medium.

4.3.3.5 *Optimisation of Western Blotting Protocol.*

Prior to commencing western blotting on ribozyme treated samples, an experiment was conducted to determine the protein levels of whole cell lysates required to obtain a band, representing EGFr protein, of detectable intensity. A431 cells were harvested directly from 24-well plates using hot laemmli buffer (section 2.7.1.1) and increasing quantities of whole cell lysate protein subjected to 7.5% SDS-PAGE, blotting and immuno-detection using antibody E-3138 targeted to the intracellular domain of EGFr, as described in sections 2.7.3-2.7.5. Increased loading resulted in bands of increasing intensity (Figure 4.14a), which when analysed by densitometry (section 2.3.2.2) and plotted graphically, (Figure 4.14b) proved to increase in a linear fashion. These results suggested optimal loading of between 15 – 20μg of cell lysates per well. A431 cell numbers in the region of $8 \times 10^4 - 1 \times 10^5$ are required to achieve this level of protein.

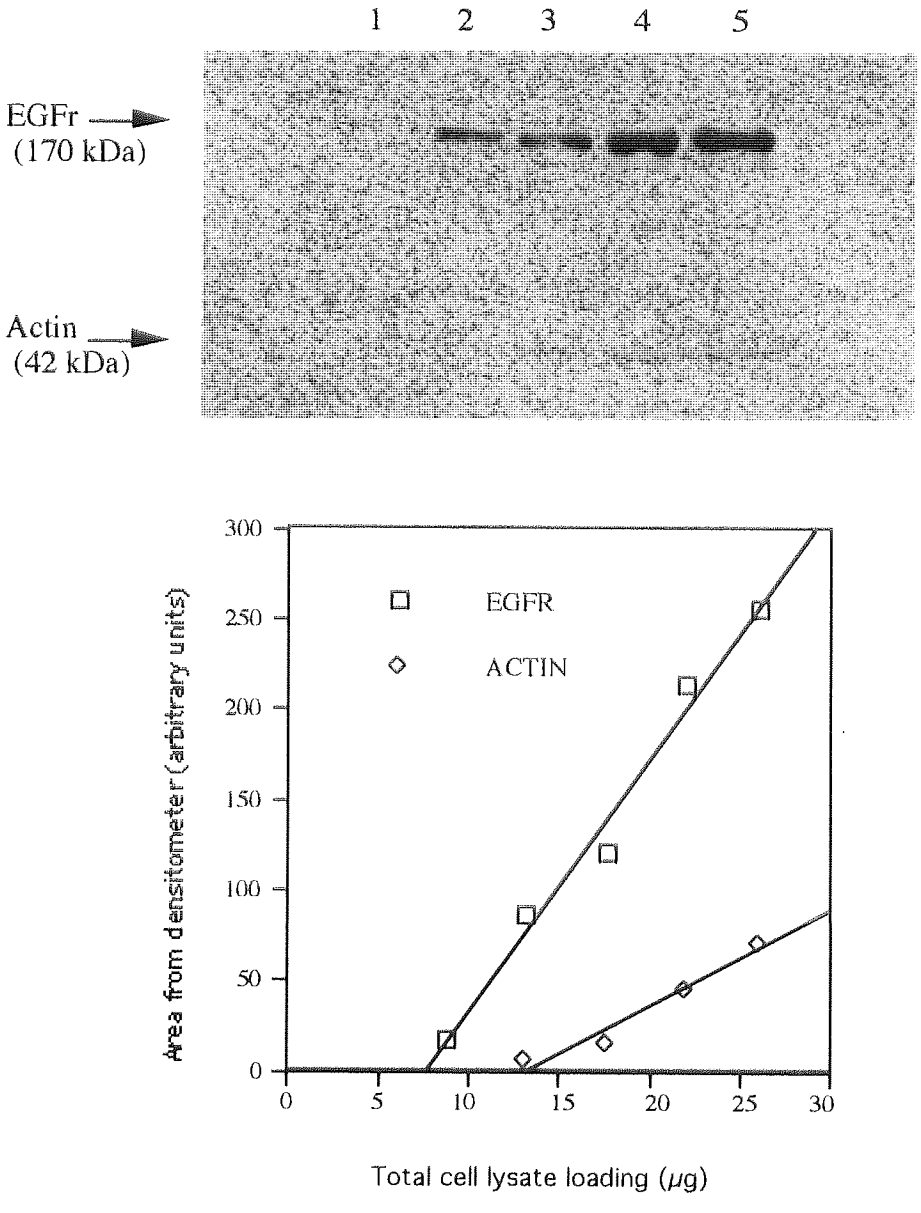

Figure 4.14 *Optimisation of protein loading for Western blotting of EGFr using antibody E-3138.* Cells were lysed directly in laemmli buffer from 24-well plates as described in section 2.7.1.1. Cell samples were subjected to 7.5% SDS-PAGE at 100V for 1.5h. The proteins were then transferred onto nitrocellulose membrane at 30V overnight and the membrane probed with anti-EGFr antibody E-3138 and anti-actin antibody A-2066 as described in sections 2.7.1-2.7.5. (**a**) western blot image. Loading per well: **1**. 8.8μg (4.4 x 10^4 cells); **2**. 13.2 μg (6.6 x 10^4); **3**. 17.6μg (8.8 x 10^4); **4** 22μg (1.1 x 10^5); **5**. 26μg (1.3 x 10^5). (**b**). Graphical representation of blot.

4.3.3.6 *Effect of Chimeric anti-EGFr Ribozymes on Proliferation and Target Protein Expression of A431 Cells.*

To determine the efficacy of the twenty chimeric ribozymes targeted to various sites along EGFr mRNA, the influence of both ribozyme concentration and incubation time were studied.

4.3.3.6.1 *Treatment with Ribozyme over 24 hours*

Studies which have successfully demonstrated efficacy using synthetic, exogenously delivered ribozymes *ex vivo* have reported IC_{50} values at concentrations in the order of nano Molar (nM) (Jarvis *et al.*, 1996; Sioud, 1996; Kisich *et al.*, 1999). Consequently, it was decided that all twenty ribozymes would initially be screened at two concentrations, 0.1μM and 1μM and their effect on A431 cell growth examined. A431 cells were treated with ribozyme for a period of twenty-four hours at 37°C in serum-free medium as described in section 4.2.3.2. LipofectAMINE™ was used to enhance delivery at concentrations determined optimal in section 4.3.3.3. The results are depicted in Figure 4.15.

At both concentrations, statistical analysis revealed no significant decrease in cell number following ribozyme treatment when compared to the untreated control for any of the twenty ribozymes under investigation. Furthermore, when western blot analysis was conducted on cells treated with the five ribozymes that had displayed the greatest percentage reduction in cell number at each concentration, no significant decrease in EGFr protein expression was evident following treatment with either 0.1μM (Figure 4.16a) or 1μM ribozyme (Figure 4.16b).

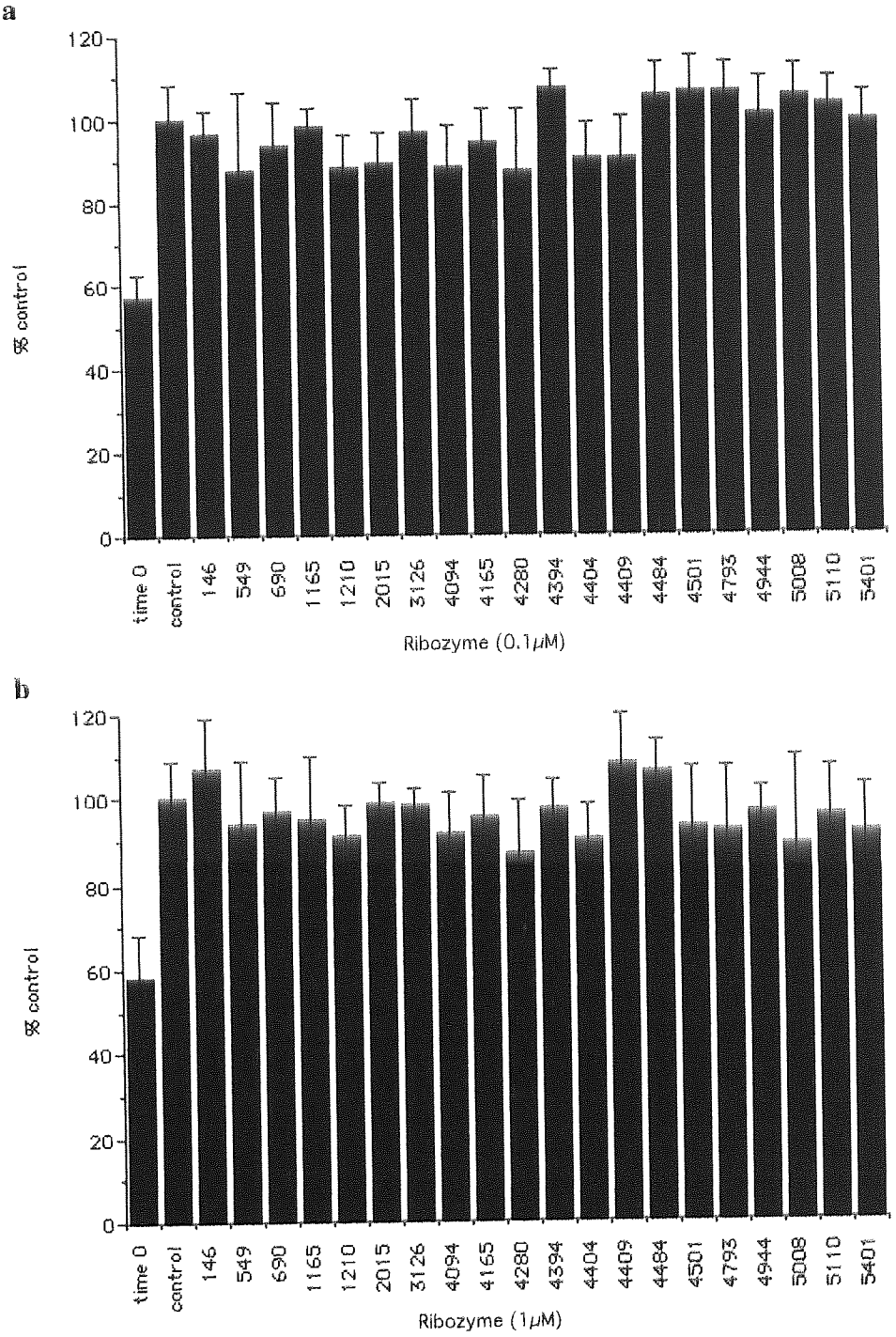

Figure 4.15 *Effect of ribozyme treatment on proliferation of A431 cells over 24 hours.* Chimeric ribozymes targeting various sites along EGFr mRNA were complexed with LipofectAMINE™ and delivered to A431 cells in serum-free medium at a concentration of either: (a) 0.1μM ribozyme (7μg/ml Lipofectamine, (+/-) charge ratio of 5) or (b) 1μM (10μg/ml LipofectAMINE™) as described in sections 4.2.3.2 and 4.2.4.2. Cells were incubated at 37°C in the presence of ribozyme for a period of 24 hours at which time cell number was determined by crystal violet assay. Control contained LipofectAMINE alone. Data represents the mean n=6±SD.

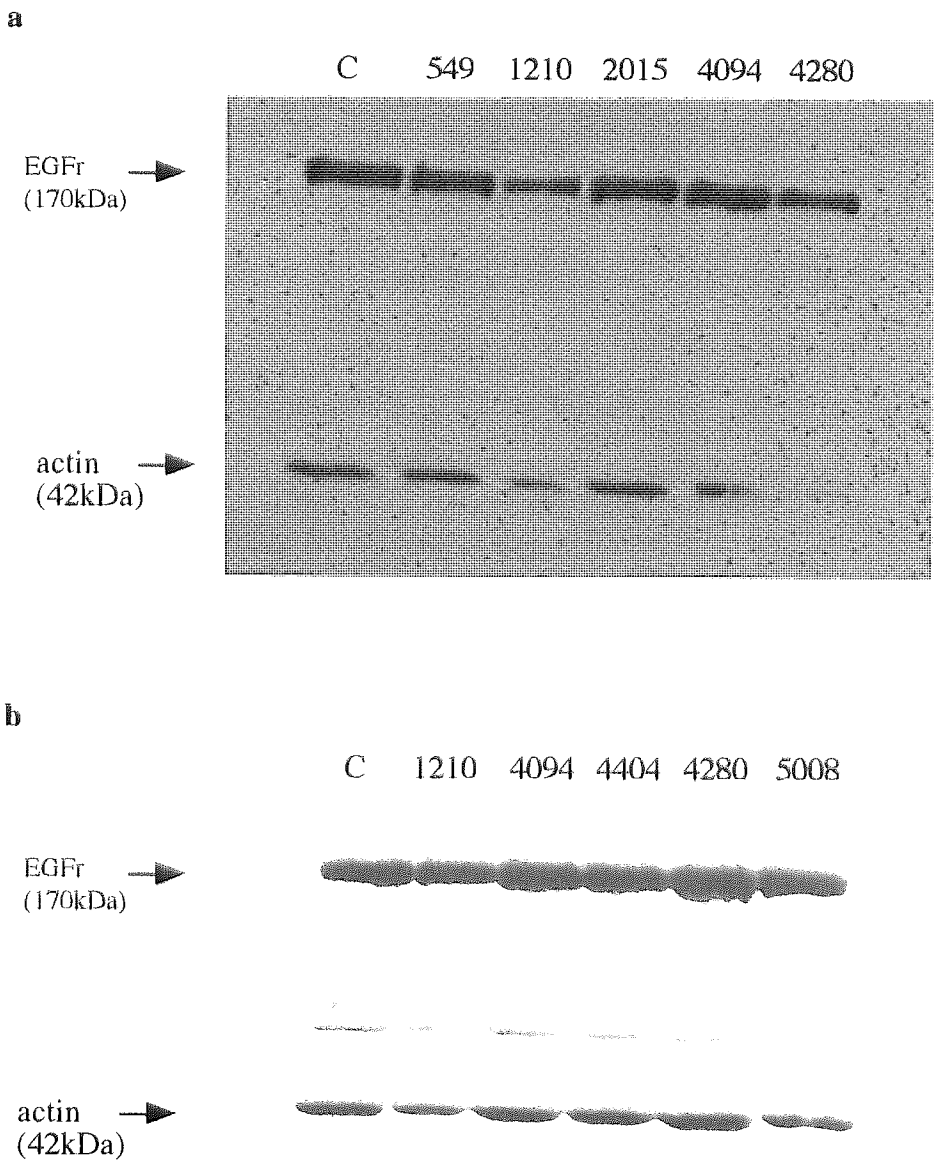

Figure 4.16 *Effect of ribozyme treatment over 24 hours on EGFr expression in A431 cells.* A431 cells were plated in 24-well plates and cultured for 24 hours in the presence of five lead ribozymes identified from each of the above two proliferation experiments (Figure 4.15 a and b). The chimeric ribozymes targeting various sites along EGFr mRNA were complexed with LipofectAMINE™ and delivered to A431 cells in serum-free medium at a concentration of either: **a** 0.1μM ribozyme (7μg/ml LipofectAMINE™:(+/-) charge ratio of 5) or **b** 1μM (10μg/ml LipofectAMINE™) as detailed in sections 4.2.4.2. Cells were incubated at 37°C in the presence of ribozyme for a period of 24 hours at which time cells were lysed and total cell lysates (20μg protein per well) analysed by 7.5% SDS-PAGE and immunoblotting with anti-EGFr antibody E-3138 (section 2.7). Images depict representative blots from duplicate experiments.

4.3.3.6.2 *Treatment with Ribozyme over 4 days*

The half-life of EGFr protein is reported to be approximately 6-10 hours (King *et al.*, 1980). Longer incubation times with the ribozymes may be required, therefore, to see any significant reduction in the target protein levels. Consequently the effect of exposing A431 cells to anti-EGFr ribozymes over a period of 4 days was investigated. Since, previous stability studies (Chapter Three) had revealed that a similarly modified 2'-O-methyl/ 2'-C-allyl chimeric ribozyme exhibited a half-life of ~ 20 hours in neat FBS, it was decided to reapply fresh doses of ribozyme to the cells every 24 hours during this period (see section 4.2.3.3 for method details). The experiment was repeated using 0.1μM and 1μM ribozyme. As with the previous study, LipofectAMINE™ was used to enhance delivery at concentrations determined as optimal in section 4.3.3.3.

Increased incubation times with the ribozymes failed to cause a significant decrease in cell proliferation (Figure 4.17) at either of the concentrations tested. To establish if any reduction in EGFr expression could be detected, western blotting analysis was undertaken on five lead ribozymes from each concentration used. As depicted in representative blots shown in Figure 4.18, none of the ribozymes appeared to significantly down regulate target protein levels, determined by the percentage of EGFr expression relative to actin.

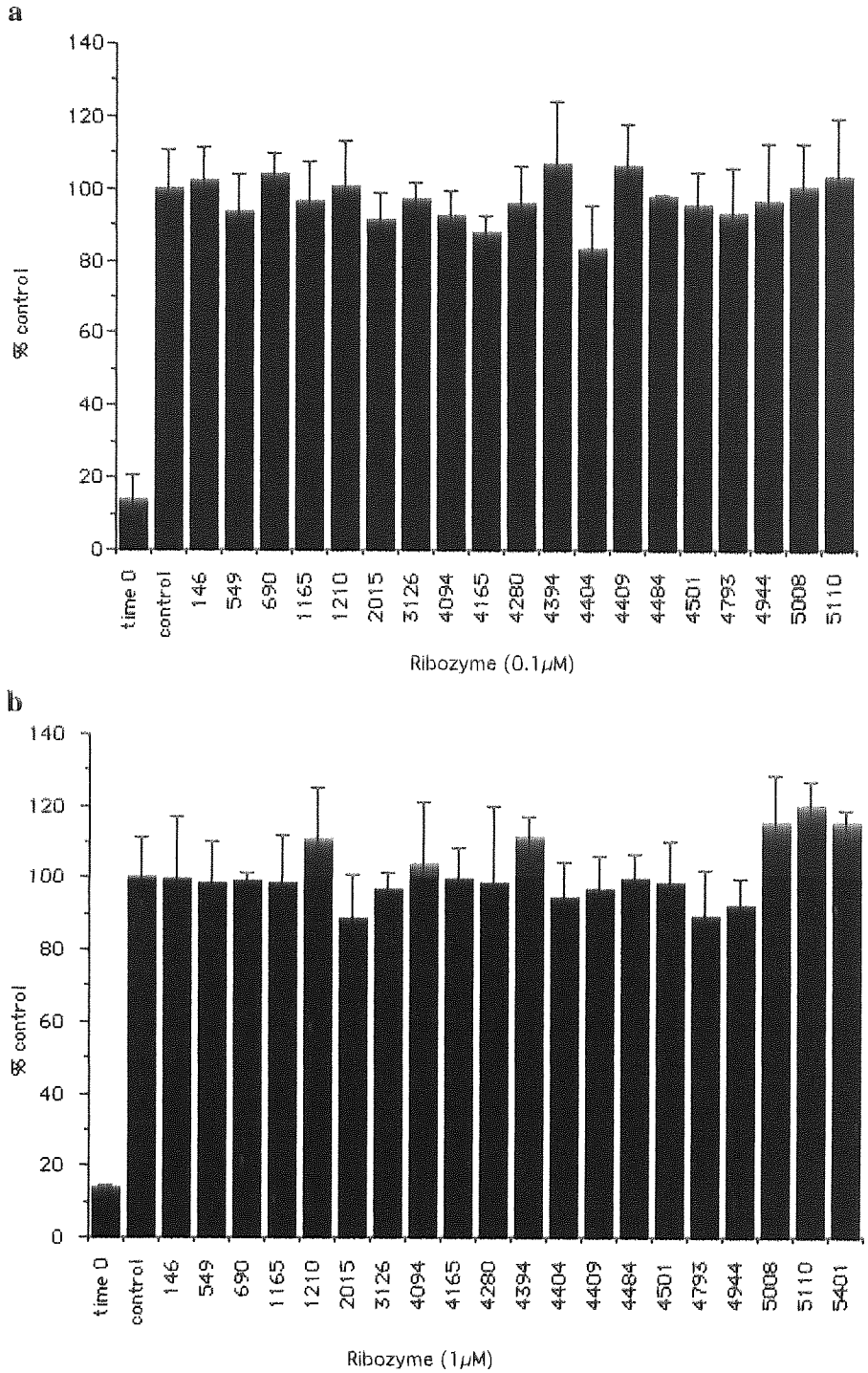

Figure 4.17 *Effect of ribozyme treatment on proliferation of A431 cells over 4 days.* Chimeric ribozymes targeting various sites along EGFr mRNA were complexed with LipofectAMINE™ and delivered to A431 cells every 24 hours at a concentration of either: (a) 0.1μM ribozyme (7μg/ml Lipofectamine:(+/-)charge ratio of 5) or (b) 1μM (10μg/ml LipofectAMINE™) as described in section 4.2.3.3. Cells were incubated at 37°C in the presence of ribozyme for a period of 4 days at which time cell number was determined by crystal violet assay. Data represents the mean (n=6±SD)cell number expressed as a % of control (no ribozyme).

a

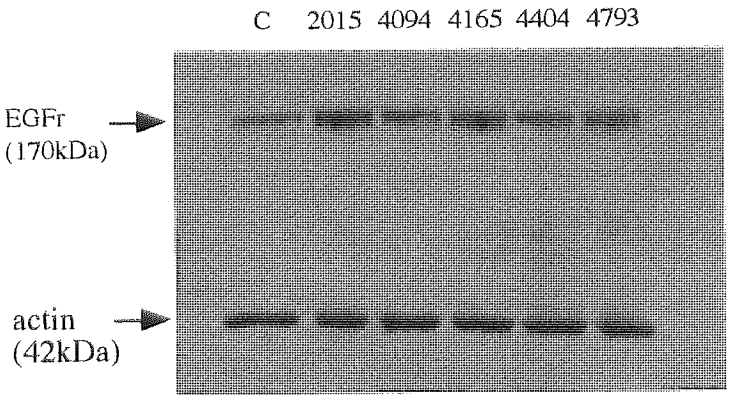

b

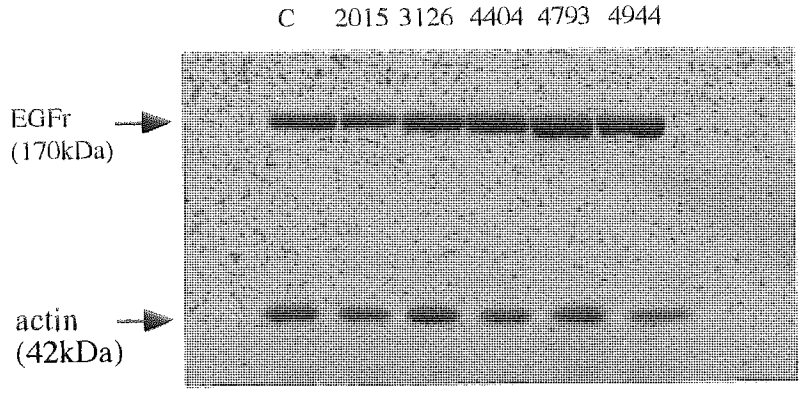

Figure 4.18. *Effect of ribozyme treatment over 4 days on EGFr expression in A431 cells.* A431 cells were plated in 24-well plates and cultured for 4 days in the presence of five lead ribozymes identified from each of the above two proliferation experiments (Figure 4.17 a and b) as described in section 4.2.3.3. The chimeric ribozymes targeting various sites along EGFr mRNA were complexed with LipofectAMINE™ and delivered to A431 cells every 24 hours at a concentration of either: **a** 0.1μM ribozyme (7μg/ml LipofectAMINE™:(+/-) charge ratio of 5) or **b** 1μM (10μg/ml LipofectAMINE™) as detailed in sections 4.2.4.2. Cells were incubated at 37°C in the presence of ribozyme for a period of 4 days at which time cells were lysed and total cell lysates (20μg protein per well) analysed by 7.5%SDS-PAGE and immunoblotting with anti-EGFr antibody E-3138 (section 2.7). Images depict representative blots of duplicate experiments. C represents untreated EGFr expression in untreated A431 cells.

4.3.3.6.3 *Effect of Ribozyme Treatment when A431 cells are Stimulated with EGF*

Epidermal growth factor EGF is a potent mitogen for a number of cell types in culture or *in vivo* (Sherrill & Kyte, 1996). Furthermore, the EGFr half-life in human fibroblasts reduces from approximately 10 hours to about 1 hour in the presence of EGF (Kawamoto *et al.*, 1983). Consequently, stimulation of A431 cells with EGF could enhance the effects of treatment with anti-EGFr ribozymes on growth inhibition and EGFr expression. A431 cells are, however, atypical in their response to EGF: while lower doses of EGF are reported to promote growth, higher concentrations have been found to inhibit proliferation (Gill and Lazar, 1981; Barnes, 1982; Kawamoto *et al.*, 1983). It is important, therefore to ensure that stimulatory and not inhibitory concentrations of EGF are used for these studies. Inhibitory growth effects of EGF have been observed at concentrations as low as 1 ng/ml (Barnes, 1982) whereas Kawamoto *et al.*(1983) reported growth stimulation at 10-400 pg/ml. The effect of a range of concentrations of EGF on growth of A431 cells was therefore investigated (Table 4.5). Cells were incubated in the presence of EGF over a period of 4 days as detailed in section 4.2.3.4 at which time cell number was determined by means of a trypan blue exclusion assay.

Table 4.5 *Effect of EGF on A431 cell growth.*

EGF concentration (ng/ml)	% control cell number
0	100.0 ± 2.4
0.01	108.7 ± 7.9
0.1	99.9 ± 1.07
1.0	91.1 ± 4.2
10.0	69.9 ± 5.5
100.0	53.9 ± 2.4

A431 cells incubated for 96 hours at 37°C with DMEM medium containing 10% FBS in the presence EGF at the indicated concentrations as described in section 4.3.2.4. Values listed represent the mean (n=3 ± SD) percentage of the untreated control cell number (% EGF-treated / control).

The results, summarised in Table 4.5, support previous findings. Higher doses of EGF clearly inhibited cell growth during this period since the decrease in cell number was statistically significant ($p<0.01$) at EGF concentrations of 10 and 100ng/ml. An increase in cell number was, however, observed when a concentration of 0.01ng/ml EGF was applied, indicating growth stimulation at this concentration, although statistical analysis revealed that this increase was not quite significant ($p=0.07$). In view of the increase in growth observed at this concentration of EGF, it was decided to screen the efficacy of the twenty chimeric ribozymes on A431 cells stimulated with 0.01ng/ml of EGF. In retrospect, however, further studies should have been undertaken to determine a concentration of EGF that resulted in a significant increase in cell growth.

In this experiment, A431 cells were incubated with 0.1μM ribozyme (complexed with LipofectAMINE at the optimal (+/-) charge ratio of 5 to enhance delivery) for four days in the continued presence of 0.01ng/ml of EGF as described in section 4.2.3.5. The efficacy of these ribozymes in inhibiting cell proliferation was initially determined (Figure 4.19). Once again, no significant reduction in cell number was evident for any of the ribozymes tested. Two of the most promising ribozymes in reducing cell growth, egfr.1210 and egfr.5110, were further analysed for their effect on EGFr expression in A431 cells as described previously (section 4.2.2.2). Analysis by densitometry of the resulting blot, a representative example of which is shown in Figure 4.20, revealed that, after normalising for protein loading, treatment with either of these ribozymes failed to result in any detectable reduction in EGFr expression.

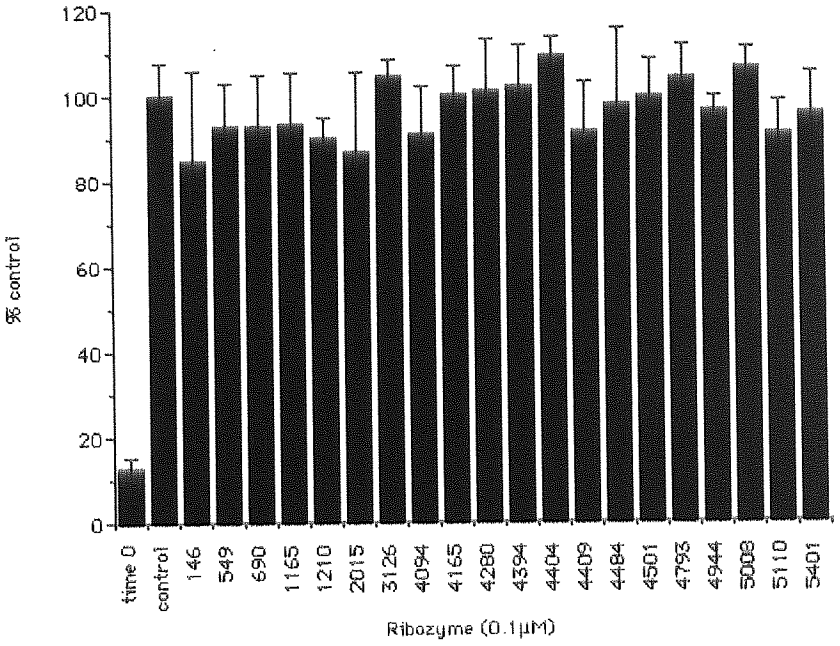

Figure 4.19 *Effect of ribozyme treatment over 4 days on proliferation of A431 cells stimulated with EGF.* Cells were incubated at 37°C in the presence of 0.1μM ribozyme in medium containing 10% FBS and 0.01ng/ml EGF for a period of 4 days as described in section 4.2.3.5. Cell number was determined by crystal violet assay. Data represents the mean (n=4±SD) cell number expressed as a % of control (no ribozyme).

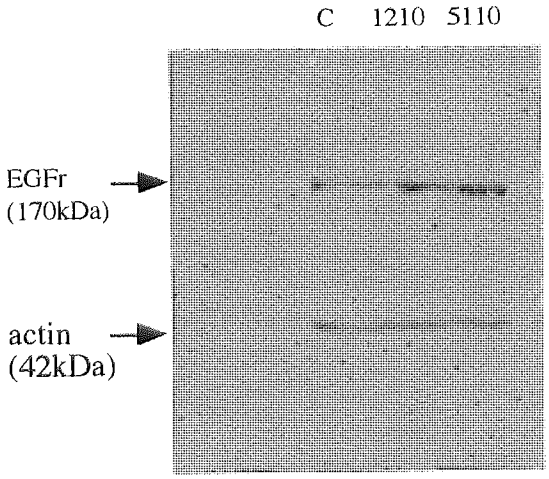

Figure 4.20 *Effect of ribozyme treatment over 4 days on EGFr expression in A431 cells stimulated with EGF.* A431 cells were plated in 24-well plates and cultured for 4 days in the continued presence of 0.1μM ribozyme in medium containing 10% FBS and 0.01ng/ml EGF. Cells were lysed and analysed by 7.5% SDS-PAGE and immunoblotting with anti-EGFr antibody E-3138 (section 2.7). Images depict representative blots of duplicate experiments. C represents EGFr expression in lysed, untreated A431 cells.

4.3.3.7 Stability of 2'-O-Methyl Chimeric Ribozyme in A431 Cells

Chemically stabilised ribozymes, modified in a similar manner to the ribozymes used in these efficacy studies had proved to be extremely stable in both FBS and U87-MG cells (see Chapter Three, section 3.3.1). In addition, complexation of nucleic acids to cationic liposomes has been shown to enhance stability (see Gaughan and Whitehead, 1999 for review). It is unlikely, therefore, that poor stability was responsible for the lack of efficacy demonstrated by these ribozymes on growth inhibition and EGFr expression of A431 cells. In order to discount this possibility, the intracellular stability of an internally [^{32}P]-labelled 2'-O-methyl chimeric ribozyme was assessed in A431 cells over a period of 4 days. Figure 4.21 demonstrates that the ribozyme did indeed exhibit considerable nuclease resistance; densitometric analysis of the autoradiograph image revealed that over 65% of the intracellular ribozyme remained intact over this period.

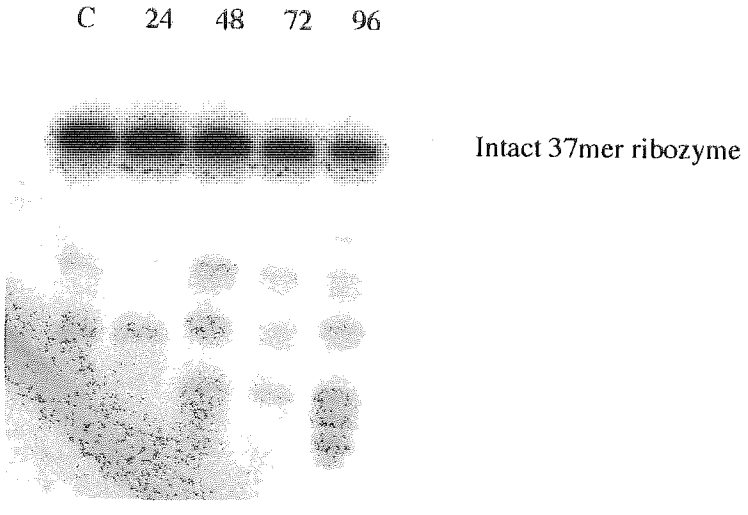

Figure 4.21 *Intracellular stability of internally [^{32}P]-labelled 2'-O-methyl chimeric ribozyme in A431 cells.* The radiolabelled ribozyme, complexed with LipofectAMINE™ (at the optimal +/- charge ratio of 5) was added to A431 cells at a final concentration of 0.1μM in serum-free medium (see section 4.2.5). Following a 4 hour uptake period, the medium was replaced with complete (10% FBS) medium and cells incubated at 37°C. The ribozyme was recovered from lysed cells at the time points indicated and analysed on 20% PAGE (7M urea). Degradation times are given in hours. C represents ribozyme in serum-free medium only.

4.3.3.8 *Efflux of Ribozyme from A431 Cells over 96 hours*

It is also a possibility that the internalised ribozymes, potentially still complexed to LipofectAMINE™, were transported out of the cells before reaching their target site. An efflux study was accordingly undertaken to evaluate the percentage of ribozyme transported out of the cell during these efficacy studies. The export of 0.1μM internally [^{32}P]-labelled ribozyme, delivered with the aid of LipofectAMINE™, was measured following an initial four-hour incubation period, over a duration of 96 hours and compared to the efflux profile of ribozyme alone as described in section 4.2.6. The results, representing the rate of loss of radiolabelled ribozyme from A431 cells as a function of time, are shown in Figure 4.22 below.

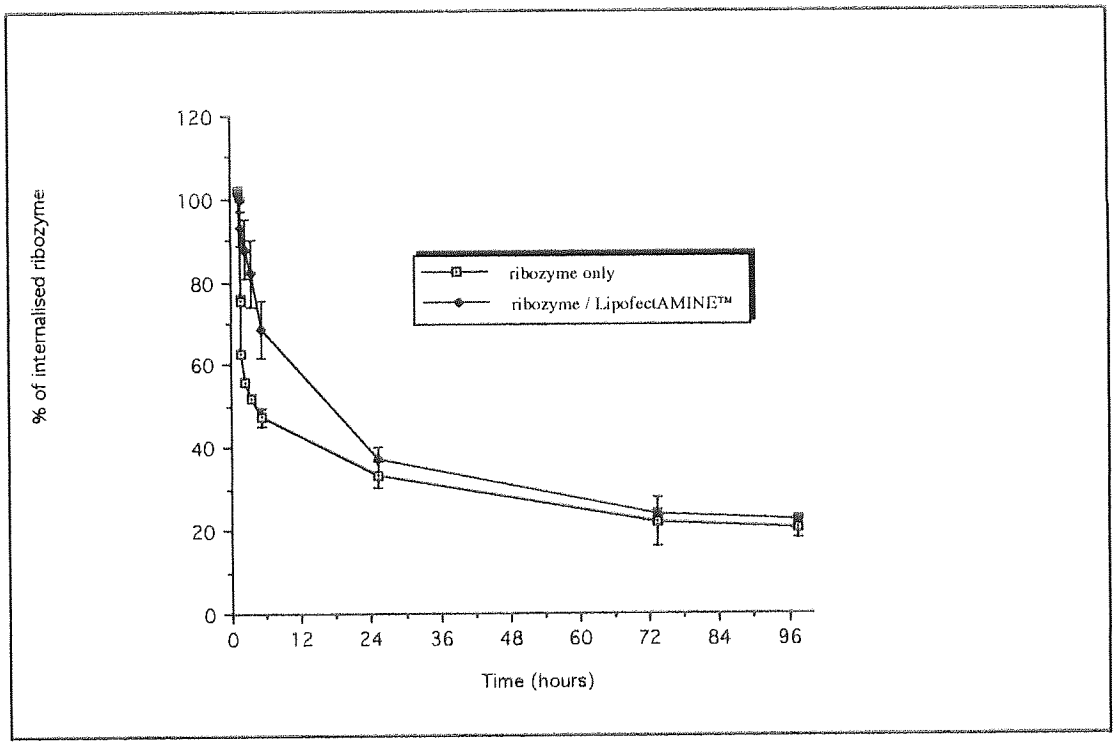

Figure 4.22 *Efflux of chimeric ribozyme from A431 cells over 96 hours.* Efflux profile over time of ribozyme complexed with LipofectAMINE™ ((+/-) charge ratio of 5) compared to ribozyme only. After a four-hour incubation with 0.1μM ribozyme at 37°C, A431 cells were washed with PBS and incubated with fresh DMEM medium (without ribozyme) for different periods. The efflux is represented by the mean percentage of [^{32}P]-labelled ribozyme remaining in the cell (n=3 ± SD).

Although a significant proportion of ribozyme delivered with the aid of LipofectAMINE™ was transported out of the cell within 24 hours, efflux data revealed that 35.43 ± 3.25% of internalised ribozyme remained sequestered within the cell during this time period. It has been proposed that the biphasic trend in efflux rates of nucleic acids may be indicative of intracellular trafficking (see section 3.3.3.2), with initial rapid efflux representing localisation in 'shallow' compartments near the surface of the cell, while the slower rate of efflux represents transport from deeper compartments such as late endosomes or lysosomes (Tonkinson and Stein, 1994). The rates of efflux of ribozyme delivered complexed with LipofectAMINE™ were compared with that of free ribozyme. It must be noted that Figure 4.22 represents the overall percentage rate of loss of internalised ribozyme from A431 cells and not the actual quantity of internalised ribozyme. The actual amount of internalised ribozyme after the initial four hour incubation period was significantly greater with the ribozyme / lipid complex than with the free ribozyme.

It was interesting to note that initially free ribozyme was transported out of the cell much more rapidly than the ribozyme/lipid complex. After six hours, approximately 55% of internalised free ribozyme had been transported out of the cell compared to only 40% of ribozyme which had been delivered complexed to LipofectAMINE™. This may indicate that during this period the ribozyme complexed to lipid was located in deeper regions of the cell than the free ribozyme and therefore less readily exported. After 24 hours, however, the efflux profiles for both free ribozyme and ribozyme/lipid were markedly similar, with no significant difference in efflux rate at all subsequent time points. This indicates that approximately 35% of internalised ribozyme, whether delivered without the aid of a delivery vehicle or delivered complexed to LipofectAMINE™, remained predominantly within deep compartments. The findings of Chapter Three suggested that

free ribozyme is taken up into the cell by an endocytic mechanism and that internalised ribozymes become trapped within endosomes. The remarkable similarity in efflux profiles between free ribozyme and ribozyme/lipid may suggest that a significant proportion of ribozyme delivered complexed to LipofectAMINE™ has remained sequestered within endosomes and is therefore unable to reach the target substrate.

4.4 CONCLUDING REMARKS

In this chapter the biological efficacy of a series of chemically stabilised synthetic ribozymes directed against the EGFr mRNA was investigated both *in vitro* and *ex vivo*.

Twenty ribozymes were designed against various sites along EGFr mRNA and synthesised with 2'-O-methyl / 2'-C-allyl modifications to enhance nuclease stability. The majority of these ribozymes (18/20) proved to be capable of cleaving complementary short RNA substrates *in vitro* with a high degree of efficiency. The value of using RNA folding algorithm programs to design small hammerhead ribozymes was highlighted, since ribozyme constructs predicted to be the most favourable by the program RNAFOLD correlated well with those ribozymes exhibiting the highest activity *in vitro*. Such programs can be utilised to discount ribozyme sequences likely to adopt catalytically inactive conformations.

The activity of these ribozymes were then evaluated in cultured A431 cells, a vulval carcinoma cell line that expresses the EGFr at levels 10-50 fold higher than that seen in other cell lines (Ullrich *et al.*, 1984). Previous research in this report (see Chapter 3) indicated that chimeric ribozymes enter cells through an endocytic mechanism which is highly inefficient and may result in the localisation of ribozymes within endosomal

vesicles (Fell *et al.*, 1997). A delivery vehicle was therefore required to enhance cellular delivery of the ribozymes to A431 cells. Following optimisation studies, the cationic liposome, LipofectAMINE™, was used to deliver the ribozymes to A431 cells for *ex vivo* efficacy studies. Cells were incubated with different concentrations of ribozyme over time points up to 4 days. Single doses and repeated doses of ribozyme were applied. However, no significant reduction in either cell proliferation or EGFr expression was observed during these studies.

The lack of activity of the twenty anti-EGFr ribozymes observed in cell culture would suggest that, even with the aid of the delivery vehicle LipofectAMINE, the ribozymes are either failing to gain access to the correct intracellular compartment or have not dissociated from the lipid and are therefore not bioavailable. This is in contrast to the findings of Zelphati and Szoka (1996) which suggest that ODNs delivered with cationic liposomes can dissociate from the lipid complex within cells, thus gaining access to cytoplasmic and nuclear targets. Unfortunately, time restraints prohibited further research on this matter, however subcellular localisation and ultrastructural studies could be performed in order to determine the intracellular destinations of these exogenously delivered ribozymes. Such studies may reveal whether it is the method of delivery or ribozyme design that is limiting cellular efficacy of these ribozymes.

CHAPTER FIVE

BIOLOGICAL ACTIVITY OF SYNTHETIC 2'-O-METHYL-MODIFIED HAMMERHEAD RIBOZYMES TARGETED TO THE RNA COMPONENT OF TELOMERASE

ABSTRACT

Telomerase is a ribonucleoprotein complex with reverse-transcriptase activity responsible for telomere elongation. High telomerase activity has been found in the majority of cancer cells, but not in normal somatic cells. As normal cells lack telomerase activity, a progressive shortening of chromosome length occurs with each cell division resulting in cell senescence. The presence of telomerase may therefore allow cells to bypass senescence and become immortal. Consequently telomerase activity has been associated with tumorigenesis and could be a highly selective target for anti-tumour drug design. The potential use of a chemically stabilised hammerhead ribozyme to inhibit telomerase activity by cleaving the RNA component in a sequence-specific manner was investigated.

A chemically modified hammerhead ribozyme, termed TEL.1, containing 2'-O-methyl ribonucleotides to enhance biological stability was designed directed against the template region of the RNA component of telomerase. The ribozyme demonstrated high catalytic activity *in vitro* against a complementary short substrate and exhibited dose-dependent inhibition of telomerase activity in human glioma U87-MG cell lysates with an IC_{50} of about 4μM.

Enhanced cellular delivery of the ribozyme to U87-MG cells was achieved using the cationic lipid formulation LipofectAMINE™. When 4μM ribozyme TEL.1 was delivered to U87-MG cells complexed to LipofectAMINE™, telomerase activity was significantly reduced to 74.5 ± 4.17% of the untreated control. Catalytically incompetent (inactive) control ribozymes or ribozymes with scrambled arm sequences failed to significantly inhibit telomerase activity indicating sequence-specific catalytic cleavage by ribozyme TEL.1. Free ribozyme showed no significant inhibitory effect demonstrating the importance of an appropriate delivery vehicle for optimum delivery of exogenously delivered synthetic ribozymes in cell culture. These findings support the potential application of exogenously delivered ribozymes as novel specific therapeutic agents directed against immortalised cancer cells.

5.1 INTRODUCTION

5.1.1 The Role of Telomere Length and Telomerase Expression in Cancer

Cancer generally develops via a multistep process involving the accumulation of independent mutations that confer a growth advantage to a cell and the successive clonal expansions of the mutated clones (Buolamwini, 1999). However, the proliferative capacity of somatic cells is limited *in vitro* and probably *in vivo* and is likely to be insufficient for the number of cell divisions required for the development of malignancy (Chadeneau *et al.*, 1995). It follows that malignant cells may ultimately exhaust their normal proliferative potential and thus tumour formation may require acquisition of an immortal phenotype. Telomere length has recently been implicated in the control of cell lifespan and telomerase, the enzyme that elongates telomeric DNA, has been proposed as an essential function for cell immortality (reviewed in: Parkinson, 1996; Shay, 1997; deLange and Jacks, 1999; Hodes, 1999).

Eukaryotic chromosomes are capped with repetitive telomere sequences which maintain chromosome stability by protecting chromosomes from degradation and terminal fusion; in humans the sequence is (TTAGGG)n (Blackburn, 1991). When replicated, chromosome ends shorten by a variable number of base pairs (50-200 terminal nucleotides) because DNA polymerase can not completely replicate the ends of linear DNA molecules (Kipling, 1995). Telomere repeats, therefore, serve as a reservoir of redundancy at chromosome ends, protecting essential DNA from erosion. The progressive shortening of telomeres has been proposed to be a mitotic clock by which cells count their divisions and a sufficiently short telomere may be a signal for senescence in normal cells. In contrast, immortal cells show no net loss of telomere

length or sequence with cell division, suggesting that maintenance of telomeres is required for cells to escape from replicative senescence and proliferate indefinitely (see reviews by: Parkinson, 1996; Shay, 1997; Hodes, 1999; McKenzie *et al.*, 1999).

Telomerase is a ribonucleoprotein polymerase that synthesises DNA, *de novo*, onto chromosomal ends using a segment of its RNA component as a template (Figure 5.1). The RNA component of human telomerase (hTR) has been cloned and sequenced, the total length identified as being approximately 450 nucleotides, the template region being from positions 46 – 56 (Feng *et al.*, 1995). The template region of human telomerase encompasses 11 nucleotides (5'-CUAACCCUAAC-3') complementary to the human telomere sequence (TTAGGG)n. More recently, the catalytic protein subunit responsible for the reverse transcriptase or lengthening activity (hTRT) has also been identified in humans (Meyerson *et al.*, 1997; Nakamura *et al.*,1997) together with a telomerase associated protein, TP1 (Harrington *et al.*, 1997).

Many recent findings have shown a positive correlation between tumour cells and telomerase activity (Kim *et al.*, 1994; Le *et al.*, 1998; Sano *et al.*, 1998; Falchetti *et al.*, 1999). Normal human somatic cells express low or undetectable telomerase activity and progressively lose their telomeric sequences with replicative senescence *in vitro* or with normal *in vivo* aging (Harley, 1990). In contrast, however, germline cells and almost all tumour cell lines and tissues express telomerase and maintain telomere length through an indefinite number of cell divisions. In fact, telomerase activity is present in almost 90% of primary human tumours but is absent in most normal cells despite the presence of the RNA component (Kim *et al.*, 1994; Broccoli *et al.*, 1995). These findings have led to the current belief that telomerase is critical for continuous cell division and its inhibition could therefore be a strategy for anti-cancer therapy.

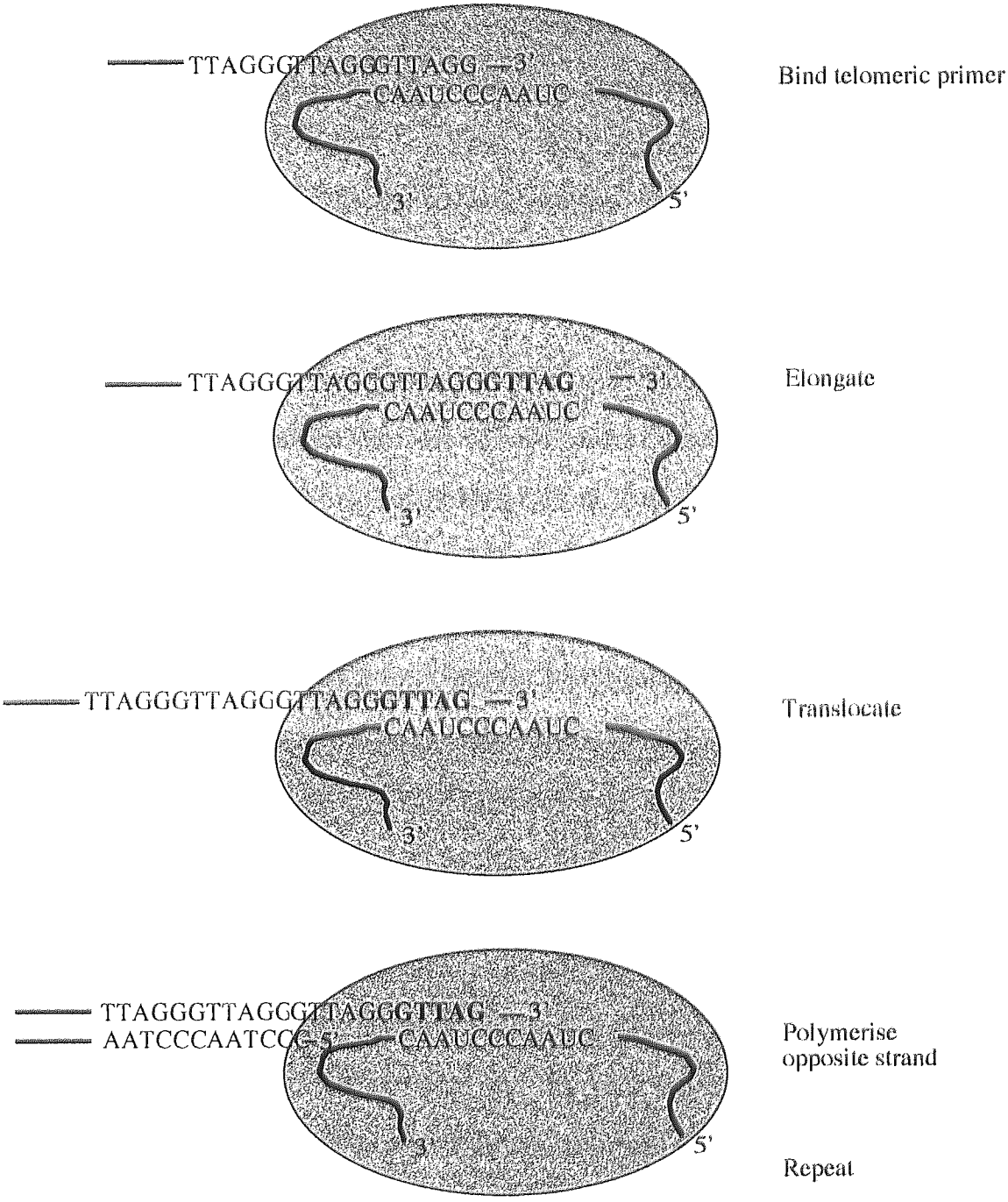

Figure 5.1 *Mechanism of telomere addition by telomerase* (adapted from Rhyu, 1995). Step 1. Chromosomal DNA binds part of the template region in telomerase RNA. Step 2. Reverse transcriptase action of telomerase results in elongation of 3'-end of chromosome. Step 3. The chromosome is translocated and repositioned to repeat the polymerisation step. Step 4. The complementary strand is synthesised by DNA polymerase. Step 5. The process is repeated .

The suggestion that telomerase is involved in tumour progression is reinforced by a study conducted by Bodnar *et al.* (1998) which clearly showed that the introduction of functional telomerase activity leads to bypassing of cellular senescence. The transfection of the catalytic subunit, hTRT, to normal retinal pigment epithelial cells and foreskin fibroblasts already expressing the RNA component of telomerase led to an increased telomere length and increased the life span of these cells by at least 20 doublings.

Telomerase activity has been observed in most brain tumours and consequently appears to be a suitable target for the treatment of brain cancers such as glioblastoma multiforme. In a study conducted by Kim *et al.* (1994), 75% of brain tumours were found to express telomerase activity. These findings were supported by a more recent study undertaken by Langford (1996). On analysing 90 human gliomas, 100% of oligodendrogliomas and 75% of all glioblastoma multiforme tumours exhibited telomerase activity. In addition, Le *et al.* (1998) reported the presence of telomerase activity in 89% of the 41 glioblastoma multiforme (grade IV) tumours analysed.

The identification and characterisation of the both the RNA component of human telomerase (hTR) and the catalytic subunit (hTRT), allows the development of highly specific anti-telomerase drugs through gene therapy / antisense therapeutics. Experiments that inhibit telomerase activity will determine the effectiveness of anti-telomerase therapy in the treatment of cancer. The aim of this chapter was to evaluate the potential use of biologically stable, synthetic hammerhead ribozymes containing 2'-O-methyl modifications as novel inhibitors of telomerase activity for anti-brain tumour applications.

5.2 MATERIALS AND METHODS

General materials and methods are detailed in Chapter Two. Any alterations, additions and specific methods relevant only to this chapter are given below.

5.2.1 Synthesis and Labelling of 2'-O-Methyl Chimeric Anti-Telomerase Ribozymes

A 36-mer hammerhead ribozyme, (TEL.1), directed against the template region of the RNA component of telomerase was synthesised as described in section 2.1.2.2. The active ribozyme contained site-specific chemical modifications to increase stability as detailed in Figure 5.2a. Most substitutions were with 2'-O-methyl residues, with five essential ribose residues situated within the catalytic core of the molecule left unmodified to retain activity. The ribozyme also contained three 3'-terminal phosphorothioate-modified deoxynucleotides in order to confer resistance against 3'- exonuclease action.

Synthesis of this ribozyme occurred in two stages: in the first stage, a 3-mer ODN 'starter' sequence containing PS inter-nucleotide linkages was synthesised using the pre-programmed 'sulfur' cycle, with the 5'-O-DMT protecting groups left on and the synthesised ODN remained attached to the solid support (see section 2.1.1.2). In the second stage, the relevant reagents were changed on the automated synthesiser and the remainder of the ribozyme sequence was added to the 3-mer 'starter' sequence using the custom designed 'Fpmp' RNA cycle as described in section 2.1.2.2. In addition, ribozymes were synthesised with either an inactivated core (Figure 5.2b) or with scrambled arms (Figure 5.2c) to act as negative controls. All chimeric ribozymes were

manually deprotected and purified by ethanol precipitation as described in section 2.1.2.4.

In order to assess *in vitro* catalytic activity of ribozymes, a region of the target telomerase RNA substrate (5'-UUUUUGUCUAACCCU-3') was also synthesised as described in section 2.1.2.3. All syntheses were performed on a 0.2μmol scale.

Ribozymes and substrates were radiolabelled at the 5'-position using [γ-^{32}P]ATP and bacteriophage T4 polynucleotide kinase as described in section 2.2.1. Following radiolabelling, ribozymes / substrates were purified by native 20% PAGE (section 2.2.4.1). Excised bands were eluted in 0.1% DEPC-treated water, desalted on NAP10 columns (section 2.2.4.2) and lyophilised.

For subcellular studies, a fluorescein label was attached to the 5'-end of the ribozyme as the terminal coupling step during automated synthesis by using fluorescein cyanoethyl phosphoramidite reagents according to the manufacturers protocol (Cruachem Ltd, Glasgow, U.K.).

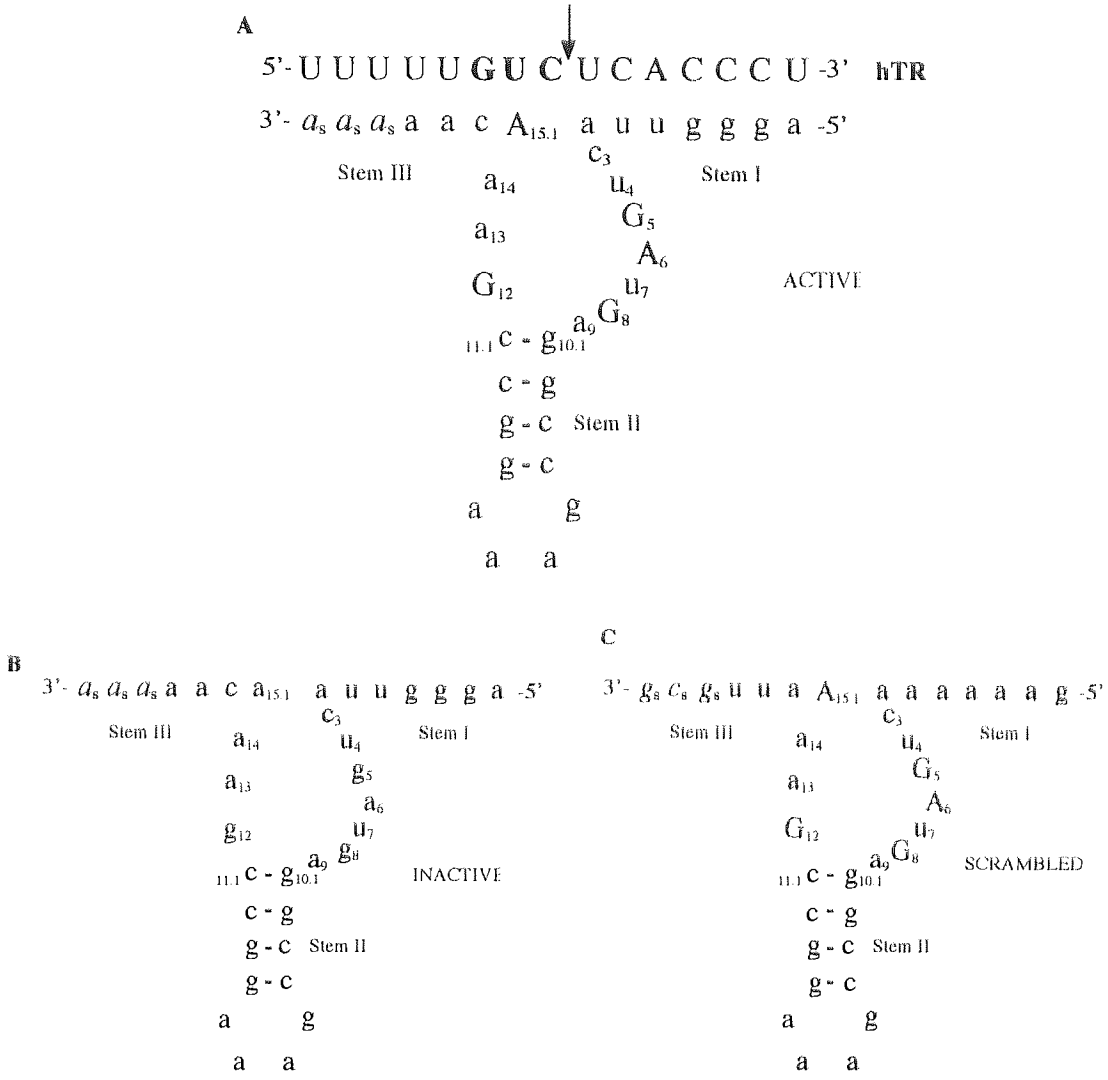

Figure 5.2 *Sequence and chemistry of chimeric synthetic ribozymes targeting the RNA component of human telomerase.* Sequence and chemistry of the active hammerhead ribozyme TEL.1 and a 15mer complementary region of telomerase RNA (**A**). Control ribozymes with either inactivated core (**B**) or with scrambled arms (**C**) are also shown. The GUC motif and human telomerase RNA cleavage site (indicated by a vertical arrow) are shown. The three 3'-treminal nucleotides (in italics) are phosphorothioate-modified deoxynucleotides. Nucleotides in lower case represent 2'-O-methylated ribonucelotides. Letters in the uppercase represent unmodified ribonucleotides. In the active ribozyme (A), stems I and III are fully complementary to telomerase RNA whereas ribozyme C contains a non complementary scrambled sequence in these binding arms. Inactive ribozyme control (B) was produced by 2'-O-methylating all ribonucelotides.

5.2.2 Ribozyme Stability Assay

5.2.2.1 *Stability in FBS / Cell Lysates*

5'-end [^{32}P]-radiolabelled ribozymes were incubated in 100μl of either neat FBS or U87-MG cell extracts at 37°C to give a final concentration of either 200nM (FBS) or 0.4μM (cell extracts). Aliquots (10μl) were removed at timed intervals, mixed with a loading buffer containing 80% formamide, 10mM EDTA,pH 8.0, 0.25% xylene cyanol, and 0.25% bromophenol blue, and frozen at –20°C prior to cell loading. Degradation profiles were analysed by 20% PAGE containing 7M urea (section 2.3.1).

5.2.2.2 *Intracellular Stability in Intact U87-MG Cells*

U87-MG cells were seeded in 24-well plates at 6 x 10^4 cells per well and used approximately 24 hours post-seeding. Cells were washed twice with sterile PBS (2 x 100μl x 5 min) and 4μM 5'-end [^{32}P]-labelled ribozyme TEL.1, complexed to the cationic lipid LipofectAMINE™ (as described in section 4.2.4.2) was added to the cells in a total volume of 200μl of serum-free medium per well. Following a four-hour incubation period at 37°C, cells were washed twice with PBS (2 x 0.5ml x 5min), lysed and harvested from the wells as described in section 5.2.3. Aliquots of 2μl were mixed with formamide loading buffer and stored at –20°C prior to gel loading. Degradation profiles were analysed by 20% PAGE containing 7M urea (section 2.3.1) and detected by autoradiography of wet gels (section 2.3.2).

5.2.3 Preparation of Cell Lysates

Total cellular extracts were made as described by Kim *et al.* (1994). Briefly, 1 x 10^6 cells were harvested and washed once in PBS, followed by ice-cold wash buffer (10mM HEPES-KOH, pH 7.5, 1.5mM $MgCl_2$ 10mM KCl and 1mM dithiothreitol). Cells were centrifuged at 12000g for 5 minutes at 4°C. The resulting cell pellet was suspended in 80μl ice-cold lysis buffer (10mM phenylmethylsulfonylamide, 5mM EGTA, 0.5% CHAPS, and 10% glycerol). Lysed cells were incubated on ice for 30 minutes and centrifuged at 20,000g at 4°C for 45 minutes. The supernatant was quick-frozen and stored at –70°C until required. The BioRad protein assay was used to measure the protein concentration of the cell extracts as described in section 2.7.2.

5.2.4 Measurement of Telomerase Activity

Telomerase activity was measured by the PCR-based telomeric repeat amplification protocol (TRAP) similar to that described by Kim *et al.* (1994). Cell extracts (4μg), prepared as described in section 5.2.3, were incubated with the TRAP reaction mixture containing 50μM deoxynucleoside triphosphates (Promega, U.K.), 0.1μg upstream primer (TS, 5'-AATCCGTCGAGCAGAGTT-3'), 5ng T4 gene 32 protein (Boehringer Mannheim, U.K.), 3U *Taq* DNA polymerase (ICN,U.K.), 20mM Tris.HCl, pH 8.3, 1.5mM MgCl2, 63mM KCl, 1μM EGTA, pH 8.0, 0.1mg/ml BSA, and 0.5 -1μl [α^{32}P]dCTP (specific activity 3000 Cimmol^{-1}, ICN) in a total volume of 50μl. The reaction mixture was incubated at ambient temperature for 30 minutes. Reverse primer (0.1μg) (CX, 5'-GCGCGGCTTACCCTTACCCTTACCCTAA-3') was added manually to each reaction tube. Reactants were placed in a thermal cycler for 29 cycles at 94°C for 30 seconds, 50°C for 30 seconds, and 72°C for 90 seconds. The PCR products were

electrophoresed on an 8% acrylamide gel (19:1 acrylamide/*N,N'*-methylenebisacrylamide weight ratio, ICN) in 0.5 x Tris borate EDTA at 250V for 3 hours (section 2.3.1). Telomerase activity was detected by autoradiography of wet gels (section 2.3.2) following exposure of films for a period of between 5 – 10 days. The amplified telomerase products are of heterogenous length, with a ladder pattern of bands each representing the addition of a hexanucleotide telomeric repeat by telomerase.

5.2.5 Ribozyme Activity in Cell Lysates

20μg of U87-MG cell lysates, prepared as described in section 5.2.3, were treated with increasing concentrations of ribozyme TEL.1 and incubated at 37°C for 30 minutes. Telomerase activity of 4μg of ribozyme-treated cell lysate was then determined by the PCR-based telomeric repeat amplification protocol TRAP as described in section 5.2.4.

5.2.6 Cellular Delivery of Ribozyme TEL.1 to U87-MG Cells using Cationic Liposomes

Cationic lipid / ribozyme complexes were prepared as previously described in section 4.2.4.2. U87-MG cells were seeded onto 24-well plates at a concentration of 6 x 10^4 cells/well as described in section 2.6 and used 20-24 hours post-seeding. At this time, cells were washed twice with sterile PBS (2 x 0.5ml x 5 min) and the liposome / ribozyme complex was added to cells in a total volume of 200μl of serum-free DMEM medium. The percentage of complexed, 5'-end [^{32}P]-radiolabelled ribozyme that became associated to U87-MG cells after a period of 4 hours was determined as described in section 2.8 and normalised to cell number (% cell association per 1 x 10^5 cells).

5.2.7 Ribozyme Activity in Intact U87-MG Cells

U87-MG cells were seeded in 24-well plates at 6 x 10^4 cells per well. Approximately 24 hours later, cells were washed twice with sterile PBS (2 x 0.5ml x 5 min) and either free ribozyme or ribozyme complexed to LipofectAMINE™ was added at the appropriate concentration in a total volume of 200μl of serum-free medium per well. Following a four-hour incubation period at 37°C, cells were washed twice with PBS and harvested with trypsin (200μl per well x 10 minutes) as described in section 2.4.3. Cells were then lysed, as described in section 5.2.3. and the level of telomerase activity of each sample determined by analysing 4μg cell lysate by TRAP assay (see section 5.2.4).

5.3 RESULTS AND DISCUSSION

5.3.1 Design of Biologically Stable, Synthetic Hammerhead Ribozymes Targeting the RNA Component of Telomerase

Target site selection is generally based on three criteria: i) biological significance of the target RNA, ii) the presence of an appropriate target triplet sequence and iii) accessibility of this sequence to ribozyme action (Macpherson *et al.*, 1999). These three factors were considered in the design of ribozymes targeting telomerase.

The RNA component of the human enzyme telomerase (hTR) provides the template for elongation of chromosomal DNA. The identification and characterisation of the RNA component of human telomerase (Feng *et al.*, 1995) allows ribozymes to be designed against the active site of the enzyme. Synthetic hammerhead ribozymes can be designed to cleave any sequence containing an NUX triplet (see section 1.2.1), but the most commonly used cleavage site by naturally occurring catalytic RNA motifs is the GUC triplet (Symons, 1992). Seven GUC sites were identified along the length of hTR and hammerhead ribozymes, containing 7 base pairing nucleotides in stems I and III, were designed against these potential cleavage sites. The base sequence of the hammerhead ribozyme motif used in this study (see Figure 5.2) was designed to promote optimal intracellular activity based on the findings of Jarvis *et al.* (1996b) and discussed in section 4.3.1.1

The computer program RNAFOLD was used to predict the intramolecular secondary structures of each candidate ribozyme (as described in section 4.2.1) and eliminate potentially inactive ribozymes. Only two ribozymes folded into the desired secondary

structures: TEL.1 targeted at its 5'-terminus spanning nucleotides 44-46 and TEL.2 targeted at position 323-325, as sequenced by Feng *et al.* (1995).

At the time that this study was instigated, previous research by Feng *et al.* (1995) had indicated that antisense inhibition of human telomerase requires nucleic acids complementary to sequences in and around the template region of hTR and that antisense distal from the template are not inhibitory. The target sequence of ribozyme TEL.2, therefore, was considered to be too far from the hTR template to be effective. The target sequence of ribozyme TEL.1 is, however, located around the template region of the RNA component. Although RNA generally exhibits a high degree of intramolecular folding that can prevent the hybridisation of complementary or antisense nucleic acids (Milner *et al.*, 1997; Akhtar, 1998), this template region site is known to be an open structure to facilitate chromosomal telomere binding and extension (Kipling, 1995). The hybidisation accessibility of this region has since been confirmed in studies with complementary nucleic acids (Norton *et al.*, 1996; Kanazawa *et al.*, 1996; Yokoyama *et al.*, 1998; Tao *et al.*, 1999.). Consequently, ribozyme TEL.1 was selected for future efficacy studies.

As all RNA ribozymes are extremely unstable in the biological milieu (see Chapter Three), chemical modifications were applied to enhance nuclease resistance. The ribozymes used in this study, however, were not supplied by Ribozyme Pharmaceuticals Inc., as had been the case for previous research (Chapters Three and Four), but were synthesised 'in house' at Aston University. Consequently, commercially available reagents at the time of this research limited the type of modifications that could be applied to enhance stability. The active ribozyme TEL.1 was synthesised containing 2'-O-methyl modifications at selected nucleotides as detailed in Figure 5.2a. In addition, three phosphorothioate deoxynucleotides were applied to the 3'- end, to confer resistance

to 3'-endonuclease digestion. Chimeric ribozymes designed to be catalytically incompetent by 2'-O-methylating essential catalytic core nucleotides (inactive ribozyme) or housing mismatches in binding arms I and III (scrambled ribozyme) were used as controls (Figures 5.2 b, c).

5.3.2 *In vitro* Activity of Chimeric Anti-Telomerase Ribozyme against Short Synthetic Substrate

The ability of the designed ribozyme TEL.1 to cleave its target substrate was initially assessed *in vitro*. Ribozyme activity, expressed as cleavage half-time ($t_{1/2}$) of the substrate, was determined under single turnover conditions as described in sections 2.8.1 and 2.8.2. Reactions were carried out with enzyme excess (4μM ribozyme:1nM substrate). Under these conditions, the ribozyme exhibited relatively rapid cleavage of the 15-mer synthetic target sequence. As demonstrated by Figure 5.3a, the substrate was almost completely cleaved in only 30 minutes, average activity half-time of the substrate being only 7.15 ± 0.25 minutes. The control ribozymes, however, displayed no catalytic activity. When the inactive or scrambled control ribozymes were incubated with the same substrate under identical conditions, no cleavage of the substrate was observed (Figures 5.3 b,c).

The good catalytic activity exhibited by the anti-telomerase ribozyme, TEL.1, was promising. However, before proceeding with further efficacy studies, it was necessary to assess the biological stability of the ribozyme in order to ensure that the chemical modifications applied to this ribozyme offered sufficient nuclease resistance for future *in vitro* and *ex vivo* work.

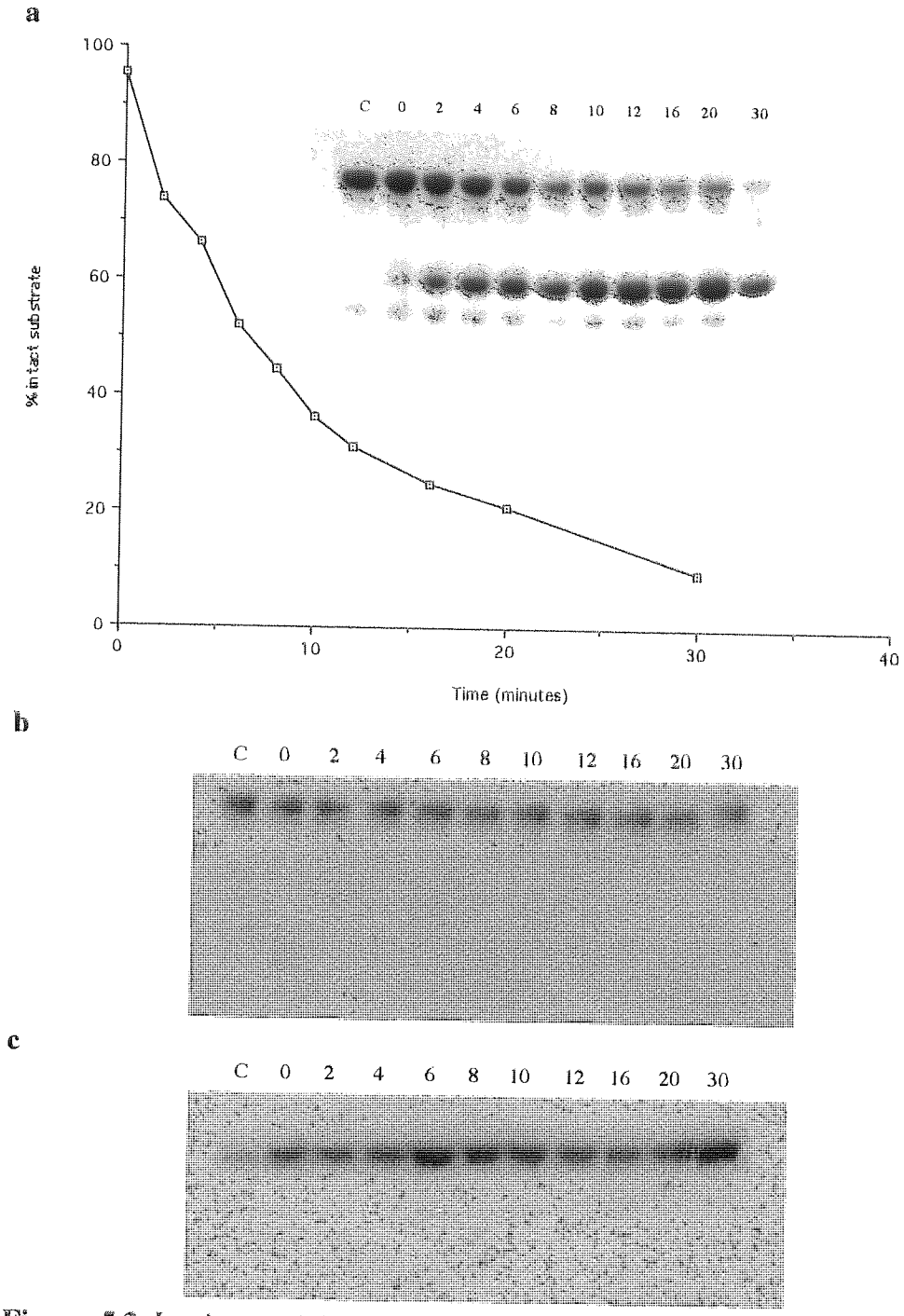

Figure 5.3 *In vitro activity of 2'-O-methyl chimeric anti-telomerase ribozymes (4μM) targeted against short synthetic telomerase RNA substrate (1nM).*(**a**) Activity of active ribozyme TEL.1. Graph is a quantitative representation of the cleavage reaction following densitometric analysis of representative autoradiograph (inset). (**b**) Activity of ribozyme with inactivated core. (**c**) Activity of ribozyme with scrambled arms. Reactions were performed in the presence of 50mM Tris.HCl (pH 7.5), 10mM $MgCl_2$ at 37°C as described in section 2.8.1-2.8.2. Reaction times are given in minutes. C represents intact substrate in Tris.HCl buffer without the addition of ribozyme.

5.3.3 Biological Stability of 2'-O-Methyl Modified Anti-Telomerase Ribozyme

In order to compare the stability of ribozyme TEL.1 with the 2'-O-methyl modified hammerhead ribozymes used in previous research (Chapters Three and Four), the degradation profile of this ribozyme was initially assessed in 100% FBS over a period of 24 hours as described in section 5.2.2.1. A representative autoradiograph demonstrating the results of this study is shown in Figure 5.4.

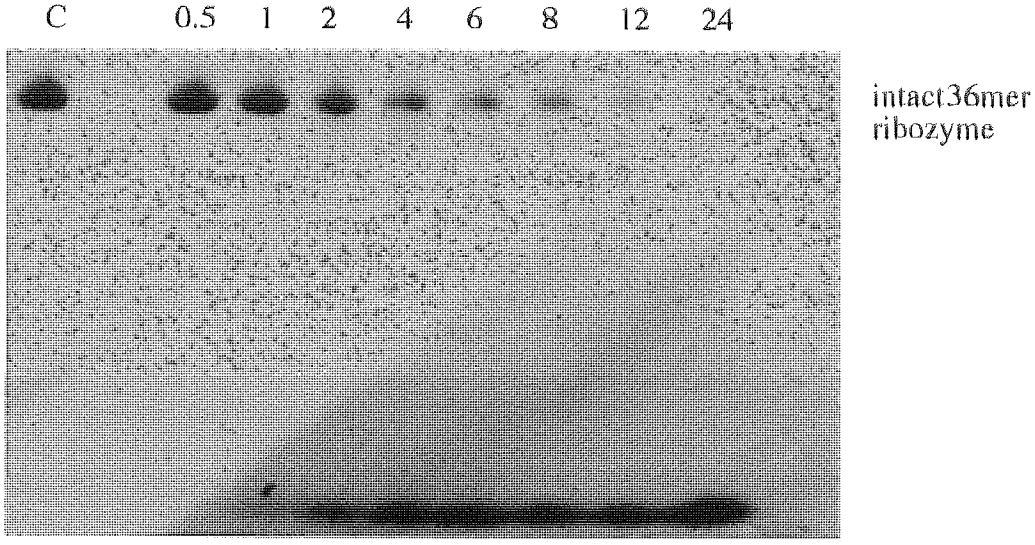

Figure 5.4 *Stability of 5'-end [^{32}P]-labelled 2'-O-methyl modified ribozyme TEL.1 in 100% foetal bovine serum (FBS).* Ribozyme was added to 100% FBS at a concentration of 200nM and incubated at 37°C for the time intervals indicated. Degradation profiles were analysed by 20% PAGE (7M Urea). Degradation times are given in hours. The control (C) represents unexposed 36-mer ribozyme.

The chimeric ribozyme appeared to remain stable in serum for up to 1 hour at 37°C. Since unmodified, all RNA, ribozymes were degraded in less than 15 seconds (section 3.2.2.1), the modifications applied to this ribozyme appear to have improved serum stability by more than 240-fold when compared with an unmodified construct. After

incubation periods in excess of one hour, however, increasing amounts of degradation products were evident, with only trace amounts of intact ribozyme remaining after a 24-hour incubation period. The stability half-life of this ribozyme ($t_{1/2}$) in FBS was estimated to be approximately 3 hours. Consequently, although the chemical modifications applied to the ribozyme, TEL.1, afforded significant stability when compared to unmodified ribozymes, they did not offer the same degree of nuclease resistance exhibited by 2'-O-methyl / 2'-amino modified and 2'-O-methyl / 2'-C-allyl modified ribozymes, which displayed stability half-lives in FBS of 18 hours and 21 hours respectively (section 3.2.2.1). The dramatically enhanced stability demonstrated by the ribozymes containing the above-mentioned U4/U7 modifications could be due to the addition of a 3'-3'-linked inverted thymidine or abasic residue at the 3'-terminus, offering increased protection against degradation by 3'-exonucleases (Beigelman *et al.*, 1995a).

The reduced stability demonstrated by ribozyme TEL.1 when compared to the 2'-O-methyl / 2'-amino modified and 2'-O-methyl / 2'-C-allyl modified ribozymes has implications for delivery strategies. The stability of chemically modified ribozymes is an important factor that must be borne in mind when considering exogenous administration of synthetic ribozymes. The frequency of the dose must be tailored to account for ribozyme stability half-life. More frequently administered doses may be required, therefore, to achieve down regulation of a target gene where ribozymes are more susceptible to nuclease degradation.

To ensure that ribozyme TEL.1 would remain intact during future activity studies in cell extracts, the stability of 5'-end [^{32}P]-labelled ribozyme was examined while incubated in U87-MG cell lysates at 37°C (see section 5.2.2.1). The ribozyme proved to be relatively stable when exposed to cellular nucleases for up to 30 minutes, after which time

progressive degradation was evident (Figure 5.5). Densitometric analysis of autoradiographs revealed that while ~70% of intact ribozyme remained after 30 minutes, only 5% remained after 2 hours incubation in the cell extracts. The degradation profile indicates that the ribozyme was particularly susceptible to the action of endonucleases and 5'-exonucleases. Increased nuclease resistance may be achieved, therefore, by adding phosphorothioate linkages at the 5'-end of the binding arm stem I. Since the ribozyme was 5'-end labelled, however, degradation products arising from the action of phosphatases can not be ruled out.

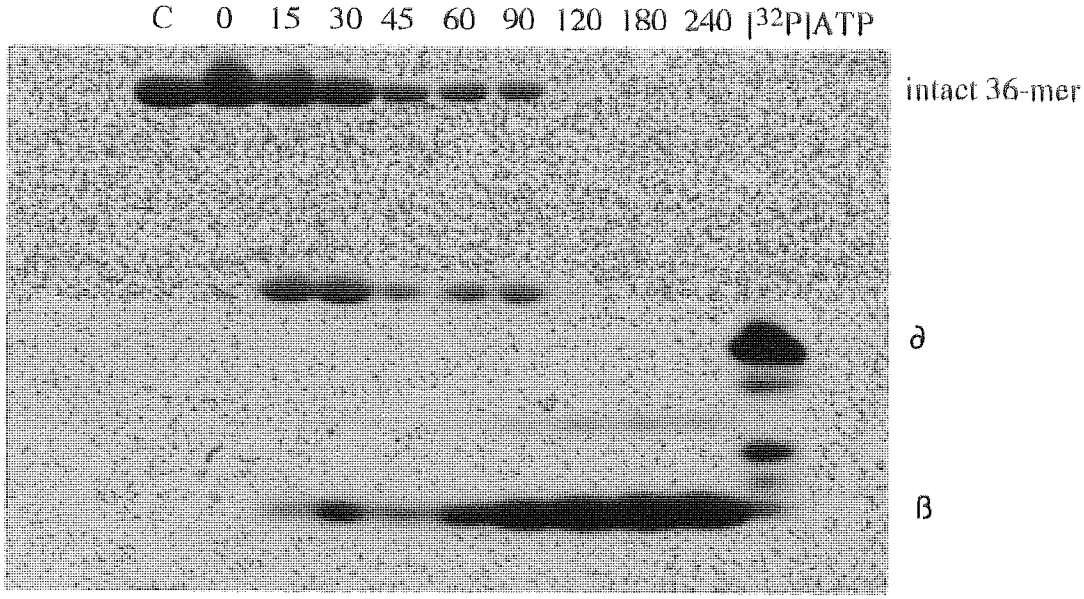

Figure 5.5 *Stability of 5'-end [^{32}P]-labelled 2'-O-methyl modified ribozyme TEL.1 in U87-MG cell lysates.* Ribozyme was added to U87-MG cell lysates at a concentration of 0.4μM and incubated at 37°C for the time intervals indicated. Degradation profiles were analysed by 20% PAGE (7M Urea). Degradation times are given in minutes. The control (C) represents unexposed intact 36-mer ribozyme. Bands ∂ and ß represent degradation products which co-migrate with the monomer [^{32}P]ATP and free phosphate respectively.

5.3.4 Telomerase Activity in Cultured Cell Lines

Positive telomerase activity is strongly associated with malignant brain tumours and is reportedly rare in benign tumours (Sano *et al.*, 1998). It is not surprising, therefore, that telomerase activity has been reported in U87-MG brain tumour cells by a number of groups (Wan *et al.*, 1998; Kiaris and Schally, 1999), A study by Kindo *et al.* (1998), however, revealed that they were unable to detect telomerase activity in this cell line.

Telomerase activity in U87-MG cell lysates was determined using the TRAP assay as described in section 5.2.4 and compared to that in lysates obtained from a primary culture of normal human astrocyte cells, IPFA (Figure 5.6). The results confirmed that this cell line was indeed telomerase positive, since the 6-bp ladder pattern characteristic of telomerase activity was clearly evident at all three protein concentrations tested. No telomerase activity, however, was detected in the lysates prepared from normal astrocyte cells supporting the belief that telomerase plays an important role in the progression of malignant tumours.

In fact, in a very recent study evaluating the diagnostic value of telomerase expression in intracranial tumours, Falchetti *et al.* (1999) reported a high degree of positivity for telomerase activity in glioblastoma tumours, while telomerase activity was poorly detected in anaplastic astrocytomas. This indicates that telomerase activity may act as a valuable tool for identifying tumours with aggressive behaviours.

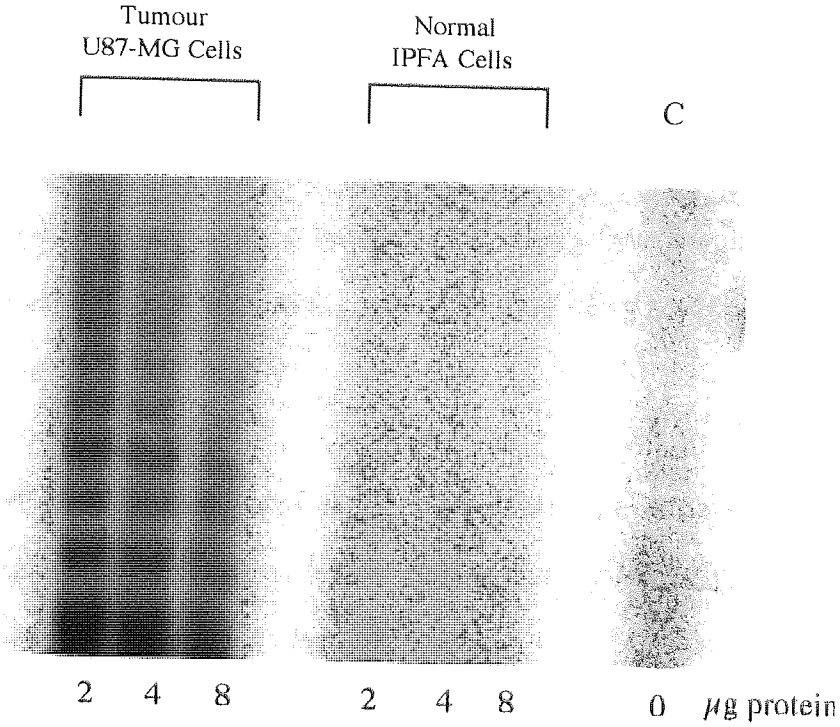

Figure 5.6 *Differential expression of telomerase activity in U87-MG glioma cell line and primary IPFA astrocytes.* Telomerase activity in the cell lysates, at the protein concentrations indicated, were analysed using the TRAP assay as described in section 5.2.4. The PCR products were electrophoresed on an 8% PAGE at 250V for 3 hours and telomerase activity visualised by autoradiography. The negative control, C ,refers to TRAP assay performed in the absence of any cell lysate protein.

5.3.5 Ribozyme Mediated Inhibition of Telomerase Activity in U87-MG Glioma Cell Lysates

The efficacy of ribozyme TEL.1 in inhibiting telomerase activity in U87-MG cell lysates was initially investigated by another member of our research team, Margaret Wan, who reported sequence–specific catalytic cleavage of the targeted RNA component of telomerase resulting in inhibition of telomerase activity (Wan, Fell and Akhtar, 1998). To confirm these findings before proceeding with experiments to determine the efficacy of this ribozyme in intact glioma cells, the ability of ribozyme TEL.1 to inhibit telomerase

activity in U87-MG cell lysates was evaluated using the TRAP assay as described in section 5.2.5. Cell lysates (20μg protein) were treated with 0 – 20μM ribozyme for 30 minutes at 37°C. A negative control, containing no cell lysate protein was included to exclude the possibility that the 6-bp ladder was resulting from amplification of primer dimers. The level of telomerase activity was quantified using scanning densitometry of gel autoradiographs (see Figure 5.7).

Inhibition of telomerase activity was clearly dose dependant, as depicted in Figure 5.7, with approximately 50% inhibition of telomerase activity occurring at 4μM. Almost complete inhibition was evident at concentrations above 20μM. These results support the previous findings of ribozyme-mediated telomerase inhibition using ribozyme TEL.1, although greater concentrations of ribozyme were required to achieve 50% inhibition. Wan *et al.* (1998) reported an IC_{50} value of around 0.4μM. The discrepancy could be due to the concentration of cell lysates used in each study. For this research, ribozyme was added to 20μg of protein (to reflect protein levels in intact cell experiments) whereas ribozyme was added to only 4μg protein in the previous study.

To confirm the specificity and mechanism of ribozyme action in inhibiting telomerase activity, the activity of the two control ribozymes were also investigated in U87-MG cell lysates. Firstly, to determine if telomerase inhibition was due to antisense effects or actual cleavage of the RNA component, the activity of increasing concentrations (0-10μM) of an inactivated ribozyme was determined. For catalytic cleavage activity, the hammerhead ribozyme requires nucleotides G_5, A_6, G_8, G_{12} and $A_{15.1}$ to be unmodified nucleotides (Paolella *et al.*, 1992; Yang *et al.*, 1992), All nucleotides within the core region of the inactivated ribozyme were 2'-O-methylated (Figure 5.2b), thus rendering the ribozyme catalytically inactive.

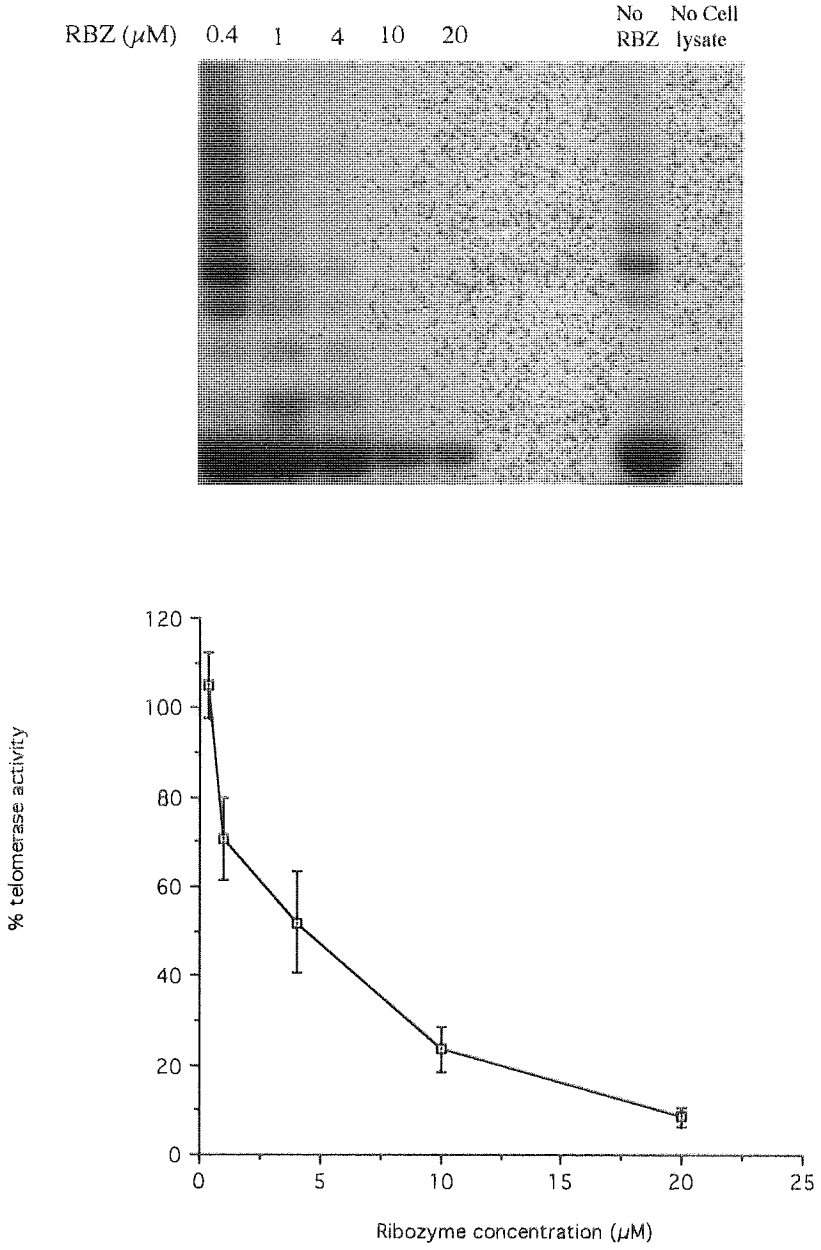

Figure 5.7 *Dose-dependent inhibition of telomerase activity in U87-MG cell lysates.* Lysates were incubated in the absence or presence of increasing concentrations (0.4-20μM) of active ribozyme TEL.1 at 37°C for 30 minutes. Telomerase activity was analysed using the TRAP assay as described in section 5.2.4. The PCR products were electrophoresed on an 8% PAGE at 250V for 3 hours and telomerase activity visualised by autoradiography. (**a**) Representative autoradiograph.(**b**) Quantitative representation of telomerase inhibition as a function of ribozyme dose. Quantification of TRAP assay gel autoradiograph was performed by densitometric analyses of two independent inhibition experiments. Bars represent range of observation.

Consequently, the inactive ribozyme control retains binding arms identical to the active version but contains a modified inactive catalytic domain, thus allowing binding to the target sequence but preventing cleavage. Any reduction in telomerase activity mediated by this ribozyme would indicate inhibition by antisense effects. As figure 5.8 demonstrates, there was no significant reduction in telomerase activity by the inactive ribozyme control at doses up to 10μM.

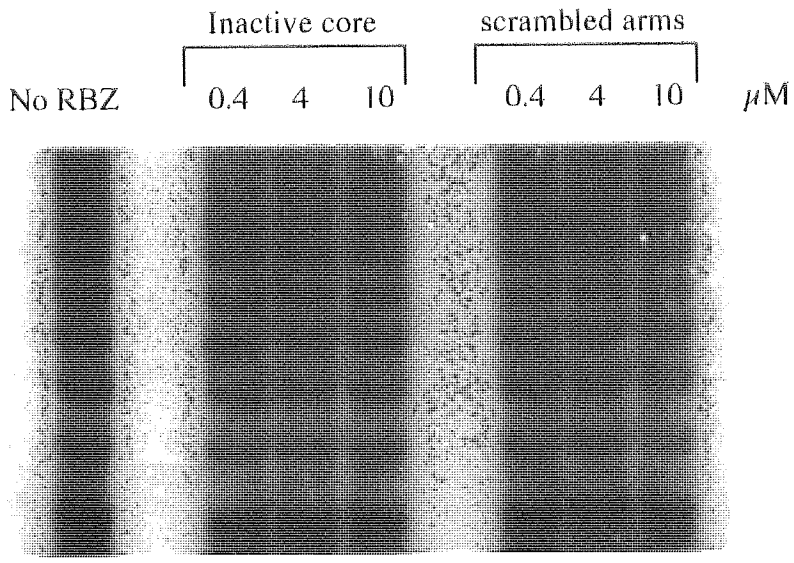

Figure 5.8 *Inactivity of scrambled and inactive control ribozymes in reducing telomerase activity in U87-MG cell lysates.* Lysates were incubated at 37°C for 30 minutes in the presence of increasing concentrations (0-10μM) of control ribozymes containing either an inactivated core (inactive) or scrambled arm sequences (scrambled). Telomerase activity was analysed using the TRAP assay as described in section 5.2.4. The PCR products were electrophoresed on an 8% PAGE at 250V for 3 hours and telomerase activity visualised by autoradiography.

To determine the specificity of ribozyme TEL.1 on telomerase inhibition, the actions of a further ribozyme control, in which the binding arm sequence of the active ribozyme has been rearranged so that it can no longer bind to its target site (Figure 5.2c), was

investigated in U87-MG cell lysates. Like the inactive control, this ribozyme failed to significantly reduce telomerase activity at the concentrations tested (Figure 5.8), as determined by densitometry of gel autoradiographs. The inactivity demonstrated by these two control ribozymes indicates that the ribozyme must specifically bind to and cleave the RNA component of telomerase in order to reduce telomerase activity levels.

5.3.6 Enhancement of Cellular Delivery of anti-Telomerase Ribozymes using Cationic Liposomes.

Before proceeding with studies to investigate the actions of ribozyme TEL.1 in intact U87-MG cells, the issue of enhancing exogenous delivery of synthetic ribozymes must once again be addressed. Research undertaken in Chapter Three revealed that, like ODNs, exogenously delivered synthetic ribozymes enter cells by endocytic mechanisms and intracellular delivery of these molecules is very inefficient. In fact, cellular delivery can be a limiting factor with therapeutic approaches using antisense ODNs and ribozymes. This problem was clearly demonstrated in a study by Duncan *et al.* (1998) evaluating PS-ODN inhibition of telomerase activity in intact cells and cell lysates in the SKnSH neuroblastoma cell line. While they were able to demonstrate effective telomerase inhibition in cell lysates, they reported little effect when intact cells were used.

Consequently a strategy was required to improve the cellular uptake and bioavailability of the anti-telomerase ribozymes in the glioma cell line U87-MG. As discussed in sections 1.4.2.2 and 4.3.3.3, cationic liposomes have been reported as an efficient system for both ODN and ribozyme delivery. The enhancement properties of two cationic lipid formulations, LipofectAMINE™ and PerFect™ Pfx-6, had previously been investigated

in the vulval epithelial cell line, A431 (section 4.3.3.3). However, lipid-ribozyme complex optimisation is dependent upon a number of factors including cell system and ribozyme concentration. Therefore, the enhancement properties of both lipid formulations in delivering the chimeric ribozyme TEL.1 into U87-MG cells was investigated

An initial study was undertaken to determine the concentrations at which LipofectAMINE™ and PerFect™ Pfx-6 could be administered without significant toxicity. Increasing concentrations of lipid formulation (0-50μg/ml) were added to U87-MG cells and incubated at 37°C for a period of 4 hours. The results demonstrated that, in both cases, lipid concentrations of up to 10μg/ml were non-toxic, with no significant reduction in cell number evident at these concentrations (Figure 5.9). When lipid concentrations of 25μg/ml and above, were administered, however, the percentage of viable cells became markedly reduced.

This toxicity study highlighted a problem with optimising efficiency of ribozyme delivery based on charge ratio as undertaken in the previous chapter (section 4.3.3). In view of the dose dependent ribozyme mediated inhibition demonstrated in section 5.3.5, it was decided that, for initial efficacy studies in intact cells, the effect of ribozyme TEL.1 in inhibiting telomerase activity in the U87-MG cell line would be investigated at two concentrations, 4μM and 10μM. However, to achieve either a net positive or even a neutral lipid:ribozyme (+/-) charge ratio a minimum concentration of 54μg/ml of LipofectAMINE™ or 118μg/ml of PerFect™ Pfx-6 would be required. Thus, in view of the high levels of lipid required, optimal charge ratios for transfection can not be obtained without significant toxicity to the cells. A different approach was taken therefore, in determining which lipid formulation was most efficient at delivering the ribozymes to the glioma cells.

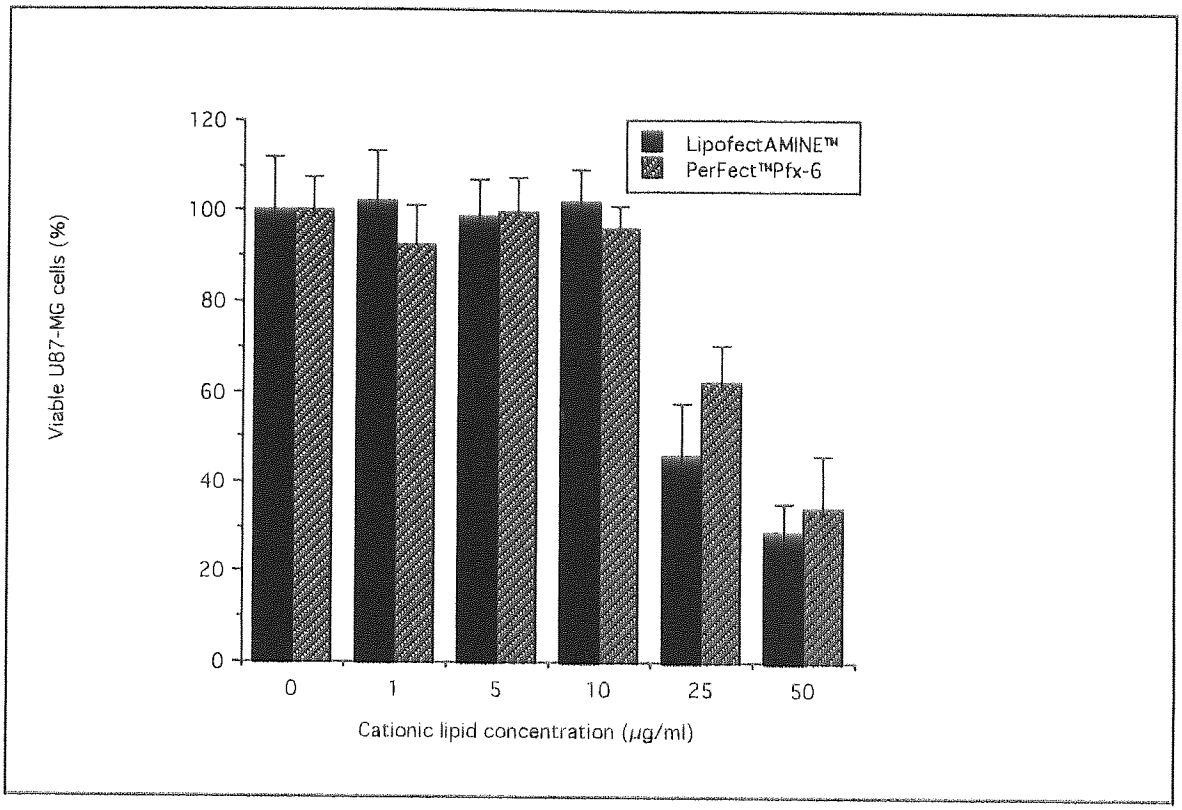

Figure 5.9 *Toxicity of cationic lipid formulations, LipofectAMINE™ and PerFect™ Pfx-6 on U87-MG cells.* Cationic lipids LipofectAMINE™ and PerFect™ Pfx-6, diluted in serum-free DMEM medium were added to U87-MG cells at concentrations ranging from 1μg/ml to 50μg/ml. The cell numbers, 4 hours after addition of the lipids are shown as a percentage of the untreated cell number. Data are expressed as mean (n=5) ± SD.

Cellular association of 5'-[^{32}P]-labelled ribozyme TEL.1 (4μM) was determined in the presence of increasing concentrations of cationic liposome formulation as described in section 5.2.6. In addition, parallel studies were performed to assess the cytotoxicity of these lipid-ribozyme complexes. Both lipid formulations significantly enhanced cellular association of the ribozyme at all concentrations tested ($p<0.001$) when compared with the free ribozyme control (Figure 5.10). While LipofectAMINE™ enhanced cellular association up to 50-fold, the presence of PerFect Pfx-6 increased association levels by up to 20-fold. In fact, ribozyme association to the glioma cells in the presence of LipofectAMINE™ was significantly greater ($p<0.001$) at each lipid concentration than that observed when ribozymes were complexed to PerFect™ Pfx-6.

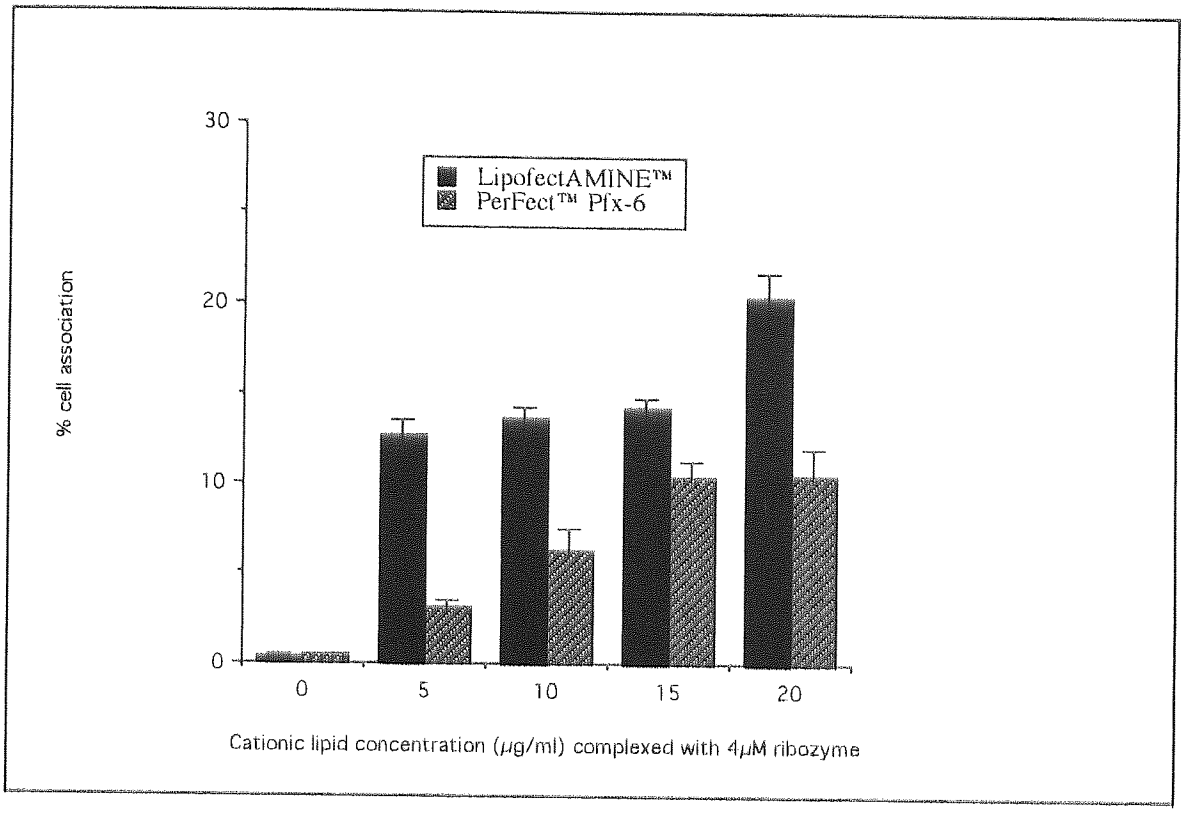

Figure 5.10 *Optimisation of ribozyme association to U87-MG cells using cationic lipids.* Cell association of 4μM 5'-[^{32}P]-radiolabelled ribozyme when complexed to either LipofectAMINE™ or PerFect™ Pfx-6 after 4 hours incubation at 37°C (see section 5.2.6). Data are expressed as mean (n=3) ± SD.

Table 5.1 *Toxicity of lipid-ribozyme complexes to U87-MG cells*

Cationic lipid conc (μg/ml) complexed with 4μM ribozyme	Viable U87-MG cells (% control)	
	LipofectAMINE™	PerFect Pfx-6™
0	100.0 ± 11.7	100.0 ± 17.7
5	102.3 ± 11.4	92.3 ± 8.88
10	98.6 ± 8.5	86.5 ± 7.69
15	74.6 ± 11.6*	82.3 ± 4.88
20	55.8 ± 7.6*	40.4 ± 11.75*

* denotes significant reduction ($p<0.05$) in viable cell number from untreated control.

Maximum association in the presence of LipofectAMINE™ was evident at a concentration of 20μg/ml, however, significant cellular toxicity was observed when concentrations greater than 10μg/ml were administered (Table 5.1). Consequently, the optimal concentration of LipofectAMINE™ required to deliver 4μM or greater of chimeric ribozyme to U87-MG glioma cells was considered to be 10μg/ml. Maximum association in the presence of PerFect™ Pfx-6, without significant loss of viable cells, was found to be 15μg/ml.

Since LipofectAMINE™ appeared to be the most effective delivery vehicle in this case, it was decided that this reagent would be the lipid of choice for facilitating delivery of ribozyme TEL.1 into U87-MG glioma cells in studies investigating ribozyme mediated inhibition of telomerase activity in intact U87-MG cells.

The subcellular distribution of ribozyme TEL.1 was studied in the presence and absence of LipofectAMINE™. To evaluate intracellular distribution, the chimeric ribozyme was labelled with FITC (section 5.2.1) and the distribution of the FITC-labelled ribozyme analysed by fluorescence microscopy (as described in section 3.2.3.11). Incubation of U87-MG cells with 4μM FITC-labelled ribozyme only (no lipid) for 4 hours resulted in a faint punctate distribution of the ribozyme located in the periphery of the cell, close to the cell membrane (Figure 5.11). As mentioned in Chapter Three (section 3.3.3.7), this distinct punctate distribution is characteristic of endosomal compartmentalisation. Cells incubated with 4μM FITC-labelled ribozyme in the presence of 10μg/ml LipofectAMINE™ exhibited a much more intense fluorescence confirming significant enhancement of ribozyme uptake facilitated by the delivery vehicle LipofectAMINE™ (Figure 5.12).

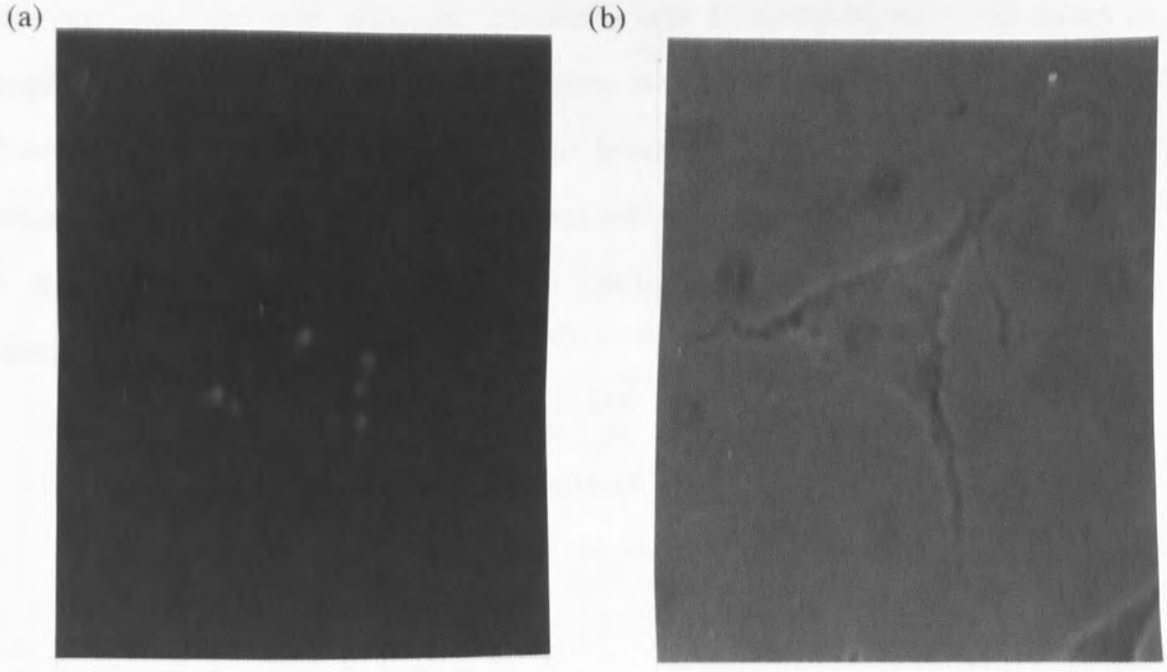

Figure 5.11 *Subcellular distribution of 4μM FITC-labelled ribozyme TEL.1 in U87-MG cells.* **(a)**. Fluorescent illumination (magnification x 40). **(b)**. Phase contrast image.

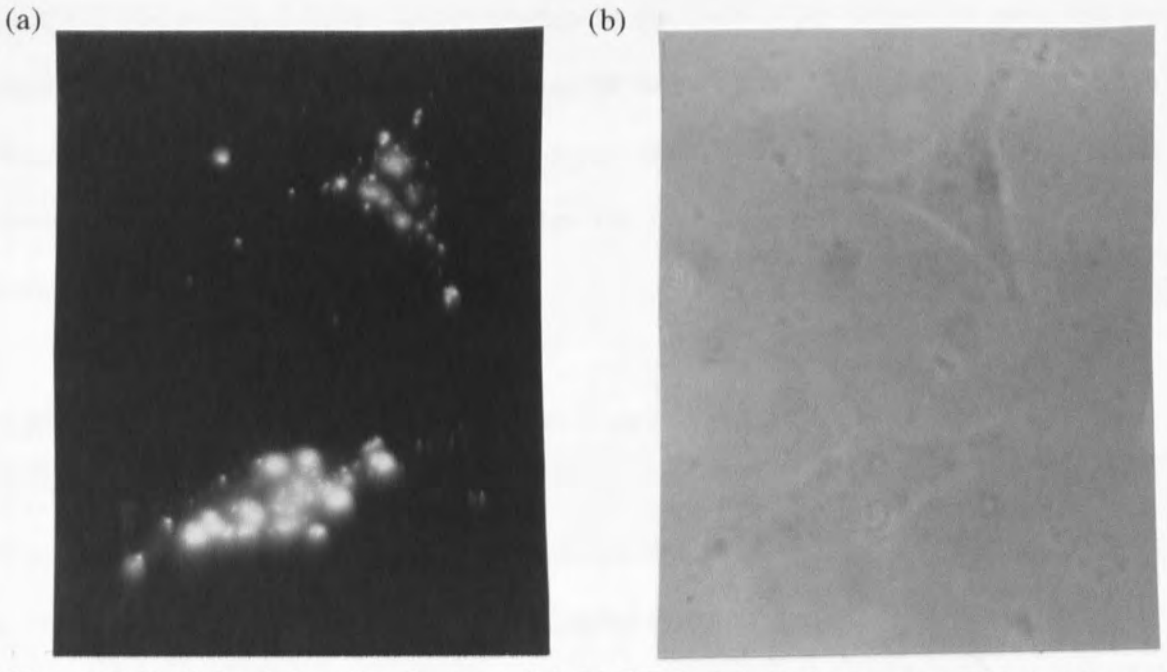

Figure 5.12 *Subcellular distribution of 4μM FITC- labelled ribozyme TEL.1 delivered with the aid of delivery vehicle LipofectAMINE™ (10μg/ml) in U87-MG cells.* **(a)**. Fluorescent illumination (magnification x 40). **(b)** Phase contrast image.

The cells incubated with ribozyme complexed with LipofectAMINE™ did appear to exhibit some diffuse cytoplasmic fluorescence as well as strong punctate cytoplasmic fluorescence. It was not clear, however, to determine from these pictures how much ribozyme, if any, was localised in the nuclear region. A nuclear stain, such as DAPI (4'-6'-diamidino-2-phenylindole) could be used to highlight the nucleus and would have clarified this matter.

What is apparent, however, is that LipofectAMINE™ not only significantly enhances ribozyme uptake in U87-MG cells but also alters the subcellular distribution. It is generally believed that cationic liposomes enter cells through the process of endocytosis (see Hope *et al.* 1998 for review). Consequently, the intense punctate fluorescence evident in Figure 5.12 could represent accumulation of the ribozyme-lipid complexes in endosomes. LipofectAMINE™ is composed of both the cationic lipid, DOSPA and the neutral fusogenic helper lipid DOPE (3:1 w/w) (see section 4.3.3.3). The presence of DOPE is reported to promote destabilisation of the endosomal membrane, releasing the ribozyme into the cytoplasm (Jaaskelainen *et al.*, 1998). The areas of more diffuse fluorescence could therefore represent ribozyme released from these endosomes into the cytoplasm. It is unclear, however, whether the ribozyme is free at this stage or still complexed with the lipid formulation.

5.3.7 Intracellular Stability of Liposome-Complexed Ribozymes

The intracellular stability of 5'-[^{32}P]-radiolabelled chimeric ribozymes complexed with LipofectAMINE™ was examined over a period of four hours (as described in section 5.2.2.2) to ensure that the ribozyme remained intact during future efficacy studies. The results, as shown in Figure 5.13, indicate that the ribozyme remained stable within the

cell during this period, as no degradation products were evident. In view of the stability profiles observed earlier in this chapter (section 5.3.3), this result suggests that the cationic liposomes protect the ribozyme against nucleases and thus enhance cellular stability. The protective effect of liposomal complexation to nucleic acids has previously been reported (see review by Amarzguioui and Prydz, 1998; Gaughan and Whitehead, 1999). For example, in one study, an all RNA ribozyme which degraded almost instantaneously in cell supernatants was shown to remain largely intact over a period of 22 hours in human osteosarcoma cells when complexed with the cationic lipid DOTMA (Kariko *et al.*, 1994).

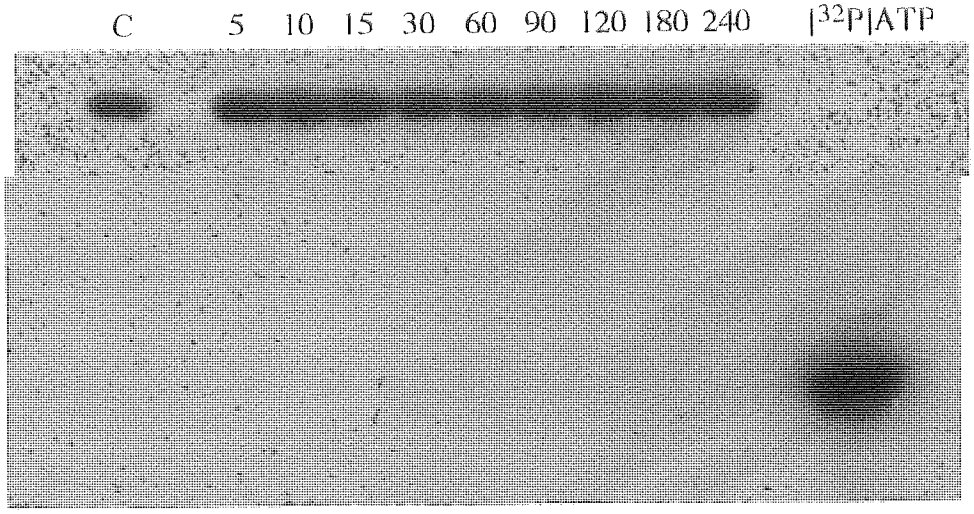

Figure 5.13 *Intracellular stability of 5'-[^{32}P]-labelled ribozyme TEL.1 complexed to LipofectAMINE™ in U87-MG cells.* The ribozyme was added to U87-MG cell culture in serum-free medium at a final concentration of 4μM with the aid of the delivery vehicle LipofectAMINE™ (10μg/ml) as described in section 5.2.2.2. The ribozyme was recovered from lysed cells at variable time points and analysed on 20% PAGE (7M urea). Incubation times are given in minutes. C represents intact ribozyme / lipid complex in serum-free medium.

5.3.8 Ribozyme Mediated Inhibition of Telomerase Activity in Intact U87-MG Cells

Ribozyme TEL.1 was delivered to U87-MG cells at two concentrations 4μM and 10μM in the presence and absence of the delivery vehicle LipofectAMINE™ as described in section 5.2.7. Cells were incubated at 37°C in the presence of the ribozyme for a period of 4 hours. After this time, telomerase activity was determined by TRAP assay (section 5.2.4) and analysed by densitometry of gel autoradiographs (section 2.3.2.2). The results are represented in Figure 5.14.

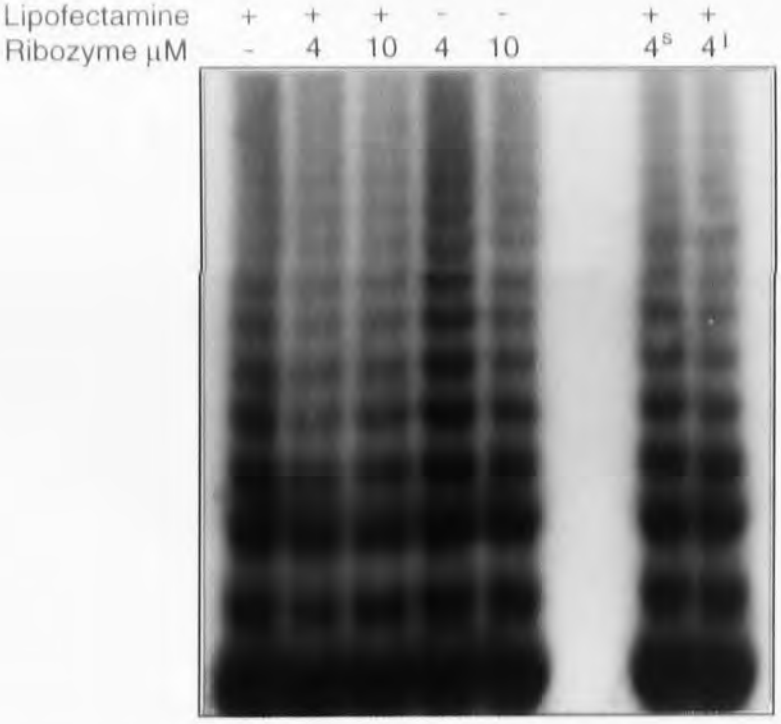

Figure 5.14 *Ribozyme-mediated inhibition of telomerase activity in intact U87-MG cells.* U87-MG cells were incubated with 4μM and 10μM ribozyme TEL.1 either in the presence or absence of the cationic lipid, LipofectAMINE™ (10μg/ml) for a period of 4 hours at 37°C (see section 5.2.7). Control ribozymes (4μM) were also delivered to cells using LipofectAMINE™ (10μg/ml). 4^s represents 4μM scrambled ribozyme, 4^I represents 4μM inactive ribozyme. Cells were then lysed (section 5.2.5) and telomerase activity of cell lysates (4μg) determined by TRAP assay as described in section 5.2.4. The PCR products were electrophoresed on an 8% PAGE at 250V for 3 hours and telomerase activity visualised by autoradiography.

The chimeric ribozyme TEL.1 did appear to inhibit telomerase activity in the intact cells when delivered using the delivery vehicle LipofectAMINE™. Densitometric analysis revealed that telomerase activity was significantly reduced to 74.5 ± 4.17% of the untreated control by 4μM ribozyme and to 77.2 ± 4.74% of the control by 10μM ribozyme. A dose response was not apparent therefore, at the concentrations of ribozyme applied in this experiment. A possible explanation could involve the ratio of ribozyme complexed to the cationic lipid. The ratio of nucleic acid to cationic lipid may be critical to the physicochemical properties of the ribozyme-liposome complex (Jaaskelainen *et al.*, 1998). In addition the ODN-liposome ratio has been shown to determine the speed of release from intracellular vesicles (Lappalainen *et al.*, 1997). As the concentration of ribozyme is increased, the net charge of the complex becomes more negative which may result in entrapment of ribozyme in endosomes. Jaaskelainen *et al.* (1994) reported that complexes prepared with excess DNA (on a charge basis) do not result in vesicle release. Alternatively, much higher doses of ribozyme may be required to inhibit telomerase activity to a greater extent than that seen in this study. A series of dose response experiments, possibly involving varying concentrations of cationic lipid, are required to investigate this further.

A recent study reported that a hammerhead ribozyme cleaved its target substrate during RNA preparation and not while in the cell (Heidenreich *et al.*, 1996b). It is possible therefore that telomerase inhibition evident in this study could be due to cleavage in cell extracts during preparation for the TRAP assay. The lack of significant effect by free ribozyme, delivered to cells without a delivery vehicle, in reducing telomerase activity largely discounts this possibility (Figure 5.14). Densitometric analysis revealed that while 4μM of free ribozyme had no effect on telomerase levels, 10μM ribozyme caused a slight

reduction in telomerase activity reducing levels to 89.5 ± 6.36% of the untreated control. This reduction, however, was not found to be statistically significant.

To establish the mechanism of action of ribozyme-mediated telomerase inhibition, the activity of the inactive and scrambled control ribozymes in intact glioma cells were also determined. Neither of the two control ribozymes, however, significantly reduced telomerase activity as shown in Figure 5.14. This indicates that telomerase inhibition resulted from cleavage of the RNA component of telomerase. Further confirmation of ribozyme activity could be established by isolating total RNA extracted from the cells and amplifying a portion of the telomerase RNA containing the GUC cleavage site by RT-PCR analysis (as described in Wan *et al.*, 1998). Substrates already cleaved by the ribozyme should not be amplified and the extent of ribozyme cleavage can then be quantified. The inclusion of an internal control would have discounted the possibility that reduced telomerase activity was due to the presence of Taq polymerase inhibitors.

5.4 CONCLUDING REMARKS

The results of this chapter demonstrate that chimeric 2'-O-methyl modified synthetic ribozymes can act as sequence-specific inhibitors of telomerase activity. The ribozyme TEL.1, directed against the template region of the RNA component of telomerase exhibited high catalytic activity *in vitro* against a complementary short substrate and dose-dependent inhibition of telomerase activity in U87-MG glioma cell lysates with an IC_{50} of around 4μM.

When delivered to intact U87-MG cells using the delivery vehicle, LipofectAMINE™, ribozyme TEL.1 significantly reduced telomerase activity whereas control ribozymes

containing either an inactive core or scrambled arm sequences failed to inhibit the activity of this ribonucleoprotein. Interestingly, when the ribozyme was delivered to the glioma cell line without the aid of the cationic lipid, no significant reduction in telomerase activity was observed, clearly demonstrating the requirement of a suitable delivery formulation to enhance intracellular bioavailability of such exogenously delivered ribozymes in cell culture.

Although other inhibitors of telomerase have now been reported (Norton *et al.*, 1996; Kanazawa *et al.*, 1996; Sun *et al.*, 1997; Naasani *et al.*, 1999; Tao *et al.*, 1999), these results suggest that synthetic chemically modified ribozymes offer the potential advantages of being highly sequence-specific catalysts that can be administered exogenously to directly cleave the RNA component and thereby inhibit telomerase activity. While there is now much interest in this field the exact role of telomerase in aging and tumorigenesis are still poorly understood. Consequently, exogenously administrable, synthetic ribozymes selective for individual components of telomerase may have important uses in further understanding the role and regulation of this ribonucleoprotein in both normal and diseased tissues, as well as in the potential therapy of telomerase-positive tumours such as Glioblastoma Multiforme.

CHAPTER SIX

DISCUSSION

Ribozymes have important potential applications as both molecular tools in the study of gene expression and as therapeutic inhibitors of disease causing genes. In this report the biological properties of chemically synthesised hammerhead ribozymes were investigated in order to assess their potential use as novel anti-brain tumour agents. Glioblastoma Multiforme (GBM) is a highly malignant form of brain cancer for which no curable treatment is currently available (Rasheed *et al.*, 1999). The over-expression of a number of genes, including the epidermal growth factor receptor (EGFr), have been implicated as a causative factor in the progression of tumours (see section 1.6). Novel forms of treatment such as oligonucleotide- and ribozyme-based therapies, which allow specific inhibition of aberrant gene expression, may hold the future of therapy for GBM.

Major limitations in the effective use of catalytic RNA as drugs, however include poor biological stability and delivery to the appropriate cells. As demonstrated in Chapter Three, unmodified RNA is extremely unstable in the biological milieu and is rapidly degraded by intra- and extra-cellular nucleases. In fact an all-RNA ribozyme was degraded almost instantaneously following exposure to foetal bovine serum (section 3.3.1.1). Site specific chemical modifications to ribozymes were therefore required that would enhance biological stability without significant loss in catalytic activity compared to unmodified RNA.

In Chapter Three, two synthetic 2'-O-methyl modified hammerhead ribozymes containing either 2'-amino groups at position U_4/U_7 (designated RPI.4782) or a 2'-C-allyl modification at U_4 only (designated RPI.5993) were characterised in terms of stability and activity. Such modifications have been reported to significantly increase stability while preserving catalytic activity (Beigelman *et al.*, 1995a). Both of these ribozyme constructs exhibited good *in vitro* cleavage activity with substantially improved nuclease stability in serum compared to all RNA and commonly used DNA oligonucleotides. Stability half-lives in 100% FBS were in excess of 18 hours. The kinetic parameters determined for the most active ribozyme RPI.4782 (K_m = 87nM; k_{cat} = 1.2min^{-1}) fall in line with typical values reported for short synthetic unmodified hammerhead ribozymes (Thompson *et al.*, 1996; Birikh *et al.*, 1997), but fall short of those exhibited by conventional protein enzymes. The issue of stability, therefore, appears to have been overcome by these site-specific modifications.

To tackle the problem of ribozyme delivery, a fundamental and precise understanding of the cellular uptake mechanisms of ribozymes is required. Before this study, very little was known about the uptake mechanisms of exogenously administered synthetic ribozymes. The surface interactions and uptake properties of the 2'-O-methyl modified ribozyme RPI.4782 were examined in the human glioma U87-MG cell line, which has been shown to exhibit many of the phenotypic features of primary glioblastoma (Yazakai *et al.*, 1996).

The cellular association of internally [^{32}P]-labelled ribozyme RPI.4782 to U87-MG glioma cells was found to be temperature, energy and pH dependent and involved an active process that could be competed with cold ribozyme of the same chemistry and sequence, antisense PS- and PO- oligonucleotides, the 2'-O-methyl / 2'-C-allyl ribozyme

RPI.5993, as well as a variety of other polyanions. These data are consistent with an endocytic mechanism of entry into cultured glioma cells and show many similarities to those observed by many research groups for antisense ODNs (for reviews see Akhtar and Juliano, 1992; Akhtar, 1998). Furthermore, as PO-ODN and PS-ODN are generally considered to enter cells via receptor mediated, adsorptive or fluid phase endocytosis, the fact that ribozyme association can be inhibited by ODNs indicates that there could be an overlap in their mechanism of entry and that ribozymes may compete for cell uptake via one or more of these process. Fluid phase endocytosis is however unlikely to account for a significant fraction of ribozyme uptake since the cellular association of the fluid phase marker, mannitol, was significantly lower than cellular association of the ribozyme. Subcellular distribution studies of fluorescently labelled ribozymes confirmed an extranuclear, punctate localisation within the cell indicative of entrapment of ribozyme within endocytic vesicles (Shoji *et al.*, 1991). Indications from this research are that the predominant mechanism of uptake for exogenously delivered ribozymes is by adsorptive and / or receptor mediated endocytosis, mediated by a variety of cell surface proteins and possibly other membrane components. Various cell surface ODN binding proteins have been postulated (see section 1.4.2.1 for review) together with suggested ODN binding to glycoproteins and even cell surface lipids (Beck *et al.*, 1996). Further research is required to establish if any of these putative binding components are also involved in ribozyme uptake into cultured cells.

These findings suggest that it is the large molecular weight and polyanionic characteristics of the ribozyme molecule that governs cellular uptake mechanism rather than the defined 'wishbone' conformation that the hammerhead construct adopts in solution (Pley *et al.*, 1994; Tuschl *et al.*, 1994; Scott *et al.*, 1995). Research on the secondary structure of G-quartet-containing ODNs that form tetraplexes in solution,

however, suggest that the magnitude of nucleic acid uptake is affected by secondary structure although the gross cellular mechanism remains the same (Agrawal *et al.*, 1996). Cell association of ribozyme to cultured cells is extremely inefficient with only ~ 1-3% of administered ribozyme becoming associated. In addition, the entry of chimeric ribozymes by endocytosis suggests that internalised ribozyme may become trapped within endosomes and unavailable for action against target mRNA. These observations will facilitate the development of delivery strategies to enhance ribozyme uptake and bioavailability.

There is a growing body of evidence indicating that elevated levels of EGFr expression and the consequent induction of tyrosine kinase activity can play a pivotal role in the initiation and development of several human malignancies (Coulson *et al.*, 1996). The biological efficacy of 2'-O-methyl chimeric ribozymes directed against the EGFr mRNA was investigated both *in vitro* and in cell culture.

Several factors that contribute to the intracellular efficacy of ribozymes must be considered in their design for inhibition of gene expression. The first step requires the rational design of effective ribozymes with sequences complementary to accessible sites within the target mRNA. With the aid of the computer program RNAFOLD (Zuker, *et al.*, 1991), twenty ribozymes were designed against various sites along EGFr mRNA, the majority of which (18/20) exhibited high *in vitro* catalytic activity against complementary short substrates. On analysis, the value of using such RNA folding algorithm programs to eliminate ribozyme designs which may adopt catalytically inactive conformations was highlighted. Ribozyme constructs predicted to be the most favourable by the program correlated well with those exhibiting the highest activity *in vitro*. Such activity may not however be reflected in the cell where many factors can influence performance such as

secondary and tertiary folding of the mRNA and the presence of RNA binding proteins. Efficient cleavage sites on long substrate mRNA can not easily be identified and it is generally believed that the value of computational secondary-structure prediction of the target RNA to identify accessible sites is limited (Bramlage *et al.*, 1999). The approach taken in this report was to screen the most favourable ribozyme designs directly in cell culture. However, although this strategy has been successful in identifying active sequences of ODNs (Monia *et al.*, 1996), it is both cost and labour intensive with no guarantees of success. Recently two cost-efficient strategies based on combinatorial chemistry have been reported (Birikh *et al.*, 1997b; Milner *et al.*, 1997). The first of these involves RNase H mapping of target mRNA with random ODN libraries. Sites accessible for hybridisation, as determined by mRNA cleavage fragments produced by the enzyme, are selected by combining the targeted mRNA transcript with a random library of chemically synthesised ODNs (see review by Akhtar, 1998). Birikh *et al.*(1997b), used this technique to identify accessible sites along human acetylcholinesterase RNA and found that the RNase H mapping technique demonstrated a high predictive power for favourable ribozyme cleavage sites. In view of the lack of efficacy of the twenty anti-EGFr ribozymes observed in cell culture (Chapter Four), an RNase H mapping strategy directed against a full transcript of EGFr mRNA could be performed to establish if the negative results seen are due to the inaccessibility of target sites. A potential disadvantage of this technique, however, is that accessible sites are broadly defined since RNase H cleavage can occur at many sites within the ODN: mRNA duplex (Akhtar *et al.*, 1998). This may be an important factor in ribozyme design because a few, even single, nucleotide shifts in antisense designs can alter efficacy (Monia *et al.*, 1997). The second approach involves hybridisation of target mRNA to scanning antisense arrays (Milner *et al.*, 1997) and allows more precise identification of open structures within mRNA.

Although the application of this method is still in its infancy, it offers great potential in both ODN and ribozyme design.

The activity of the 2'-O-methyl chimeric anti-EGFr ribozymes were evaluated in cultured A431 cells, a cell line which expresses amplified levels of EGFr (Ullrich *et al.*, 1984). The findings from earlier in this report (Chapter Three) had indicated that ribozymes enter cultured cells through an endocytic mechanism which is highly inefficient and can result in internalised ribozymes becoming trapped in endocytic vesicles. A delivery vehicle was therefore required to enhance cellular delivery of these ribozymes to A431 cells. Cationic liposomes have been reported to enhance nucleic acid delivery (see section 1.4.2.2 for review) and facilitate endosomal exit of ODNs by a putative lipid exchange mechanism (Zelphati and Szoka, 1996). In fact, the effective use of liposomes has been reported in facilitating delivery and efficacy of pre-synthesised ribozymes (Jarvis *et al.*, 1996; Bramlage *et al.*, 1999; Kisish *et al.*, 1999). Two different commercially available cationic liposomes, LipofectAMINE™ and PerFect™ Pfx-6 were investigated as a means of improving the efficiency of ribozyme delivery to A431 cells. Optimisation studies showed that optimal association of ribozymes to A431 cells was achieved when the overall charge ratio was net positive, although maximum association of the lipid/ribozyme complex was dependent upon a number of factors including ribozyme concentration, lipid concentration and formulation.

Using LipofectAMINE™ as a delivery vehicle, ribozymes were delivered to A431 cells at different concentrations, in single and continuous doses and over time points of up to four days. Despite the fact that the ribozymes were taken up by the cells and that they remained largely stable throughout these experiments, no significant reduction in either cell proliferation or EGFr expression was observed during these studies. The lack of

activity of the twenty anti-EGFr ribozymes observed in cell culture would suggest that, even with the aid of the delivery vehicle LipofectAMINE™, the ribozymes are either failing to gain access to the correct intracellular compartment or have not dissociated from the lipid and are therefore not bioavailable. This is in contrast to the findings of Zelphati and Szoka (1996) which suggest that ODNs delivered with cationic liposomes can dissociate from the lipid complex within cells, thus gaining access to cytoplasmic and nuclear targets. Unfortunately, time restraints prohibited further research on this matter. Clearly, it is important to determine the intracellular destinations of these ribozymes to establish whether it is the method of delivery or ribozyme design that is limiting cellular efficacy of such exogenously delivered ribozymes. Suggested work in this field would include both fluorescent subcellular localisation studies coupled with more detailed ultrastructural analysis by immuno-electron microscopy.

An important determinant on ribozyme efficacy is co-localisation of the ribozyme with the target RNA. In a study to determine the efficacy of synthetic ribozymes delivered using hemagglutinating virus conjugated (HVJ)-cationic liposomes, co-localisation of ribozyme with target was determined by tagging the ribozyme with FITC (green) while the target protein, Tax, was identified by using TRITC-labelled (orange) anti-Tax monoclonal antibodies (Kitajima *et al.*, 1997). Subcellular distibution of both ribozyme and target protein were then identified using fluorescent microscopy. The same principle could be utilised to determine whether any anti-EGFr ribozymes actually reach the target EGFr mRNA. A more detailed examination of ribozyme localisation could also be confirmed by immuno-electron microscopy. The predominant localisation of PS-ODNs within endosomes has been clearly demonstrated using this method (Beltinger *et al.*, 1995). Furthermore, research undertaken using this technique by a member of the research group (Andrew Hudson, Aston University) detected biotin-labelled ribozymes,

delivered without the aid of a delivery vehicle, localised mainly within distinct endocytic vesicles, although a small proportion of internalised ribozymes was observed free within the nucleus and cytoplasm. Lappalainen *et al.* (1997) examined the intracellular distribution of digoxigenin-labelled ODNs delivered by cationic liposomes using electron microscopy. Endocytosis was reported to be the main pathway of cellular uptake of such liposomes. The type of liposome and the charge of the oligo-liposome complex however was found to be important for determination of the intracellular distribution of ODNs.

The presence of telomerase, a ribonucleoprotein responsible for telomere elongation, has been strongly associated with brain tumour progression (for reviews see Parkinson, 1996; Shay, 1997; deLange and Jacks, 1999; Hodes, 1999). Furthermore, telomerase activity has been observed in most brain tumours (Kim *et al.*, 1994; Langford, 1996; Le *et al.*, 1998) and consequently appears to be a suitable target for the treatment of brain cancers such as glioblastoma multiforme. A chemically modified hammerhead ribozyme, termed, TEL.1, containing 2'-O-methyl ribonucleotides to enhance biological stability was designed directed against the template region of the RNA component of telomerase. This ribozyme demonstrated high catalytic activity *in vitro* against a complementary short substrate and dose-dependent inhibition of telomerase activity in U87-MG glioma cell lysates with an IC_{50} of around 4μM. Enhanced cellular delivery of the ribozyme to this cell line was achieved using the cationic lipids formulation LipofectAMINE™. Fluorescent distribution studies revealed that the use of this delivery vehicle not only enhanced cellular uptake but also affected ribozyme distribution.

When delivered to intact U87-MG cells using the delivery vehicle, LipofectAMINE™, ribozyme TEL.1 significantly reduced telomerase activity whereas control ribozymes containing either an inactive core or scrambled arm sequences failed to inhibit the

activity of this ribonucleoprotein. This indicates that telomerase inhibition resulted from specific cleavage of the RNA component of telomerase. The efficacy demonstrated by TEL.1 suggests that synthetic chemically modified ribozymes offer the potential to be highly sequence-specific catalysts that can be administered exogenously to inhibit telomerase activity for anti-brain tumour applications. Such novel inhibitors of telomerase activity have important applications in understanding the role and regulation of telomerase activity in both normal and tumour cells. While there is now much interest in this field, the exact role of telomerase is still poorly understood. It has been reported that such strategies may be ineffectual due to possible alternative (ALT) pathways for maintaining telomere length (Bryan *et al.*, 1997). Research involving the use of telomerase inhibiting ribozymes will determine the effectiveness of anti-telomerase therapy in the treatment of cancer.

It is interesting to note that when ribozyme TEL.1 was delivered to the glioma cell line without the aid of the cationic lipid, LipofectAMINE™, no significant reduction in telomerase activity was observed, clearly demonstrating the requirement of a suitable delivery formulation to enhance intracellular bioavailability of such exogenously delivered ribozymes in cell culture. The effectiveness of cationic lipids, however, is not universal and lipid complexes with ribozymes will require optimisation for a given cell / nucleic acid system. The findings revealed in this report regarding the cellular uptake mechanisms of ribozymes, together with further investigations on the intracellular distribution of ribozymes, should facilitate this process.

Demonstrations of biological efficacy using synthetic chemically modified ribozymes *in vivo* (Lyngstadaas *et al.*, 1995 ; Flory *et al.*, 1996) however suggest that cellular uptake in animal models is sufficient to achieve biological effects in the absence of such delivery

methods. These examples show that for disease in which local or *ex vivo* application is possible, direct delivery of chemically stabilised ribozymes may be sufficient without the aid of a delivery vehicle. Such localised delivery, following surgical debulking, would be appropriate in the treatment of GBM in order to bypass the blood brain barrier. A disadvantage of administering exogenously delivered synthetic ribozymes is that multiple administrations are required, since ribozymes would be needed at the target site for long periods of time to exert the desired biological effects (Akhtar and Juliano, 1992). A sustained release delivery system, such as biodegradable polymers, may therefore be advantagous *in vivo*. Synthetic hammerhead ribozymes were successfully incorporated into biodegradable poly L-lactic acid polymer films and sustained release of ribozyme observed *in vitro* (Hudson *et al.*, 1996). Clearly optimum delivery of synthetic ribozymes is essential both *ex vivo* and *in vivo* if they are to fulfil their potential as novel therapeutic agents.

The development of nuclease stable synthetic ribozymes as both potential therapeutic agents and as biological tools has progressed significantly in the last few years. There is little doubt that despite the obstacles concerning delivery, exogenously administered ribozymes offer enormous potential as novel specific inhibitors of disease causing genes. In fact this optimism is reflected in the fact that the first chemically synthesised ribozyme, ANGIOZYME, has very recently successfully completed Phase 1 clinical trials (see section 1.5). Providing a methodical approach is adopted to optimising the various factors that govern the intracellular bioavailability of synthetic ribozymes, their full potential in molecular medicine should be realised.

REFERENCES

Agrawal, S. (1996). Antisense oligonucleotides: towards clinical trials. *Trends in Biotechnology*. **14**, 376-387.

Agrawal, S. (1999). Factors affecting the specificity and mechanism of action of antisense oligonucelotides. *Antisense and Nucleic Acid Drug Development*. **9**, 371-375.

Agrawal, S., Iadarola, P.L., Temsamani, J., Zhao, Q.Y., and Shaw, D.R. (1996). Effect of G-rich sequences on the synthesis, purification, hybridisation, cell uptake and hemolytic activity of oligonucleotides. *Biorganic and Medicinal Chemistry Letters*. **6**, 2219-2224.

Agrawal, S., and Iyer, R.P. (1995). Modified oligonucleotides as therapeutic and diagnostic agents. *Current Opinions in Biotechnology*. **6**, 12-19.

Akhtar, S. (1995). *Delivery Strategies for Antisense Oligonucleotides Therapeutics*. CRC Press Inc., London, U.K.

Akhtar, S. (1998). Antisense technology: selection and delivery of optimally acting antisense oligonucleotides. *Journal of Drug Targeting*. **5**, 225-234.

Akhtar, S. and Agrawal, S (1997). In vivo studies with antisense oligonucleotides. *Trends in Pharmaceutical Sciences*. **18**, 12-18.

Akhtar, S., Beck, G.F., Hawley, P., Irwin, W.J. and Gibson, I. (1996). The influence of polarised epithelial (Caco-2) differentiation on the cellular binding of phosphodiester and phosphorothioate oligonucleotides. *Antisense Research and Development*. **6**, 197- 206.

Akhtar, S. and Juliano, R.L. (1992). Cellular uptake and intracellular fate of antisense oligonucleotides. *Trends in Cell Biology*. **2**, 139-143.

Alberts, B., Bray, D., Lewis, J., Raff, M., Roberts, K., and Watson., J.D. (1989). Cell signalling. In: *The Molecular Biology of the Cell*. Garland Publishing, New York, USA.

Alexander, E. and Leoffler, J.S. (1998). Radiosurgery for primary malignant brain tumours. *Seminars in Surgical Oncology*. **14**, 79-87.

Ali, M., Lemoine, N.R., and Ring, C.J.A. (1994). The use of DNA viruses as vectors for gene therapy. *Gene Therapy*, **1**, 367-384.

Amarzguioui, M. and Prydz, H. (1998). Hammerhead ribozyme design and application. *Cellular and Molecular Life Sciences*. **54**, 1175-1202.

Arndt, G.M. and Rank, G.H. (1997). Colocalisation of antisense RNAs and ribozymes with their target mRNAs. *Genome*. **40**, 785-797.

Aurup, H., Heidenreich, O., and Eckstein, F. (1995). Stabilized RNA analogues for antisense and ribozyme applications. In: Akhtar, S (ed) *Delivery Strategies for Antisense Oligonucleotide Therapeutics*. CRC Press Inc. London, UK., pp161-177.

Ayers, D., Cutherbertson, J.M. Schroyer, K., and Sullivan, S.M. (1996). Polyacrylic acid mediated ocular delivery of ribozymes. *Journal of Controlled Release*. **38**, 167-175.

Barnes, D.W. (1982). Epidermal growth factor inhibits growth of A431 human epidermoid carcinoma in serum-free cell culture. *The Journal of Cell Biology*. **93**, 1-4.

Bassi, G.S., Mollegaard, N.E., Murchie, A., Von Kitzing, E., and Lolley, D.M.J. (1995). Ionic interactions and the global conformation of the hammerhead ribozyme. *Nat. Struct. Biol.* **2**, 45-55.

Beck, G.F., Irwin, W.J., Nicklin, P.L., and Akhtar, S. (1996). Interactions of phosphodiester and phosphorothioate oligonucleotides with intestinal epithelial caco-2 cells. *Pharmaceutical Research*. **13**, 1028-1037.

Been, M.D. (1994). Cis- and trans- acting ribozymes from a human pathogen, hepatitis delta virus. *Trends in Biological Sciences*. **19**, 251-257.

Beigelman, L., McSwiggen, J., Draper, K., Gonzalez, C., Jensen, K., Karpeisky, A., Matulic-Adamic, J., DiRenzo, A., Haeberli, P., Sweedler, D., Tracz, D., Grimm, S., Wincott, F., Thackray, V., and Usman, N. (1995a). Chemical modification of Hammerhead Ribozymes. *Journal of Biological Chemistry*. **270**, 25701-25708.

Beigelman, L., Karpeisky, K., and Usman, N., (1995b). Synthesis of 6-aza- & 6-methyl-pyrimidine ribonucleoside phosphoramidites and their incorporation into hammerhead ribozymes. *Nucleosides and Nucleotides*. **14**, 895-899.

Beigelman, L., Karpeisky, K., Matulic-Adamic, J., Haeberli, P., Sweedler, D., and Usman, N. (1995c). Synthesis of 2'-modified nucleotides and their incorporation into hammerhead ribozymes. *Nucleic Acids Research.* **23**, 4434-4442.

Beltinger, C., Saragovi, H.U., Smith, R.M., LeSauter, L., Shah, H., DeDionisio, L., Christensen, L., Raile, A., Jarett, L., and Gewirtz, A.M. (1995). Binding, uptake and intracellular trafficking of phosphorothioate-modified oligodeoxynucleotides. *The Journal of Clinical Investigation.* **95**, 1814-1823.

Benimetskaya, L., Loike, J., Khaled, Z., Wright, S., Kai, T., and Stein, C.A. (1997). Mac-1 (CD11b/CD18) is a cell surface oligodeoxynucleotide binding protein. *Nature Medicine.* **3**, 414-420.

Bennett, C.F. (1995). Intracellular delivery of oligonucleotides with cationic liposomes. In: Akhtar, S (ed). *Delivery strategies for antisense oligonucleotides therapeutics.* CRC Press Inc., London, U.K.

Bennett, C.F. (1998). Antisense oligonucleotides: Is the glass half full or half empty? *Biochemical Pharmacology.* **55**, 9-19.

Bennett, C.F., Chaing, M.Y., Chan, Y., Shoemaker, J.H.E and Mirabelli, C.K. (1992). Cationic lipids enhance cellular uptake and activity of phosphorothioate antisense oligonucleotides. *Molecular Pharmacology.* **41**, 1023- 1025.

Bennett, R.M. (1993). As nature intended? The uptake of DNA and oligonucleotides by eukaryotic cells. *Antisense Research and Development.* **3**, 235-241.

Bennett, R.M., Gabor, G.T., and Merritt, M.M. (1985) DNA binding to human leukocytes. *Journal of Clinical Investigation.* **76**, 2182- 2190.

Berlin, R.D. and Oliver, J.M. (1980). Characterisation of FITC-Dextran as an indicator of fluid phase pinocytosis. *Journal of Cell Biology.* **85**, 660-671.

Bertrand, E. and Rossi, J. (1994). Facilitation of hammerhead ribozyme catalysis by the nucleocapsid protein of HIV-1 and the heterogeneous nuclear ribonucleoprotein A1. *EMBO Journal.* **73**, 2904-2912.

Birikh, K.R, Heaton, P.A and Eckstein, F. (1997). The structure, function and application of the hammerhead ribozyme. *European Journal of Biochemistry.* **248**, 1-16.

Birikh, K.R., Berlin, Y.A., Soreq, H. and Eckstein, F. (1997). Probing accessible sites for ribozymes on human acetylcholinesterase RNA. *RNA*. **3**, 429-437.

Black, P.McL. (1991). Brain Tumours, Parts 1 and 2. *New England Journal of Medicine*. **324**. 1471-1476, 1555-1564.

Blackburn, E.H. (1991). Structure and function of telomeres. *Nature*. **350**, 569-573.

Blackburn, G.M. and Gait, M.J. (1990). Antisense oligonucleotide technology (Chapter 9), In: *Nucleic Acids in Chemistry and Biology*. IRL Press. Oxford, U.K, 339-377.

Blasco, M.A., Lee, H-W., Hande, M.P., Samper, E., Lansdorp, P.M., DePinho, R.A. and Greider, C.W. (1997). Telomere shortening and tumour formation by mouse cells lacking telomerase RNA. *Cell*. **91**, 25-34.

Blasco, M.A., Rizen, M., Greider, C.W. and Hanahan, D. (1996). Differential regulation of telomerase activity and telomerase RNA during multi-stage tumorigenesis. *Nature Genetics*. **12**, 200-204.

Bodnar, A.G., Ouellette, M., Frolikis, M., Holt, S.E., Chui, C-P., Morin, G.B., Harley, C.B., Shay, J.W., Lichsteiner, S., and Wright, W.E. (1998). Extension of life-span by introduction of telomerase into normal human cells. *Science*. **279**, 349-352.

Bramlage, B., Alefelder, S., Marschall, P., and Eckstein, F. (1999). Inhibition of luciferase expression by synthetic hammerhead ribozymes and their cellular uptake. *Nucleic Acids Research*. **27**, 3159-3167.

Bratty, J., Chartrand, P., Ferbeyre, G., and Cedergren, R. (1993). The hammerhead RNA domain, a model ribozyme. *Biochemica et Biophysica Acta*. **1216**. 345-359.

Broccoli, D., Young, J.W. and de Lange, T. (1995). Telomerase activity in normal and malignant hematopoitic cells. *Proceedings of the National Acadamy of Sciences, USA*. **92**, 9082-9086.

Brown, S.A. and Jarvis, T.C. (1997). Optimisation of lipid mediated ribozyme delivery to cells in culture. *Methods in Molecular Biology*. **74**, 59-68.

Brown, T. and Brown, D.J.S. (1989). Modern machine aided methods of oligodeoxynucleotide synthesis. In: Eckstein, F (ed). *Oligonucleotides and Analogues.* Oxford University Press. Oxford, U.K.

Bruner, J.M. (1994). Neuropathology of malignant gliomas. *Seminars in Oncology*, **21**, 126-138.

Buolamwini, J.K. (1999). Novel anti-cancer drug discovery. *Current Opinions in Chemical Biology*. **3**, 500-509.

Carola, C and Eckstein, F. (1999). Nucleic acid enzymes. *Current Opinion in Chemical Biology*. **3**, 274-283.

Cech, T.R. and Bass, B.L. (1986). Biological catalysis by RNA. *Annual Reviews in Biochemistry*. **55**, 599-644.

Cech, T.R. and Uhlenbeck, O.C. (1994). Hammerhead nailed down. *Nature*. **372**, 39-40.

Cech, T.R., Zaug, A.J. and Grabowski, P.J. (1981). *In vitro* splicing of the ribosomal RNA precurser of *Tetrahymena*: involvement of a guanoside nucleotide in the excision of the intervening sequence. *Cell*, **27**, 487-496.

Chadeneau, C., Siegel, P., Harley, C.B., Muller, W.J., and Bacchetti, S. (1995). Telomerase activity in normal and malignant tissues. *Oncogene*, **11**, 893-898.

Chamberlain, M.C. and Kormanik, P.A. (1998). Practical guidelines for the treatment of malignant gliomas. *West Journal of Medicine*. **168**, 114-120.

Christoffersen, R.E., McSwiggen, J., and Konings, D. (1994). Application of computational technologies to ribozyme biotechnology products. *Journal of Molecular Structure*. **311**, 273-284.

Ciardiello, F and Totora, G. (1998). Interactions between the epidermal growth factor receptor and type I protein kinase A: biological significance and therapeutic implications. *Clinical Cancer Research*. **4**, 821-828.

Cluoet-D'Orval, B. and Uhlenbeck, O.C. (1996). Kinetic characterisation of I/II format hammerhead ribozymes. *RNA*. **2**, 483-491.

Cohn, Z.A. and Ehrenreich, B.A. (1969). The uptake, storage and intracellular hydrolysis of carbohydrates by macrophages. *The Journal of Experimental Medicine*. **129**, 201-255.

Collins, R.A. and Olive, J.E. (1992). Reaction conditions and kinetics of self cleavage of a ribozyme derived from *Neurospora* VS RNA. *Biochemistry*. **32**, 2794-2799.

Coulson, J.M., Poyner, D.R., Chantry, A., Irwin, W.J. and Akhtar, S. (1996). A non-antisense sequence-selective effect of a phosphorothioate oligodeoxynucleotide directed against the epidermal growth factor receptor in A431 cells. *Molecular Pharmacology*. **50**, 314-325.

Crooke, S.T. (1992) Therapeutic applications of oligonucleotides. *Annual Review of Pharmacology*. **32**, 329-379.

Dahm, S.C., Derrick, W.B. and Uhlenbeck, O.C. (1993). Evidence for the role of a solvated metal hydroxide in the hammerhead cleavage mechanism. *Biochemistry*. **32**, 13040-13045.

Dash, P., Lotan, I., Knapp, M., Kandel, E.R., and Goelet, P. (1987). Selective elimination of mRNAs in vivo: complementary oligodeoxynucleotides promote RNA degradation by an Rnase H-like activity. *Proceedings of the National Academy of Sciences, USA*. **84**, 7896-7900.

Davies, D.E. and Chamberlin, S.G. (1996). Targeting the Epidermal Growth Factor Receptor for therapy of carcinomas. *Biochemical Pharmacology*. **51**, 1101-1110.

De Lange, T and Jacks, T. (1999). For better or worse? Telomerase inhibition and cancer. *Cell*. **98**, 273-275.

Denman, R.B. (1993). Using RNAFOLD to predict the activity of small catalytic RNAs. *Biotechniques*. **15**, 1090-1094.

Desjardins, J.P., Sproat, B.S., Beijer, B., Blaschke, M., Dunkel. M., Gerdes, W., Ludwig, J., Reither, V., Rupp, T and Iverson, P.L. (1996). Pharmacokinetics of a synthetic, chemically modified hammerhead ribozyme against the rat cytochrome P-450 3A2 mRNA after single intravenous injections. *The Journal of Pharmacology and Experimental Therapeutics*. **278**, 1419-1427.

Downward, J., Yarden, E., Mayes, G., Scrace, N., Totty, P., Stockwell, A., Ullrich, J., Schlessinger I and Waterfield, M.D. (1984). Close similarity of epidermal growth factor receptor and V-erbB oncogene protein sequences. *Nature*. **307**, 521-527.

Duncan, V.E. Ajmani, P.S. and Hughes, J.A. (1998). Cellular delivery is a major obstacle for oligodeoxynucleotide inhibition of telomerase activity. *Anticancer Research*. **18**, 4105-4108.

Eastman, S.J., Siegel, C., Tousignant, J., Smith, A.E., Cheng,S.H., and Scheule, R.K. (1997). Biophysical characterization of cationic lipid:DNA complexes. *Biochimica et Biophysica Acta*. **1325**. 41-62.

Eckstein, F. (1985). Nucleoside phosphorothioates. *Annual Reviews of Biochemistry*, **54**, 367-402.

Elkins, D.A. and Rossi, J.J. (1995). Cellular delivery of ribozymes. In: Akhtar, S (ed). *Delivery Strategies for Antisense Oligonucleotide Therapeutics*. CRC Press Inc., London, UK. 17-37.

Endicott, J.A. and Ling, V (1989). The biochemistry of P-glycoprotein-mediated drug resistance. *Annual Reviews in Biochemistry*. **58**, 137-171.

England, T.E., Gumport, R.L. and Uhlenbeck, O.C. (1977). Nucleoside pyrophosphates are substrates for T4-induced RNA ligase. *Proceedings of the National Academy of Sciences, USA*. **74**, 4839-4842.

Falchetti, M.L., Pallini, R., Larocca, L.M., Verna, R., and D'Ambrosio, E. (1999). Telomerase expression in intracranial tumours: prognostic potential for malignant gliomas and meningliomas. *Journal of Clinical Pathology*. **52**, 234-236.

Farhood, H., Serbina, N., and Huang, L. (1995). The role of dioleoyl-phosphatidylethanolamine in cationic liposome mediated gene transfer. *Biochimicia et Biophysica Acta*. **1235**, 289-295.

Fedor, M.J. and Uhlenbeck, O.C. (1992). Kinetics of intermolecular cleavage by hammerhead ribozymes. *Biochemistry*, **31**, 12042-12054.

Feldkemo, M.M., Lau, N and Guha, A. (1997). Signal transduction pathways and their relevance in human astrocytomas. *Journal of Neurooncology*. **35**, 223-248.

Fell, P.L., Hudson, A.J., Reynolds, M.A., Usman, N and Akhtar, S. (1997). Cellular uptake properties of a 2'-amino / 2'-O-methyl- modified chimeric hammerhead ribozyme targeted to the epidermal growth factor receptor. *Antisense and Nucleic Acid Drug Development*. 7, 319-326.

Fenstermaker, R.A., Capala, J., Barth, R.F., Hujer, A., Kung, H-J., and Kaetzel, D.M. (1995). The effect of epidermal growth factor receptor (EGFR) expression on in vivo growth of rat C6 glioma cells. *Leukemia*. **9**, S106-S112.

Feng, J., Funk, W.D., Wang, S.S., Weinrich, S.L. Avilion, A.A., Chiu, C.P., Adams, R.R., Chang, E., Allsopp, R.C., Yu, J., Le, S., West, M.D., Harley, C.B., Andrews, W.H., Greider, C.W., and Villeponteau, B. (1995). The RNA component of human telomerase. *Science*. **69**, 1236-1241.

Ferscht, A. *(1977)* The basic equation of enzyme kinetics. In*: Enzyme Structure and Mechanism*. Ferscht, A (ed.), W.H. Freeman and Company, Belfast University Press, U.K.

Filion, M.C., and Phillips, N.C. (1997). Toxicity and immunomodulatory activity of liposomal vectors formulated with cationic lipids toward immune effector cells. *Biochimica et Biophysica Acta*. **1329**. 345-356.

Filmus, J., Pollak, M., Cairncross, J.G., and Buick, R.N. (1985). Amplified, overexpressed and rearranged epidermal growth factor receptor gene in a human astrocytoma cell line. *Biochemical and Biophysical Research Communications*. **131**: 207-215.

Flory, C.M., Pavco, P.A., Jarvis, T.C., Lesch, M.E., Wincott, F.E., Beigelman, L., Hunt, S.W., and Schrier, D.J. (1996). Nuclease-resistant ribozymes decrease stromelysin mRNA levels in rabbit synovium following exogenous delivery to the knee joint. *Proceedings of the National Academy of Sciences, USA*. **86**, 6454-6458.

Forster, A.C and Symons, R. (1987). Self cleavage of plus and minus strand RNAs of a virusoid and a structural model for the active sites. *Cell*. **49**, 211-220.

Freshney, R.I. (1992). Measurement of viability and cytotoxicity. In*: Animal Cell Culture, A Practical Approach*. Second Edition. IRL Press, Oxford, U.K.

Fry, D.W. (1999). Inhibition of the epidermal growth factor receptor family of tyrosine kinases as an approach to cancer chemotherapy: progression from reversible to irreversible inhibitors. *Pharmacological Therapies*. **82**, 207-218.

Fu, D.J. and McLaughlin, L.W. (1992). Importance of specific purine amino and hydroxyl groups for efficient cleavage by a hammerhead ribozyme. *Proceedings of the National Acadamy of Sciences, USA*. **89**, 3985-3989.

Furnari, F.B., Huang, H-J.S, and Cavenee, W.K. (1995). Genetics and malignant progression of human brain tumours. *Cancer Surveys*. **25**, 233-275.

Gait, M.J. Grasby, J.A., Karn, J., Mersmann, K., and Pritchard, C.E. (1995). Synthetic ribonucleotides analogues specific for RNA structure-function studies. *Nucleosides and Nucleotides*. **14**, 1133-1144.

Gao, W.Y., Storm, C., Egan, J.S., and Chengo, Y.C. (1993). Cellular pharmacology of phosphorothioate homooligodeoxynucleotides in human cells. *Molecular Pharmacology*. **43**, 45-50.

Gaughan, D.J. and Whitehead, A.S. (1999). Function and biological applications of catalytic nucleic acids. *Biochimica et Biophysica Acta*. **1445**, 1-20.

Gewirtz, A.M., Sokol, D.L., and Ratajczak, M.Z. (1998). Nucleic acid therapeutics: State of the art and future prospects. *Blood*. **92**, 712-736.

Gerwitz, A.M., Stein, C.A. and Glazer, P.M., (1996). Facilitating oligonucleotide delivery: helping antisense deliver on its promise. *Proceedings of the National Academy of Sciences, USA*. **93**, 3161-3163.

Geselowitz, D.A. and Neckers, L.M. (1995). Bovine serum albumin is a major oligonucleotide-binding found on the surface of cultured cells. *Antisense Research and Development*. **5**, 213-217.

Giannini, C.D., Roth, W.K., Piiper, A., and Zeuzem, S. (1999). Enzymatic and antisense effects of a specific anti-Ki-ras ribozyme in vitro and in cell culture. *Nucleic Acids Research*. **27**, 2737-2744.

Gill, G.N. and Lazar, C.S. (1981). Increased phosphotyrosine content and inhibition of proliferation of EGF-treated A431 cells. *Nature*. **392**. 305-307.

Gish, G and Eckstein, F. (1989). Phosphorothioates in molecular biology. *Trends in Biochemical Sciences*. **14**, 97-100.

Goodarzi, G., Watabe, M., and Watabe, K. (1991). Binding of oligonucleotides to cell membranes at acidic pH. *Biochemical and Biophysical Research Communications*. **181**, 1343-1351.

Goodchild, J. (1992). Enhancement of ribozyme catalytic activity by a contiguous oligodeoxynucleotide (facilitator) and by 2'-O-methylation. *Nucleic Acids Research*, **20**, 4607-4612.

Griffiths, A.D., Potter, B.V.L., and Eperon, I.C. (1987). Stereospecificity of nucleases towards phosphorothioate- substituted RNA; stereochemistry of transcription by T7 RNA polymerase. *Nucleic Acids Research*. **15**, 4145-4162.

Griffiths, B. (1992). Scaling up of animal cell cultures. In; Freshney, R.I. (ed). *Animal Cell Culture, A Practical Approach*. IRL Press, Oxford, U.K.

Gu, J-L., Nadler, J and Rossi, J. (1997). Use of a hammerhead ribozyme with cationic liposomes to reduce leukocyte type 12-lipooxygenase expression in vascular smooth muscle. *Molecular and Cellular Biochemistry*. **172**, 47-57.

Guo, H.C.T and Collins, R.A. (1995). Efficient trans-cleavage of a stem loop RNA substrate by a ribozyme derived from Neurospora VS RNA. *EMBO Journal*. **14**, 368.

Guerrier-Takada, C.D.A, Gardiner, K., Marsh, T., Pace, N., and Altman, S. (1983). The RNA moiety of ribonuclease P is the catalytic subunit of the enzyme. *Cell*, **35**, 849-857.

Hackel, P.O., Zwick, E., Prenzel, N., and Ullrich, A. (1999). Epidermal growth factor receptors: critical mediators of multiple receptor pathways. *Current Opinion in Cell Biology*. **11**, 184-189.

Hacker, H., Mischak, H., Miethke, T., Liptay, S., Scmid, R., Sparwasser, T., Heeg, K., Lipford, G.B., and Wagner, H. (1998). cpG-DNA-specific activation of antigen-presenting cells requires stress kinase and is preceded by non-specific endocytosis and endosomal maturation. *EMBO Journal*. **17**, 6230-6240.

Haigler, H., Ash, J.F., Singer, S.J. and Cohen, S. (1978). Visualisation by fluorescence of the binding and internalisation of epidermal growth factor in human carcinoma cells. *Proceedings of the National Academy of Sciences, USA*. **75**, 3317-3321.

Hampel, A. (1998). The hairpin ribozyme: Discovery, Two dimensional model and development for gene therapy. *Progress in Nucleic Acid Research and Molecular Biology*. **58**, 1-39.

Hampel, A., Tritz, R., Hicks, M., and Cruz, P. (1990). "Hairpin' catalytic RNA model: Evidences for helices and sequence requirement for the substrate RNA. *Nucleic Acids Research*. **18**, 299-304.

Han, Y., Caday, C.G., Nanda, A., Cavenee, W.K., and Su Huang, H-J. (1996). Tyrphostin AG 1478 preferentially inhibits human glioma cells expressing truncated rather than wild-type epidermal growth factor receptors. *Cancer Research*. **56**, 3859-3861.

Hanss, B., Leal-Pinto, E., Bruggeman, L.A., Copeland, T.D., and Klotman, P. (1998). Identification and characterisation of a cell membrane nucleic acid channel. *Proceedings of the National Academy of Sciences, USA*. **95**, 1921-1926.

Harley, C.B., Futcher, A.B., and Greider, C.W. (1990). Telomeres shorten during aging of human fibroblasts. *Nature*. **345**, 458-460.

Harrington, L., Zhou, W., McPhail, T., Oulton, R., Yeung, D.S., Mar, V., Bass, M.B., and Robinson, M.O. (1997). Human telomerase contains evolutionary conserved catalytic and structural subunits. *Genes Development*. **11**, 3109-3115.

Haseloff, J. and Gerlach, W.L. (1988). Simple RNA enzymes with new and highly specific endoribonuclease activities. *Nature*. **334**, 585-591.

Hawley, P and Gibson, I. (1996). Interaction of oligonucleotides with mammalian cells. *Antisense and Nucleic Acid Drug Development*. **6**, 185-195.

Heidenreich, O., Beneseler, F., Fahrenholtz, A., and Eckstein, F. (1994). High activity and stability of hammerhead ribozymes containing 2'-modified pyrimidine nucleosides and phosphorothioates. *Journal of Biological Chemistry*. **269**, 2131-2138.

Heidenreich, O., Pieken, W. and Eckstein, F. (1993). Chemically modified RNA: approaches and applications. *The FASEB Journal*, **7**, 90-96.

Heidenreich, O., Xu, X., Swiderski, P., Rossi, J.J., and Nerenberg, M. (1996a). Correlation of activity with stability of chemically modified ribozymes in nuclei suspension. *Antisense and Nucleic Acid Drug Development.* **6**, 111-118.

Heidenreich, O., Xu, X and Nerenberg, M. (1996b). A hammerhead ribozyme cleaves its target RNA during RNA preparation. *Antisense and Nucleic Acid Drug Development.* **6**, 141-144.

Helene, C and Toulme, J-J. (1990). Specific regulation of gene expression by antisense, sense and antigene nucleic acids. *Biochimica et Biophysica Acta.* **1049**, 99-125.

Henry, P. and Mecca, M.J. (1995). A comparison of the in vitro activity of DNA- armed and all RNA hammerhead ribozymes. *Nucleic Acids Research*, **23**, 3928-3936.

Hendry,P., McCall, M.J., Santiago, F.S. and Jennings, P.A. (1995). In vitro activity of minimised hammerhead ribozymes. *Nucleic Acids Research.* **23**, 3922-3927.

Herschlag, D., Khosla, M., Tsuchihashi, Z., and Karpel, R.L. (1994). An RNA chaperone activity of non-specific RNA binding proteins in hammerhead ribozyme catalysis. *EMBO Journal.* **13**, 2913-2924.

Hertel, K.J., Herschlag, D., and Uhlenbeck, O.C. (1994). A kinetic and thermodynamic framework for the hammerhead ribozyme reaction. *Biochemistry.* **33**, 3374-3385.

Hertel, K.J., Herschlag, D. and Uhlenbeck, O.C. (1996). Specificity of hammerhead ribozyme cleavage. *EMBO Journal.* **15**, 3751-3757.

Hertel, K.J., Pardi., A., Uhlenbeck, O.C., Koizumi, M., Ohtsuka, E., Uesugi, S., Cedergren, R., Eckstein, F., Gerlach, W.L., Hodgson, R., and Symons, R.H. (1992). Numbering system for the hammerhead. *Nucleic Acids Research.* **20**, 3252.

Hertel, K.J., Stage-Zimmermann, T.K., Ammons, G., and Uhlenbeck, O.C. (1998). Thermodynamic dissection of the substrate-ribozyme interaction in the hammerhead ribozyme. *Biochemistry.* **37**, 16983-16988.

Hodes, R.J. (1999). Telomere length, ageing and somatic cell turnover. *Journal of Experimental Medicine.* **190**, 153-156.

Hoi Sang, U., Espiritu, O.D., Kelley, P.Y., Klauber, M.R. and Hatton, J.D. (1995a). The role of the epidermal growth factor receptor in human gliomas: I. The control of cell growth. *Journal of Neurosurgery*. **82**, 841-846.

Hoi Sang, U., Espiritu, O.D., Kelley, P.Y., Klauber, M.R. and Hatton, J.D. (1995b). The role of the epidermal growth factor receptor in human gliomas: II. The control of glial process extension and the expression of glial fibrillary acidic protein. *Journal of Neurosurgery*. **82**, 847-857.

Homann, M., Tabler, M., Tzortzakaki, S., and Sczakiel, G (1994). Extension of helix II of an HIV-1 directed hammerhead ribozyme with long antisense flanks does not alter kinetic parameters in vitro but causes loss of inhibitory potential in living cells. *Nucleic Acids Research*. **22**, 3951-3957.

Hope, M.J., Mui, B., Ansell, S and Ahkong, Q.F. (1998). Cationic lipids, phosphatidylethanolamine and the intracellular delivery of polymeric, nucleic acid-based drugs (review). *Molecular Membrane Biology*. **15**, 1-14.

Hudson, A.J., Lewis, K.J., Rao, V.M., and Akhtar, S. (1996). Biodegradable polymer matrices for the sustained exogenous delivery of a biologically active c-myc hammerhead ribozyme. *International Journal of Pharmaceutics*. **136**, 23-29.

Hudson, A.J., Normand, N., Ackroyd, J., and Akhtar, S (1999). Cellular delivery of hammerhead ribozymes conjugated to a transferrin receptor antibody. *International Journal of Pharmaceutics*. **182**, 49-58.

Hughes, J., Avroutskaya, A., Sasmor, H.M., Guinosso, C.K., Cook, P.D., and Juliano, R.L. (1995). Oligonucleotide transport across membranes and into cells: Effects of chemical modifications. In: Akhtar, S. (ed). *Delivery Strategies for Antisense Oligonucleotide Therapeutics*. CRC Press Inc., London, U.K.

Iverson, P., Zhu, S., Meyer, A. and Zon, G. (1992). Cellular uptake and subcellular distribution of phosphorothioate oligonucleotides into cultured cells. *Antisense Research and Development*. **2**, 211-222.

Jaeger, J .A. Turner, D.H., and Zuker, M. (1989). Improved predictions of secondary structures for RNA, *Proceedings of the National Academy for Sciences, USA*. **86**, 7706-7710.

Jaaskelainen, I., Monkkonen, J and Urtti, A. (1994). Oligonucleotide-cationic liposome interactions. A physicochemical study. *Biochimica et Biophysica Acta.* **1195**, 115-123.

Jaaskelainen, I., Sternberg, B., Monkkonen, J and Urtti, A. (1998). Physicochemical and morphological properties of complexes made of cationic liposomes and oligonucleotides. *International Journal of Pharmaceutics.* **167**, 191-123.

James, H.A., and Gibson, I. (1998). The therapeutic potential of ribozymes. *Blood.* **91**, 371-382.

James, H., Mills, K., and Gibson, I. (1996). Investigating and improving the specificity of ribozymes directed against the bcr-abl translocation. *Leukemia.* **10**, 1054-1064.

Jarvis, T.J., Alby, L.J., Beaudry, A.A., Wincott, F.E., Beigelman, L., McSwiggen, J.A., Usman, N and Stinchcomb, D.T. (1996). Inhibition of Vascular Smooth Muscle cell proliferation by ribozymes that cleave c-myb mRNA. *RNA.* **2**, 419-428.

Jarvis, T.C., Wincott, F.E., Alby, L.J., McSwiggen, J.A., Beigelman, L., Gustofson, J., DiRenzo, A., Levy, K., Arthur, M., Matulac-Damic, J., Karpeisky, A., Gonzalez, C., Woolf, T.M., Usman, N and Stinchcomb, D.T. (1996b). Optimizing the cell efficacy of synthetic ribozymes. *Journal of Biological Chemistry.* **271**, 29107-29112.

Joyce, G.F. (1998). Nucleic acid enzymes: playing with a fuller deck. *Proceedings of the National Academy of Sciences, USA.* **95**, 5845-5847.

Juliano, R.L. and Akhtar, S. (1992). Liposomes as a drug delivery system for antisense oligonucleotides. *Antisense Research and Development.* **2**, 165–176.

Kanazawa, Y., Ohkawa, K., Ueda, K., Mita, E., Takehara, T., Sasaki, Y., Kasahara, A and Hayashi, N. (1996). Hammerhead ribozyme-mediated inhibition of telomerase activity in extracts of human hepatocellular carcinoma cells. *Biochemical and Biophysical Research Communications.* **225**, 570-576.

Kariko, K. Megyeri, K., Xiao, Q., and Barnathan, E.S. (1994). Lipofectin-aided cell delivery of ribozyme targeted to human urokinase receptor mRNA. *FEBS letters*, **352**, 41-44.

Kawamoto, T., Sato, J.D., Le, A., Polikoff, J., Sato, G.H., and Mendelsohn, J. (1983). Growth stimulation of A431 cells by epidermal growth factor: Identification of high-affinity receptors for epidermal growth factor by an anti-receptor monoclonal antibody. *Proceedings of the National Academy of Sciences*, USA. **80**, 1337-1431.

Khazaie, K., Schirrmacher, V and Lichter, R.B. (1993). EGF receptor in neoplasia and metastasis. *Cancer Metastasis Reviews*. **12**, 255-274.

Kiaris, H. and Schally, A.V. (1999). Decrease in telomerase activity in U87-MG human glioblastomas after treatment with an antagonist of growth hormone-releasing hormone. *Proceedings of the National Academy of Sciences, USA*. **96**, 226-231.

Kiehntopf, M., Brach, M., Licht, T., Petscauer, S., Karawajew, L., Kirschning, C., and Herrmann, F. (1994). Ribozyme mediated cleavage of the Mdr-1 transcript restores chemosensitivity in previously resistant cancer cells. *EMBO Journal*, **13**, 4645-4652.

Kilpatrick, M.W., Phylactou L.A., Godfrey, M., Wu, C.H., and Wu, G.Y. (1996). Delivery of a hammerhead ribozyme specifically down regulates the production of fibrillin-1 by cultured dermal fibroblasts. *Human Molecular Genetics*. **5**, 1939-1944.

Kim, N.W., Piatyszek, M.A., and Prowse, K.R. (1994). Specific association of human telomerase activity with immortal cells and cancer. *Science*. **266**, 2011-2015.

Kindo, Y., Kondo, S., Tanaka, Y., Haqqi, T., Barna, B.P., and Cowell, J.K. (1998). Inhibition of telomerase increases the susceptibility of human glioblastoma cells to cisplatin-induced apoptosis. *Oncogene*. **16**, 2243-2248.

King, A.C., Willis, R.A., and Cuatrecasas, P. (1980). Accumulation of epidermal growth factor within cells does not depend on receptor cycling. *Biochemical and Biophysical Research Communications*. **97**, 840-845.

Kisich, K.O., Stecha, P.F., Harter, H.A. and Stinchcomb, D.T. (1995). Inhibition of TNF secretion by murine macrophages following in vivo and in vitro ribozyme treatment. *The Journal of Cellular Biochemistry*. **19A**, 291.

Kisich, K.O., Malone, R.W., Feldstein, P.A., and Erikson, K.L. (1999). Specific inhibitions of macrophage TNF-alpha expression by in-vivo ribozyme treatment. *Journal of Immunology*. **163**, 2008-2016.

Kitajima, I., Shinohara, T., Minor, T., Bibbs, L., Bilakovic S.J. and Nerenberg, M. (1992). Human T-Cell Leukaemia Virus Type-1 tax transformation is associated with increased uptake of oligonucleotides in vitro and in vivo. *The Journal of Biological Chemistry*. **267**, 25881- 25888.

Konopka, K., Rossi, J.J., Swiderski, P, Slepushkin, V.A., and Duzgunes, N. (1998). Delivery of an anti-HIV-1 ribozyme into HIV-infected cells via cationic liposomes. *Biochimica et Biophysica Acta*. **1372**, 55-68.

Kore, A.R., Vaiah, N.K., Kutzke, U, and Eckstein, F. (1998). Sequence specificity of the hammerhead ribozyme revisited; the NHH rule. *Nucleic Acids Research*. **26**, 4116-4120.

Krieg, A.M. and Stein, C.A. (1995). Phosphorothioate oligodeoxynucleotides: Antisense or anti-protein? *Antisense Research and Development*. **5**, 241.

Krieg, A.M., Love-Homan, L., Yi, A.K. and Harty, J.T. (1998). CpG DNA induces sustained IL-12 expression in vivo and resistance to Listeria monocytogenes challenge. *Journal of Immunology*. **161**, 2428-2434.

Kruger, M., Beger, C. and Wong-Staal, F. (1999). Use of ribozymes to inhibit gene expression. *Methods in Enzymology*. **306**, 207-225.

Kurpad, S.N., Zhao, X-G., Wikstrand, C.J., Batra, S.K., McLendon, R.E., and Bigner, D.D. (1995). Tumour antigens in astrocytic gliomas, *GLIA*. **15**, 244-256.

Lange, W., Cantin, E.M., Finke, J., and Dolken, G. (1994). In vitro and In vivo effects of synthetic ribozymes targeted against BCR / ABL mRNA. *Leukemia*, **7**,1786-1794.

Langford, L.A. (1996). Telomerase activity in brain tumours. *Lancet*. **346**, 1267-1268.

Lappalainen, K., Miettinen, R., Kellokoski, J., Jaaskelainen, I. and Syrjanen, S. (1997). Intracellular distribution of oligonucleotides delivered by cationic liposomes: Light and electron microscopic study. *The Journal of Histochemistry and Cytochemistry*. **45**, 265-274.

Le, S., Zhu,.J., Anthony, D.C., Greider, C.W., and Black, P.M. (1998). Telomerase activity in human gliomas. *Neurosurgery*. **42**, 1120-1124.

Leopold, L.H., Shore, S.K., Newkirk, T.A., Reddy, R.M., and Reddy, E.P. (1995). Multi-unit ribozyme mediated cleavage of bcr-abl mRNA in myeloid leukaemias. *Blood.* **85**, 2162-2170.

Lesser, G.L. and Grosman, S. (1994). The chemotherapy of high grade astrocytomas. *Seminars in Oncology.* **21**, 220-235.

Levis, J.T., Butler, W.O., Tseng, B.Y. and Tso, P.O.P. (1995). Cellular uptake of oligodeoxyribonucleoside methylphosphonates. *Antisense Research and Development.* **5**, 251-259.

Lewis, J.G., Lin, K-Y., Kothvale, A., Flanagan, W.M., Matteuchi, M.D., DePrince, R.B., Mook, R.A., Hendren, R.W. and Wagner, R. (1996). A serum-resistant cytofectin for cellular delivery of antisense oligodeoxynucleotides and plasmaid DNA. *Proceedings of the National Academy of Sciences, USA.* 93, 3176-3181.

Li, Y and Breaker, R.B. (1999). Deoxyribozymes: new players in the ancient game of biocatalysis. *Current Opinions in Structural Biology.* **9**, 315-323.

Loke, S.L., Stein, S.L., Zhang, X.H., Mori, K., Nakanisdhi, M., Subasinghe, C., Cohen, J., and Neckers, L.M. (1989). Characterization of oligonucleotide transport into living cells. *Proceedings of the National Academy of Sciences, USA.* **86**, 3474-3478.

Louis, D.N. and Gusella, J.F. (1995). A tiger behind many doors: multiple genetic pathways to malignant glioma. *Trends in Genetics.* **11**, 412-415.

Ludwig, J., Blaschke, M., and Sproat, B.S. (1998). Extending the cleavage rules for the hammerhead ribozyme: mutating adenosine$^{15.1}$ to inosine$^{15.1}$ changes the cleavage site specificity from $N^{16.2}U^{16.1}H^{17}$ to $N^{16.2}C^{16.1}H^{17}$. *Nucleic Acids Research.* **26**, 2279-2285.

Lyngstadaas, S.P., Risnes, S., Sproat, B.S., Thrane, P.S. and Prydz, H.P. (1995). A synthetic, chemically modified ribozyme eliminates amelogenin, the major translation product in developing mouse enamel in vivo. *EMBO Journal.* **14**, 5224-5229.

McKenzie, K.E., Umbricht, C.B. and Sukumar, S. (1999). Application of telomerase research in the fight against cancer. *Molecular Medicine Today.* **5**, 114-122.

Macejak, D.G., Lin, H., Webb, S., Chase, J., Jensen, K., Jarvis, T.C., Leiden, J.M. and Couture, L. (1999). Adenovirus-mediated expression of a ribozyme to c-myb mRNA inhibits smooth muscle cell proliferation and neointima formation in vivo. *Journal of Virology*. **73**, 7745-7751,

Mackay, S.L., Tannahill, C.L., Auffenber, T., Ksontini, R., Copeland, E.M. and Moldawer, L.L. (1999). Characterisation in vitro and in vivo of hammerhead ribozymes directed against murine tumor necrosis factor alpha. *Biochemical and Biophysical Research Communications*. **260**, 390-397.

Macpherson, J.L., Ely, J.A., Sun, L-Q, and Symonds, G.P. (1999). Ribozymes in gene therapy of HIV-1. *Frontiers in Bioscience*. **4**, 497-505.

Marshall, W.S. and Caruthers, M.H. (1993). Phosphorothioate DNA as a potential therapeutic drug. *Science*. **259**, 1565-1569.

Marschall, P., Thomson, J.B., and Eckstein, F. (1994). Inhibition of Gene Expression with Ribozymes. *Cellular and Molecular Neurobiology*. **14**. 523-538.

Martuza, R.L., Malick, A., Markert, J M., Ruffner, K.L., and Cohen, D.M. (1991). Experimental therapy of human glioma by means of a genetically engineered virus mutant. *Science*. **252**, 854-855.

Masuda,Y., Kobayashi, H., Holland, J.F., and Ohnuma, T. (1998). Reversal of multidrug resistance by a liposome-MDR1 ribozyme complex. *Cancer Chemotherapy and Pharmacology*. **42**, 9-16.

Mendelsohn, J. (1997). Epidermal growth factor receptor inhibition by a monoclonal antibody as anticancer therapy. *Clinical Cancer Research*. **3**, 2703-2707.

Meyerson, M., Counter, C.M., Eaton, E.N., Elisen, L.W., Steiner, P., Caddle, S.D., Ziagura, L., Beijersbergen, R.L., Davidoff, M.J., Liu, Q.Y., Bachetti, S., Haber, D.A., and Weinberg, R.A. (1997). hEST 2, the putative human telomerase catalytic subunit gene is upregulated in tumour cells during immortalisation. *Cell*. **90**, 785-795.

Middleton, T., Herlihy, W.C.; Schimmel, P.R and Munro, H.N. (1985). Synthesis and purification of oligoribonucleotides using T4 RNA ligase and reverse-phase chromatography. *Analytical Biochemistry*. **144**, 110-117.

Miller, W.A., Hercus, T., Waterhouse, P.M., and Gerlach, W.L. (1991). A satellite RNA of barley yellow dwarf virus contains a novel hammerhead structure in the self cleaving domain. *Virology*. **183**, 711-720.

Milligan, J.F., Matteucci, M.D. and Martin, J.C. (1993). Current concepts in antisense drug design. *The Journal of Medicinal Chemistry*. **36**, 1923 – 1931.

Mills, K.I., Walsh, V., Gilkes, A.F., Goringe, A., Twomey, C., James, H.A., and Gibson, I (1996). In vitro ribozyme treatment of 32D cells expressing a BCR-ABL construct prolongs the survival of SCID mice. *Blood*. **88**, 577a.

Milner, N., Mir, K.U., and Southern, E.M. (1997). Selecting effective antisense reagents on combinatorial oligonucleotide arrays. *Nature Biotechnology*. **15**, 537-541.

Modjtahedi, H., and Dean, C. (1994). The receptor for EGF and its ligands: expression, prognostic value and target for therapy in cancer (review). *The International Journal of Oncology*. **4**, 277-296.

Moghal, N and Sternberg, P.W. (1999). Multiple positive and negative regulators of signalling by the EGF-receptor. *Current opinions in Cell Biology*. **11**, 190-196.

Monia, B.P., Johnston, J.F., Geiger, T., Muller, M., and Fabbro, D. (1996). Antitumor-activity of a phosphorothioate antisense oligodeoxynucleotide targeted against c-raf kinase. *Nature Medicine*. **2**, 668-675.

Morvan, F; Bernard, R. and Imbach, J.L. (1990). Modified oligonucleotides. Solid phase synthesis and preliminary evaluation of phosphorothioate RNA as potential antisense agents. *Tetrahedron Letters*, **31**, 7149-7152.

Murray, J.B. Terwey, D.P., Karpeisky, A., Usman, N., Beigelman, L., and Scott,W.G. (1998). The structural basis of hammerhead ribozyme self-cleavage. *Cell*. **92**, 665-673.

Naasani, I, Seimiya, H, Yamori, T, and Tsuruo, T (1999). FJ5002: a potent telomerase inhibitor identified by exploiting the disease-oriented screening program with COMPARE analysis. *Cancer Research*. **59**, 4004-4011.

Nakai, D., Seita, T., Terasaki, T., Iwasa, S., Shoji, S., Mizushima, Y and Sugiyama, Y. (1996). Cellular uptake mechanism for oligonucleotides: Involvement of endocytosis in the uptake of phosphodiester oligonucleotides by a human colorectal adenocarcinoma cell line, HCT-15. *The Journal of Pharmacology and Experimental Therapeutics*. **278**, 1362-1372.

Nakamura, T.M., Morin, G.B., Chapman, K.B., Weinrich, S.L., Andrews, W.H., Lingner, J., Harley, C.B. and Cech, T.R. (1997). Telomerase catalytic subunit homologs from fission yeast and human. *Science*. **277**, 955-959.

Noonberg, S.B., Garovoy, M.R., and Hunt, C.A. (1993). Characteristics of oligonucleotide uptake in human keratinocyte culture. *Journal of Investigative Dermatology*. **101**, 727- 731.

Norton, J.C., Piatysek, M.A., Wright, W.E., Shay, J.W. and Corey, D.R. (1996). Inhibition of human telomerase activity by peptide nucleic acids. *Nature Biotechnology*. **14**, 615-619.

O'Rouke, D.M., Zhang, X and Greene, M.I. (1997). Principles of receptor-mediated inhibition of erbB family receptor kinases: prospects for new therapies for human cancers. *Proceedings of the Association of American Physicians*. **109**, 209-219.

Ohta, Y., Kijima, H., Ohkawa, T., Kashani-Sabet, M. and Scanlon, K.J. (1996). Tissue-specific expression of an anti-ras ribozyme inhibits proliferation of human malignant melanoma. *Nucleic Acids Research*. **24**, 938-942.

Olsen, D.B., Benseler, F., Aurup,H., Pieken, W.A., and Eckstein, F. (1991). Study of a hammerhead ribozyme containing 2'-modified adenosine residues. *Biochemistry*, **31**, 9735-9741.

Ostrowski, L.E., Bigner, S.H., Humphrey, P.A. and Bigner, D.D. (1994). Genetic alterations and gene expression in human malignant gliomas. In: Pretlow, G., and Pretlow, T.P. (ed). *Biochemical and Molecular Aspects of Selected Cancers*. San Diego, Academic Press, 143-168.

Paolella, G., Sproat, B.S., and Lamond, A.I. (1992). Nuclease resistant ribozymes with high catalytic activity. *The EMBO Journal*. **11**, 1913-1919.

Parkinson, E.K. (1996). Do telomerase antagonists represent a novel anti-cancer strategy? *British Journal of Cancer*. **73**, 1-4.

Parry, T.J., Cushman, C., Gallegos, A.M., Agrawal, A.B., Richardson, M., Andrews, L.E., Maloney, L., Mokler, V.R., Wincott, W., and Pavco, P.A. (1999). Bioactivity of anti-angiogenic ribozyme targeting Flt-1 and KDR mRNA. *Nucleic Acids Research*. **27**, 2569-2577.

Perreault, J.P., Wu, T., Cousineau, B., Ogilvie, K.K., and Cedergren, R.J. (1990). Mixed deoxyribo and ribooligonucleotides with catalytic activity. *Nature*. **334**, 56.

Perriman, R., Breuning, G., Dennis, E.S., and Peacock, W.J. (1995). Effective ribozyme delivery in plant cells. *Proceedings of the National Academy of Sciences, USA*. **92**, 6175-6179.

Perriman, R., Delves, A., and Gerlach, W.L. (1992). Extended target-site specificity for a hammerhead ribozyme. *Gene*. **113**, 157-163.

Pieken, W.A., Olsen, D.B., Benseler, F., Aurup, H., and Eckstein, F. (1991). Kinetic characterization of ribonuclease resistant 2'-O-modified hammerhead ribozymes. *Science*. **253**, 314-317.

Pierga, J.Y and Magdelenat, H (1994) Applications of antisense oligonucleotides in oncology. *Cellular and Molecular Biology*. **40**, 237-261.

Pley, H.W., Flaherty, K.M. and McKay,D.B. (1994). Three-dimensional structure of a hammerhead ribozyme. *Nature*. **372**, 68-74.

Ponten, J and Macintyre, E.H. (1968). Long term culture of normal and neoplastic human glia. *Acta Pathology and Microbiology Scandinavia*. **74**, 465-486.

Puttaraju, M., Perrotta, A.T., and Been, M.D. (1993). A circular trans acting hepatitis delta virus ribozyme. *Nucleic Acids Research*. **21**, 4253-4258.

Raschke, W.C., Baird, S., Ralph, P. and Nakoinz, I. (1978). Functional macrophage cell lines transformed by Abelson Leukemia Virus. *Cell*. **15**, 261-267.

Rasheed, B.K., Wiltshire, R.N., Bigner, S.H., and Bigner, D.D. (1999). Molecular pathogenesis of malignant gliomas. *Current Opinions in Oncology*. **11**, 162-167.

Reddy, D.S. (1996). Antisense oligonucleotides: a new class of potential anti-AIDS and anticancer drugs. *Drugs of Today*, **32**, 113-137.

Ringertz, N. (1950). "Grading" of gliomas. *Acta Pathology and Microbiology Scandinavia*. **27**, 51-64.

Rojanasakul, Y (1996). Antisense oligonucleotide therapeutics: drug delivery and targeting. *Advanced Drug Delivery Reviews*. **18**, 115-131.

Rossi, J.J. (1994). Making ribozymes work in cells. *Current Biology*, **4**, 469-471.

Rossi, J.J. (1995). Controlled, targeted, intracellular expression of ribozymes: progress and problems. *Trends in Biotechnology*. **13**, 301-306.

Rossi, J.J. (1998). Therapeutic Ribozymes: Principles and Applications. *Biodrugs*. **9**, 1-10.

Ruffner, D.E., Stormo, G.D. and Uhlenbeck, O.C. (1990). Sequence requirements of the hammerhead RNA self-cleavage reaction. *Biochemistry*. **29**, 10695- 10702.

Sambrook, J., Fritsch, E.F., and Maniatis, T. (1989*). Molecular Cloning: A Laboratory Manual*. Volumes 1-3 (second Edition). Cold Spring Habour Laboratory Press. Cold Spring Harbour, New York, USA.

Santoro, S.W. and Joyce, J.F. (1998). Mechanism and utility of an RNA-cleaving DNA enzyme. *Biochemistry*. **37**, 13330-13342.

Sakamoto, N., Wu, C.H. and Wu, G.Y. (1996). Intracellular cleavage of hepatitis C virus RNA and inhibition of viral protein translation by hammerhead ribozymes. *Journal of Clinical Investigation*. **98**, 2720-2728.

Sandberg, J.A., Bouhana, K.S., Gallegos, A.M., Agrawal, A.B., Brimm, S.L., Wincott, F.E., Reynolds, M.A., Pavco, P.A and Parry, T.J. (1999). Pharmacokinetics of an anti-angiogenic ribozyme (ANGIOZYME) in the mouse. *Antisense Nucleic Acid Drug Development*. **9**. 271-277.

Sano, T., Asai, A., Mishima, K., Fijimaki, T., and Kirino, T. (1998). Telomerase activity in 144 brain tumours. *British Journal of Cancer*. **77**, 1633-1637.

Scanlon, K.J., Ohta, Y., Ishida, H., Kijima, H., Ohkawa, T., Kaminski, A., Tsai, J., Horng, G and Kashani-Sabet, M. (1995). Oligonucleotide-mediated modulation of mammalian gene expression. *The FASEB Journal.* **9**, 1288-1296.

Scherr, M., Grez, M., Ganser, A and Engels, J.W. (1997). Specific hammerhead ribozyme-mediated cleavage of mutant N-ras mRNA in vitro and ex-vivo. Oligoribonucleotides as therapeutic agents. *Journal of Biological Chemistry.* **272**,14304-14313.

Scott, W.G., Finch, J.T., and Klug, A. (1995). The crystal structure of an all RNA hammerhead ribozyme : a proposed mechanism for catalytic cleavage. *Cell.* **81**, 991-1002.

Sczakiel, G. (1996). Hammerhead ribozymes with long flanking sequences: a structural and kinetic view. *Nucleic Acids and Molecular Biology.* **10**, 231-241.

Sen, D and Geyer, C.R. (1998). DNA enzymes. *Current Opinions in Chemical Biology.* **2**, 680-687.

Shapiro, W.R., and Shapiro, J.R. (1998). Biology and treatment of malignant gliomas. *Oncology.* **12**, 233-240.

Shay, J.W. (1997). Telomerase in development and cancer. *Journal of Cell Physiology.* **173**, 266-270.

Sherrill, J.M. and Kyte, J. (1996). Activation of epidermal growth factor receptor by epidermal growth factor. *Biochemistry.* **35**, 5705-5718.

Shimayama, T., Nishikawa, F., Nishikawa, S., and Taira, K. (1993). Nuclease resistant chimeric ribozymes containing deoxyribonucleotides and phosphorothioate linkages. *Nucleic Acids Research.* 21, 2605-2611.

Shimayama, T., Nishikawa, M., and Taira, K. (1995). Generality of the NUX rule - kinetic analysis of the results of systematic mutations in the trinucleotide at the cleavage site of the hammerhead ribozymes. *Biochemistry.* **34**, 3649-3654.

Shoji, Y., Akhtar, S., Periasamy, A., Herman, B., and Juliano, R.L. (1991). Mechanism of cellular uptake of modified oligodeoxynucleotides containing methyl phosphonate linkages. *Nucleic Acids Research.* **19**, 5543-5550.

Shoji, Y.Y., Shimada, J., Mizushima, Y., Iwasawa, A., Nakamura, Y., Inouye, K., Azuma, T., Sakurai, M and Tateo, N. (1996). Cellular uptake and biological effects of antisense oligodeoxynucleotide analogues targeted to herpes simplex virus. *Antimicrobial Agents and Chemotherapy*. **40**, 1670-1675.

Sion-Vardy, N., Vardy, D., Rodeck, U., Kari, C., Levin, R.M. and Malkowicz, S.B. (1995). Antiproliferative effects of tyrosine kinase inhibitors (Tyrphostins) on human bladder and renal carcinoma cells. *Journal of Surgical Research*. **59**, 675-680.

Sioud, M. (1996). Ribozyme modulation of lipopolysaccharide-induced tumour necrosis factor-alpha production by peritoneal cells in vitro and in vivo. *The European Journal of Immunology*. **26**, 1026-1031.

Sioud, M and Jepersen, L (1996). Enhancement of hammerhead ribozyme catalysis by glyceraldehyde-3-phosphate dehydrogenase. *Journal of Molecular Biology*. **257**, 775-789.

Sioud, M., Natwig, J.B. and Forre, O. (1992). Preformed ribozyme destroys tumour necrosis factor mRNA in human cells. *Journal of Molecular Biology*. **223**, 831-835.

Snyder, D.S., Wu, Y., Wang, J.L., Rossi, J.J, Swiderski, P., Kaplan, B.E., and Forman, S.J. (1993). Ribozyme mediated inhibition of bcr-abl gene expression in a Philadelphia chromosome-positive cell line. *Blood*. **82**, 600-605.

Sporn, M.B., and Roberts, A.B. (1985). Autocrine growth factors and cancers. *Nature*. **313**, 745-747.

Sproat, B.S. (1996). Synthetic catalytic oligonucleotides based on hammerhead ribozyme. *Nucleic Acids and Molecular Biology*. **10**, 265-281.

Stein, C.A. (1997). Controversies in the cellular pharmacology of oligodeoxynucleotides. *Antisense and Nucleic Acid Drug Development*. **7**, 207-209.

Stein, C.A., Mori, K., Loke, S.L. Subasinghe, C., Cohen, J.S. and Neckers, L.M. (1988). Phosphorothioate and normal oligodeoxyribonucleotides with 5'-linked acridine: characterisation and preliminary kinetics of cellular uptake. *Gene*. **72**, 333-341.

Stein, C.A., Tonkinson, J.L., Zhang, L-M., Yakubov, L., Gervasoni, J., Taub, R and Rotenberg, S. (1993). Dynamics of the internalisation of phosphodiester oligonucelotides in HL60 cells. *Biochemistry*. **32**, 4855-4861.

Steinmetz, A and Schackert, G. (1996). Malignant gliomas of the brain and surgical limitations. *Onkologie*. **19**, 6-14.

Stegmann, T and Legendre, J-Y. (1997). Gene transfer mediated by cationic lipids: lack of correlation between lipid mixing and transfection. *Biochimica et Biophysica Acta*. **1325**, 71-79.

Stryer, L. (1988). Protein conformation, dynamics and function. In. *Biochemistry*. Third Edition. W.H. Freeman and Company, New York, USA.

Sullenger, B.A. and Cech, T.R. (1993). Tethering ribozymes to a retroviral packaging signal for destruction of viral RNA. *Science*. **262**, 1566-1569.

Sullivan, S.M. (1993). Liposome-mediated uptake of ribozymes. *A Companion to Methods in Enzymology*. **5**, 61-66.

Sullivan, S.M. (1994). Development of ribozymes for gene therapy. *The Journal of Investigative Dermatology*. **100**, 85S-89S.

Sun, D.Y., Thompson, B., Cathers, B.E., Salazar, M., Kerwin, S. M., Trent, T.C., Neidle, S and Hurley, L.H. (1997). Inhibition of human telomerase by a G-quadraplex-interactive compound. *Journal of Medicinal Chemistry*. **40**, 2113-2116.

Symons ,R.H. (1992). Small catalytic RNAs. *Annual Review of Biochemistry*. **61**, 641-671.

Tanner, N.K. (1999). Ribozymes: the characteristic and properties of catalytic RNAs. *FEMS Microbiology Reviews*. **23**, 257-275.

Tao, M., Miyano-Kurosaki, N., Takai, K and Takaku, H. (1999). Specific inhibition of human telomerase activity by transfection reagent, FuGENE6-antisense phosphorothioate oligonucleotide complex in HeLa cells. *FEBS letters*. **454**, 312-316.

Tayler, N.R., Kaplan, B.E., Swiderski, P., Li, H., and Rossi, J.J. (1992). Chimeric DNA-RNA hammerhead ribozymes have enhanced in vitro catalytic efficiency and increased stability in vivo. *Nucleic Acids Research*, **20**, 4559-4565.

Temsamani, J., Kubert, M., Tang, J., Padmapriya, A. and Agrawal, S. (1994). Cellular uptake of oligodeoxynucleotide phosphorothioates and their analogues. *Antisense Research and Development*. **4**, 35-42.

Thierry, A.R. and Tackle, G.B. (1995). Liposomes as a delivery system for antisense and ribozymes compounds. in :Akhtar, S (ed), *Delivery Strategies for Antisense Oligonucleotide Therapeutics*, CRC Press Inc., London, UK.

Thompson, J.B., Tuschl T., and Eckstein, F. (1993). Activity of hammerhead ribozymes containing non-nucleotidic linkers. *Nucleic Acids Research*. **21**, 5600-5603.

Thompson, J.B., Tuschl, T. and Eckstein, F. (1996). The hammerhead ribozyme. *Nucleic Acids and Molecular Biology*. **19**, 172-196.

Tidd, D.M. (1996). Ribonuclease-H mediated antisense effects in intact human leukaemia cells. *Biochemical Society Transactions*. **24**, 619-623.

Tidd, D.M. and Warenius, H.M. (1989). Partial protection of oncogene, antisense oligodeoxynucleotides against serum nuclease degradation using terminal methylphosphonate groups. *British Journal of Cancer*. **60**, 343-350.

Tonkinson, J.L. and Stein, C.A. (1994). Patterns of intracellular compartmentalization, trafficking and acidification of 5'-fluorescein labelled phosphodiester and phosphorothioate oligodeoxynucleotides in HL60 cells. *Nucleic Acids Research*. **22**, 4268-4275.

Traxler, P., and Furet, P. (1999). Strategies towards the design of novel and selective protein tyrosine kinase inhibitors. *Pharmacological Therapies*. **82**, 195-206.

Tuschl, T. and Eckstein, F. (1993). Hammerhead ribozymes: The importance of stem loop II for activity. *Proceedings of the National Academy of Sciences, USA*. **90**, 6991-69.

Tuschl, T., Gohlke, C., Jovin, T.M., Westhof, E., and Eckstein, F. (1994). A three dimensional model for the hammerhead ribozyme based on fluorescence measurements. *Science*. **266**, 785-788.

Tsuchihashi, Z., Khosla, M., and Herschlag, D. (1993). Protein enhancement of hammerhead ribozyme catalysis. *Science*. **262**, 99-102.

Uhlenbeck, O.C. (1987). A small catalytic oligoribonucleotide. *Nature*. **328**, 596-600.

Uhlmann, E., and Peyman, A. (1990). Antisense oligonucleotides: a new therapeutic principle. *Chemical Reviews*, **90**, 544-579.

Ullrich, A., Coussens, J.S., Hayflick, T.J., Dull, A., Tam, A.W., Lee, J., Yarden, Y., Libermann, T.A., Schlessenger, J., Downward, J., Mayers, E.L.V., Whittle, N., Waterfield, M.D. and Seeburg, P.H. (1984). Human Epidermal Growth Factor Receptor cDNA sequence and aberrant expression of the amplified gene in A431 epidermoid carcinoma cells. *Nature*. **309**, 418-425.

Usman, N and Cedergren, R. (1992). Exploiting the chemical synthesis of RNA. *Trends in Biochemical Science*. **17**, 334-339.

Usman, N and McSwiggen, J.A. (1996). Catalytic RNA (ribozymes) as drugs. *Annual Reports in Medicinal Chemistry*. **30**, 285-294.

Usman, N. and Stinchcomb, D.T. (1996). Design, synthesis, and function of therapeutic hammerhead ribozymes. *Nucleic Acids and Molecular Biology*. **10**, 243-263.

Vaish, N.K., Heaton, P.A., Fedorova, O., and Eckstein, F. (1998). In vitro selection of a purine nucleotide-specific hammerhead-like ribozyme. *Proceedings of the National academy of Sciences USA*. **92**, 2158-2162.

Vlassov, V.V., Balakireva, L.A., and Yakubov, L.A. (1994). Transport of oligonucleotides across natural and model membranes. *Biochimica et Biophysica Acta*. **1197**, 95-108.

Voldborg, B.R., Damstrup, L., Spang-Thomsen, M and Poulsen, H.S. (1997). Epidermal growth factor receptor (EGFR) and EGFR mutations, function and possible role in clinical trials. *Ann Oncology*. **8**, 1197-1206.

Wan, M.S.K., Fell, P.L. and Akhtar, S. (1998). Synthetic 2'-O-methyl modified hammerhead ribozymes targeted to the RNA component of telomerase as sequence-specific inhibitors of telomerase activity. *Antisense and Nucleic Acid Drug Development*. **8**, 309-317.

Wells, A. (1999). EGF receptor. *International Journal of Biochemical Cell Biology.* **31**, 537-643.

Werner, M and Uhlenbeck, O.C. (1995). The effect of base mismatches in the substrate recognition helices of hammerhead ribozymes on binding and catalysis. *Nucleic Acids Research.* **23**, 2092-2096.

Westaway, S.K., Larson, G.P., Li, S., Zaia, J.A. and Rossi, J.J. (1995). A chimeric tRNA(Lys3)-ribozyme inhibits HIC replication following virion assembly. *Nucleic Acids Symposium.* **33**, 194-199.

Williams, D.M., Pieken, W.A., and Eckstein, F. (1992). Function of specific 2'-hydroxyl groups of guanosines in a hammerhead ribozyme probed by 2'-modifications. *Proceedings of the National Academy of Sciences, USA.* **89**, 918-921.

Wincott, F., DiRenzo, A., Shaffer, C., Grimms, S., Tracz, D., Workman, C., Sweedler, D., Gonzalez, C., Scaringe, S., and Usman, N. (1995). Synthesis, deprotection, analysis and purification of RNA and ribozymes. *Nucleic Acids Research.* **23**, 2677-2684.

Witters, L., Kumar, R., Mandil, M., Bennet, C.F., Miraglia, L., and Lipton, A. (1999). Antisense oligonucleotides to the epidermal growth factor receptor. *Breast Cancer Research Treatment.* **53**, 41-50.

Wong, A.J., Zoltick, P.W., and Moscatello, D.K. (1994). The molecular biology and molecular genetics of atrocytic neoplasms. *Seminars in Oncology.* **21**,139-148.

Wong-Staal, F, Poeschla, E., and Looney, D. (1998). A controlled, phase 1 clinical trial to evaluate the safety and effects in HIV-1 infected humans of autologous lymphocytes transduced with a ribozyme that cleaves HIV-1 RNA. *Human Gene Therapy.* **9**, 2407-2425.

Wu, H.N., Lin, Y-J., Lin, F-P., Makino, S., Chang, M-F., and Lai, M.M.C. (1989). Human hepatitis delta virus RNA subfragments contain auto-cleavage activity. *Proceeding of the National Academy of Sciences, USA.* **86**, 1831-1836.

Wu-Pong, S., Weiss, T.L. , and Hunt, C.A. (1994). Antisense c-myc oligonucleotide cellular uptake and activity. *Antisense Research and Development.* **4**, 155-163.

Wu-Pong, S., Weiss, T.L., and Hunt, C.A. (1994b) Calcium dependent cellular uptake of a c-myc antisense oligonucleotide. *Cellular and Molecular Biology*. **40**, 843-850.

Yakubov, L.A., Deeva, E.A., Zarytova, V.F., Ivanova, E.M., Ryte, A.S., and Yurchenko, L.V. (1989). Mechanism of oligonucleotide uptake by cells: involvement of specific receptors? *Proceedings of the National Academy of Sciences*, USA. **86**, 6454-6458.

Yao, G.Q., Corrias, S. and Cheng, Y.C. (1996). Identification of two oligoribonucleotide binding proteins on plasma membranes of human cell lines. *Biochemical Pharmacology*. **51**, 431-436.

Yamazaki, H., Kijima, H., Ohnishi, Y., Abe, Y., Oshika, Y., Tsuchida, T., Tokunaga, T., Tsugu, A., Ueyama, Y., Tamaoki, N., and Nakamura, M. (1998). Inhibition of tumour growth by ribozyme mediated suppression of aberrant epidermal growth factor receptor gene expression. *Journal of the National Cancer Institute*. **90**, 581-587.

Yang, J.H., Usman, N., Chartrand, P., and Cedergren, R.J. (1992). Minimum ribonucleotide requirement for catalysis by the RNA hammerhead domain. *Biochemistry*. **31**, 5005-5009.

Yazaki, T., Ahmed, S., Chahlavi, A., Zylber-Katz, E., Dean, N.M., Rabkin, S.D., Martuza, R.L. and Glazer, R.I. (1996). Treatment of glioblastoma U87 by systemic administration of an antisense protein kinase C-α phosphorothioate oligodeoxynucleotide. *Molecular Pharmacology*. **50**, 236-242.

Yokoyama, Y., Takahashi, Y., Shinohara, A., Lian, Z., Wan,X., Niwa, K., and Tamaya, T. (1998). Attenuation of telomerase activity by a hammerhead ribozyme targeting the template region of telomerase RNA in endometrial carcinoma cells. *Cancer Research*. **58**, 5406-5410.

Zamecnik, P., and Stephenson., M. (1978). Inhibition of Rous sarcoma virus replication and cell transformation by a specific oligodeoxynucleotide. *Proceedings of the National Academy of Sciences, USA*. **75**, 280-284.

Zabner, J. (1997). Cationic lipids used in gene transfer. *Advanced Drug Delivery Reviews*. **27**, 17-28.

Zelphati, O., and Szoka, F.C.Jr. (1996). Mechanism of oligonucleotide release from cationic liposomes. *Proceedings of the National Academy of Sciences, USA.* **93**, 11493-11498.

Zhenodarova, S.M. (1993). Synthetic endoribonucleases (a review). *Molecular Biology.* **27**, 137-152.

Zhao, J.J. and Pick, L (1993). Generating loss of function phenotypes of the fushi tarazu gene with a targeted ribozyme in Drosophila. *Nature.* **365**, 448-451.

Zhao, Q., Matson, S., Herrera, C.J., Fisher, E., Yu, H., and Kreig, A.M. (1993). Comparison of cellular binding and uptake of antisense phosphodiester, phosphorothioate and mixed phosphorothioate and methylphosphonate oligonucleotides. *Antisense Research and Development.* **3**, 53-66.

Zhao, Q., Temsamani, J., Iadarola, P.L., Jiang, Z.W. and Agrawal, S. (1997). Pattern and kinetics of cytokine production following administration of phosphorothioate oligonucleotides in mice. *Antisense Nucleic Acid Drug Development.* **79**, 495-502.

Zhou, X., and Huang, L. (1994). DNA transfection mediated by cationic liposomes containing lipopolylysine: characterisation and mechanism of action. *Biochimica et Biophysica Acta.* **1189**, 195-203.

Zuker, M., Jaeger, J., and Turner, D. (1991). A comparison of optimal and suboptimal RNA secondary structures predicted by free energy minimization with structures determined by phylogenetic comparison. *Nucleic Acids Research.* **19**, 2707-2714.

Zuker, M and Steigler, P. (1981). Optimal computer folding of large RNA sequences using thermodynamics and auxiliary information. *Nucleic Acids Research.* **9**, 133-148.

APPENDIX I

Publications

- Fell, P.L., Hudson, A.J., Reynolds, M.A., Usman, N and Akhtar, S. (1997). Cellular uptake properties of a 2'-amino / 2'-O-methyl- modified chimeric hammerhead ribozyme targeted to the epidermal growth factor receptor. *Antisense and Nucleic Acid Drug Development*. **7**, 319-326.

- Wan, M.S.K., Fell, P.L. and Akhtar, S. (1998). Synthetic 2'-O-methyl modified hammerhead ribozymes targeted to the RNA component of telomerase as sequence-specific inhibitors of telomerase activity. *Antisense and Nucleic Acid Drug Development*. **8**, 309-317.